CAL REPORT NO. BM-2820-F-1

DEVELOPMENT OF ADVANCED TECHNIQUES FOR THE IDENTIFICATION OF V/STOL AIRCRAFT STABILITY AND CONTROL PARAMETERS

Final Report
(May 1969 to December 1970)

August 1971

Robert T. N. Chen
Bernard J. Eulrich
J. Victor Lebacqz

CORNELL AERONAUTICAL LABORATORY, INC.
Buffalo, New York

APPROVED FOR PUBLIC RELEASE; DISTRIBUTION UNLIMITED

Under Contract No. N00019-69-C-0534
NAVAL AIR SYSTEMS COMMAND
DEPARTMENT OF THE NAVY
WASHINGTON, D.C.

359

Unclassified

Security Classification

DOCUMENT CONTROL DATA - R&D

(Security classification of title, body of abstract and indexing annotation must be entered when the overall report is classified)

1. ORIGINATING ACTIVITY (Corporate author) Cornell Aeronautical Laboratory, Inc. P. O. Box 235 Buffalo, New York 14221	2a REPORT SECURITY CLASSIFICATION Unclassified 2b GROUP

3 REPORT TITLE

DEVELOPMENT OF ADVANCED TECHNIQUES FOR THE IDENTIFICATION OF V/STOL AIRCRAFT STABILITY AND CONTROL PARAMETERS

4 DESCRIPTIVE NOTES (Type of report and inclusive dates)

Final Report (May 1969 to December 1970)

5. AUTHOR(S) (Last name, first name, initial)

Chen, Robert T.N.; Eulrich, Bernard J.; Lebacqz, J. Victor

6 REPORT DATE	7a TOTAL NO. OF PAGES	7b NO OF REFS
August 1971	340	76

8a CONTRACT OR GRANT NO. N00019-69-C-0534 New b. PROJECT NO. c. d	9a. ORIGINATOR'S REPORT NUMBER(S) BM-2820-F-1 9b OTHER REPORT NO(S) (Any other numbers that may be assigned this report)

10 AVAILABILITY/LIMITATION NOTICES

Approved for Public Release; Distribution Unlimited

11. SUPPLEMENTARY NOTES	12. SPONSORING MILITARY ACTIVITY Naval Air Systems Command Department of the Navy

13. ABSTRACT

Contemporary analyses of transition flight of V/STOL aircraft are based on aerodynamic data measured in a wind tunnel or on analytical prediction using methods developed for conventional aircraft. The validity and accuracy of these techniques for V/STOL aircraft has not yet been established, and it is essential that they be correlated with flight test data through parameter identification. In spite of the complicated nature of V/STOL dynamics in transition, some method of identifying these characteristics is required. This report documents the development of identification techniques to meet this requirement.

The report first presents the selection of a mathematical model to represent a V/STOL aircraft (the X-22A). This is followed by a discussion of available identification techniques. Based upon a thorough knowledge of the requirements of this program and the limitations of the available techniques, advanced techniques suitable for identification of V/STOL aircraft stability and control parameters are developed. These advanced techniques, which were developed by CAL, are: a suboptimal fixed-point nonlinear data smoothing technique for estimation of parameters and unknown forcing inputs to detect the modeling errors; a start-up procedure for the fixed-point smoothing algorithm; and an improved computational algorithm for the variances of the fixed-point smoothed estimates. The developed techniques are then applied to the identification of the X-22A stability and control parameters from computer-generated data, Princeton Dynamic Model Track data, and available X-22A flight data.

DD FORM 1 JAN 64 1473

Unclassified

Security Classification

Unclassified
Security Classification

14 KEY WORDS	LINK A ROLE	LINK A WT	LINK B ROLE	LINK B WT	LINK C ROLE	LINK C WT
Parameter Identification						
V/STOL Aircraft						
Nonlinear Filtering						
Identifiability						
Flight Data Analysis						
Fixed-Point Smoothing						
Modelling and Measurement Error Analysis						
Input Design						

INSTRUCTIONS

1. ORIGINATING ACTIVITY: Enter the name and address of the contractor, subcontractor, grantee, Department of Defense activity or other organization (*corporate author*) issuing the report.

2a. REPORT SECURITY CLASSIFICATION: Enter the overall security classification of the report. Indicate whether "Restricted Data" is included. Marking is to be in accordance with appropriate security regulations.

2b. GROUP: Automatic downgrading is specified in DoD Directive 5200.10 and Armed Forces Industrial Manual. Enter the group number. Also, when applicable, show that optional markings have been used for Group 3 and Group 4 as authorized.

3. REPORT TITLE: Enter the complete report title in all capital letters. Titles in all cases should be unclassified. If a meaningful title cannot be selected without classification, show title classification in all capitals in parenthesis immediately following the title.

4. DESCRIPTIVE NOTES: If appropriate, enter the type of report, e.g., interim, progress, summary, annual, or final. Give the inclusive dates when a specific reporting period is covered.

5. AUTHOR(S): Enter the name(s) of author(s) as shown on or in the report. Enter last name, first name, middle initial. If military, show rank and branch of service. The name of the principal author is an absolute minimum requirement.

6. REPORT DATE: Enter the date of the report as day, month, year, or month, year. If more than one date appears on the report, use date of publication.

7a. TOTAL NUMBER OF PAGES: The total page count should follow normal pagination procedures, i.e., enter the number of pages containing information.

7b. NUMBER OF REFERENCES: Enter the total number of references cited in the report.

8a. CONTRACT OR GRANT NUMBER: If appropriate, enter the applicable number of the contract or grant under which the report was written.

8b, 8c, & 8d. PROJECT NUMBER: Enter the appropriate military department identification, such as project number, subproject number, system numbers, task number, etc.

9a. ORIGINATOR'S REPORT NUMBER(S): Enter the official report number by which the document will be identified and controlled by the originating activity. This number must be unique to this report.

9b. OTHER REPORT NUMBER(S): If the report has been assigned any other report numbers (*either by the originator or by the sponsor*), also enter this number(s).

10. AVAILABILITY LIMITATION NOTICES: Enter any limitations on further dissemination of the report, other than those imposed by security classification, using standard statements such as:

(1) "Qualified requesters may obtain copies of this report from DDC."

(2) "Foreign announcement and dissemination of this report by DDC is not authorized."

(3) "U. S. Government agencies may obtain copies of this report directly from DDC. Other qualified DDC users shall request through

__________________________."

(4) "U. S. military agencies may obtain copies of this report directly from DDC. Other qualified users shall request through

__________________________."

(5) "All distribution of this report is controlled. Qualified DDC users shall request through

__________________________."

If the report has been furnished to the Office of Technical Services, Department of Commerce, for sale to the public, indicate this fact and enter the price, if known.

11. SUPPLEMENTARY NOTES: Use for additional explanatory notes.

12. SPONSORING MILITARY ACTIVITY: Enter the name of the departmental project office or laboratory sponsoring (*paying for*) the research and development. Include address.

13. ABSTRACT: Enter an abstract giving a brief and factual summary of the document indicative of the report, even though it may also appear elsewhere in the body of the technical report. If additional space is required, a continuation sheet shall be attached.

It is highly desirable that the abstract of classified reports be unclassified. Each paragraph of the abstract shall end with an indication of the military security classification of the information in the paragraph, represented as *(TS)*, *(S)*, *(C)*, or *(U)*.

There is no limitation on the length of the abstract. However, the suggested length is from 150 to 225 words.

14. KEY WORDS: Key words are technically meaningful terms or short phrases that characterize a report and may be used as index entries for cataloging the report. Key words must be selected so that no security classification is required. Identifiers, such as equipment model designation, trade name, military project code name, geographic location, may be used as key words but will be followed by an indication of technical context. The assignment of links, rules, and weights is optional.

Unclassified
Security Classification

Details of illustrations in
this document may be better
studied on microfiche

DEVELOPMENT OF ADVANCED TECHNIQUES FOR THE IDENTIFICATION OF V/STOL AIRCRAFT STABILITY AND CONTROL PARAMETERS

Robert T. N. Chen
Bernard J. Eulrich
J. Victor Lebacqz

CAL Report No. BM-2820-F-1

August 1971

APPROVED FOR PUBLIC RELEASE; DISTRIBUTION UNLIMITED

Prepared Under Contract N00019-69-C-0534
for

NAVAL AIR SYSTEMS COMMAND
DEPARTMENT OF THE NAVY
WASHINGTON, D. C.

FOREWORD

The study whose results are reported herein was performed under Contract N00019-69-C-0534 for the Naval Air Systems Command, Department of the Navy, by the Flight Research Department of the Cornell Aeronautical Laboratory, Inc. (CAL), Buffalo, New York. Dr. Robert T. N. Chen was the CAL Project Engineer. Technical monitors for the Naval Air Systems Command were Messrs. Raymond Siewert and Fred Pierce.

The authors wish to express their deep appreciation to Messrs. Siewert and Pierce for their many valuable discussions and suggestions during the course of this work. The authors also wish to thank many members of the Flight Research Department who have contributed ideas, encouragement, and work during this study. Particular gratitude must be given to Mr. N. Weingarten who performed the computer evaluations of the conjugate gradient, quasilinearization, and suboptimal input design methods; to Mr. C. L. Mesiah who did an excellent job in computer programming and performed data handling; to Messrs. E. G. Rynaski, J. M. Schuler, W. R. Deazley, and R. P. Harper, Jr., who supervised and guided this work; and to Mrs. J. A. Martino, Misses D. Kantorski, D. Hoyler, and J. Weirich for their assistance during publication.

Grateful acknowledgment is also given to Dr. J. T. Fleck and Mr. D. Larson of the Computer Mathematics Department of CAL for their help in the use of their modified spline functions computer program and quasilinearization computer program at the early stage of this project; and to Dr. James Tyler of Systems Control Inc. for his valuable discussions and the subcontract work which is reported in Reference 55.

ABSTRACT

Contemporary analyses of transition flight of V/STOL aircraft are based on aerodynamic data measured in a wind tunnel or on analytical prediction using methods developed for conventional aircraft. The validity and accuracy of these techniques for V/STOL aircraft has not yet been established, and it is essential that they be correlated with flight test data through parameter identification. In spite of the complicated nature of V/STOL dynamics in transition, some method of identifying these characteristics is required. This report documents the development of identification techniques to meet this requirement.

The report first presents the selection of a mathematical model to represent a V/STOL aircraft (the X-22A). This is followed by a discussion of available identification techniques. Based upon a thorough knowledge of the requirements of this program and the limitations of the available techniques, advanced techniques suitable for identification of V/STOL aircraft stability and control parameters are developed. These advanced techniques, which were developed by CAL, are: a suboptimal fixed-point nonlinear data smoothing technique for estimation of parameters and initial state of nonlinear dynamic systems having a large number of parameters and unknown forcing inputs; a method for estimating the unknown forcing inputs to detect the modeling errors; a start-up procedure for the fixed-point smoothing algorithm; and an improved computational algorithm for the variances of the fixed-point smoothed estimates. The developed techniques are then applied to the identification of the X-22A stability and control parameters from computer-generated data, Princeton Dynamic Model Track data, and available X-22A flight data.

TABLE OF CONTENTS

Section		Page
I	INTRODUCTION.	1
II	MATHEMATICAL MODEL AND FORMULATION OF THE PROBLEM.	6
	2.1 Mathematical Model	6
	2.2 Formulation of the Problem.	13
III	REVIEW OF IDENTIFICATION TECHNIQUES.	20
	3.1 Equation-Error Methods	21
	3.1.1 Comparison of the Numerical Results	28
	3.1.2 Concluding Remarks on the Equation-Error Methods.	29
	3.2 Measurement-Error Methods	31
	3.2.1 Description of Various Measurement-Error Methods	32
	3.2.2 Basic Characteristics of Measurement-Error Methods	44
	3.2.3 Numerical Results of Computer-Generated Data	48
	3.3 Methods Treating Both Measurement and Process Noise	50
IV	PARAMETER IDENTIFIABILITY	65
	4.1 Identifiability for Noiseless Measurements - Linear Stationary Systems.	66
	4.2 Sensitivity Vector Functions.	70
	4.3 Problem of Uniqueness Due to Data	78
	4.4 Concluding Remarks	79
V	DEVELOPMENT OF ADVANCED IDENTIFICATION TECHNIQUES	82
	5.1 Description of the Developed Techniques	84
	5.1.1 Initial Estimator Program	84
	5.1.2 Multi-Corrected Extended Kalman Filter.	85
	5.1.3 Fixed-Point Smoothing.	88
	5.1.4 Computation of Unknown Forcing Function	90
	5.1.5 Better Prediction of the Quality of the Estimated Parameters	91
	5.2 Derivation of Locally Iterated Filter Smoother and Fixed-Point Smoothing Algorithm.	96

TABLE OF CONTENTS (CONTINUED)

Section		Page
	5.3 Computations of the Unknown Forcing Function . .	105
	5.4 Improved Covariance Computation.	108
VI	NUMERICAL VERIFICATION OF ADVANCED TECHNIQUES TECHNIQUES	116
	6.1 Data Generation	116
	6.2 Effects of Using Acceleration Measurements . . .	118
	6.3 Effects of Reusing Data	120
	6.4 Effects of Multi-Corrections - The Use of Locally Iterated Filter-Smoother.	121
	6.5 Effects of Different Start-Up Procedures	122
	6.6 Fixed-Point Smoothing Results.	124
	6.7 Residual Consistency Test	126
	6.8 Sensitivity of Estimates to Process Noise	128
VII	APPLICATION OF ADVANCED TECHNIQUES TO EXPERIMENTAL DATA	153
	7.1 Application to Princeton Data	153
	7.1.1 Test Apparatus and Coordinate Transformation .	153
	7.1.2 Equations of Motion for PDMT Quad Duct Test Model	155
	7.1.3 Conversion of Princeton Test Data to Identification Computer Program Data Format	161
	7.1.4 Identification Results Using Princeton Data . . .	162
	7.2 Application to X-22A Flight Data	168
	7.2.1 Data Selection and Digitization	168
	7.2.2 Selection of Noise Levels	170
	7.2.3 Results at Fixed-Duct Incidence.	172
	7.2.4 Results in Slow Transition	177
VIII	CONCLUSIONS	241
IX	RECOMMENDATIONS.	244
APPENDIX A -	LINEAR TIME-VARYING MATHEMATICAL MODEL FOR THE X-22A IN TRANSITION - AN ALTERNATE IDENTIFICATION MODEL. .	247
APPENDIX B -	A STATISTICAL ANALYSIS OF THE ESTIMATES FROM THE EQUATION-ERROR METHODS . .	249

TABLE OF CONTENTS (CONCLUDED)

Section		Page
APPENDIX C -	DENERY'S INITIAL ESTIMATOR	263
APPENDIX D -	COMPUTER-GENERATED DATA FOR IDENTIFICATION STUDY	266
APPENDIX E -	PERTURBED PARAMETERS.	270
APPENDIX F -	DESIGN OF INPUT	271
APPENDIX G -	MATHEMATICAL PRELIMINARIES	285
APPENDIX H -	ACTUAL BIAS AND COVARIANCE IN MULTI-CORRECTED EXTENDED KALMAN FILTER	295
APPENDIX I -	CORRELATED PROCESS AND MEASUREMENT NOISE	301
APPENDIX J -	EFFECTS OF CALIBRATION ERRORS AND SENSOR/FILTER DYNAMICS	306
APPENDIX K -	SENSITIVITY FUNCTIONS FOR THE KALMAN FILTER	316
APPENDIX L -	DERIVATION OF THE EQUATIONS OF MOTION FOR PDMT QUAD DUCT TEST MODEL	323
	REFERENCES	333

LIST OF ILLUSTRATIONS

Figure		Page
2-1	Constant Attitude Slow Level Transition - X-22A ($\theta = 0$) .	19
3-1	Quasilinearization Solution for the Minimum.	54
3-2	Quasilinearization Solution for the Local Minimum . .	55
5-1a	A Systematical Recycling Scheme	112
5-1b	An Alternate Recycling Scheme - SCI's Forward-Backward Filtering	112
5-2	Block Diagram of the CAL Identification Program. . .	113
5-3	Local Iterative Filter-Smoother (The Multi-Correction Scheme)	114
5-4	Fixed-Point Smoother Working in Conjunction With Local Iterative Filter-Smoother.	114
5-5	Reference Trajectory	115
5-6	Updating of Reference Trajectory	115
6-1	Computer Generated Data 3C-1	130
6-2	Computer Generated Data 3D-1	131
6-3	Transient Response Matching to Data 2D-2, Typical Kalman	132
6-4	Transient Response Matching to Data 2C-1, Typical Kalman	133
6-5	Transient Response Matching to Data 2D-1	134
6-6	Transient Response Matching to Data 3D-1, $F_1(1)$ Filter	135
6-7	Filtered Estimates (States and Parameters), Data 3D-1, F_{CR} (1) Filter	137
6-8	Residual Sequence for R and Q True Data 3D-1, F_{CR} (1) Filter	138
6-9	Residual Sequence for True R and 4Q, Data 3D-1, F_{CR} (1) Filter	139
7-1	Space-Fixed and Body-Fixed Axis Systems	179
7-2	Model and Error Link Mass Arrangement	180
7-3	Princeton Dynamic Model Track Quad Model Geometry (taken from Reference 60).	181
7-4	Transient Response Matching to Princeton Data No. 55 Linear Kalman Without Acceleration, Initial Estimate: EOM	182

Figure		Page
7-5	Transient Response Matching to Princeton Data No. 55 Linear Kalman Without Acceleration, Initial Estimate: Global.	183
7-6	Transient Response Matching to Princeton Data No. 154 With Acceleration Measurements and Modeling Error, F_{CR} (1)	184
7-7	Transient Response Matching to Princeton Data No. 154 With Acceleration Measurements and Modeling Error, F_1 (1).	186
7-8	Transient Response Matching to Princeton Data No. 154 With Acceleration Measurements, No Modeling Error, F_{10} (1)	188
7-9	Transient Response Matching to Princeton Data No. 154 Without Acceleration Measurements, No Modeling Error, F_{10} (1)	190
7-10	Transient Response Matching to Princeton Data No. 157 Using Parameter Identified From No. 154 (F_1 (1) with Accel. and Q)	192
7-11	Transient Response Matching to Princeton Data No. 55 With Acceleration Measurements and Model Error	194
7-12	Transient Response Matching to Flight Data 2F197, Linear Kalman	197
7-13	Transient Response Matching to Flight Data 2F203, Linear Kalman	198
7-14	Transient Response Matching to Flight Data 2F197, E.O.M. vs. 13 Parameter Model	199
7-15	Transient Response Matching to Flight Data 2F197, F_{10} (2) Without Acceleration Measurements	200
7-16	Transient Response Matching to Flight Data 2F197, F_{10} (2) With Acceleration Measurements	201
7-17	Transient Response Matching to Flight Data 2F203, F_{10} (2) With Acceleration Measurements	203
7-18	Transient Response Matching to Flight Data 2F203, Parameter Estimate from 2F197	204

LIST OF ILLUSTRATIONS (CONCLUDED)

Figure		Page
7-19	Transient Response Matching to Flight Data 2F197, Parameter Estimate from 2F203	205
7-20	Transient Response Matching to Flight Data 2F198, F_{10} (1)	206
7-21	Transient Response Matching to Flight Data 2F198, F_{CR} (1)	207
7-22	Transient Response Matching to Flight Data 2F198, F_1 (1)	208
7-23	Transient Response Matching to Flight Data 2F195, F_{10} (1)	211
7-24	Transient Response Matching to Flight Data 2F195, F_1 (1)	212
7-25	Slow Transition Flight Data 2F197	213
7-26a	Transient Response Measurement to Flight Data 2F197 in Transition	214
7-26b	Selected Filter Estimates, Flight Data 2F197 in Transition	215
7-26c	Residual Sequences, Flight Data 2F197 in Transition	216
B-1	$f(\hat{a}_1)$ for $\varkappa/\sigma = 0$	260
B-2	$f(\hat{a}_1)$ for $\varkappa/\sigma = 1.0$	261
B-3	$f(\hat{a}_1)$ for $\varkappa/\sigma = 10.0$	261
F-1	State Responses to Designed Input	280

LIST OF TABLES

Table		Page
3-1	Effects of Process and Measurement Noise on Parameter Estimates Using the "Equations-of-Motion" Method . . .	56
3-2	Effects of Process and Measurement Noise on Parameter Estimates Using the Modified Spline Function Method. . .	57
3-3a	Effects of Process and Measurement Noise on Parameter Estimates Using Polynomial Estimator - Fifth Degree . .	58
3-3b	Effects of Process and Measurement Noise on Parameter Estimates Using Polynomial Estimator - Ninth Degree . .	59
3-4a	Effects of Process and Measurement Noise on Parameter Estimates Using Denery's Estimator - 10% Increase of the True Values as Nominal Values.	60
3-4b	Effects of Process and Measurement Noise on Parameter Estimates Using Denery's Estimator - Nominal Values Being About 50% of the True Values	61
3-5	Comparison of Methods Using Linearized Model	62
3-6	Comparison of Methods Using Nonlinearized Model . . .	63
4-1	Parameter Identification for Noiseless Data Using a "Least-Squares" Method.	81
6-1a	Computer-Generated Data Characteristics for Data 2A-1, 2B-1, 2C-1, 2D-1 and 2A-2 through 2D-2	140
6-1b	Computer-Generated Data Characteristics for Data 3C-1 (Measurement Noise only) and 3D-1 (Both Process and Measurement Noise)	142
6-2	Kalman Filter Estimates With and Without Acceleration Measurements	144
6-3	Kalman Filter Estimates for Different Recycling Techniques With Acceleration Measurements	145
6-4a	Kalman Filter Estimates for Different Recycling Techniques and Multi-Correction Technique With Acceleration Measurements	146
6-4b	Effects of the Multi-Correction for Case 2C-1	147
6-4c	Effects of Multi-Correction	148
6-5	Effects of Multi-Correction for Case 3D-1	149
6-6a	Variance Comparison [P(0)] for Different Start-Up Procedures.	150
6-6b	Parameter Estimates Employing Different Start-Up Procedures and an Improved Final Variance Computation .	151

Table		Page
6-7	Sensitivity of Parameter Estimates to Variations in Q	152
7-1	Linear Kalman Run on Data No. 55 Using Equations-of-Motion Method as Initial Estimator	217
7-2	Linear Kalman Run on Data No. 55 Using Global Values as Initial Estimators	218
7-3	Scale Factors for Converting Model Values to X-22A Values	219
7-4	Flight Conditions and Reference Values of Princeton Data Runs	220
7-5	Noise Levels for Princeton Data Runs	221
7-6	Parameter Estimation From Nonlinear Program for Princeton Data No. 154	222
7-7	Parameter Estimation From Nonlinear Program for Princeton Data No. 154 and No. 157	223
7-8	Parameter Estimation From Nonlinear Program for Princeton Data No. 55 and No. 58	224
7-9	Comparison of the Effects of Linear and Nonlinear Kinematic Coupling for No. 55	225
7-10	Flight Conditions for X-22A Flights	226
7-11	Noise Statistics From Flight Records	227
7-12	Flight Conditions and Reference Values for X-22A Fixed-Duct Flight Data	228
7-13	Previous Results Using Linear Kalman Program Using Recycling (Without Acceleration Measurement)	229
7-14	Parameter Estimation From Nonlinear Kalman Without Acceleration Measurements With and Without Nonlinear Aerodynamics	230
7-15	Parameter Estimation From Nonlinear Kalman Without Acceleration Measurements With and Without Nonlinear Aerodynamics	231
7-16	Parameter Estimate From Nonlinear Kalman Without Acceleration Measurements	232
7-17	Parameter Estimation from Nonlinear Kalman	233
7-18	Comparison of Initial Variances $[P(0)]$ for Different Start-Up Procedures	234
7-19	Parameter Estimates From Nonlinear Kalman X-22A Data at $\lambda = 45°$	235
7-20	Parameter Estimation From Nonlinear Kalman X-22A Data at $\lambda = 45°$	236

LIST OF TABLES (CONCLUDED)

Table		Page
7-21	Results of Fixed-Point Smoothing for Initial Aircraft States	237
7-22	Comparison of Parameter Estimates Using Princeton Data and X-22A Data	238
7-23	Reference Values Used for Slow Transition Identification	239
7-24	Parameter Estimation on Slow Transition Flight Data 2F197	240
D-1	Actual Parameter Values Used in Generating Data	269
D-2	Measurement and Process Noise Characteristics	269
F-1	Effect of Input on the Initial Estimator (Equations-of-Motion Method)	281
F-2	Effects of Input on Kalman Filtering	282
F-3	A Sample Run of Suboptimal Input Design	283
J-1	Data Generation	310
J-2	Measurement Noise Characteristics and Sensor and Filter Dynamics	311
J-3	Summary of Initial Estimator - Equations of Motion	312
J-4	Case 1A - Sensitivity With Respect to P(0)	313
J-5	Case 2A - Sensitivity With Respect to P(0)	314
J-6	Summary of Extended Kalman - 5 Passes	315

LIST OF SYMBOLS

Nomenclature and symbols which have been used as consistently as possible in the main body of this report are presented in this list. Less commonly employed symbology have been excluded.

Axis System	Body axes are used throughtout. The axis system is orthogonal and positive according to the right-handnrule. The x -axis is fixed in the plane of symmetry aligned with the fuselage reference. z is positive down and y is positive to the right. The origin is at the center of gravity (c. g.)
Accel.	Abbreviation for acceleration measurements (n_x , n_z , and $\dot{q}$)
Aero.	Abbreviation for aerodynamic coefficients
B	Collective propeller blade angle, deg. Positive B gives increased thrust
$\mathcal{B}_k$	Fixed-point smoother gain matrix at time t_k
C, C_i	Cross-covariance matrix between process noise and measurement noise
CR	Cramer-Rao lower bound covariance matrix of estimation error
$E\{\ \}$	Expectation operator
E. O. M.	Abbreviation for equations-of-motion estimator
$f(x,p,m)$	Vector valued function which represents the dynamics of the aircraft
$f(x\|y)$	Conditional probability density function of x given y
$F_x(y)$	Mnemonic which defines the type of Kalman filter and start-up covariance matrix, P_0 , employed for identification where:

If x = constant (e. g. , 10), P_0 for the initial parameter estimates is equal to the variances of these estimates obtained from the E. O. M. estimator each multiplied equally by the constant x

If x = CR, P_0 for the initial parameter estimates was formed from the diagonal elements of the Cramer-Rao lower bound matrix

y is an integer signifying the number of corrections or iterations employed in the locally iterated filter. If y is not present, the filter is the extended Kalman filter

g	Gravitational constant, 32.2 ft/sec
g_1	Process noise effective matrix
$g_i(x_{i-1})$	Symbology to define nonlinear integration of the system differential equations from time t_{i-1} to t_i with initial condition x_{i-1}
G_k	Gain matrix in unknown forcing function algorithm at time t_k
$h(\ )$	Nonlinear measurement or observation vector used to represent the measurement system
H_k	$\partial h/\partial x$ evaluated at the reference trajectory at time t_k, where x is the augmented state vector
I_x, I_y, I_z	Moments of inertia about x, y, z body axes, slug-feet^2
I_n	Denotes the n x n identity matrix
J	Scalar performance index or cost functional
$ln(\ )$	Natural logarithm of ( )
m	$(\eta \quad B \quad \delta_{ES})^T$, Control input vector
M	Pitching moment, ft-lb
$M_0(u)$, $M_q(u)$, $M_w(u)$, $M_\eta(u)$, $M_B(u)$, $M_\delta(u)$	Dimensional pitching moment stability and control derivatives expressed as a polynomial function of u, e.g., $M_0(u) = M_{01} + M_{0u}u + M_{0u^2}u^2 + M_{0u^3}u^3$
n_x	Accelerometer measurement along the x axis, g's or ft/sec
n_z	Accelerometer measurement along the z axis, g's or ft/sec
N	Number of data points minus one (the first at time t_0)
P	Represents the unknown vector of the coefficients (or stability and control derivatives) of the equations of motion to be identified
P_{xx}	Covariance matrix of x, and defined by $P_{xx} = E\left\{[x-E(x)][x-E(x)]^T\right\}$
$P_0, P(0)$	Covariance matrix of initial estimates
$P_{k/k-1}$	Error covariance matrix of the difference between the true state and the state estimate at time t_k given data up to time t_{k-1}
P_k	Error covariance matrix of the difference between the true state and the state estimate at time t_k given data up to time t_k

$P_{0\|N}$	Fixed-point smoother error covariance matrix for the initial state given data up to time t_N
q	Angular pitch rate about the y body axis, rad/sec or deg/sec. Since the vehicle is restricted to longitudinal motions only, $q = \dot{\theta}$
Q, Q_k	Process noise covariance matrix
R, R_i	Measurement error or noise covariance matrix
t, t_i	Time, sec
T	Transformation matrix from perturbed to nonperturbed parameters
u, w	Components of linear velocity along the x, z body axes, ft/sec
$\vec{u}$	$(1 \ u \ u^2 \ u^3)^T$ vector, 4 x 1, whose elements are powers of u
$\vec{u}_d$	$(0 \ 1 \ 2u \ 3u^2)^T$ time derivative of $\vec{u}$ vector
v, v_i	Zero mean white Gaussian measurement noise vector sequence
V	$\sqrt{u^2 + w^2}$ Total velocity of c. g., ft/sec or knots
$\forall(\ )$	For all ( )
$w(t)$	Zero mean vector of white Gaussian noise which denotes process noise in continuous representation of aircraft dynamics
w_i	Zero mean white Gaussian vector sequence which denotes process noise in discrete representation of aircraft dynamics
$\hat{w}_{k\|N}$	Smoothed estimate of the unknown forcing function at time t_k given data up to time t_N
X, Z	Body axis components of aerodynamic and thrust forces along the x, z axis, lb
x	Used interchangeably to denote the aircraft state vector $(q \ \theta \ u \ w)^T$ or the augmented state vector $(q \ \theta \ u \ w \ \vdots \ p^T)^T$. The meaning is clear from the context
$x_0, x(0), x(t_0)$	Initial state at time t_0
$\hat{x}_{k\|k}$	Filtered state estimate at time t_k given data up to time t_k
$\hat{x}_{k\|k-1}$	Extrapolated or predicted state estimate at time t_k given data up to time t_{k-1}
$\hat{x}_{k\|N}$	Fixed-point or fixed-interval smoothed estimate at time t_k given data up to time t_N

$\hat{x}_{k-1\|k}$	One state smoothed estimate at time t_{k-1} given data up to time t_k
$x_0(u)$, $x_w(u)$, $x_\lambda(u)$, $x_B(u)$, $x_\delta(u)$	Dimensional X force stability and control derivatives expressed as a polynomial function of u e.g., $x_w(u) = x_{w_1} + x_{w_u} u + x_{w_{u^2}} u^2 + x_{w_{u^3}} u^3$
y	Denotes observation or measurement vector
$z_0(u)$, $z_w(u)$, $z_\lambda(u)$, $z_B(u)$, $z_\delta(u)$	Dimensional Z force stability and control derivatives expressed as a polynomial function of u, e.g., $z_w(u) = z_{w_1} + z_{w_u} u + z_{w_{u^2}} u^2 + z_{w_{u^3}} u^3$
α	Angle of attack $= \tan^{-1}\left(\frac{w}{u}\right)$ at c. g., deg or rad
α_V	Angle of attack vane measurement at forward boom, deg or rad, $= \tan^{-1}\left(\frac{w - q\,23}{u}\right)$
γ	Flight path angle, deg
δ_B	Power setting, inches
δ_{ES}	Longitudinal stick position, inches, (positive δ_{ES} gives positive M)
Δw	$w - w_r$
$\Delta\delta_{ES}$	$\delta_{ES} - \delta_{ES_r}$
Δq	$q - q_r$
ΔB	$B - B_r$
$\Delta\lambda$	$\lambda - \lambda_r$ — Perturbations from defined references
Δt	Sample time, sec
θ	Pitch angle defining attitude of the x body axis relative to the horizontal, deg or rad
λ	Duct tilt angle – $\lambda = 0$ when duct axes are aligned with the x body axis, deg
σ	Standard deviation or square root of variance
$\sigma_{x_i}^2$	Variance of x_i, defined by $E\left\{\left[x_i - E(x_i)\right]^2\right\}$
σ_{CR}	Standard deviation of estimates from the Cramer-Rao lower bound matrix

σ_{EM}, σ_{EQ}	Standard deviation of the parameter estimates calculated in the equations-of-motion initial estimator program
$\Phi_{k,k-1}$	Transition matrix from t_{k-1} to t_k for linearized equations of motion about a reference trajectory
$\mathcal{K}_k$	Kalman or locally iterated filter gain matrix at time t_k

Commonly Used Subscripts

a	Denotes augmented state vector, i.e., includes aircraft states and unknown parameters to be identified
r, R	Denotes reference trajectory
0	May denote initial condition at time t_0 or trim value
t	Denotes trim value
-1	Matrix inverse
$\wedge$	Estimate
T	Matrix transposition

Some Mathematical Notations

$x(z,u)$	Functional notation, i.e., x is a function of the variables z and u. Scalar or vector functions are clear from context.
$\dot{(\;)}$	$d(\;)/dt$ Derivative with respect to time
$(\;)^T$	Transpose of ( ) matrix
$tr[M]$	Trace of matrix M

$$\bar{x} \triangleq E\{x\}$$

$$\frac{\partial f(x)}{\partial x} \triangleq \begin{bmatrix} \frac{\partial f_1}{\partial x_1} & \frac{\partial f_1}{\partial x_2} & \cdots & \frac{\partial f_1}{\partial x_p} \\ \vdots & \vdots & & \vdots \\ \frac{\partial f_n}{\partial x_1} & \frac{\partial f_n}{\partial x_2} & \cdots & \frac{\partial f_n}{\partial x_p} \end{bmatrix}$$

where $f(x)$ is an n-vector functional and x is a p-vector

$\nabla_x(f) \triangleq \frac{\partial f}{\partial x} \triangleq f_x$

( ) or [ ] Used interchangeably to denote matrixes or vectors

SECTION I

INTRODUCTION

The transition of a VTOL aircraft from hovering flight to conventional flight and vice versa involves large changes in the vehicle's aerodynamic characteristics. Contemporary analyses for transition flights are based on aerodynamic data measured in a wind tunnel or on analytical prediction using the same methods as for conventional aircraft. The validity and accuracy of these techniques for VTOL aircraft have not yet been established. Parameter identification can be used to determine the validity of these techniques and at the same time yield an independent and more powerful method of data analysis.

The realization that existing parameter identification techniques were inadequate to handle the complex and unique problems of a VTOL, such as the X-22A, served as a powerful motivation for this study. At the onset of the study, no known technique had been developed that could cope with the problems of significant nonlinearities, large numbers of parameters, imperfect mathematical modeling, and noisy measurements, all of which characterize the VTOL identification problem.

The identification of V/STOL aircraft characteristics in transition flight is one of the most complex identification problems yet to be attacked. First, this complexity arises from the fact that the equations of motion are, in general, nonlinear and time varying over most of the transition range, in contrast to the equations for a conventional aircraft, which are frequently well represented by linear, constant coefficient "small perturbation" approximations. Secondly, a more fundamental difficulty is the relative uncertainty in formulating the V/STOL equations of motion due to the complex interaction and incomplete definition of propulsive and aerodynamic forces and moments. A large number of parameters is usually required to describe these forces and moments. For example, in a previous study (Reference 1), an identification model was obtained using a Taylor series expansion about a reference trajectory; unfortunately, even with a low order (third order) Taylor's series expansion, and with physical arguments to eliminate negligible derivatives, there remain in the model more than 60 derivatives which vary as a function of the thrust vector angle. Thus, we are faced with an identification problem of a nonlinear, time varying system having a large number of parameters. Finally, measurements of the dynamic motions of the vehicle are usually corrupted with noise. Although this is a problem common to all types of aircraft, it appears to be more acute for V/STOL aircraft. Based on available flight records, the noise levels in the measurements of the V/STOL aircraft motions are significantly higher than those of conventional aircraft.

The particular features of the V/STOL identification problem may therefore be summarized as:

1. nonlinear dynamic motions, represented by
2. large numbers of parameters, containing
3. significant modeling errors and whose
4. measurements are contaminated with noise.

In spite of the complicated nature of this V/STOL parameter identification problem, some practical identification techniques must be developed. Clearly, the parameter identification technique for the V/STOL aircraft must be capable of:

1. determining, to the best possible accuracy, the numerical values of the unknown parameters, i.e., stability and control derivatives in the mathematical model chosen, and
2. detecting the dynamic modeling errors to improve the mathematical model which better represents the V/STOL aircraft dynamics.

Although the sec   apability is occasionally overlooked, it becomes an important part of the identification problem for V/STOL aircraft and will be discussed at length later. For conventional aircraft, the form of the equations is generally well known, and the first capability becomes of primary importance. Before the advent of the digital computer, the usual method of obtaining numerical values of the parameters was through analog matching techniques, a method which still finds use today. With the advent of digital computers, the capability to handle large amounts of data in equations that might need to be solved numerically became feasible. This capability led first to so-called "equation error" techniques, such as the well known classical least squares, or equations-of-motion method, and then to more advanced "response-error" techniques, such as quasilinearization, Newton-Raphson, conjugate gradient, and so on.

The merits or debits of all these techniuqes are a function of the quality of their parameter estimates in the presence of various types of uncertainty, or noise. For the aircraft problem, as well as most others, there are two types of noise that are of importance:

1. Measurement noise. The parameters of the mathematical model are estimated in all cases by making use of measurements of the state and/or accelerations of the system over a time span. Since no measurement is perfect, these measurements will have uncertainties, or noise, which will affect the parameter estimates.
2. Process noise. Process noise may, in general, consist of unknown random inputs to the system (e.g., gusts, fuel change) and errors in the mathematical model (e.g., neglecting a stability derivative in the model).

Essentially, equation-error techniques give biased estimates in the presence of measurement noise, and pure response-error techniques give biased estimates for nonlinear systems in the presence of process noise. Although response-error techniques such as quasilinearization can be shown to exhibit certain advantages over equation-error techniques, they do not have the second capability of detecting errors in the assumed model, which is an important part of the V/STOL identification problem.

With the knowledge of the limitations given above, the present study of V/STOL identification techniques was undertaken. Without going into the mathematical details at this point, the identification technique developed by CAL essentially consists of a three-stage process:

1. Initial estimates of the parameters, and their variances, in the assumed equations are obtained by a method that is essentially an equation-error technique. Since the variances obtained by this method do not adequately represent estimation errors, an improved variance estimate is obtained by a Cramer-Rao lower bound computation, thereby facilitating a better initialization of the locally iterated filter-smoother algorithm.

2. An extended Kalman filter, utilizing a "local iteration" or "multi-correction" algorithm, is used to refine the initial estimates of the parameters. Although the extended Kalman filter gives biased estimates when applied to a nonlinear problem, which is inherent to parameter identification, it can be shown that the multi-correction scheme reduces biases due to nonlinearities by improving the reference trajectory between data points.

3. A fixed-point smoothing algorithm, which actually works in conjunction with the multi-corrector at each data point, is used to further refine the parameter estimates and separate out the effects of process noise. This step is extremely important as a first attempt at determining the mathematical modeling error, as well as improving the parameter estimates. Also, a more accurate variance computation of the parameter estimate is obtained.

These techniques are fairly general and are, theoretically speaking, applicable to the identification of unknown parameters, initial state, and unknown forcing functions of a wide class of nonlinear dynamic systems. As such, these techniques may have potential applicability to identification of stability and control parameters of many flight vehicles other than V/STOL aircraft, especially for these vehicles in large motion such as in spins and post-stall gyrations. However, as the number of unknown parameters increases, the computer time increases rapidly, and therefore the analysis of a large amount of data for systems with a large number of unknown parameters may not be economically feasible.

This report is organized as follows: Section II discusses the selection of a mathematical model to represent the X-22A aircraft and formulates the identification problem. A discussion of identification techniques is given in Section III. Section IV discusses the identifiability of the parameters. The development of final identification techniques for the V/STOL aircraft and numerical verification are presented in Sections V and VI, respectively. Applications of these advanced techniques to experimental data are given in Section VII. Finally, the conclusions and recommendations are given in Sections VIII and IX, respectively.

SECTION II

MATHEMATICAL MODEL AND FORMULATION OF THE PROBLEM

In this section, the formulation of the equations of motion used to represent the X-22A dynamics will first be discussed. With the determination of a mathematical model of the X-22A aircraft and the definition of the data which will be available, the problem of identifying the stability and control parameters of the X-22A aircraft will then be formulated.

2.1 Mathematical Model

The general description of a VTOL aircraft such as the X-22A poses a fundamental difficulty. In general, VTOL aircraft exhibit highly nonlinear behavior, the result of complex interactions of aerodynamic and propulsive forces and moments during transition maneuvers. In particular, the dynamic motions in the plane of symmetry exhibit pronounced nonlinearities during transitions, and, as such, pose the most difficult modeling problem. It is the purpose of the formulation to define a mathematical model of the plane-of-symmetry dynamics that is simple enough to facilitate the determination of its unknown parameters yet complex enough to include the paramount features of the VTOL aircraft in transition. Specifically, the task is to determine a representation of $\mathscr{x}$, $\mathscr{z}$, $\mathscr{m}$ in the following equations of motion, written with respect to a body-fixed axis system:

$$\begin{aligned} \dot{u} + qw + g\sin\theta &= \mathscr{x} \\ \dot{w} - qu - g\cos\theta &= \mathscr{z} \\ \dot{q} &= \mathscr{m} \end{aligned} \qquad (2.1)$$

where

$q = \dot{\theta}$

$\mathscr{x} = \dfrac{X}{\text{mass of the aircraft}}$

$\mathscr{z} = \dfrac{Z}{\text{mass of the aircraft}}$

$\mathscr{m} = \dfrac{M}{\text{pitching moment of inertia, } I_y}$

X, Z = aerodynamic (including thrust) forces along body axes, forward and downward respectively

M = aerodynamic pitching moment

The aerodynamic forces and moment (x , z , m) in these equations are functions of the flight variables and the control motions. For a VTOL aircraft such as the X-22A, there are three independent control variables: thrust inclination (λ), thrust magnitude (B), and pitching moment magnitude (δ_{ES}). Excluding unsteady aerodynamics, then, we may write:

$$
\begin{aligned}
x &= x(u, w, q, \lambda, B, \delta_{ES}) = \dot{u} + qw + g \sin\theta \\
z &= z(u, w, q, \lambda, B, \delta_{ES}) = \dot{w} - qu - g \cos\theta \\
m &= m(u, w, q, \lambda, B, \delta_{ES}) = \dot{q} \\
q &= \dot{\theta}
\end{aligned}
\tag{2.2}
$$

As can be seen, there are four equations in seven (7) unknowns: u , w , q , θ , λ , B , δ_{ES} . Therefore, three variables must be specified to determine the other four. For example, if an attainable <u>reference trajectory</u> $w(t)$, $u(t)$, $\theta(t)$ is specified, then $q(t)$, $\lambda(t)$, $B(t)$, $\delta_{ES}(t)$ may be determined. In this example, $u(t)$, $w(t)$ may be chosen to be uniformly accelerating (or decelerating) with $\theta(t) = 0$; for the X-22A however, $\lambda(t)$ is somewhat constrained, and such a trajectory might not be achievable.

For the X-22A, it is reasonable to specify $\dot{\lambda}(t)$ (usually as a constant rate of change of duct angle), $\gamma(t) = \theta(t) - \alpha(t)$ and $\theta(t)$. In this case, $u(t)$, $q(t)$, $B(t)$, $\delta_{ES}(t)$ may then be determined for the reference trajectory. One might then be tempted to expand equations (2.2) in a Taylor series about this determined trajectory, as was done in Reference 1. There, the specifications were: $\gamma(t) = 0$, $\dot{\lambda} = -3$ deg/sec and $\theta(t)$ varying between 0° at $\lambda = 90°$ to the value required for level flight at $\lambda = 0°$. Then the determined trajectory may be written as $\underline{r_0}(\lambda) = \left[u_0(\lambda), w_0(\lambda), q_0(\lambda), B_0(\lambda), \delta_{ES}(\lambda)\right]^T$ and the x -force may be expanded as:

$$
x(\lambda, \underline{r}) \approx \sum_{j=0}^{k} \frac{1}{j!} \left[\left(\sum_{i=1}^{5} \Delta r_i \frac{\partial}{\partial r_i} \right)^j x(\lambda, \underline{r}) \right]_{\lambda, \underline{r_0}}
\tag{2.3}
$$

where $\Delta \underline{r} = r - \underline{r_0}(\lambda)$

$r_i = u, w, q, B, \delta_{ES}$

Unfortunately, such a representation has several drawbacks. The first is that a large number of parameters is required for an adequate representation of the x force. For example, a third-order expansion (K=3) results in more than 60 derivatives at each duct incidence, and if a polynomial fit of the λ variation is assumed, then more than 240 parameters would need to be identified. The second, more fundamental, difficulty with this approach is its strong local property. As we have seen, $u_0(t), w_0(t)$ and $B_0(t)$ for the reference trajectory are determined by the specification of $\lambda_0(t)$, $\gamma_0(t)$ and $\theta_0(t)$. The choice of $\lambda_0(t)$ indicates whether the reference is a takeoff (accelerating) or landing (decelerating) trajectory. For the X-22A aircraft, the value of $B_0(t)$ and $u_0(t)$, for a given duct angle, are widely different for accelerating or decelerating transitions.* Since the stability derivatives in (2.3) are strong functions of both u_0 and B_0, this in turn means that the derivatives determined by expansion about a takeoff trajectory are invalid for a decelerating trajectory. Hence, (2.3) cannot apply to both. A somewhat more general formulation is required.

As the initial step toward this formulation, let us draw an analogy with the "quasi-steady" representation of the aerodynamics of a conventional airplane. Consider equations (2.2) in equilibrium, level, steady flight. In this case, $\gamma=0$, $\dot{u}=\dot{w}=\dot{q}=\dot{\theta}=0$, and we are left with three equations (since $q=0$) in five unknowns (u, $\theta=\alpha$, λ, δ_{ES}, B). Therefore, two of the unknowns must be specified to determine the other three. A logical choice is u and λ, and thus:

$$
\begin{aligned}
\theta &= \theta(u,\lambda) \\
B &= B(u,\lambda) \\
\delta_{ES} &= \delta_{ES}(u,\lambda)
\end{aligned}
\qquad (2.4)
$$

Note that these equations are analogous to the equilibrium relationships for a conventional airplane, where the controls and angle of attack are specified as a function of the single variable u, but that the additional control (λ) now makes $\theta=\alpha$, B (or power), and δ_{ES} functions of two variables. At a

* This difference arises from the fact that an accelerated transition requires a larger thrust (B) to accelerate, and, since more of the weight is then supported by thrust rather than lift, a smaller velocity and angle of attack.

fixed duct angle, clearly, they are directly comparable.

Near equilibrium flight, then, the stability and control derivatives may be written as a function of the two variables u and λ if the dependence on the other variables is nearly linear (as it is for a conventional airplane). Since this is not a perturbation about a prescribed trajectory, but is instead a general quasi-steady representation of the aerodynamics, it should be applicable to both accelerated and decelerated transitions near equilibrium. Note, however, that equations (2.5) are now nonlinear:

$$\begin{aligned} x &= x_0(u,\lambda) + x_w(u,\lambda)w + x_{\delta_B}(u,\lambda)\delta_B + x_{\delta_{ES}}(u,\lambda)\delta_{ES} \\ z &= z_0(u,\lambda) + z_w(u,\lambda)w + z_{\delta_B}(u,\lambda)\delta_B + z_{\delta_{ES}}(u,\lambda)\delta_{ES} \\ m &= m_0(u,\lambda) + m_w(u,\lambda)w + m_q(u,\lambda)q + m_{\delta_B}(u,\lambda)\delta_B + m_{\delta_{ES}}(u,\lambda)\delta_{ES} \end{aligned} \tag{2.5}$$

To determine the validity of this model, time histories for a portion of a takeoff transition from the full "global" digital computer program* were compared with those from the model. The stability derivatives were assumed to be represented by polynomials in u and λ :

$$\begin{aligned} i\,(u,\lambda) &= \vec{u}^{\,T} A_i \vec{\lambda} \\ \vec{u}^{\,T} &= (1,\ u,\ u^2,\ u^3) \\ \vec{\lambda} &= (1,\ \lambda,\ \lambda^2,\ \lambda^3)^T \\ A_i &= \text{a 4x4 constant matrix} \\ i &= x_w,\ x_{\delta_B},\ \ldots,\ m_{\delta_{ES}} \end{aligned} \tag{2.6}$$

* A complete set of six-degree-of-freedom nonlinear equations of motion with available aerodynamic data of the X-22A were programmed on CAL's IBM 360/65 computer (see Reference 1). These equations will be called the "global" program henceforth.

The terms $x_o(u,\lambda)$, $z_o(u,\lambda)$, and $m_o(u,\lambda)$ in (2.4) are computed by:

$$\begin{aligned}
x_o(u,\lambda) &= g\sin\theta_o(u,\lambda) - \left[x_w(u,\lambda)w_o(u,\lambda) + x_B(u,\lambda)B_o(u,\lambda) + x_{\delta_{ES}}(u,\lambda)\delta_{ES_o}(u,\lambda)\right] \\
z_o(u,\lambda) &= -g\cos\theta_o(u,\lambda) - \left[z_w(u,\lambda)w_o(u,\lambda) + z_B(u,\lambda)B_o(u,\lambda) + z_{\delta_{ES}}(u,\lambda)\delta_{ES_o}(u,\lambda)\right] \qquad (2.7) \\
m_o(u,\lambda) &= -\left[m_w(u,\lambda)w_o(u,\lambda) + m_B(u,\lambda)B_o(u,\lambda) + m_{\delta_{ES}}(u,\lambda)\delta_{ES_o}(u,\lambda)\right]
\end{aligned}$$

Here, $w_o(u,\lambda)$, $B_o(u,\lambda)$, $\delta_{ES_o}(u,\lambda)$ are the trim (equilibrium) values of vertical velocity, collective pitch, and longitudinal stick position. These trim values, and the derivatives $x_w(u,\lambda)$, etc. were obtained from the digital computer program with global aerodynamics, with the polynomial representation being achieved by a least-squares fit. The particular transition chosen was $\dot{\lambda} = -3$ deg/sec from $\lambda = 30°$ to $\lambda = 15°$, a 0.4 inch longitudinal stick step, and a ramp collective input. These responses of the model matched those of the global computer program quite well, thereby indicating the validity of the model (2.5).

Unfortunately, when duct angle is changing, the number of parameters in this model is still much too high for efficient identification. Also, although the model was shown to be valid for a transition of moderate acceleration, it probably wouldn't be valid for transitions far off the equilibrium condition. This model, then, is best suited to provide an accurate representation of the X-22A dynamics at fixed duct incidence, which reduces the number of parameters to be identified by a factor of four. With λ fixed, equations (2.5) become:

$$\begin{aligned}
\dot{u} + qw + g\sin\theta &= x_o(u) + x_w(u)w + x_B(u)B + x_{\delta_{ES}}(u)\delta_{ES} \\
\dot{w} - qu - g\cos\theta &= z_o(u) + z_w(u)w + z_B(u)B + z_{\delta_{ES}}(u)\delta_{ES} \qquad (2.8) \\
\dot{q} &= m_q(u)q + m_o(u) + m_w(u)w + m_B(u)B + m_{\delta_{ES}}(u)\delta_{ES}
\end{aligned}$$

Equations (2.8) were verified by comparing time histories as previously described. At $\lambda = 30°$, the model time histories were an excellent match to those of the global program when the stability derivatives were represented by second- and third-order polynomials in u, and the matches were only slightly degraded by using only first-order polynomials. This mathematical model, then, may be used for identification of fixed-duct data.

As we have seen, both a pure perturbation about an accelerated reference trajectory (Equation 2.3) and a quasi-steady representation around equilibrium (Equations 2.5) do not yield equations that are tractable for identification. We have, however, obtained a model that is valid and useful at fixed duct incidence (Equations 2.8), and our purpose now is to obtain a similar model, by a combination of perturbation expansion and quasi-steady representation, that will be valid for transitions.

Consider an ideal level transition with zero pitch attitude. This is feasible from a duct angle above 15 degrees; and, in fact, this technique was used in many occasions during Phase I of the Military Preliminary Evaluation of the X-22A (Reference 2). Upon constraining the transition to be at constant flight path angle (zero in this case), and zero pitch attitude, and choosing a given $\lambda(t)$, it can readily be shown that a unique $u-\lambda$ profile exists from Equations (2.2) and (2.4). We may therefore choose the following references for slow and fast transitions: $\theta = 0$, γ = constant and

$\dot{\lambda} \approx$ 0 (equilibrium - slow conversion and reconversion)

$\dot{\lambda} =$ - 5 deg/sec - fast conversion

$\dot{\lambda} =$ 5 deg/sec - fast reconversion

Figure 2-1 shows the $u-\lambda$ profile for the slow transition with $\theta = \gamma = 0$. The solid line represents the profile obtained from the digital program with global aerodynamics and the "circles" are taken from Reference 3. The profiles for fast conversion and fast reconversion can be obtained from the digital program or from the flight records in Reference 2.

We may now expand Equations (2.5) about the chosen reference trajectory. Note that the unique $u-\lambda$ profile means that the coefficients are now functions of only u or λ ; we choose to make them functions of u so that, at fixed duct incidence, they will reduce to Equations (2.8). Retaining only first-order terms in the state and control variables (with the exception of)
Equations (2.5) therefore become (after substitution into 2.1):

$$
\begin{aligned}
\dot{u} + qw + g\sin\theta &= x_{o_R}(u) + x_w(u)\Delta w + x_B(u)\Delta B + x_{\delta_{ES}}(u)\Delta\delta_{ES} + x_\lambda(u)\Delta\lambda \\
\dot{w} - qu - g\cos\theta &= z_{o_R}(u) + z_w(u)\Delta w + z_B(u)\Delta B + z_{\delta_{ES}}(u)\Delta\delta_{ES} + z_\lambda(u)\Delta\lambda \qquad (2.9)\\
\dot{q} &= m_{o_R}(u) + m_q(u)\Delta q + m_w(u)\Delta w + m_B(u)\Delta B + m_{\delta_{ES}}(u)\Delta\delta_{ES} + m_\lambda(u)\Delta\lambda
\end{aligned}
$$

(Note: Here the subscript R denotes the reference trajectory and $\Delta w \triangleq w - w_R(u)$, etc.)

The following comments concerning these equations are in order:

1. Although we have been forced to return to an expansion about a reference trajectory as in Equations (2.3), the resulting Equations (2.9) result in fewer parameters to be identified.
2. Equations (2.9) reduce to (2.8) when $\Delta\lambda = 0$ (fixed duct incidence).
3. Equations (2.9) also have fewer parameters to identify than do Equations (2.5), and are applicable to both slow and fast transitions.
4. Equations (2.9) reduce to linear equations with time-varying coefficients if only first-order perturbations in u are retained (see Appendix A).
5. The fact that the reference transition may not be at constant pitch attitude throughout $(q_R \neq 0)$ is accounted for by $m_{o_R}(u)$.

Equations (2.9) then, were adopted as the mathematical model of the X-22A dynamic motions in transition, and Equations (2.8) were adopted at fixed duct incidence. These equations are now used to formulate the parameter identification problem.

2.2 Formulation of the Problem

The uncoupled longitudinal equations of motion for the X-22A in transition flight as described by Equation (2.9) are now used as the mathematical model for the X-22A aircraft for the development of the identification techniques. Recall that the derivatives in Equation (2.9) are expressed as third degree polynomials in forward speed u, i.e.,

$$\left.\begin{array}{l} m_{o_g}(u) \triangleq a_1^T \vec{u} \\ m_q(u) \triangleq a_2^T \vec{u} \\ \hline m_\lambda(u) \triangleq a_6^T \vec{u} \\ \hline g_\lambda(u) \triangleq a_{16}^T \vec{u} \end{array}\right\} \quad (2.10)$$

where

$$\vec{u} = (1, u, u^2, u^3) \quad (2.11)$$

Define the parameter vector p to be

$$p = (a_1^T, a_2^T, \ldots, a_{16}^T)^T \quad (2.12)$$

and the state x and the control vector m to be

$$x = (q, \theta, u, w)^T \quad (2.13)$$

$$m = (\Delta\lambda, \Delta B, \Delta\delta_{ES})^T \quad (2.14)$$

respectively. In view of the fact that the model (2.9) is by no means perfect, dynamic modeling errors and possible unknown external excitations are simulated by unknown forcing inputs, $w(t)$. The equations of motion (2.9) may now be alternatively written as:

$$\dot{x} = f(x, p, m) + g_1 w(t), \qquad x(0) = x_0 \quad (2.15)$$

where x_0 is the unknown initial condition, $g_1 = I_4$,

$$f(x,p,m) = \begin{bmatrix} m_0(u) + m_w(u)\Delta w + m_q(u)\Delta q + m_\lambda(u)\Delta\lambda + m_B(u)\Delta B + m_{\delta_{ES}}(u)\Delta\delta_{ES} \\ \dot{\theta} \\ x_0(u) + x_w(u)\Delta w + x_\lambda(u)\Delta\lambda + x_B(u)\Delta B + x_{\delta_{ES}}(u)\Delta\delta_{ES} - qw - g\sin\theta \\ z_0(u) + z_w(u)\Delta w + z_\lambda(u)\Delta\lambda + z_B(u)\Delta B + z_{\delta_{ES}}(u)\Delta\delta_{ES} + qu + g\cos\theta \end{bmatrix} \tag{2.16}$$

and

$$w(t) = \left[w_1(t)\ ,\ 0\ ,\ w_3(t)\ ,\ w_4(t) \right]^T \tag{2.17}$$

Consideration has also been given to the simulation of random gusts.*
Denote, for convenience, the acceleration vector to be

$$h_1(x, \dot{x}) \triangleq \begin{bmatrix} n_x \\ n_z \\ \dot{q} \end{bmatrix} = \begin{bmatrix} \frac{1}{g}(\dot{u} + qw) + \sin\theta \\ \frac{1}{g}(\dot{w} - qu) - \cos\theta \\ \dot{q} \end{bmatrix} \tag{2.18}$$

---

* If gusts are considered, g_1 is the gust effectiveness matrix and $w(t)$ is a gust vector, i.e.,

$$g_1 = g_1(x,p,m) = \begin{bmatrix} m_q(u) & 0 & m_u(u) & m_w(u) \\ 0 & 0 & 0 & 0 \\ 0 & 0 & x_u(u) & x_w(u) \\ 0 & 0 & z_u(u) & z_w(u) \end{bmatrix} , \quad w(t) = \begin{bmatrix} q_g \\ 0 \\ u_g \\ w_g \end{bmatrix}$$

where

$$\begin{aligned} m_u &= \vec{u}_d^{\,T} \left[a_1 + \Delta w\, a_2 + \Delta q\, a_3 + \Delta B\, a_4 + \Delta\delta_{ES}\, a_5 + \Delta\lambda\, a_6 \right] \\ x_u &= \vec{u}_d^{\,T} \left[a_7 + \Delta w\, a_8 + \Delta B\, a_9 + \Delta\delta_{ES}\, a_{10} + \Delta\lambda\, a_{11} \right] \\ z_u &= \vec{u}_d^{\,T} \left[a_{12} + \Delta w\, a_{13} + \Delta B\, a_{14} + \Delta\delta_{ES}\, a_{15} + \Delta\lambda\, a_{16} \right] \\ \vec{u}_d^{\,T} &= (0\ ,\ 1\ ,\ 2u\ ,\ 3u^2) \end{aligned}$$

We may now formulate the problem of identifying V/STOL aircraft parameters, the unknown initial state, and the unknown forcing inputs as follows:

Given: (a) the nonlinear dynamic system (2.15)

(b) a set of discrete measurements for the state and the accelerations, which are corrupted with measurement noise $v_1(t_i)$, and $v_2(t_i)$, respectively.

$$\left.\begin{aligned} z_1(t_i) &= x(t_i) + v_1(t_i) \\ z_2(t_i) &= h_1(x(t_i), \dot{x}(t_i)) + v_2(t_i) \end{aligned}\right\} \quad i = 1, 2, \ldots, N \qquad \begin{aligned} &(2.19a)^* \\ &(2.19b) \end{aligned}$$

(c) a set of discrete measurements for the control vector

$m(t_i)$, $i = 1, 2, \ldots, N$.

Find: the unbiased, minimum variance (efficient) estimates for x_0, p, and $w(t_i)$, $i = 1, 2, \ldots, N$

A few comments concerning the above formulation are now in order:

(1) By annexing the parameter vector p to the state vector x, i.e.,

$$x_a = \begin{bmatrix} x \\ \hdashline p \end{bmatrix} \tag{2.20}$$

---

* For current instrumentation on the X-22A, there is no w sensor. Consequently, measurements from the α vane sensor are utilized. In this case, the measurements are nonlinear functions of the states: $\alpha_v = \tan^{-1} \frac{w - q\ell}{u}$ + noise, where α_v is the α vane measurement. The vane is located at ℓ ft ahead of c.g. of the aircraft.

it is readily seen that Equations (2. 15) and (2. 19) can be rewritten as

$$x_a = \left[\begin{array}{c} f(x, p, m) \\ \hline 0 \end{array}\right] + \left[\begin{array}{c} w(t) \\ \hline 0 \end{array}\right] \qquad , x_a(0) = x_{a_0} \tag{2.21a}$$

$$y \triangleq \left[\begin{array}{c} z_1 \\ \hline z_2 \end{array}\right] = \left[\begin{array}{c} x \\ \hline h(x, p, m) \end{array}\right] + \left[\begin{array}{c} v_1 \\ \hline v_2 + g_2 w \end{array}\right] \tag{2.21b}$$

where

$$h(x, p, m) = \begin{bmatrix} x_0(u) + x_w(u)\Delta w + x_{\delta_{ES}}(u)\Delta\delta_{ES} + x_\theta(u)\Delta\theta + x_\lambda(u)\Delta\lambda \\ z_0(u) + z_w(u)\Delta w + z_{\delta_{ES}}(u)\Delta\delta_{ES} + z_\theta(u)\Delta\theta + z_\lambda(u)\Delta\lambda) \\ m_0(u) + m_w(u)\Delta w + m_{\delta_{ES}}(u)\Delta\delta_{ES} + m_\theta(u)\Delta\theta + m_q(u)\Delta q + m_\lambda(u)\Delta\lambda \end{bmatrix}$$

$$g_2 = \begin{bmatrix} 0 & 0 & 1 & 0 \\ 0 & 0 & 0 & 1 \\ 1 & 0 & 0 & 0 \end{bmatrix}$$

From Equation (2. 21) we see that the problem stated above can now be restated as follows: Given (a), (b), and (c), find the best (efficient) estimates of x_{a_0} and $w(t_i)$, $i = 1, 2, \ldots, N$.

(2) Regardless of the statistical properties (or more precisely, the conditional probability density function)

$$f(x_{a_0} | y_1, y_2, \ldots y_N) \triangleq f(x_{a_0} | Y(N)) \tag{2.22a}$$

and

$$f(w_i | Y(N)) \ , \ i = 1, 2, \ldots N \tag{2.22b}$$

a best (efficient) estimate for the above problem is the conditional expectation of (2. 22a) and (2. 22b), i.e.,

$$\hat{x}_{a_0|N} = E\left\{f(x_{a_0} | Y(N))\right\} \tag{2.23a}$$

$$w_{i|N} = E\left\{f(w_i | Y(N))\right\} \tag{2.23b}$$

This is shown in Appendix G.

(3) If the statistical properties of x_{a_0} , $w(t)$, and $v(t) = \left[v_1^T(t) \,\vdots\, v_2^T(t) + [g_2 w(t)]^T \right]^T$ are known, and if they are normally distributed such that

$$E\{x_{a_0}\} = \bar{x}_{a_0}$$
$$E\{(x_{a_0} - \bar{x}_{a_0})(x_{a_0} - \bar{x}_{a_0})^T\} = P_{a_0}$$

and $w(t)$ and $v(t)$ are zero mean with covariance matrices

$$E\{w(t)\, w^T(\tau)\} = Q(t)\,\delta(t-\tau)$$
$$E\{v(t)\, v^T(\tau)\} = R(t)\,\delta(t-\tau)$$
$$E\{w(t)\, v^T(\tau)\} = C(t)\,\delta(t-\tau)$$

respectively, then it has been shown (References 4 - 7) that the maximum likelihood (Bayesian) fixed-interval smoothed estimate of $x_a(t)$ for $0 \le t \le t_N$ given the data $y(t)$, $0 \le t \le t_N$ is equivalent to minimizing the cost functional

$$J = \frac{1}{2}\left\{ \| x_{a_0} - \bar{x}_{a_0} \|^2_{P^{-1}_{a_0}} + \int_0^{t_N} \| z(t) \|^2_{N^{-1}} \, dt \right\} \tag{2.24}$$

with respect to $w(t)$, $0 \le t \le t_N$, subject to the constraint in Equation (2.21a), where

$$z(t) \triangleq \left[\begin{array}{c} \begin{bmatrix} w(t) \\ \hline 0 \end{bmatrix} \\ \hline y - h(x_a, m) \end{array} \right] \tag{2.25a}$$

$$N \triangleq \begin{bmatrix} \bar{Q}(t) & C(t) \\ C'(t) & R(t) \end{bmatrix} , \quad \bar{Q} \triangleq \left[\begin{array}{c|c} Q & 0 \\ \hline 0 & 0 \end{array} \right] \tag{2.25b}$$

and $\|x\|^2_A \triangleq x^T A x$.

It should be emphasized that unless (2.21) is linear, the fixed-point smoothed estimate $\hat{x}_{a_0|N}$ as stated in comment 2 does not necessarily lie on the fixed-interval estimate as formulated above at time $t = 0$. This has been pointed out by Cox in Reference 5.

(4) As will be discussed later in Section V, the a priori information P_{a_0} for the unknown parameter is almost always lacking. If in addition to the lack of the a priori information P_{a_0}, the process noise is also absent, then, for the discrete measurements contaminated with Gaussian noise where

$$E\left\{ v(t_i) \right\} = 0$$

$$E\left\{ v(t_i)\, v(t_j)^T \right\} = R_i\, \delta_{ij}$$

the likelihood function becomes

$$\ln f(Y(N) \mid x_{a_0}) = + C\ \frac{1}{2} \sum_{i=1}^{N} \left\| y_i - h(x_{a_i}, m_i) \right\|^2_{R_i^{-1}} \qquad (2.26)$$

where C is some positive constant independent of x_{a_0}.

Thus, the classical (non-Bayesian) maximum likelihood estimate for x_{a_0} has the same cost functional as what is commonly called a measurement (or output) error method. The latter will be discussed in the next section.

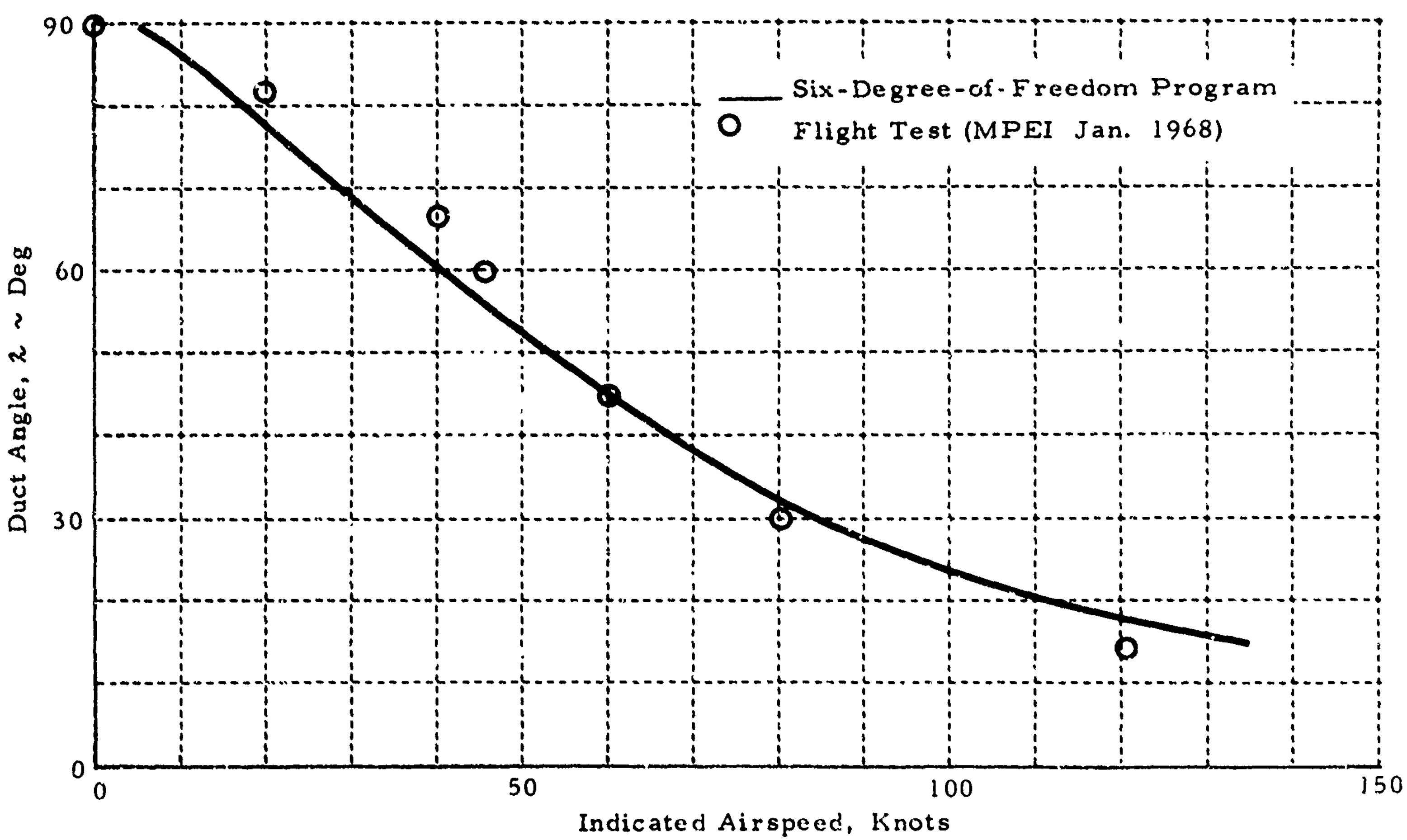

Figure 2-1 Constant Attitude Slow Level Transition - X-22A (θ 0)

SECTION III

REVIEW OF IDENTIFICATION TECHNIQUES

Parameter identification has been playing one of the major roles in the field of physical science and engineering. Literally hundreds of papers and reports have been devoted to this subject. Since the V/STOL parameter identification problem, as formulated in the preceding section, is basically a nonlinear estimation problem, attention was therefore focused on those methods which are directly applicable to nonlinear systems or which can readily be extended to nonlinear systems.

Perhaps due to poor communication among the various authors, much work has been duplicated and triplicated; each author often has coined a different name for basically the same technique. For an uninitiated engineer it would be a big job indeed to sort out which technique is the most suitable for his problem. The first important point, then, is to recognize that the many available parameter identification techniques may be classified into three major groups, as follows:

1. Equation-error methods (or process-error methods),
2. Measurement-error methods (or response-error methods), and
3. Methods treating both measurement and process errors.

As shown later in the report, equation-error techniques give biased estimates in the presence of measurement noise, but they are noniterative and hence the simplest for parameter identification from a computational point of view. Furthermore, this group of methods is equally applicable to both linear and nonlinear systems. The response-error methods are iterative. Although these methods give unbiased estimates in the absence of process noise, they generally produce biased estimates of the unknown parameters in the presence of process noise. Again, these methods are equally applicable to linear and nonlinear systems. The third group, which treats both the measurement and process errors, has the capability of obtaining unbiased estimates in the presence of process noise and of estimating the unknown forcing inputs (or the process errors), thus providing an indication of the errors in the dynamic model assumed.

Although the methods in the third group are undoubtedly the most suitable for use in parameter identification of V/STOL aircraft because of the capability of detecting the modeling errors, it is felt appropriate at this point to examine, in some depth, the basic characteristics of all the three groups as stated above. In was with a clear understanding of the merits and debits of these available techniques that a final technique for the parameter identification of V/STOL aircraft was developed as discussed in Section V.

3.1 Equation-Error Methods

The equation-error methods for aircraft parameter identification may be conveniently classified into two categories:

(a) Methods which use the acceleration measurements in addition to the state variable measurements.

(b) Methods which use only the state variable measurements.

Under category (a), only the so-called "equations-of-motion (error) method" (References 8, 9, and 10) was considered here. Under category (b), three methods were studied. They are:

(i) Modified spline function method (Reference 11).

(ii) Polynomial estimator.

(iii) Denery's method (Reference 12).

There are many more methods of the integral transform variety available in this category; however, since frequency domain techniques are, generally speaking, not readily extended to nonlinear systems, the integral transform methods were not considered in this report. Some statistical properties of the equation error methods are discussed in Appendix B.

Equations-of-Motion (Error) Method (References 8-10)

This method was originally developed in CAL's Flight Research Department for conventional airplane identification. It is essentially a classical linear regression method and a general discussion of the method is given below as applied to VTOL aircraft identification.

From Equation (2.15) and (2.19), i.e.,

$$\dot{x} = f(x, p, m) + w(t) \tag{2.15}$$

$$z_1 = x + v_1(t) \tag{2.19a}$$

$$z_2 = h_1(x, \dot{x}) + v_2(t) \tag{2.19b}$$

where
x = the state vector for our problem, (4-vector)
p = the unknown parameter vector (q-vector)
z_1 = state measurements (4-vector)
z_2 = measurement of the accelerations (3-vector)
m = control vector (r-vector)
v_1, v_2 = error vectors

It is desired to estimate the parameter vector p that is the best fit to Equation (2.15), in the least squares sense, using a set of data

$$\begin{aligned} Z_1(N) &= \left[z_{11}(t_0), z_{11}(t_1), \ldots, z_{11}(t_N); \ldots; z_{14}(t_0), z_{14}(t_1), \ldots z_{14}(t_N)\right]^T \\ Z_2(N) &= \left[z_{21}(t_0), z_{21}(t_1), \ldots, z_{21}(t_N); \ldots; z_{23}(t_0), z_{23}(t_1), \ldots z_{23}(t_N)\right]^T \\ M(N) &= \left[m_1(t_0), m_1(t_1), \ldots, m_1(t_N); \ldots; m_r(t_0), m_r(t_1), \ldots m_r(t_N)\right]^T \end{aligned} \tag{3.1}$$

Since p enters into the vector-valued function f linearly, the substitution of the above set of data (3.1) into (2.15) results in a set of $3(N+1)$ linear equations

$$Z_2(N) = A_N p + w(N) \tag{3.2}$$

where A_N is a $3(N+1) \times q$ constant matrix consisting of data $Z_1(N)$ and $M(N)$ and $w(N) \triangleq \left[w_1(t_0), w_2(t_0), \ldots, w_1(t_N); \ldots; w_3(t_0), w_3(t_1), \ldots, w_3(t_N)\right]^T$.

Let us assume that A_N is non-stochastic. Actually, A_N is obviously stochastic because $Z_1(N)$ is a random vector for $v_1 \neq 0$. Therefore, our assumption here is only an approximation. For details see Appendix B. Let us further assume that

$$E\{w(N)\} = 0$$

$$\operatorname{cov}\{w(N)\} = \sigma^2 I_{3(N+1)}$$

Then the problem posed above becomes a simple classical linear regression problem with non-stochastic regressor (A_N). The least square solution to (3.2) is

$$\hat{p} = (A_N^T A_N)^{-1} A_N^T Z_2(N) \tag{3.3}$$

and the covariance of $\hat{p}$ is

$$\operatorname{cov}(\hat{p}) = \sigma^2 (A_N^T A_N)^{-1} \tag{3.3a}$$

Since σ^2 in the above equation is usually not known in practice, it has to be first estimated in order to obtain a covariance of the estimated parameter using (3.3a). To do this, let us consider the error vector of the fit.

$$\hat{\epsilon} = Z_2(N) - \hat{Z}_2(N)$$

where $\hat{Z}_2(N) = A_N(\hat{p})$. Thus,

$$\hat{\epsilon} = A_N(p - \hat{p}) + w(N)$$

Using Equation (3.3), it is readily shown that the above equation becomes

$$\hat{\epsilon} = \left[I - A_N (A_N^T A_N)^{-1} A_N^T\right] w(N)$$

$$= M w(N)$$

where $M \triangleq I - A_N (A_N^T A_N)^{-1} A_N^T$. It is easy to show that $M = M^T$ and $M^2 = M$, and hence the error sum of squares becomes

$$\hat{\epsilon}^T \hat{\epsilon} = w(N)^T M^T M w(N) = w^T(N) M w(N) \tag{3.3b}$$

Thus, since M is non-stochastic by the virtue of the assumption that A_N is non-stochastic and since the trace operator is a linear operator, it can readily be shown that

$$E\left\{\hat{\epsilon}^T\hat{\epsilon}\right\} = E\left\{w^T(N)\,M w(N)\right\}$$
$$= tr\; E\left\{M w w^T\right\}$$
$$= \sigma^2\; tr\, M$$
$$= \sigma^2\left[3(N+1)-q\right]$$

We may therefore approximate σ^2 by

$$\hat{\sigma}^2 = \frac{\hat{\epsilon}^T\hat{\epsilon}}{3(N+1)-q} \tag{3.3c}$$

and thus, using (3.3a) and (3.3c), an approximate estimate of the covariance of the estimated parameters can be written as

$$cov(\hat{p}) = \frac{\hat{\epsilon}^T\hat{\epsilon}}{3(N+1)-q}\;(A_N^T A_N)^{-1} \tag{3.3d}$$

It should be emphasized that the above relation is based on the assumption that A_N is non-stochastic. Some problems associated with this basic assumption are discussed in Section V.

Using (3.3), both the linear* and nonlinear representations of the VTOL aircraft dynamics in transition were programmed for digital computation. As an example, consider the nonlinear representation for the pitching moment equation in Equation (2.8)

$$\dot{q}(t) = m_0(u) + m_w(u)\Delta w + m_q(u)\Delta q + m_B(u)\Delta B + m_{\delta_{ES}}(u)\Delta\delta_{ES} + m_\lambda(u)\Delta\lambda \tag{3.4}$$

where $m_0(u)$ etc. are third-order polynomials in u and $\Delta w = w(t) - w_R(t)$, and where the subscript R denotes the reference values.

Using (3.3), (3.4) becomes

$$\hat{p} = (A_q^T A_q)^{-1} A_q^T \underline{\dot{q}} = P_q A_q^T \underline{\dot{q}} \tag{3.5}$$

*The linear representation is obtained by setting $\lambda_R(t)$ = constant and $q_R = 0$ in Appendix A.

where

$$P_q \triangleq (A_q^T A_q)^{-1}$$

$$\hat{p} = (a_1^T \; a_2^T \; . \; . \; . \; a_6^T)^T$$

$$m_0(u) = a_1^T \vec{u} \qquad a_1^T = (a_{10}, a_{11}, a_{12}, a_{13})$$

$$m_w(u) = a_2^T \vec{u} \qquad \text{-------}$$

$$m_q(u) = a_3^T \vec{u} \qquad a_6^T = (a_{60}, a_{61}, a_{62}, a_{63})$$

$$m_\delta(u) = a_4^T \vec{u} \qquad \vec{u} = (1, u, u^2, u^3)^T$$

$$m_{\delta_{es}}(u) = a_5^T \vec{u} \qquad \underline{\dot{q}} = (\dot{q}(t_0), \dot{q}(t_1), \ldots, \dot{q}(t_N))^T$$

$$m_\lambda(u) = a_6^T \vec{u}$$

and

$$A_q = \begin{bmatrix} 1 & u(t_0) & u^2(t_0) & u^3(t_0) & \Delta w(t_0) \cdots \Delta w(t_0)u^3(t_0) \cdots & \Delta\lambda(t_0) & \Delta\lambda u(t_0) \cdots & \Delta\lambda u^3(t_0) \\ 1 & u(t_1) & u^2(t_1) & u^3(t_1) & \Delta w(t_1) \cdots \Delta w(t_1)u^3(t_1) \cdots & \Delta\lambda(t_1) & \Delta\lambda u(t_1) \cdots & \Delta\lambda u^3(t_1) \\ \vdots & \vdots & \vdots & \vdots & \vdots & \vdots & \vdots & \vdots \\ 1 & u(t_N) & u^2(t_N) & u^3(t_N) & \Delta w(t_N) \cdots \Delta w(t_N)u^3(t_N) \cdots & \Delta\lambda(t_N) & \Delta\lambda u(t_N) \cdots & \Delta\lambda u^3(t_N) \end{bmatrix}$$

Modified Spline Function Method

A spline (see Reference 11) is a thin strip that is bent so as to pass through a given set of data points. Using the deformed strip as a guide, a line can be traced through these points; the resulting curve is continuous and has a continuous first derivative. Analytically, a spline function is usually generated by minimizing the integral of the curvature of the entire function subject to the constraint that the function passes through all the data points. In this construction scheme it is further assumed that the functions and their first two derivatives are continuous within the set of data points.

In many practical situations, the data are contaminated with some random errors (such as quantization errors or measurement noise). Consequently, it becomes desirable to relax the constraint that the conventional spline function must pass through the data points. The resulting function is called a modified spline function (also called floppy spline function). A scheme to generate a modified spline function has been developed by D. Larson and J. Fleck of CAL, and has been reported in detail in Reference 11. They also developed a computer program for generating the modified spline function using the technique they developed.

When this computer program is used to perform as an initial estimator for parameter identification, the measured state variable data and weights are read in. The spline routine uses these data to fit a floppy spline curve through the measured data points of each state variable, and then evaluates the resulting curve and its time derivative at each of the desired time points. Once all of the derivatives of the state variables are known, the initialization routine uses the least squares technique to obtain the initial estimates of the parameters.

Polynomial Estimator

This method also uses only the measurements of the state variables. First, the state variables are fitted with a polynomial in t using a least square method. The time rates of the changes of the state variables are then calculated from the polynomials used to fit the state variables. The equations-of-motion error method is then applied to obtain the estimates of the unknown parameters.

Like the preceding two methods, here we also assume that all the state variables are measurable. For computational simplicity, all the state variables are represented by polynomials of the same degree. Consider the linear representation of the VTOL aircraft dynamics.

$$\left.\begin{aligned} \dot{x} &= Fx + Gm \\ y &= x + v \end{aligned}\right\} \qquad (3.6)$$

where

$$x = (q, \theta, u, w)^T$$

$$m = (1, \delta_{ES}, B)^T$$

We fit a set of n-degree polynomials to these state variables' measurements. Let

$$y = Ab \tag{3.7}$$

where

$$A = \begin{pmatrix} a_{10} & a_{11} & \cdots & a_{1n} \\ a_{20} & a_{21} & & a_{2n} \\ a_{30} & \vdots & \ddots & \vdots \\ a_{40} & \cdot & & a_{4n} \end{pmatrix}$$

$$b = (t^0, t^1, t^2, \ldots, t^n).$$

At each time instance t_i

$$y(t_i) = Ab(t_i).$$

Hence

$$\left[y(t_0), y(t_1), \ldots, y(t_N) \right] = A \left[b(t_0), b(t_1), \ldots, b(t_N) \right]$$

or $S = A\mathrm{X}$.

Thus, in a least square sense, A is given by

$$A = S\mathrm{X}^T (\mathrm{X}\mathrm{X}^T)^{-1} \tag{3.8}$$

where

$$S = \begin{bmatrix} q(t_0) & q(t_N) \\ \theta(t_0) & \theta(t_N) \\ u(t_0) & u(t_N) \\ w(t_0) & w(t_N) \end{bmatrix}$$

$$\mathrm{X} = \begin{bmatrix} 1 & 1 & 1 \\ 0 & \Delta & N\Delta \\ 0 & (\Delta)^2 & \vdots \\ \vdots & \vdots & \vdots \\ 0 & (\Delta)^n & (N\Delta)^n \end{bmatrix}$$

$$\Delta = t_{i+1} - t_i$$

We now substitute (3.7) into (3.6); the result is:

$$A\dot{b} = \left[F \,\vdots\, G \right] \begin{bmatrix} Ab \\ \hdashline m \end{bmatrix}$$

Once again, using the least squares method, we have

$$\left[F \,\vdots\, G \right] = A\mathrm{X}_d \left[(A\mathrm{X})^T \,\vdots\, M^T \right] \left\{ \begin{bmatrix} A\mathrm{X} \\ \hdashline M \end{bmatrix} \left[(A\mathrm{X})^T \,\vdots\, M^T \right] \right\}^{-1} \tag{3.9}$$

where

$$
X_d = \begin{bmatrix} 0 & 0 & & 0 \\ 1 & 1 & & 1 \\ 0 & 2\Delta & \cdots & N\Delta \\ \vdots & \vdots & & \vdots \\ 0 & n\Delta^{n-1} & & n(N\Delta)^{n-1} \end{bmatrix} \qquad M = \begin{bmatrix} 1 & \cdots & 1 \\ \delta_{ES}(t_0) & \cdots & \delta_{ES}(t_N) \\ B(t_0) & \cdots & B(t_N) \end{bmatrix}
$$

Equation (3.9) is the desired result. It is to be noted that like the preceding two methods this approach is also applicable to nonlinear systems.

Denery's Initial Estimator (Reference 12)

This method of performing the initial estimation of the unknown parameters was recently developed by D. Denery. Its special feature is its similarity to the method of quasilinearization, which we shall discuss later. Thus, a unified estimation procedure can be used for first obtaining the initial estimates and then subsequently improving these estimates through further iterations. However, this method is applicable only to linear systems.

The basic idea of this method is to relate the unknown parameters of the system to a set of new parameters that affect the output in a linear fashion. In so doing, linear regression can then be used to obtain this set of new parameters which, in turn, permit the calculation of the original unknown parameters using the relationship between these two sets of parameters. Details are discussed in Appendix C.

3.1.1 Comparison of the Numerical Results

The equations-error methods discussed in 3.1 were programmed for digital computation using the linearized equations of motion of the VTOL aircraft dynamics, which describe the fixed-operating point, fixed-duct angle motions of the vehicle (see Appendix D, Equation D.2a). The results of the computer runs are shown in Tables 3-1 through 3-4. The data used are explained in Appendix D. From these numerical experiments, the following observations may be made:

(i) For data without measurement error (Data 1-0), the equations-of-motion method and Denery's method give the correct parameter estimates. However, the polynomial estimator and the modified spline function method do not obtain the correct estimates.

(ii) As the noise to signal ratio increases, the estimates of all four methods deteriorate, confirming the statistical analysis conducted in Appendix B.

(iii) Although for noiseless data, Denery's method gives the correct estimates regardless of nominal values of the parameters F_N and G_N that have been assumed (see Appendix C), for noisy data the estimates are significantly affected by the values of F_N and G_N used.

(iv) The estimates using the polynomial estimator depend heavily upon the degree of polynomial assumed for the state variables. The numerical results suggest that the higher degree polynomial fit (ninth degree) is more accurate than the lower degree (fifth degree). However, the estimates for the ninth degree fit do not appear to be better than those using the modified spline function method.

(v) From the computational point of view, the equations-of-motion method is the simplest, provided that the acceleration measurements are available; Denery's method is the most complicated one, in that it requires solutions of a large number of sensitivity equations.

3.1.2 Concluding Remarks on the Equation-Error Methods

From the above discussions and the numerical experimentations the following remarks are in order.

(1) It has been shown (Appendix B) that the initial estimators discussed in Section 3.1 are asymptotically biased, i.e., the use of longer data records does not help reduce the bias of the estimates.

(2) A formula has been derived, for the linear case, for the calculation of the bias when the equations-of-motion method is used to obtain the initial estimates and if the noise is normally distributed. (See Appendix B).

(3) If the acceleration measurements are available, then the equations-of-motion method is recommended for initial parameter estimation, since this method is applicable to both linear and nonlinear systems, and since its computational procedure is the simplest. If the acceleration measurements are not available, then the modified spline function method is recommended.

(4) For linear systems, Denery's method is a good alternate to the above two methods, since its computational algorithm is similar to the method of quasilinearization, and a single computer program can therefore be easily devised.

As stated at the beginning of Section III, in the absence of process noise the measurement-error methods will remove the bias in these initial estimates obtained using equation-error methods. The iterative measurement-error methods such as quasilinearization method, the extended Kalman filtering method, and the conjugate gradient technique are applicable to both linear and nonlinear systems. For linear systems there appear to be other methods that are capable of removing the bias of the initial estimates. From the statistical analysis performed in Appendix B, it is clear that these methods may be classified into the following two groups:

(a) Estimate the noise statistics and remove the effects of the noise from the regressor (Reference 13).

(b) Introduce a set of "instrumental variables" (see References 13, 14, and 15) which make the resulting regressor uncorrelated with the errors in the least square fit. (See discussion in Appendix B.)

3.2 Measurement-Error Methods

We now proceed to examine the basic characteristics of the second group - the measurement-error methods. As we stated in the comment at the end of Section II, this group of methods essentially employs the likelihood function for the system (including additive white Gaussian measurement noise) as the performance index. Indeed, from (2.26) it is clear that maximizing the likelihood function $\ln f\left(Y(N)/x_0\right)$ is equivalent to minimizing the deterministic cost function

$$J_d = \frac{1}{2}\sum_{i=1}^{N} \left\| y_i - h\left(x_{a_i}, m_i\right)\right\|^2_{R_i^{-1}} \tag{3.10}$$

Therefore, from the statistical point of view, the estimate of the initial augmented state $x_{a_0} = \left(x_0^T, p^T\right)^T$ obtained from minimizing (3.10) is the classical (non-Bayesian) maximum likelihood estimate for the initial augmented state of a continuous system with discrete measurements corrupted by additive, white, Gaussian noise. From a deterministic point of view, the minimum of the cost function used in this group of methods is the sum of the weighted least squares in the output errors.

For analytical simplicity, we shall consider (3.11), which is the equivalent continuous counterpart of (3.10), for use as the performance index.

$$J = \int_0^{t_f} \left[y(t) - h(x,p,m)\right]^T R^{-1} \left[y(t) - h(x,p,m)\right] dt \tag{3.11}$$

The problem for this group of methods can now be stated as follows:

Given: (1) a continuous nonlinear dynamic system (2.15) with $w(t) = 0^*$, and a set of continuous measurements $y(t)$, $0 \leq t \leq t_f$ as given in (3.12a) and (3.12b)

$$\dot{x} = f(x, p, m) \quad , \quad x(0) = x_0 \tag{3.12a}$$

$$y(t) = h(x, p, m) + v(t) \tag{3.12b}$$

respectively, where $E\{v(t)\} = 0$, and $E\{v(t)v^T(\tau)\} = R(t)\delta(t-\tau)$.

(2) a set of noise free continuous measurements for the control vector $m(t)$, $0 \leq t \leq t_f$.

Find: An estimate of the parameter vector and the initial state that minimizes (3.11)

For sake of generality in the following discussion, let x be an n-vector, p be a q-vector, and y an m-vector.

3.2.1 Description of Various Measurement-Error Methods

Clearly, the problem posed above is essentially a nonlinear parameter minimization problem, for which many iterative methods are available to obtain a solution. In this report, the following methods are discussed.

1. Quasilinearization (Differential correction, parameter influence coefficient, Gauss-Newton procedure, "Modified" Newton-Raphson).
2. Gradient methods and their simplified computation.
3. Basic Newton's procedure and Goodwin's simplifications.
4. Conjugate gradient method.

---

* Discussions will be given later on the effect of the process noise on the estimates from this group of methods.

5. Method of invariant imbedding (for case without process noise)
6. Extended Kalman filter (for case without process noise)

A sketch of these methods will first be given. This will then be followed by an examination of the basic characteristics of this group of methods. Their merits and debits will then be assessed, based on the computational complexity as well as from the results of numerical experiments using computer-generated data.

Quasilinearization Method (References 16 - 18)

This method is also referred to as Gauss-Newton procedure (Reference 19), parameter-influence-coefficient method (Reference 19), "modified" Newton-Raphson method (Reference 20), etc. It begins with the linearizations of the trajectory and the output about the initial estimates $\hat{p}$ and $\hat{x}_0$:

$$x(\hat{x}_0 + \Delta x_0, \hat{p} + \Delta p) \approx x(\hat{x}_0, \hat{p}) + \left[\frac{\partial x}{\partial x_0}, \frac{\partial x}{\partial p}\right] \begin{bmatrix} \Delta x_0 \\ \Delta p \end{bmatrix} \tag{3.13}$$

$$h(x, p, m) \approx h(x(\hat{x}_0, \hat{p}), \hat{p}, m) + \frac{\partial h}{\partial x} \left[\frac{\partial x}{\partial x_0}, \frac{\partial x}{\partial p}\right] \begin{bmatrix} \Delta x_0 \\ \Delta p \end{bmatrix} + \frac{\partial h}{\partial p} \Delta p \tag{3.14}$$

The sensitivity matrices $\partial x/\partial x_0$ and $\partial x/\partial p$ are obtained from the solutions to the following set of linear time-varying differential equations:

$$\frac{d}{dt}\left(\frac{\partial x}{\partial x_0}\right) = \left(\frac{\partial f}{\partial x}\right)\left(\frac{\partial x}{\partial x_0}\right), \quad \frac{\partial x}{\partial x_0}(0) = I_n \tag{3.15}$$

$$\frac{d}{dt}\left(\frac{\partial x}{\partial p}\right) = \left(\frac{\partial f}{\partial x}\right)\left(\frac{\partial x}{\partial p}\right) + \frac{\partial f}{\partial p}, \quad \frac{\partial x}{\partial p}(0) = 0 \tag{3.16}$$

where I_n is the n[th] order identity matrix. From (3.11) the gradient of the performance index with respect to the initial state and the parameter is

$$\nabla J_{x_a} \triangleq \begin{bmatrix} \nabla J_{x_0} \\ \nabla J_p \end{bmatrix} = -\int_0^{t_f} \left[\frac{\partial h}{\partial x} \frac{\partial x}{\partial x_0} \;\middle|\; \frac{\partial h}{\partial p} + \frac{\partial h}{\partial x} \frac{\partial x}{\partial p} \right]^T R^{-1} \left(y(t) - h(x, p, m)\right) dt \tag{3.17}$$

Using (3.14) and equating the gradient ∇J_{x_a} in (3.17) to zero which defines the extremal, yields a new estimate

$$(\hat{x}_{a_0})_{new} = (\hat{x}_{a_0})_{old} + \Delta x_{a_0} \tag{3.18}$$

where

$$\Delta x_{a_0} \triangleq \begin{bmatrix} \Delta x_0 \\ \Delta p \end{bmatrix}$$

$$= \left\{ \int_0^{t_f} \left[\frac{\partial h}{\partial x} \frac{\partial x}{\partial x_0} \;\middle|\; \frac{\partial h}{\partial p} + \frac{\partial h}{\partial x} \frac{\partial x}{\partial p} \right]^T R^{-1} \left[\frac{\partial h}{\partial x} \frac{\partial x}{\partial x_0} \;\middle|\; \frac{\partial h}{\partial p} + \frac{\partial h}{\partial x} \frac{\partial x}{\partial p} \right] dt \right\}^{-1} \cdot$$

$$\int_0^{t_f} \left[\frac{\partial h}{\partial x} \frac{\partial x}{\partial x_0} \;\middle|\; \frac{\partial h}{\partial p} + \frac{\partial h}{\partial x} \frac{\partial x}{\partial p} \right]^T R^{-1} \left(y(t) - h(\hat{x}, \hat{p}, m)\right) dt \tag{3.19}$$

The Jacobian matrices $\partial f/\partial x$, $\partial f/\partial p$ in (3.15) and (3.16), $\partial h/\partial x$, $\partial h/\partial p$ in (3.14), and the computed output $h(\hat{x}, \hat{p}, m)$ are evaluated at the <u>old</u> estimate $(\hat{x}_{a_0})_{old}$. Note also that $x(\hat{x}_0, \hat{p}) \triangleq x\left[(\hat{x}_{a_0})_{old}\right]$ in (3.13) is the solution of (3.12a) using $(\hat{x}_{a_0})_{old}$.

It should be pointed out that, when acceleration measurements are not used, h is not a function of p and hence $\partial h/\partial p = 0$ in (3.17) and (3.19).

In the above derivation for the improved estimate, there is no guarantee that (3.18) will converge. It has been a common practice to use a positive number α, $0 < \alpha \leq 1$ to reduce the magnitude of the correction

$$(\hat{x}_{a_0})_{new} = (\hat{x}_{a_0})_{old} + \alpha \, \Delta x_{a_0} \tag{3.20}$$

whenever any element of Δx_{a_0} is large in magnitude compared to its corresponding $(\hat{x}_{a_0})_{old}$. An alternate scheme is to determine α by a one-dimensional search such that

$$\min_{\alpha} J\left[(\hat{x}_{a_0})_{new}\right] \tag{3.21}$$

rather than using a predetermined value such as $0 < \alpha \leq 1$.

We mention in passing that (3.19) can be used as the basis for a recursive computational scheme (Reference 21).

Gradient Method (References 22 and 23)

The gradient method is basically a linearization on the performance index with respect to the parameter vector, that is:

$$J(\hat{x}_{a_0} + \Delta x_{a_0}) = J(\hat{x}_{a_0}) + \left[\nabla_{x_{a_0}} J(\hat{x}_{a_0})\right]^T \Delta x_{a_0} \tag{3.22}$$

with a constraint on the step size Δx_{a_0} given by:

$$C = \frac{1}{2} (\Delta x_{a_0})^T S (\Delta x_{a_0}) \tag{3.23}$$

where C is a chosen constant, and S is a positive definite symmetrical matrix.

Introducing a Lagrange multiplier λ, and setting the gradient of $\tilde{J}(x_{a_0}) = 0$, where

$$\tilde{J}(x_{a_0}) \triangleq J(\hat{x}_{a_0} + \Delta x_{a_0}) + \lambda \left[C - \frac{1}{2} (\Delta x_{a_0})^T S (\Delta x_{a_0})\right]$$

yields

$$(\hat{x}_{a_0})_{new} = (\hat{x}_{a_0})_{old} + \frac{1}{\lambda} \cdot \nabla_{x_{a_0}} J\left[(\hat{x}_{a_0})_{old}\right] \tag{3.24}$$

where the gradient $\nabla_{x_{a_0}} J$ in (3.24) is given by (3.17).

The evaluation of the gradient of the performance index can be obtained more efficiently by a use of an adjoint-variable method. However, we shall not discuss it here. (See Reference 22 for details.)

Newton's Procedure and Its Connection with Quasilinearization (References 19 and 20)

The basic Newton's procedure is to first expand the performance index (3.11) in a Taylor series about the old estimate $\hat{x}_{a_0}$.

$$J(\hat{x}_{a_0}+\Delta x_{a_0}) = J(\hat{x}_{a_0}) + \left[\nabla_{x_{a_0}} J(\hat{x}_{a_0})\right]^T \Delta x_{a_0} + \frac{1}{2}(\Delta x_{a_0}) J_{x_{a_0} x_{a_0}}(\hat{x}_{a_0})\Delta \hat{x}_{a_0} \tag{3.25}$$

where $J_{x_{a_0} x_{a_0}}$ is the curvature matrix, and higher-order terms have been neglected. By imposing the condition that the gradient of the performance index with respect to the parameters and initial state be zero, i.e.,

$$\nabla_{x_{a_0}} J(\hat{x}_{a_0} + \Delta x_{a_0}) = 0$$

the change in the parameter vector is seen to be

$$\Delta x_{a_0} = -\left[J_{x_{a_0} x_{a_0}}(\hat{x}_{a_0})\right]^{-1} \nabla_{x_{a_0}} J(\hat{x}_{a_0}) \tag{3.26}$$

The new estimates of the initial state and the parameters are then obtained by using (3.27)

$$(\hat{x}_{a_0})_{new} = (\hat{x}_{a_0})_{old} + \alpha \Delta x_{a_0} \tag{3.27}$$

where $\alpha > 0$ can be obtained by a one-dimensional search along the positive real axis such that $J\left[(\hat{x}_{a_0})_{new}\right]$ = min. Notice that a large amount of computation involving second partials with respect to initial state and the parameters is required to obtain the curvature matrix $J_{x_{a_0} x_{a_0}}$. Goodwin (Reference 19) has simplified considerably the computational load by again using adjoint variables. However, aside from the fact that the computational load is heavy to obtain the curvature matrix, the other major drawback associated with Newton's procedure is the fact that unless the curvature matrix $J_{x_{a_0} x_{a_0}}$ is positive definite, there is no assurance of convergence. This can be seen by substituting (3.26) into (3.25), which yields:

$$J(\hat{x}_{a_0} + \Delta x_{a_0}) - J(\hat{x}_{a_0}) = -\frac{1}{2}\left(\nabla_{x_{a_0}} J\right)^T J_{x_{a_0} x_{a_0}}^{-1} \left(\nabla_{x_{a_0}} J\right) \tag{3.28}$$

Since $J_{x_{a_0} x_{a_0}}^{-1}$ is positive definite if and only if $J_{x_{a_0} x_{a_0}}$ is positive definite, it is clear that there is no guarantee that J will decrease. Several schemes have been devised to partially overcome this difficulty. All these schemes involve the diagonalization of the curvature matrix and hence require a solution of eigenvalues and corresponding eigenvectors of the curvature matrix – a procedure which significantly increases the computational load. We now show the connection of Newton's procedure with the quasilinearization method discussed previously.

From (3.17)

$$\frac{\partial}{\partial x_{a_{0\ell}}}\left(\nabla_{x_{a_0}} J\right) = -\int_0^{t_f} \left[\frac{\partial h}{\partial x} \frac{\partial^2 x}{\partial x_0^2 x_{a_{0\ell}}} \;\middle|\; \left(\frac{\partial^2 h_i}{\partial p_j \partial x_{a_{0\ell}}} + \sum_{k=1}^{n} \frac{\partial^2 h_i}{\partial p_j \partial x_k} \frac{\partial x_k}{\partial x_{a_{0\ell}}}\right) + \frac{\partial h}{\partial x} \frac{\partial^2 x}{\partial p \partial p_\ell}\right]^T$$

$$R^{-1} \left[y - h(x, p, m)\right] dt$$

$$-\int_0^{t_f} \left[\left(\frac{\partial^2 h_i}{\partial x_m \partial x_{a_{0\ell}}} + \sum_{k=1}^{n} \frac{\partial^2 h_i}{\partial x_m \partial x_h} \frac{\partial x_k}{\partial x_{a_{0\ell}}}\right)\left(\frac{\partial x}{\partial x_0} \;\middle|\; \frac{\partial x}{\partial p}\right)\right]^T R^{-1} \left[y - h(x, p, m)\right] dt$$

$$+\int_0^{t_f} \left[\frac{\partial h}{\partial x} \frac{\partial x}{\partial x_0} \;\middle|\; \frac{\partial h}{\partial p} + \frac{\partial h}{\partial x} \frac{\partial x}{\partial p}\right]^T R^{-1} \left[\frac{\partial h}{\partial x} \frac{\partial x}{\partial x_{a_{0\ell}}} + \frac{\partial h}{\partial p} \frac{\partial p}{\partial x_{a_{0\ell}}}\right] dt$$

where

$$\left(\frac{\partial^2 h_i}{\partial p_j \partial x_{a_{0\ell}}} + \sum_k \frac{\partial^2 h_i}{\partial p_j \partial x_k} \frac{\partial x_k}{\partial x_{a_{0\ell}}}\right)$$

and

$$\left(\frac{\partial^2 h_i}{\partial x_m \partial x_{a_{0\ell}}} + \sum_k \frac{\partial^2 h_i}{\partial x_m \partial x_k} \frac{\partial x_k}{\partial x_{a_{0\ell}}}\right)$$

are matrices with their ij and im elements as shown in the above brackets respectively.

Now, if the second partials are neglected, then

$$J_{x_{a_0} x_{a_0}} = \int_0^{t_f} \left[\frac{\partial h}{\partial x} \frac{\partial x}{\partial x_0} \,\vdots\, \frac{\partial h}{\partial p} + \frac{\partial h}{\partial x} \frac{\partial x}{\partial p} \right]^T R^{-1} \left[\frac{\partial h}{\partial x} \left(\frac{\partial x}{\partial x_0} \,\vdots\, \frac{\partial x}{\partial p} \right) + \frac{\partial h}{\partial p} \left(0 \,\vdots\, I \right) \right] dt$$

$$= \int_0^{t_f} \left[\frac{\partial h}{\partial x} \frac{\partial x}{\partial x_0} \,\vdots\, \frac{\partial h}{\partial p} + \frac{\partial h}{\partial x} \frac{\partial x}{\partial p} \right]^T R^{-1} \left[\frac{\partial h}{\partial x} \frac{\partial x}{\partial x_0} \,\vdots\, \frac{\partial h}{\partial p} + \frac{\partial h}{\partial x} \frac{\partial x}{\partial p} \right] dt \tag{3.30}$$

Clearly, from (3.26), (3.30), and (3.17)

$$\Delta x_{a_0} = \left\{ \int_0^{t_f} \left[\frac{\partial h}{\partial x} \frac{\partial x}{\partial x_0} \,\vdots\, \frac{\partial h}{\partial p} + \frac{\partial h}{\partial x} \frac{\partial x}{\partial p} \right]^T R^{-1} \left[\frac{\partial h}{\partial x} \frac{\partial x}{\partial x_0} \,\vdots\, \frac{\partial h}{\partial p} + \frac{\partial h}{\partial x} \frac{\partial x}{\partial p} \right] dt \right\}^{-1}$$

$$\times \int_0^{t_f} \left[\frac{\partial h}{\partial x} \frac{\partial x}{\partial x_0} \,\vdots\, \frac{\partial h}{\partial p} + \frac{\partial h}{\partial x} \frac{\partial x}{\partial p} \right]^T R^{-1} \left(y(t) - h(\hat{x}, \hat{p}, m) \right) dt$$

which is precisely (3.19). Thus, if the second partials are neglected, Newton's procedure reduces to the quasilinearization method discussed earlier.

<u>Conjugate Gradient Method (References 24 - 26)</u>

The conjugate gradient method begins with the construction of conjugate gradient vectors $\{a_i\}$ which have the following property

$$a_i^T J_{x_{a_0} x_{a_0}} a_j = 0, \; i \neq j, \; i, j = 1, 2, \ldots, q, \ldots, q+n \tag{3-31}$$

This is then followed by a sequence of one-dimensional searches to obtain scalars $\{\alpha_i\}$ such that

$$\min_{\alpha} J\left(\hat{x}_{a_0}^i - \alpha a_i \right) \tag{3.32}$$

and

$$\hat{x}_{a_0}^{i+1} = \hat{x}_{a_0}^{i} + \Delta x_{a_0}$$
$$\Delta x_{a_0} = -\alpha_i a_i \tag{3.33}$$

In practice, the construction of conjugate gradients by (3.31) is rarely used, since it requires the information of the curvature matrix $J_{x_{a_0} x_{a_0}}$. Instead the following construction scheme is used:

$$a_i = \begin{cases} \nabla_{x_{a_0}} (\hat{x}_{a_0}^i) & i = 1 \\ \nabla_{x_{a_0}} J(\hat{x}_{a_0}^i) + \dfrac{\|\nabla_{x_{a_0}} J(\hat{x}_{a_0}^i)\|^2}{\|\nabla_{x_{a_0}} J(\hat{x}_{a_0}^{i-1})\|^2} a_{i-1} & i \geq 2 \end{cases} \tag{3.34}$$

where the norm $\| \cdot \|$ is the $q+n$ -dimensional Euclidean norm (i.e., the square root of the sum of the square of the $q+n$ -components) and the gradient $\nabla_{x_{a_0}} J(\hat{x}_{a_0}^i)$ in (3.13) is given by (3.17).

Thus, the first iteration is basically a gradient method. However, the search directions in the second iteration and iterations thereafter use a linear combination of the gradient and the previous search direction. In addition to the simplicity of the algorithm, it has a good convergence property. Indeed,

$$\frac{d}{d\alpha} J(\hat{x}_{a_0}^i - \alpha a_i)\Big|_{\alpha=0} < 0, \text{ if } \nabla_{x_{a_0}} J(\hat{x}_{a_0}^i) \neq 0$$

and hence

$$J(\hat{x}_{a_0}^{i+1}) < J(\hat{x}_{a_0}^i).$$

To show this, one observes that

$$\frac{d}{d\alpha} J(\hat{x}_{a_0}^i - \alpha a_i)\Big|_{\alpha=0} = \left[\nabla_{x_{a_0}} J(\hat{x}_{a_0}^i - \alpha a_i)\right]^T (-a_i)\Big|_{\alpha=0}$$
$$= -\left[\nabla_{x_{a_0}} J(\hat{x}_{a_0}^i)\right]^T a_i$$

From (3.32) it is then seen that

$$\frac{d}{d\alpha} J(\hat{x}_{a_0}^{i} - \alpha a_i)\Big|_{\alpha=\alpha_i} = 0 = -\left[\nabla_{x_{a_0}} J(\hat{x}_{a_0}^{i+1})\right]^T a_i , \quad \forall i$$

and from (3.33)

$$a_i = \nabla_{x_{a_0}} J(\hat{x}_{a_0}^{i}) + \beta a_{i-1} , \qquad i \geq 2$$

where

$$\beta = \frac{\|\nabla_{x_{a_0}} J(\hat{x}_{a_0}^{i})\|^2}{\|\nabla_{x_{a_0}} J(\hat{x}_{a_0}^{i-1})\|^2}$$

Hence,

$$\begin{aligned} -\left[\nabla_{x_{a_0}} J(\hat{x}_{a_0}^{i})\right]^T a_i &= -\left[\nabla_{x_{a_0}} J(\hat{x}_{a_0}^{i})\right]^T\left[\nabla_{x_{a_0}} J(\hat{x}_{a_0}^{i}) + \beta a_{i-1}\right] \\ &= -\|\nabla_{x_{a_0}} J(\hat{x}_{a_0}^{i})\|^2 < 0 , \quad \text{if } \nabla_{x_{a_0}} J(\hat{x}_{a_0}^{i}) \neq 0. \end{aligned}$$

Using the definition of $\hat{x}_{a_0}^{i+1}$, it is readily established that $J(\hat{x}_{a_0}^{i+1}) < J(\hat{x}_{a_0}^{i})$.

The preceding four methods are all nonrecursive (or batch processing) methods; the entire data set is utilized each time the estimates are updated. As a summary, we list the information utilized in each method to obtain the correction term Δx_{a_0} which improves initial state and parameter estimates in the following table:

Methods	Information used in correction, Δx_{a_0}
Quasilinearization	Gradient and a modified curvature matrix
Gradient Method	Gradient only
Newton Procedure	Gradient and curvature matrix
Conjugate Gradient	Conjugate gradients

We next discuss two recursive methods that sequentially update the estimate of the parameter and the current state at each data point. These two methods, as do many more nonlinear filtering methods, belong to the third group of identification methods, in that they may treat both measurement and process noise. Clearly, these methods are equally applicable for parameter and state estimation in the absence of process noise, and have been chosen here to demonstrate the recursive nature of the computation. We have more to say later in Section 3.3 and Section V about the estimation of parameters and state in noisy nonlinear dynamic systems based on noisy nonlinear measurements.

Invariant Imbedding Method (References 27 and 28)

Rewrite (3.12a) and (3.12b) in an augmented state form, (2.21a) and (2.21b) respectively, i.e.,

$$\dot{x}_a = f_a\,(x_a\,, m) \tag{3.35a}$$

$$y = h\,(x_a\,, m) + v \tag{3.35b}$$

Then the Jacobian matrices $\partial f_a/\partial x_a$, $\partial h/\partial x_a$ are

$$\frac{\partial f_a}{\partial x_a} = \left[\begin{array}{c|c} \frac{\partial f}{\partial x} & \frac{\partial f}{\partial p} \\ \hline 0 & 0 \end{array}\right] \tag{3.36a}$$

$$\frac{\partial h}{\partial x_a} = \left[\begin{array}{c|c} \frac{\partial h}{\partial x} & \frac{\partial h}{\partial p} \end{array}\right] \tag{3.36b}$$

Using the invariant imbedding technique, it can be shown (References 27 and 28) that the estimate of the augmented state is computed recursively as follows:

$$\frac{d}{dt}\,\hat{x}_a(t) = f_a\,(\hat{x}_a\,, t) + P(t)\left(\frac{\partial h}{\partial x_a}\right)^T R^{-1}\left[y(t) - h\left(\hat{x}_a\,, m\right)\right] \tag{3.37a}$$

$$\dot{P}(t) = \frac{\partial f_a}{\partial \hat{x}_a}\,P(t) + P(t)\left(\frac{\partial f_a}{\partial \hat{x}_a}\right)^T + P\left[\left(\frac{\partial h}{\partial \hat{x}_a}\right)^T R^{-1}\left(y - h\left(\hat{x}_a\,, m\right)\right)\right]_{\hat{x}_a} P \tag{3.37b}$$

where the term

$$\left[\left(\frac{\partial h}{\partial \hat{x}_a}\right)^T R^{-1}\left(y-h(\hat{x}_a, m)\right)\right]_{\hat{x}_a}$$

in (3.37b) is an $(n+q)(n+q)$ square matrix whose i^{th} column is

$$\frac{\partial}{\partial x_i}\left[\left(\frac{\partial h}{\partial \hat{x}_a}\right)^T R^{-1}\left(y-h(\hat{x}_a, m)\right)\right]$$

Thus, (3.37b) can be rewritten as

$$\begin{aligned}\dot{P}(t) = &\left(\frac{\partial f_a}{\partial \hat{x}_a}\right) P + P\left(\frac{\partial f_a}{\partial \hat{x}_a}\right)^T - P\left(\frac{\partial h}{\partial \hat{x}_a}\right)^T R^{-1}\left(\frac{\partial h}{\partial \hat{x}_a}\right) P \\ &+ P\left[\sum_{k} \frac{\partial^2 h_k}{\partial x_i \partial x_j} R^{-1}\left(y_k - h_k(\hat{x}_a, m)\right)\right] P\end{aligned} \tag{3.38}$$

In (3.38), the square bracket is an $(n+q) \times (n+q)$ matrix whose i, j element is contained in the bracket. Note that this term vanishes if h is a linear function of x. The initial conditions $x_a(0)$, and $P(0) = P_0$ are usually guessed. For the moment we shall not dwell on the question of how to choose these two initial conditions. An in-depth discussion will be given in Section V.

Extended Kalman Filter (for the case without process noise)

The derivation of an extended Kalman filter for the noisy nonlinear continuous system with noisy discrete nonlinear measurements as formulated in Section 2 is given in Section 5.2. Here, for the sake of comparison with other methods discussed in this section, we present a simpler version for a system without process noise and with noisy continuous measurements.

The name "extended" stems from the attempts which have been made to apply the Kalman filtering technique developed for linear systems to nonlinear systems through successive linearization at each data point.

Let $\bar{x}_a(0)$ be the mean of $x_a(0)$, and P_0, R be the covariance matrices of $x_a(0)$ and v respectively, i.e.,

$$\left.\begin{array}{l} E\left[x_a(0)\right] = \bar{x}_a(0)\ , \quad E\left[\left(x_a(0)-\bar{x}_a(0)\right)\left(x_a(0)-\bar{x}_a(0)\right)^T\right] = P_0 \\ E\left[v\right] = 0 \quad , \qquad E\left[v(t)v^T(t_i)\right] = R\delta(t-t_i) \\ E\left[\left(x_a(0)-\bar{x}_a(0)\right)v^T(t)\right] = 0\ , \quad \forall t \end{array}\right\} \tag{3.39}$$

Then the estimate of the augmented state is computed using (from References 29 - 32)

$$\frac{d}{dt}\hat{x}_a = f_a(\hat{x}_a, t) + P(t)\left(\frac{\partial h}{\partial \hat{x}_a}\right)^T R^{-1}\left[y(t) - h(\hat{x}, t)\right], \quad \hat{x}_a(0) = \bar{x}_a(0) \tag{3.40a}$$

$$\dot{P}(t) = \frac{\partial f_a}{\partial \hat{x}_a} P + P\left(\frac{\partial f_a}{\partial \hat{x}_a}\right)^T - P\left(\frac{\partial h}{\partial \hat{x}_a}\right)^T R^{-1}\left(\frac{\partial h}{\partial \hat{x}_a}\right) P, \qquad P(0) = P_0 \tag{3.40b}$$

It can be seen from (3.37a), (3.38), and (3.40) that the invariant imbedding method and extended Kalman filtering are <u>identical</u> if h is a linear function of x. It should be pointed out that, in contrast to the linear case, equations (3.40a) and (3.40b) are coupled equations, because the Jacobian matrices $\partial f_a/\partial \hat{x}_a$ and $\partial h/\partial \hat{x}_a$ are evaluated along the estimated augmented state $\hat{x}_a(t)$. The decoupling of the variance (equation (3.40b)) from (3.40a) can be achieved by evaluating the Jacobian matrices about the trajectory computed using the previous estimated initial conditions of the augmented state $\hat{x}_{a_0}$. This version of extended Kalman filter is equivalent to the quasilinearization method, as shown in Reference 21.

From the above descriptions of the various measurement error methods, it is clear that the conjugate gradient method has the advantages of computational simplicity and good convergence properties. The Newton's procedure is the most complicated from the computational viewpoint; further, the convergence is not guaranteed. The gradient method, although computationally simple, has a slow rate of convergence (see, for instance, Reference 19). The method of quasilinearization has had some encouraging applications in the past (References 12 and 33) for the extraction of stability and control derivatives of conventional aircraft whose dynamics may be represented by linear equations. It has moderate computational complexity. Numerical experience (References 12 and 33) has indicated that the rate of convergence is fast (quadratic) if it converges at all. The sequential computational schemes, as indicated earlier, have the capability of treating both measurement and process noise. From the computational point of view, the extended Kalman filter is much simpler than the invariant imbedding method, which requires the computation of the second-order partials. For these analytical and computational reasons, it was decided to numerically assess the following three methods:

1. Quasilinearization method
2. Conjugate gradient method, and
3. Extended Kalman filter.

However, before we present the numerical results, it seems appropriate to first examine the basic characteristics of this group of methods.

3.2.2 Basic Characteristic of Measurement-Error Methods

From the above descriptions for the various measurement-error methods, it is clear that the computational scheme of these methods is basically iterative; the batch processing schemes are globally iterative and the sequential methods are locally iterative by updating the trajectory at each data point. Aside from the iterative feature, this group of methods has its own associated statistical properties. Furthermore, there is a problem associated with the uniqueness of the solution. Let us first discuss the statistical properties.

Statistical Properties of the Measurement-Error Methods

In Section V, we shall discuss at length the statistical properties of sequential estimation schemes such as those discussed in 3.2.1. Consequently, we shall discuss here only the statistical properties of the batch processing methods. The following properties are formally established:

(i) If the process noise $w(t)$ (or modeling error) is absent, and if the measurement noise is zero mean white Gaussian as formulated in 4.2, then the batch process estimates are asymptotically efficient (i.e., consistent and minimum mean-square).

(ii) If the process noise (or modeling error) is absent, and if the measurement noise is nonwhite (time correlated) but stationary and ergodic, then the batch process estimates are asymptotically unbiased.

(iii) Regardless of white or nonwhite zero mean measurement noise, if the process noise $w(t)$ (or modeling error) is present, then the estimates are asymptotically biased if the dynamical system and/or the measurement system are nonlinear; however, the estimates are asymptotically unbiased if both the system dynamics and the measurement system are linear.

The first property is very clear, since under the stated conditions the estimator is identical to the maximum likelihood (non-Bayesian) estimator as explained at the beginning of the Section 3.2. Consequently, the assertion follows (see for example, Reference 34).

To establish the second property, one first notes from (3.19) that the regressor is nonstochastic (see Appendix B). Also, as $\Delta x_a \to 0$, (3.19) implies

$$\frac{1}{t_f}\int_0^{t_f}\left[\frac{\partial h}{\partial x}\frac{\partial x}{\partial x_0}\,\Big|\,\frac{\partial h}{\partial x}\frac{\partial x}{\partial p}+\frac{\partial h}{\partial p}\right]^T R^{-1}\left\{h\left[x(x_0,p),p,m\right]+v \right. \tag{3.41}$$

$$\left. -h\left[x(\hat{x}_0,\hat{p}),\hat{p},m\right]\right\}\longrightarrow 0$$

Thus, assuming the process is ergodic, then, since $E\{v(t)\}=0$,

$$E\left\{h\left[x(\hat{x}_0,\hat{p}),\hat{p},m\right]\right\} = h\left[x(x_0,p),p,m\right]$$

as $t_f \to \infty$. This implies

$$E\left[\hat{x}_a(0)\right] = \hat{x}_{a_0} \quad as \quad t_f \to \infty$$

as asserted in the second property.

To establish (iii), we note that, in lieu of (3.13) and (3.14), the linearization about the trajectory becomes

$$x(\hat{x}_0 + \Delta x, \hat{p} + \Delta p, w) \approx x(\hat{x}_0, \hat{p}, 0) + \begin{bmatrix} \frac{\partial x}{\partial x_0} & \frac{\partial x}{\partial p} \end{bmatrix} \begin{bmatrix} \Delta x_0 \\ \Delta p \end{bmatrix} + \frac{\partial x}{\partial w} w \tag{3.42a}$$

$$h[x, p, m] = h[x(\hat{x}_0, \hat{p}, 0), \hat{p}, m] + \left[\frac{\partial h}{\partial x} \frac{\partial x}{\partial x_0} \,\middle|\, \frac{\partial h}{\partial x} \frac{\partial x}{\partial p} + \frac{\partial h}{\partial p} \right] \begin{bmatrix} \Delta x_0 \\ \Delta p \end{bmatrix} + \frac{\partial h}{\partial x} \frac{\partial x}{\partial w} w \tag{3.42b}$$

Hence, in place of (3.19), we have

$$\Delta x_{a_0} = \left\{ \int_0^{t_f} \left[\frac{\partial h}{\partial x} \frac{\partial x}{\partial x_0} \,\middle|\, \frac{\partial h}{\partial x} \frac{\partial x}{\partial p} + \frac{\partial h}{\partial p} \right]^T R^{-1} \left[\frac{\partial h}{\partial x} \frac{\partial x}{\partial x_0} \,\middle|\, \frac{\partial h}{\partial x} \frac{\partial x}{\partial p} + \frac{\partial h}{\partial p} \right] dt \right\}^{-1} \cdot$$

$$\cdot \int_0^{t_f} \left[\frac{\partial h}{\partial x} \frac{\partial x}{\partial x_0} \,\middle|\, \frac{\partial h}{\partial x} \frac{\partial x}{\partial p} + \frac{\partial h}{\partial p} \right]^T R^{-1} \left\{ y(t) - h[x(\hat{x}_0, \hat{p}, 0), \hat{p}, m] - \frac{\partial h}{\partial x} \frac{\partial x}{\partial w} w \right\} dt \tag{3.43}$$

Thus, the regressor is still nonstochastic, but in lieu of (3.41) we have

$$\frac{1}{t_f} \int_0^{t_f} \left[\frac{\partial h}{\partial x} \frac{\partial x}{\partial x_0} \,\middle|\, \frac{\partial h}{\partial x} \frac{\partial x}{\partial p} + \frac{\partial h}{\partial p} \right]^T R^{-1} \left\{ h[x(x_0, p, w), p, m] + v - h[x(\hat{x}_0, \hat{p}, 0), \hat{p}, m] - \frac{\partial h}{\partial x} \frac{\partial x}{\partial w} w \right\} \longrightarrow 0 \tag{3.44}$$

Since $E\{w(t)\} = E\{v(t)\} = 0$, and since

$h[x(x_0, p, w), p, m] = h[x(x_0, p, 0), p, m]$ if f and h are linear

$h[x(x_0, p, w), p, m] \neq h[x(x_0, p, 0), p, m]$ if f and/or h are nonlinear

the assertion (iii) is established.

Nonuniqueness Problem

All the parameter estimation schemes with a performance index (3.11) are essentially methods for solving the nonlinear simultaneous algebraic equations

$$\frac{\partial J}{\partial p_i} = 0 \quad \forall i \tag{3.45}$$

Indeed, equation (3.19) is essentially a scheme of solving equation (3.45) using Newton's method (with curvature matrix simplified). Since equations (3.45) are simultaneous nonlinear algebraic equations in the unknown parameters, the existence of multi-roots is by no means rare; when multiple roots are present, the solutions for the unknown parameters will be nonunique. Indeed, even for a simple system

$$\dot{x} = ax + b \tag{3.46a}$$

where $x(0) = 0$ and a, b are the unknown parameters to be identified, using data

$$y(t) = 1 - \frac{1}{2}\left(e^{-t} + e^{-2t}\right) \tag{3.46b}$$

and $t_f = 1$, which resembles (but not identically) a first-order response, it can be shown that there are two sets of solutions for a and b that satisfy (3.45) in the vicinity of the origin. They are:

1. $a = 0$ $\quad$ $b = 0.88$
2. $a = -1.57$ $\quad$ $b = 1.48$

If one begins with an estimate within the domain of convexity of the minimum ($a = -1.57$, $b = 1.48$), a use of the quasilinearization method converges to that minimum. On the other hand, if one begins with a poor estimate, which is within the domain of convexity of the local minimum ($a = 0$, $b = 0.88$), then the subsequent iterations converge to that local minimum. Results of the computer runs are shown in Figures 3-1 and 3-2.

3.2.3 Numerical Results from Computer-Generated Data

For the reasons discussed at the end of Section 3.2.1, the following three methods were chosen for numerical experimentations using the computer-generated data (see Appendix D for a detailed description). They are:

1. Quasilinearization Method
2. Conjugate Gradient Method
3. Extended Kalman Filter

Digital computer programs were written for these techniques using the nonlinear mathematical model chosen to represent the X-22A aircraft (2.9). Both acceleration and state variable measurements were used. The linearized equations of motion (D.2) were also programmed on a computer for each of these methods to save computer time in detailed evaluations. Table 3.5 shows a comparison of the results using the data generated from the linearized model. Acceleration measurements were not used, and the equations-of-motion method was used as the initial estimator. In performing the linear search (3.32) in the conjugate gradient algorithm, the step size was first determined automatically on the basis of a norm of the gradient (3.17). The linear search was then performed by successively doubling the step size until the performance index began to increase. Quadratic interpolation was then applied to determine the optimal α_i. The convergence criteria used were: (i) change in the components of the parameter, and (ii) change in the performance index. A similar procedure was applied to the quasilinearization method for the one-dimensional search.

For the extended Kalman filter runs, the discrete version of the filter rather than the continuous version (3.40) was used. The discrete version of the extended Kalman filter is derived in Section V, and is:

$$
\left.
\begin{aligned}
\hat{x}_{k|k} &= \hat{x}_{k|k-1} + \psi_k \left[y_k - h(\hat{x}_{k|k-1}) \right] \\
\psi_k &= P_{k|k-1} H_k^T \left[H_k P_{k|k-1} H_k^T + R_k \right]^{-1} \\
P_{k|k-1} &= \Phi_{k,k-1} P_{k-1} \Phi_{k,k-1}^T + \Gamma_k Q_k \Gamma_k^T \\
P_k &= (I - \psi_k H_k) P_{k|k-1} \\
\hat{x}_{k|k-1} &= g_k(\hat{x}_{k-1|k-1})
\end{aligned}
\right\} \qquad (3.47)
$$

where $\hat{x} \triangleq \hat{x}_a$ is the augmented state $(x^T, \rho^T)^T$ (for notational convenience the subscript " a " is dropped in the above algorithm); ψ_k is the filter gain; $P_{k|k-1}$ is the extrapolated covariance matrix; Γ_k is the gust effective matrix, and P_k is the covariance matrix of the estimate $\hat{x}_{k|k-1}$. The Kalman runs were initialized using the param... and variances computed from the equations-of-motion method (equations (3.3)and (3.3d), respectively). The initial aircraft state and its covariance matrix were chosen to be the state at the first data point and R , respectively. The notation F_k for the Kalman runs in Table 3.5 is to mean that the initial P_o used to start up the extended Kalman is

$$
P_o = \begin{pmatrix} R & 0 \\ 0 & kP_{\epsilon e} \end{pmatrix},
$$

where $P_{\epsilon e}$ is a diagonal matrix whose diagonal elements are variances computed using (3.3d). The results clearly show that the conjugate gradient method does not give satisfactory results. For the case in which process noise is absent and the measurement noise level is moderate (1-C data), the results using quasilinearization and the extended Kalman filter are comparable. However, with the presence of moderate process noise (1-D data), the parameters estimated from the extended Kalman filter are clearly superior. Table 3.6 shows a comparison of the results of the parameters estimated from the quasilinearization program and extended Kalman filter program using a nonlinear model with acceleration measurements. Again, the Kalman estimates appear to be better.

From the numerical experimentation and the analysis of the basic characteristics associated with the measurement error methods, the following remarks are in order:

1. If the process noise or modeling errors are absent, then the quasilinearization method is a sound identification technique; however, numerically, problems such as convergence and nonuniqueness of the solution do exist.

2. The conjugate gradient method does not appear suitable for VTOL aircraft parameter identification.

3. The extended Kalman filter is a promising technique for VTOL parameter identification.

4. Since process noise (gusts, model errors, etc.) is always present, the quasilinearization method is less promising than the extended Kalman filter.

3.3 Methods Treating Both Measurement and Process Noise

As formulated in Section II, the problem of identifying V/STOL stability and control parameters is basically a problem of estimating parameters and states in a noisy nonlinear dynamic system utilizing noisy nonlinear measurements. This problem has been the subject matter of many papers and reports in the past few years. However, frequently motivated by the desire to estimate the current state and parameters for control purposes (see for example, References 35, 36, and 37), the majority of the effort has been in the area of nonlinear filtering. Schwartz and Stear (Reference 38) recently presented a computational comparison of six currently available higher-order (second-order) nonlinear filtering techniques with the extended Kalman filter, which is a first-order nonlinear filter. They concluded that, as far as their numerical experimentation was concerned, the added complexity of the higher order was not warranted.

However, as we discussed earlier, a fundamental difficulty associated with identification of the V/STOL aircraft parameters is its modeling problem. Consequently, the identification technique must have the capability of detecting the modeling errors. Filtering alone is not capable of doing so; the detection of the modeling errors can only be done through data smoothing. Bryson and Frazier (Reference 4) were the first to formulate the smoothing problem for a continuous nonlinear system; they formulated the problem as a deterministic optimal control problem with a quadratic performance index. Although the solution to the nonlinear smoothing problem was obviously formidable and was not attempted, they were the first to obtain the recursive solutions to the linear case. Cox (References 5 and 6) later provided a general formulation of the estimation of state and parameters of nonlinear systems with Gaussian process and measurement noise, and for the linear case he rederived the smoothing solution of Bryson and Frazier. Subsequently, Rauch (References 39 and 40) obtained a solution for the discrete linear case. In his thesis, Fraser (Reference 41) discussed extensively the computational aspects of the linear smoothing problems. Meditch (Reference 42) made an attempt to solve a nonlinear fixed-interval problem by directly solving the two-point boundary value problem using successive approximations. The computational load is formidable even for a second-order problem; furthermore, as new data are received, a new two-point boundary value problem has to be solved.

In order to investigate in some depth the feasibility of applying a smoothing technique to the V/STOL parameter identification problem, Systems Control, Inc., Palo Alto, California, under subcontract to CAL, examined two smoothing algorithms and concluded that

1. Standard Smoothing Algorithm of Rauch
   - requires large storage for filtered state and covariance matrices and hence is difficult to implement.

2. A Simplified Smoothing Algorithm

- requires the use of only the data but
- it has computation difficulty.

An alternate simplified "smoothing" algorithm using backward filtering was proposed. Although this method is not capable of estimating the unknown forcing functions, the parameter estimates may be significantly improved by "appropriately" increasing the covariance from the results of the first forward filter run to start up the backward filter. However, in all of the above work, the primary concern has been with the fixed-interval rather than the fixed-point smoothing problem. Fixed-point smoothing is the important problem associated with parameter identification, as will be discussed in Section 5.1.3.

The problem of fixed-point smoothing for a linear system was first derived by Rauch (Reference 39) for discrete systems and later by Meditch (References 43 and 44) for continuous systems. Unfortunately, very little work has been done toward solving the fixed-point smoothing problem for nonlinear systems, a problem of considerable importance in parameter identification. In a recent paper, Kagiwada (Reference 45) employed invariant imbedding to obtain a sequential approximate solution for the fixed-point smoothing problem for continuous nonlinear systems with continuous nonlinear measurements. Because of the deterministic approach of using the least square cost functional, the quality of the obtained estimates is usually hard to interpret. Furthermore, it is interesting to note that the filtering pass is identical to the Detchmendy-Sridhar filter (Reference 27). The Detchmendy-Sridhar filter is only first order in the system dynamics nonlinearity, and therefore the bias of the estimates may be significant when system nonlinearity is severe. Thus, the development of a new technique which does not have this limitation for V/STOL parameter identification is required.

The development of a new technique is described in detail in Section V. In developing the technique, a continuous nonlinear system driven by white Gaussian noise with noisy discrete nonlinear measurements was considered to characterize the model - as formulated in Section II.

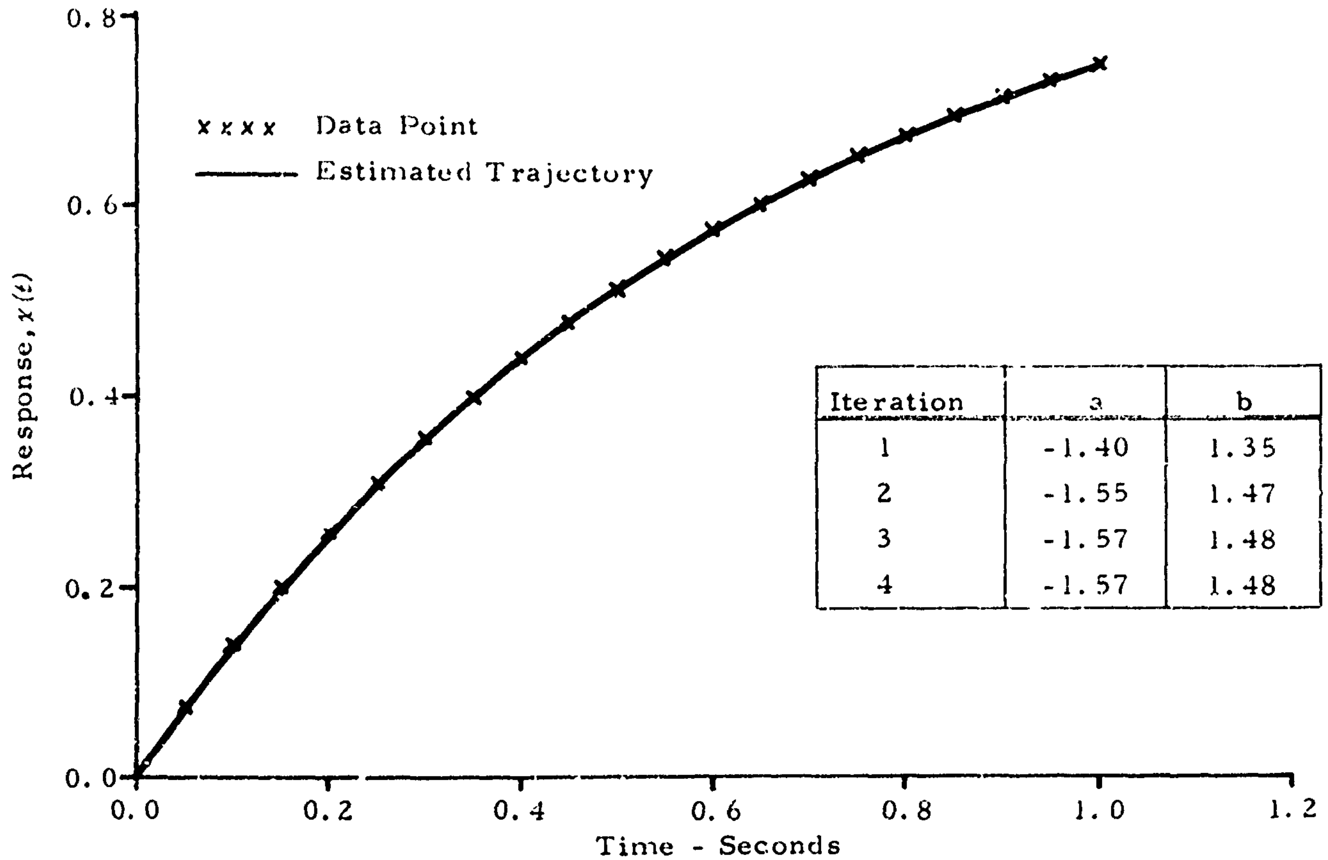

Iteration	a	b
1	-1.40	1.35
2	-1.55	1.47
3	-1.57	1.48
4	-1.57	1.48

Figure 3-1 Quasilinearization Solution for the Minimum

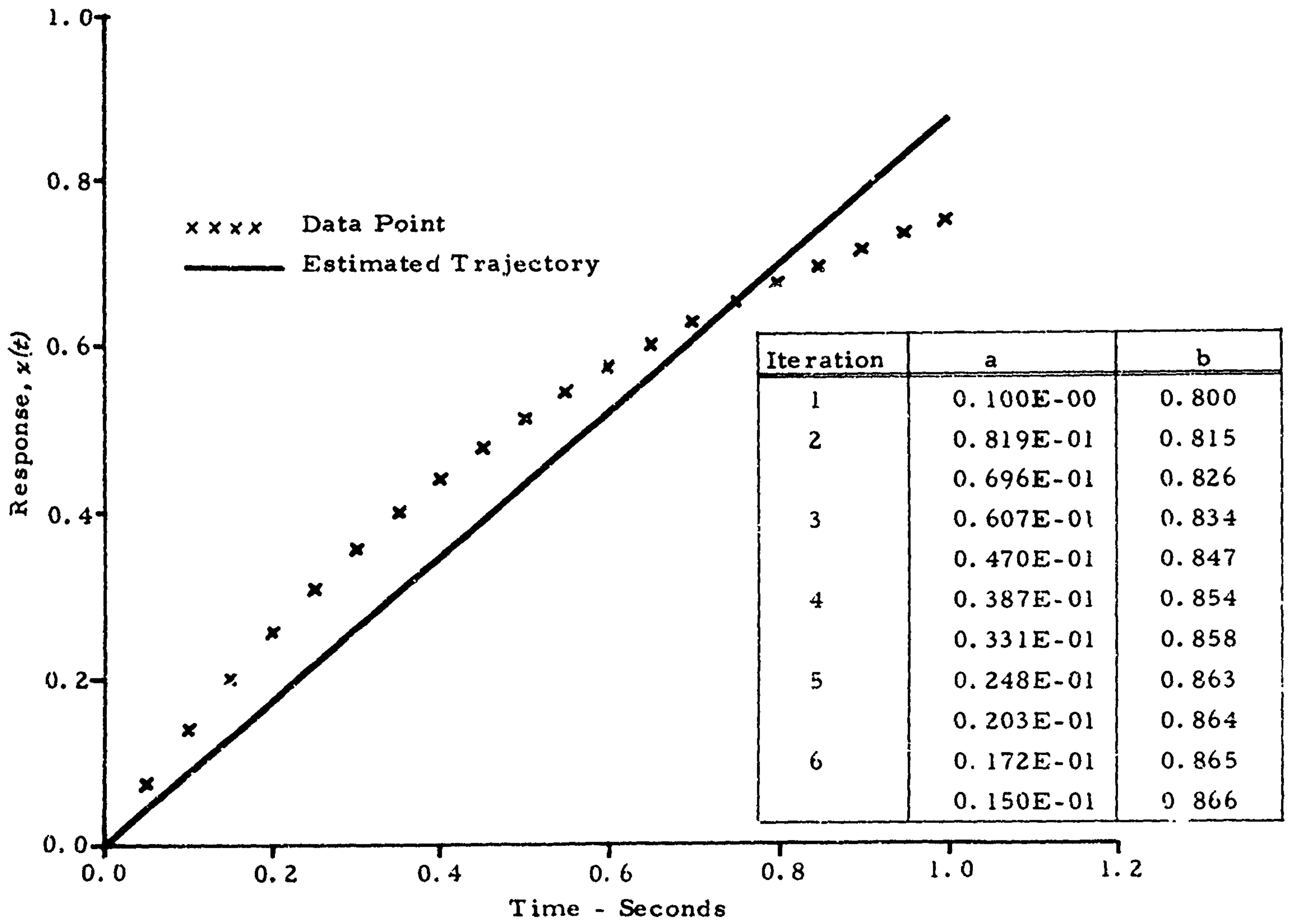

Iteration	a	b
1	0.100E-00	0.800
2	0.819E-01	0.815
	0.696E-01	0.826
3	0.607E-01	0.834
	0.470E-01	0.847
4	0.387E-01	0.854
	0.331E-01	0.858
5	0.248E-01	0.863
	0.203E-01	0.864
6	0.172E-01	0.865
	0.150E-01	0.866

Figure 3-2 Quasilinearization Solution for the Local Minimum

TABLE 3-1 - Effects of Process and Measurement Noise on Parameter Estimates Using the "Equations-of-Motion" Method *

Data / Parameters	Actual	1-A	1-B	1-C	1-D	1-0 +
m_u	-0.0044	-0.004233	-0.004383	-0.00171	-0.003190	-0.0044
m_w	-0.0075	-0.007304	-0.007518	-0.0023	-0.006190	-0.0075
m_q	-0.625	-0.5575	-0.6329	-0.5488	-0.2966	-0.625
$m_{\delta_{ES}}$	0.480	0.4538	0.4945	0.2990	0.4047	0.480
X_u	-0.150	-0.1451	-0.1484	-0.06531	-0.09615	-0.150
X_w	0.021	0.03184	0.02665	0.1889	0.1324	0.021
$X_{\delta_{ES}}$	1.370	0.9849	1.024	-3.5716	-3.008	1.370
Z_u	-0.216	-0.2060	-0.2163	-0.07619	-0.1845	-0.216
Z_w	-0.650	-0.6275	-0.6540	-0.3657	-0.6045	-0.650
$Z_{\delta_{ES}}$	1.660	0.7585	2.543	-7.506	3.907	1.660

* Columns 1-A through 1-D in Tables 3-1 through 3-4 refer to data contaminated with varying degrees of noise. See Table D-2, Appendix D for explanation and definition of noise levels. The control perturbation is shown below:

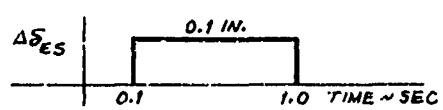

\+ This column refers to noise free data.

TABLE 3-2 - Effects of Process and Measurement Noise on Parameter Estimates Using Modified Spline Function Method

Data / Parameters	Actual	1-A	1-B	1-C	1-D	1-0
M_u	-0.0044	-0.00436	-0.00432	-0.00463	-0.00342	-0.00426
M_w	-0.0075	-0.00800	-0.00799	-0.00900	-0.00864	-0.00783
M_q	-0.625	-0.3416	-0.4223	-0.1426	0.5056	-0.3874
$M_{\delta_{ES}}$	0.480	0.4219	0.4571	0.4142	0.2910	0.4218
X_u	-0.150	-0.1794	-0.1840	-0.3840	-0.2713	-0.1331
X_w	0.021	-0.01797	-0.02642	-0.3885	-0.1644	0.06725
$X_{\delta_{ES}}$	1.370	2.5892	2.7601	15.8283	8.8060	-0.2758
Z_u	-0.216	-0.2145	-0.2078	-0.2268	-0.09582	-0.2071
Z_w	-0.650	-0.6463	-0.6454	-0.6556	-0.4532	-0.6352
$Z_{\delta_{ES}}$	1.660	1 4168	2.6179	2.4869	0.6194	0.9045

TABLE 3-3a - Effects of Process and Measurement Noise on Parameter Estimates Using Polynomial Estimator - Fifth Degree

Data / Parameters	Actual	1-A	1-B	1-C	1-D	1-0
M_u	-0.0044	-0.004722	-0.004265	-0.005028	-0.001646	-0.004598
M_w	-0.0075	-0.008286	-0.007303	-0.009393	-0.001477	-0.0079106
M_q	-0.625	-0.5135	-0.5777	-0.2452	-0.9620	-0.57963
$M_{\delta_{ES}}$	0.480	0.4675	0.4661	0.4167	0.4031	0.47660
X_u	-0.150	-0.2282	-0.2286	-0.4796	-0.3904	-0.1638
X_w	0.021	-0.1218	-0.1197	-0.5492	-0.3662	-0.009245
$X_{\delta_{ES}}$	1.370	5.669	5.554	16.784	12.691	2.497
Z_u	-0.216	-0.3349	-0.3413	-0.4187	-0.2489	-0.3101
Z_w	-0.650	-0.9137	-0.9266	-1.064	-0.7220	-0.8684
$Z_{\delta_{ES}}$	1.660	11.416	12.988	14.797	9.125	10.257

TABLE 3-3b - Effects of Process and Measurement Noise on Parameter Estimates Using Polynomial Estimator - Ninth Degree

Data / Parameters	Actual	1-A	1-B	1-C	1-D	1-0
M_u	-0.0044	-0.004251	-0.004161	-0.004549	-0.003353	-0.004136
M_w	-0.0075	-0.00760	-0.007398	-0.008775	-0.008339	-0.007230
M_q	-0.625	-0.4437	-0.5232	-0.1633	0.3959	-0.5095
$M_{\delta_{ES}}$	0.480	-0.4293	0.4616	0.3800	0.2842	0.4378
X_u	-0.150	-0.2111	-0.2173	-0.4545	-0.3416	-0.1492
X_w	0.021	-0.08973	-0.1017	-0.5211	-0.3015	0.02280
$X_{\delta_{ES}}$	1.370	4.650	5.080	16.612	11.748	1.302
Z_u	-0.216	-0.2238	-0.2131	-0.2300	-0.1173	-0.2141
Z_w	-0.650	-0.6593	-0.6521	-0.6507	-0.4908	-0.6452
$Z_{\delta_{ES}}$	1.660	1.629	2.708	0.3606	1.0023	1.453

TABLE 3-4a - Effects of Process and Measurement Noise on Parameter Estimates Using Denery's Estimator - 10% Increase of the True Values as Nominal Values

Data / Parameters	Actual	1-A	1-B	1-C	1-D	1-0	Nominal*
M_u	-0.0044	-0.004295	-0.00566	-0.004487	-0.01057	-0.00438	-0.00484
M_w	-0.0075	-0.007605	-0.009908	-0.007553	-0.02395	-0.007457	-0.00825
M_q	-0.625	-0.4698	-0.5033	-0.5597	1.861	-0.6254	-0.6875
$M_{\delta_{ES}}$	0.480	0.4327	0.4679	0.4357	0.1484	0.4784	0.528
X_u	-0.150	-0.1802	-0.2455	-0.1471	-1.255	-0.1503	-0.165
X_w	0.021	-0.002718	-0.03766	0.06494	-1.445	0.02079	0.0231
$X_{\delta_{ES}}$	1.370	2.308	-3.730	-1.697	1.487	1.369	1.507
Z_u	-0.216	-0.2177	-0.2621	-0.2052	-0.3541	-0.2159	-0.2376
Z_w	-0.650	-0.6519	-0.7229	-0.6143	-0.8904	-0.6503	-0.715
$Z_{\delta_{ES}}$	1.660	1.384	1.465	-0.8986	2.097	1.661	1.82[illegible]

* Nominal values in F_N and G_N (see Appendix C)

TABLE 3-4b - Effects of Process and Measurement Noise on Parameter Estimates Using Denery's Estimator - Nominal Values Being About 50% of the True Values

Parameters \ Data	Actual	1-A	1-B	1-C	1-D	1-0	Nominal *
M_u	-0.0044	-0.004296	-0.006223	-0.005581	-0.01135	-0.004327	-0.0066
M_w	-0.0075	-0.007333	-0.01082	-0.008234	-0.02506	-0.007290	-0.01125
M_q	-0.625	-0.5282	-0.4542	-0.6655	1.652	-0.6398	-0.9375
$M_{\delta_{ES}}$	0.480	0.4307	0.4507	0.4064	0.2379	0.4750	0.720
X_u	-0.150	-0.1512	-0.2144	-0.2632	-1.033	-0.1509	-0.225
X_w	0.021	0.03810	0.03613	0.4138	-1.172	0.01984	0.0315
$X_{\delta_{ES}}$	1.370	-0.001137	-7.072	-1.633	1.205	1.387	0.2052
Z_u	-0.216	-0.2181	-0.2946	-0.2697	-0.3910	-0.2143	-0.324
Z_w	-0.650	-0.6463	-0.7703	-0.6815	-0.9601	-0.6470	-0.975
$Z_{\delta_{ES}}$	1.660	0.7379	1.280	-2.737	3.892	1.535	2.490

* Nominal values in F_N and G_N (see Appendix C)

TABLE 3-5

Comparison of Methods * Using Linearized Model

Parameters	Actual Param. Values	1-C Data (Moderate Meas. Noise)				1-D Data (Moderate Meas. & Process Noise			
		E.O.M	Conjugate Gradient	Quasi	Kalman ** (F_{10})	E.O.M.	Conjugate Gradient	Quasi	Kalman ** (F_{10})
M_u	-0.0044	-0.00171	-0.002681	-0.00443	-0.00473	-0.00319	No Solutions Obtained	-0.00453	-0.00424
M_w	-0.075	-0.002301	-0.003988	-0.00655	-0.00800	-0.00619		-0.00689	-0.00847
M_q	-0.625	-0.5488	-0.5619	-0.9142	-0.5542	-0.2966		-1.2957	-0.3217
$M_{\delta_{ES}}$	0.180	0.2990	0.3185	0.5069	0.4464	0.4047		0.7585	0.4967
X_u	-0.150	-0.06531	-0.07989	-0.1225	-0.1761	-0.09615		-0.9571	-0.1965
X_w	0.071	0.1889	0.2031	0.1075	0.0152	0.1324		-1.4357	-0.0229
$X_{\delta_{ES}}$	1.370	-3.5716	-3.7183	-2.5962	-0.1671	-3.008		57.778	0.6127
Z_u	-0.216	-0.07619	-0.07736	-0.1946	-0.2358	-0.1845		-0.0573	-0.1616
Z_w	-0.650	-0.3657	-0.3686	-0.5887	-0.6775	-0.6045		-0.3435	-0.5916
$Z_{\delta_{ES}}$	1.660	-7.506	-7.1038	-1.5345	1.2135	3.907		-5.3359	4.7322

* Without using acceleration measurements; the control perturbation is shown below.

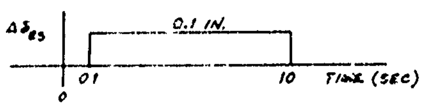

** F_{10} : Denotes the Kalman filter run for which the initial covariance matrix P_0 for the parameters is equal to variances of the parameters estimated from the E.O.M. estimator multiplied equally by 10.

TABLE 3-6

Comparison of Methods Using Nonlinear Model

Parameter	Actual Value	2-C-1 + Moderate Measurement Noise: Equation of Motion Estimates	2-C-1 + Moderate Measurement Noise: Quasilin-* earization	2-C-1 + Moderate Measurement Noise: Kalman** F_{10}	2-D-1 + Moderate Measurement Noise: Equation of Motion Estimates	2-D-1 + Moderate Measurement Noise: Quasilin-* earization	2-D-1 + Moderate Measurement Noise: Kalman** F_1
M_0 (1)	.50518	-1.281	-1.2896	.686	-.6691	-.6691	.4758
M_0 (u)	-.00308	.02197	.02216	-.0064	.019898	.019898	.00205
M_0 (u^2)	-6.2×10^{-6}	-9.3×10^{-5}	-9.53×10^{-5}	8.6×10^{-6}	-.0001136	-.0001136	-4.3×10^{-5}
M_w (1)	-.001747	.02061	.01953	-.00294	.01094	.01094	-.00163
M_w (u)	-5.53×10^{-5}	-.000228	-.000216	-4.3×10^{-5}	-.0001804	-.0001804	-7.64×10^{-5}
M_q (1)	-.497	-2.850	-2.6792	-.760	-1.2881	-1.2881	-.8519
M_q (u)	-.00163	.01777	.01649	.00065	.007815	.007815	.00315
M_δ (1)	.3275	.37613	.46712	.336	-.7305	-.7305	-.581
M_δ (u)	.001167	.0006687	.0001056	.0011	.009188	.009188	.0080
X_0 (1)	18.30	-15.884	-128.84	13.93	-19.148	-19.1477	-5.671
X_0 (u)	-.09167	.4332	1.587	-.0297	.4802	.4802	.2408
X_0 (u^2)	-.0003	-.00232	-.00468	-.000523	-.002485	-.002485	-.00149
X_w (1)	.2211	.6174	.9214	-.257	.6933	.6933	.4469
X_w (u)	-.001587	-.00464	-.0068	-.00189	-.005292	-.005292	-.00318

\+ See Table D-2, Appendix D for explanation and definition of noise levels. 2-C-1 and 2-D-1 data were generated using the control perturbation shown below

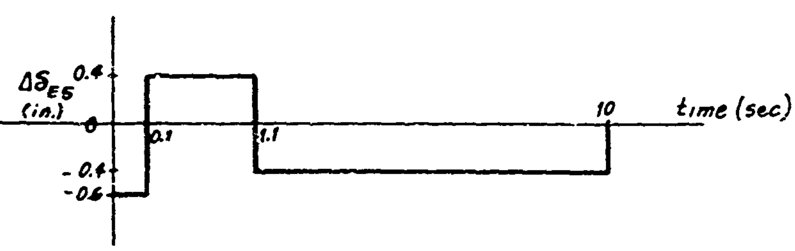

TABLE 3-6 (cont)

Parameter		Actual Value	2-C-1† Moderate Measurement Noise			2-D-1† Moderate Measurement Noise		
			Equation of Motion Estimates	Quasilin-* earization	Kalman** F_{10}	Equation of Motion Estimates	Quasilin-* earization	Kalman** F_1
X_δ	1	-.778	-21.395	370.6	1.584	-28.6304	-28.6363	7.115
	u	.0184	.17822	-2.82	.000191	.23474	.23479	-.0396
Z_0	1	-32.17	-30.454	-7.8956	-47.99	13.1365	13.1373	2.514
	u	.910	.99062	.7929	1.146	.4669	.4669	.630
	u^2	-.007	-.00777	-.00770	-.00796	-.006384	-.006384	-.0071
Z_w	1	-.2939	.009735	.0001115	-.148	-.51487	-.51487	-.6462
	u	-.00287	-.004593	-.004019	-.0039	-.0006755	-.0006754	.00032
Z_δ	1	-.3507	-138.557	-254.6	.533	-155.795	-155.798	-99.59
	u	.01667	1.0839	1.991	.01507	1.23168	1.23168	.812

* In these quasilinearization runs, the term $\partial h / \partial p$ in (3.19) was neglected.

** F_1, F_{10} : Denote the Kalman filter runs for which the initial covariance matrix P_0 for the parameters is equal to variance of the parameters estimated from the E.O.M. estimator multiplied by 1 and 10 respectively.

SECTION IV

PARAMETER IDENTIFIABILITY

The identifiability of parameters is concerned with the ability to solve for all the unknown parameters from the given data. It is intuitively obvious that those parameters which have no effects on the data cannot be identified. Consider a hovering X-22A aircraft in calm air, for example. Then, for application of a collective input ΔB_c, all the stability and control parameters with the exception of the vertical damping Z_w and the vertical control effectiveness Z_{δ_c} will not affect the data. Since in this situation only Z_w and Z_{δ_c} affect the data, it is intuitively clear that no parameters other than these two can be identified.

Perhaps it was Lee (Reference 46) who first discussed the identifiability of a system. He examined the identifiability of a single output linear autonomous discrete system and found that the system was identifiable if and only if the initial state vector (initial conditions of the system) excited all the natural modes of the system. Subsequently, Fisher (Reference 47) studied the identifiability of a continuous single input linear time-invariant system and concluded that the system was identifiable if and only if the system was completely controllable and the control function was not linearly related to the state variables.

It was not until recently that the problem of identifiability of nonlinear systems was touched upon. In identifying the orbit parameters from lunar orbiter tracking, Pfeiffer (Reference 48) loosely defined unobservable, weakly observable, and strongly observable parameters. He defined the observability of these parameters in terms of the diagonal elements of an orthogonal transformation of the matrix in the normal equation resulting from a linearization of orbit equations about the nominal trajectory. Experience in linear systems has indicated that identifiability is a property different from observability; the former depends on both system and input, the latter, however, depends on the system only. Because of this, a clear cut condition for the identifiability of nonlinear systems has been lacking.

Closely related to the identifiability problem is the problem of the uniqueness of the solutions. There appear to be two different uniqueness problems: one stems from the system configuration, and the other from the data (inputs and outputs) given. The latter problem was discussed in Section 3.2. Comparatively speaking, it has received less treatment than that stemming from the system configuration. Lavi & Strauss (Reference 49) were perhaps the first to mention this problem; unfortunately, without offering their own study, they only suggested that this problem should be investigated.

In the early stages of our study of the identification of VTOL aircraft parameters, it was found that identification techniques such as quasilinearization did not give unique solutions - the solutions depended upon the initial estimates. This prompted an investigation into the problem of identifiability and uniqueness of the solutions. Some results of this investigation are presented here.

4.1 Identifiability for Noiseless Measurements - Linear Stationary Systems

To begin with, it seems instructive to analyze the simplest case, namely the case in which the system is linear and the data (output) are noiseless. Consider the following problem:

Given - A multi-input, multi-output linear time-invariant system

System S-1
$$\begin{cases} \dot{x}(t) = Fx(t) + Gu(t) & (4.1a) \\ y(t) = Hx(t) & (4.1b) \end{cases}$$

where x is the state, n-vector

u is the control vector, r-vector

y is the output, m-vector

and the data $u(t)$ and $y(t)$ are given for $0 \leq t \leq t_f$

Find: the triple (F, G, H)

(a) Uniqueness problem and the maximum number of independent parameters -

It is readily seen that there is no unique solution for the triple (F, G, H). Indeed, there are infinite sets of (F, G, H) that are satisfied by the equations (4. 1a) and (4. 1b) with the data given. To see this, let us consider a nonsingular linear transformation M such that

$$\tilde{x} = Mx \tag{4.2}$$

then

$$\dot{\tilde{x}} = MFM^{-1}\tilde{x} + MGu \tag{4.3a}$$

$$y = HM^{-1}\tilde{x} \tag{4.3b}$$

Note that, as far as input-output relationships are concerned, systems (4. 1) and (4. 3) are completely equivalent; therefore, the solution for (F, G, H) is not unique. It is to be noted also that in equations (4. 1), there is a total of $n(n+m+r)$ parameters. However, these parameters are not independent insofar as the input-output relationships are concerned. In fact, it can be shown that there is a maximum of only $n(m+r)$ independent parameters (Reference 12).

As a result of the points discussed above, it can then be shown that only the transfer function matrix relating the outputs to the inputs can be identified. The transfer function matrix for the system (4. 1) is unique, and is independent of the coordinate systems (4. 2). Indeed, from (4. 3)

$$\begin{aligned} y(s) &= HM^{-1}\left[sI - MFM^{-1}\right]MG\,u(s) \\ &= HM^{-1}\left[sM^{-1} - FM^{-1}\right]^{-1}Gu(s) \\ &= H\left[sI - F\right]^{-1}Gu(s) \end{aligned} \tag{4.4}$$

which is the transfer function matrix for (4.1).

(b) Identifiability conditions and the solution -

In order to avoid the nonuniqueness problem for the triple (F , G , H), consider the special, but important, case in which all of the state variables are measurable, i.e., $H = I$. Then:

$$\text{System } S\text{-}2 \quad \begin{cases} \dot{x} = Fx(t) + Gu(t) & (4.5\text{a}) \\ y(t) = x(t) & (4.5\text{b}) \end{cases}$$

From (4.5a)

$$x(t) - x(0) = F\int_0^t x(\tau)d\tau + G\int_0^t u(\tau)d\tau$$

Let

$$\hat{x}(t) = x(t) - x(0) \qquad \text{- n-vector function}$$

$$z(t) = \int_0^t x(\tau)\,d\tau \qquad \text{- n-vector function}$$

$$V(t) = \int_0^t u(\tau)d\tau \qquad \text{- r- ector function}$$

Then

$$\hat{x}(t) = (F \mid G) \begin{bmatrix} Z(t) \\ \hline V(t) \end{bmatrix} \tag{4.6}$$

Define

$$A = \int_0^{t_f} \hat{x}(t) \left[z^T(t) \mid V^T(t) \right] dt \tag{4.7a}$$

$$B = \int_0^{t_f} \begin{bmatrix} Z(t) \\ \hline V(t) \end{bmatrix} \left[Z^T(t) \mid V^T(t) \right] dt \tag{4.7b}$$

Note that

A is $n \times (n+r)$ constant matrix

B is $(n+r) \times (n+r)$ constant matrix

If B has full rank (i.e., nonsingular), then

$$A = \left[F \,\vdots\, G \right] B \tag{4.8a}$$

or

$$\left[F \,\vdots\, G \right] = AB^{-1} \tag{4.8b}$$

Thus, system (S-2) is identifiable if and only if B is nonsingular. It is clear from (4.7b) that B is nonsingular if and only if $\left[\begin{array}{c} z(t) \\ \hline V(t) \end{array} \right]$ are linearly independent. Physically, this means that all the natural modes of the system (S-2) are excited and the control functions are linearly independent of the state variables and also independent of themselves. Fisher has investigated the case in which $V(t)$ is a scalar function (i.e., a single input case) and concluded that the system (S-2) with single input is identifiable if and only if the system is controllable and the control function is linearly independent of the stable variables. In the multi-input case, this set of conditions is not sufficient, because the controllability of the pair (F , G) does <u>not</u> imply pairwise controllability (i.e., (F , g_1), (F , g_2) , . . . ,(F , g_r) are controllable where $G \triangleq (g_1, g_2, \ldots, g_r)$). Thus, we conclude that:

(i) System (S-2) is identifiable if and only if all the natural modes of the system are excited and the control functions are linearly independent of the state variables.

(ii) A sufficient condition for the system S-2 to be identifiable is that (F , g_i) , $i = 1, 2, \ldots, r$ are pairwise controllable and the control functions $u(t)$ are linearly independent of the state variables, and are also independent of themselves.

It should be pointed out that the above conditions for identifiability are restricted to linear time-invariant systems. It is conceivable that this approach cannot readily be extended to nonlinear systems, which are of major importance to the VTOL parameter identification problem. In the following section we will take a different approach which utilizes the concept of the sensitivity vector functions.

4.2 Sensitivity Vector Functions

Linear System - Deterministic Case

In this section we shall discuss the importance of the sensitivity vector functions. Unlike quantities such as natural modes, which are of use solely in linear systems, a set of the sensitivity vector functions is a unique entity in both linear and nonlinear systems. Let us consider first the system S-2. Differentiating (4.5a) with respect to a representative parameter p_i (or p_j) gives

$$\frac{d}{dt}\frac{\partial x}{\partial p_i} = F\frac{\partial x}{\partial p_i} + \frac{\partial F}{\partial p_i}x(t) \tag{4.9a}$$

$$\frac{d}{dt}\frac{\partial x}{\partial p_j} = F\frac{\partial x}{\partial p_j} + \frac{\partial G}{\partial p_j}u(t) \tag{4.9b}$$

$$\frac{\partial x}{\partial p_i}(0) = 0\ ,\ i = 1, 2, \ldots, p \qquad \frac{\partial x}{\partial p_j}(0) = 0\ ,\ j = 1, 2, \ldots, q \tag{4.9c}$$

where p and q are the total number of parameters in F and G respectively. To see clearly the sensitivity vector functions in (4.9c) consider a third-order system with all nine unknown elements in F and six unknowns in G. We have then

$$\begin{aligned}
\frac{d}{dt}\frac{\partial x}{\partial p_1} &= F\frac{\partial x}{\partial p_1} + \begin{pmatrix} x_1(t) \\ 0 \\ 0 \end{pmatrix} \\
\frac{d}{dt}\frac{\partial x}{\partial p_2} &= F\frac{\partial x}{\partial p_2} + \begin{pmatrix} x_2(t) \\ 0 \\ 0 \end{pmatrix} \qquad \text{where } x(t) \triangleq \begin{pmatrix} x_1(t) \\ x_2(t) \\ x_3(t) \end{pmatrix} \\
\frac{d}{dt}\frac{\partial x}{\partial p_3} &= F\frac{\partial x}{\partial p_3} + \begin{pmatrix} x_3(t) \\ 0 \\ 0 \end{pmatrix} \\
\frac{d}{dt}\frac{\partial x}{\partial p_4} &= F\frac{\partial x}{\partial p_4} + \begin{pmatrix} 0 \\ x_1(t) \\ 0 \end{pmatrix} \\
&\ \vdots \\
\frac{d}{dt}\frac{\partial x}{\partial p_9} &= F\frac{\partial x}{\partial p_9} + \begin{pmatrix} 0 \\ 0 \\ x_3(t) \end{pmatrix}
\end{aligned} \tag{4.10a}$$

$$\frac{d}{dt}\frac{\partial x}{\partial p_{10}} = F\frac{\partial x}{\partial p_{10}} + \begin{pmatrix} u_1(t) \\ 0 \\ 0 \end{pmatrix}$$

$$\frac{d}{dt}\frac{\partial x}{\partial p_{11}} = F\frac{\partial x}{\partial p_{11}} + \begin{pmatrix} u_2(t) \\ 0 \\ 0 \end{pmatrix} \qquad \frac{\partial x}{\partial p_i}(0) = 0\,,\ i = 1,2,\ldots,15$$

$$\vdots$$

$$\frac{d}{dt}\frac{\partial x}{\partial p_{14}} = F\frac{\partial x}{\partial p_{14}} + \begin{pmatrix} 0 \\ 0 \\ u_1(t) \end{pmatrix} \tag{4.10b}$$

$$\frac{d}{dt}\frac{\partial x}{\partial p_{15}} = F\frac{\partial x}{\partial p_{15}} + \begin{pmatrix} 0 \\ 0 \\ u_2(t) \end{pmatrix}$$

$$\text{where} \quad u(t) \triangleq \begin{pmatrix} u_1(t) \\ u_2(t) \end{pmatrix}$$

The solution to the first equation in (4.10a) for example, is well known and is given by

$$\frac{\partial x}{\partial p_1}(t) = \int_0^t e^{F(t-\tau)} \begin{pmatrix} 1 \\ 0 \\ 0 \end{pmatrix} x_1(\tau)\,d\tau \tag{4.11}$$

Since the transition matrix e^{Ft} is nonsingular, i.e., all its columns (and hence its rows) are linearly independent, and since the integration (4.11) is a linear operation, it is readily seen from (4.10) that

(i) If $x_1(t)$, $x_2(t)$ and $x_3(t)$ are linearly independent and the control functions $u_1(t)$ and $u_2(t)$ are linearly independent and are also linearly independent of $x_1(t), x_2(t)$ and $x_3(t)$, then all the sensitivity vector functions are linearly independent.

(ii) The sensitivity functions are linearly dependent if the state variables are linearly dependent or the control functions are linearly dependent among themselves or are linearly dependent upon the state variables.

It is not difficult to see that these statements hold for a general case other than a third-order system.

The above conclusions can be combined to become:

Theorem 1

The sensitivity vector functions are nontrivial and are linearly independent if the state variables are linearly independent and the control functions are linearly independent and also linearly independent of the state variables.

Using spectral decomposition (References 50 and 51) and using the well known fact that a modal matrix (matrix consisting of all the eigenvectors) of F is nonsingular, it can readily be shown that the state variables are linearly independent if and only if all the natural modes of the system are excited.

Using this fact we establish the following important result:

Theorem 2

The sensitivity vector functions are nontrivial and are linearly independent if and only if all the natural modes of the system are excited and the control functions are linearly independent among themselves and are also linearly independent of the state variables.

The above theorem clearly indicates that the linear independency of the sensitivity vector functions is equivalent to the identifiability conditions.

Thus, we have established the following theorem:

Theorem 3

System (S-2) is identifiable if and only if all the sensitivity vector functions are nontrivial and are linearly independent.

From Theorem 3 it becomes apparent that an approach that uses sensitivity vector functions in lieu of equation (4.8) is possible. Denery (Reference 12) recently proposed a method for obtaining an initial parameter estimate using sensitivity vector functions and a state observer concept (Reference 52),as we discussed in 3. 1.

Special Case of System S-1 When H is Known

At this point, it is important to point out once again that the triple (F , G , H) in the system S-1 is, in general, not identifiable. However, if H is known and is square and nonsingular, then the above results still hold. If, on the other hand, H is not a square matrix, then the output sensitivity vectors

$$\frac{\partial y}{\partial p_i} = H \frac{\partial x}{\partial p_i}$$

are no longer linearly independent even if $\partial x/\partial p_i$ are. In other words, the output sensitivity vector functions are not linearly independent if the number of the unknown parameters in F and G is more than $n\,(m+r)$. This is illustrated in the following simple examples.

Example 1. Let the true values of the following single input - single output linear system

$$\dot{x} = Ax + bu$$
$$y = h'x$$

be

$$A = \begin{pmatrix} -1 & 0 \\ 0 & -2 \end{pmatrix} \qquad b = \begin{pmatrix} 1 \\ 1 \end{pmatrix} \qquad h' = \begin{pmatrix} 1 \\ 1 \end{pmatrix}$$

It is readily seen that the system is controllable and observable. Note that the system can have only a maximum number of four (2x (1+1)) independent parameters.

Let h be known and the nonzero parameters in A and b be unknowns. Note that there are four parameters and hence the condition for maximum number of independent parameters is met. A perturbation of those parameters from their true values yields the following (state) sensitivity vector equations with zero initial conditions:

$$\frac{d}{dt}\frac{\partial x}{\partial a_{11}} = A\frac{\partial x}{\partial a_{11}} + \begin{pmatrix} x_1(t) \\ 0 \end{pmatrix}$$

$$\frac{d}{dt}\frac{\partial x}{\partial a_{22}} = A\frac{\partial x}{\partial a_{22}} + \begin{pmatrix} 0 \\ x_2(t) \end{pmatrix}$$

$$\frac{d}{dt}\frac{\partial x}{\partial b_1} = A\frac{\partial x}{\partial b_1} + \begin{pmatrix} u(t) \\ 0 \end{pmatrix}$$

$$\frac{d}{dt}\frac{\partial x}{\partial b_2} = A\frac{\partial x}{\partial b_2} + \begin{pmatrix} 0 \\ u(t) \end{pmatrix}$$

Let the control function $u(t)$ be a unit step function for the sake of algebraic simplicity. A straightforward computation shows that

$$\frac{\partial x}{\partial a_{11}}(t) = \begin{bmatrix} (1-e^{-t})-te^{-t} \\ 0 \end{bmatrix}$$

$$\frac{\partial x}{\partial a_{22}}(t) = \begin{bmatrix} 0 \\ \frac{1}{4}(1-e^{-2t})-\frac{1}{2}te^{-2t} \end{bmatrix}$$

$$\frac{\partial x}{\partial b_1}(t) = \begin{bmatrix} (1-e^{-t}) \\ 0 \end{bmatrix}$$

$$\frac{\partial x}{\partial b_2}(t) = \begin{bmatrix} 0 \\ \frac{1}{2}(1-e^{-2t}) \end{bmatrix}$$

It is clear that these (state) sensitivity vector functions are linearly independent. The output sensitivity functions are also linearly independent. They are

$$y_1(t) \triangleq h'\left(\frac{\partial x}{\partial a_{11}}\right) = (1-e^{-t}) - te^{-t}$$

$$y_2(t) \triangleq h'\left(\frac{\partial x}{\partial a_{22}}\right) = \frac{1}{4}(1-e^{-2t}) - \frac{1}{2}te^{-2t}$$

$$y_3(t) \triangleq h'\left(\frac{\partial x}{\partial b_1}\right) = (1-e^{-t})$$

$$y_4(t) \triangleq h'\left(\frac{\partial x}{\partial b_2}\right) = \frac{1}{2}(1-e^{-2t})$$

Example 2. Now we consider the case when the true values of A and b are

$$A = \begin{pmatrix} -1 & 1 \\ 0 & -3 \end{pmatrix} \qquad b = \begin{pmatrix} 1 \\ 1 \end{pmatrix}$$

Note that the system is still controllable and observable. However, there are now five unknowns. A perturbation from these true values and again using a unit step function for the control function $u(t)$ yields the following (state) sensitivity vector functions:

$$\frac{\partial x}{\partial a_{11}} = \begin{bmatrix} \frac{33}{12}(1-e^{-t}) + \frac{1}{12}(1-e^{-3t}) - \frac{3}{2}te^{-t} \\ \hline 0 \end{bmatrix}$$

$$\frac{\partial x}{\partial a_{12}} = \begin{bmatrix} \frac{1}{2}(1-e^{-t}) - \frac{1}{6}(1-e^{-3t}) \\ \hline 0 \end{bmatrix}$$

$$\frac{\partial x}{\partial a_{22}} = \begin{bmatrix} \frac{1}{6}\left\{\frac{3}{2}(1-e^{-t}) - \frac{5}{6}(1-e^{-3t}) + te^{-3t}\right\} \\ \hline \frac{1}{3}\left\{\frac{1}{3}(1-e^{-3t}) - te^{-3t}\right\} \end{bmatrix}$$

$$\frac{\partial x}{\partial b_1} = \begin{bmatrix} (1-e^{-t}) \\ \hline 0 \end{bmatrix}$$

$$\frac{\partial x}{\partial b_2} = \begin{bmatrix} \frac{1}{2}(1-e^{-t}) - \frac{1}{6}(1-e^{-3t}) \\ \hline \frac{1}{3}(1-e^{-3t}) \end{bmatrix}$$

The state sensitivity vector functions are clearly still linearly independent. However, the output sensitivity functions are no longer linearly independent. They are

$$y_1(t) \triangleq h'\left(\frac{\partial x}{\partial a_{11}}\right) = \frac{32}{12}\left(1-e^{-t}\right) + \frac{1}{12}\left(1-e^{-3t}\right) - \frac{3}{2}\, t e^{-t}$$

$$y_2(t) \triangleq h'\left(\frac{\partial x}{\partial a_{12}}\right) = \frac{1}{2}\left(1-e^{-t}\right) - \frac{1}{6}\left(1-e^{-3t}\right)$$
$$= y_4(t) - y_5(t)$$

$$y_3(t) \triangleq h'\left(\frac{\partial x}{\partial a_{22}}\right) = \frac{1}{4}\left(1-e^{-t}\right) - \frac{1}{36}\left(1-e^{-3t}\right) - \frac{1}{6}\, t e^{-t}$$

$$y_4(t) \triangleq h'\left(\frac{\partial x}{\partial b_1}\right) = \left(1-e^{-t}\right)$$

$$y_5(t) \triangleq h'\left(\frac{\partial x}{\partial b_2}\right) = \frac{1}{2}\left(1-e^{-t}\right) + \frac{1}{6}\left(1-e^{-3t}\right)$$

From these examples, it is evident that for the deterministic case, identifiability implies uniqueness. Thus, nonuniqueness due to the system configuration is of no major problem in parameter identification. The major problem of uniqueness is due to data as was briefly discussed in Section 3.2.

Linear and Nonlinear Systems with Noisy Measurements

In the above discussion, we have restricted ourselves to the noiseless linear systems. It was shown that if a system is identifiable, the solution can readily be obtained without iteration and without initial guess values for the parameters. For noisy measurements, the regressor in the normal equation (4.8a) becomes stochastic, and the initial estimates using (4.8b)are asymptotically biased. The bias can be removed using iterative techniques such as the method of quasilinearization as discussed in Section 3.2. We now continue our discussions on the importance of the sensitivity vector functions in conjunction with the use of these methods. In order to be consistent with equation (4.8a), we shall first consider the quasilinearization method.

Consider the following problem:

$$\dot{x} = f(x, p, m), \quad x(0) = \alpha \tag{4.12a}$$

$$y = x + v \tag{4.12b}$$

where

x = state vector

y = output vector

v = error vector of the measurement

m = control vector

f = vector function of appropriate dimension

As shown in Section 3.2, the quasilinearization algorithm for the parameter estimation which minimizes the performance index

$$J = \frac{1}{2}\int_0^{t_f} (y-x)^T W (y-x)\,dt \tag{4.12c}$$

where t_f denotes the final time and W is a positive definite symmetrical matrix, is as follows :

$$\hat{p}_{new} = \hat{p}_{old} + \Delta p$$

$$= \hat{p}_{old} + \left[\int_0^{t_f}\left(\frac{\partial x}{\partial p}\right)^T W \left(\frac{\partial x}{\partial p}\right)\right]^{-1} \int_0^{t_f}\left(\frac{\partial x}{\partial p}\right)^T W\,(y - x(\hat{p}))\,dt \tag{4.13}$$

where

$$\frac{d}{dt}\left(\frac{\partial x}{\partial p}\right) = \left(\frac{\partial f}{\partial x}\right)\left(\frac{\partial x}{\partial p}\right) + \left(\frac{\partial f}{\partial p}\right), \quad \frac{\partial x}{\partial p}(0) = 0 \qquad \text{for parameters}$$

$$\frac{d}{dt}\left(\frac{\partial x}{\partial p}\right) = \left(\frac{\partial f}{\partial x}\right)\left(\frac{\partial x}{\partial p}\right), \qquad \frac{\partial x}{\partial p}(0) = I_n \qquad \text{for initial conditions}$$

$$x(\hat{p}_{old}) = \int_0^t f(x, \hat{p}_{old}, m)\,dt + x(0) \tag{4.14}$$

$$\left(\frac{\partial f}{\partial p}\right) \triangleq \left.\left(\frac{\partial f}{\partial p}\right)\right|_{x(\hat{p}_{old})}$$

It is clear from (4. 13) that the sensitivity vector functions $\partial x/\partial p_i$ in the sensitivity matrix $\partial x/\partial p$ must be linearly independent in order to have the matrix inversion in (4. 13) exist. In other words, the nonlinear system (4. 12) is identifiable by the method of quasilinearization if and only if the sensitivity vector functions $\partial x/\partial p_i$ are linearly independent. From the connection established in Reference 19 between the method of quasilinearization and extended Kalman filtering, it can be shown that the above statement is also true for the method of extended Kalman filtering.

In general, the output in equation (4. 12b) is to be replaced by

$$y = g(x)$$

and the linearity of the output sensitivity vector functions

$$\frac{\partial y}{\partial p_i} = \left(\frac{\partial g}{\partial x}\right)\frac{\partial x}{\partial p_i}$$

becomes essential for the identification of the unknown parameters p in (4. 12a).

4. 3 Problem of Uniqueness Due to Data

On the basis of the previous discussion, it can be shown that, for the deterministic case, the solution for the parameters is unique if the system is identifiable. For a noniterative scheme (such as the scheme defined in equation (4. 8b)), it is clear that the solution is unique regardless of whether the system is linear or not (as long as parameters enter in the equations linearly). Furthermore, the parameters identified are the true values. Table 4-1 lists the results of two numerical experiments for both a linear and nonlinear representation of a VTOL aircraft. For an iterative scheme such as equation (4. 13), the identifiability also implies uniqueness (within a reasonable bound resulting from the convergence criterion used in the iteration). The fact that the residue vector $y - x(\hat{p})$ in equation (4. 13) can be identically zero permits the condition that $\Delta p = 0$ be automatically satisfied. i. e., the residue vector $y - x(\hat{p})$ is orthogonal to the subspace spanned by the sensitivity vector functions -- in the language of Hilbert space (Reference 50). However, due to the convergence criteria used in the iterative scheme, uniqueness, in the sense of the numerical values identified, is not computationally possible if the initial estimates are not the same (and the computer time is limited). This statement has also been confirmed by some numerical experiments.

If, on the other hand, errors exist in the measurements, then identifiability does not imply uniqueness regardless of whether or not the system is linear. In this situation, a noniterative scheme such as equation (4.8b) will give a biased parameter estimate (see Appendix B). Therefore, although the solution is unique for <u>the given data,</u> it becomes useful <u>only</u> to provide an initial estimate for the iterative methods. For iterative methods, the nonuniqueness problem has already been discussed (Section 3.2). We shall not repeat it here.

4.4 Concluding Remarks

In conclusion, the following remarks on the identifiability and uniqueness problems associated with parameter identification of linear and nonlinear systems are evident.

(i) A system, linear or nonlinear, is identifiable if and only if the sensitivity vector functions are nontrivial and are linearly independent.

(ii) The sensitivity vector functions are nontrivial and are linearly independent if and only if the state variables are linearly independent and the control functions are linearly independent and are also linearly independent of the state variables.

(iii) For the deterministic case, the solution for the parameters is unique if the system is identifiable.

(iv) If errors exist in the measurements, then the identifiability does not imply uniqueness, regardless of whether the system is linear or not.

Since the sensitivity vector functions depend not only on the system but also on the input, it is extremely desirable to design an input to increase the sensitivity and hence the parameter identifiability. Problems concerning the design of an appropriate input are discussed in Appendix F.

TABLE 4-1

Parameter Identification for Noiseless Data
Using a "Least-Squares" Method

Linear Representation			Nonlinear Representation		
parameters	true	identified	parameters	true	identified
m_u	-.0044	-.004400	m_0	.50518	.505177
m_w	-.0075	-.00749999	m_{0_u}	-.00308	-.00307997
m_q	-.625	-.624524	$m_{0_{u^2}}$	-6.2×10^{-6}	-6.20007×10^{-6}
$m_{\delta_{es}}$	.480	.479999	m_w	-.001747	-.00174696
			m_{w_u}	-.0000553	-.0000553302
x_u	-.150	-.150002	m_q	-.497	-.497336
x_w	.021	.0210088	m_{q_u}	-.00103	-.00103125
$x_{\delta_{es}}$	1.370	1.36996	$m_{\delta_{es}}$	.3275	.327503
			$m_{\delta_{es_u}}$	.001167	.00116697
z_u	-.216	-.216004			
z_w	-.650	-.649985	x_0	18.3	18.2996
$z_{\delta_{es}}$	1.660	1.65994	x_{0_u}	-.09167	-.0916648
			$x_{0_{u^2}}$	-.0003	-.000300018
			x_w	.2211	.221103
			x_{w_u}	-.001587	-.00158703
			$x_{\delta_{es}}$	-.778	-.777760
			$x_{\delta_{es_u}}$	.0184	-.0183981
			z_0	-32.171	-32.1717
			z_{0_u}	.910	.910010
			$z_{0_{u^2}}$	-.007	-.00700004
			z_w	-.2939	-.293892
			z_{w_u}	-.00287	-.00286705
			$z_{\delta_{es}}$	-.3507	-.351216
			$z_{\delta_{es_u}}$	.01667	.0166741

SECTION V

DEVELOPMENT OF ADVANCED IDENTIFICATION TECHNIQUES

The parameter identification of VTOL aircraft as formulated in Section II is fundamentally a problem of nonlinear estimation. By annexing the constant parameter vector to the state vector, it becomes apparent that parameter identification is a problem of state estimation of a nonlinear system even if the original equations of motion are linear. We note also that if accelerations or α -vane sensors are used as measurements, the measurement system is also nonlinear.

For the reasons discussed in Section III, the equations-of-motion method (a least-square method) is chosen as the initial estimator for the extended Kalman filter, which appears to be a very promising method for parameter identification for VTOL aircraft. However, as is shown in Appendix H, the extended Kalman filter is a biased estimator in the presence of nonlinearities, and nonlinearities are inherent in parameter identification problems. Since the extended Kalman filter algorithm is derived on the assumption that the estimate is unbiased, (as is true in the linear case), the quality of the estimate is overestimated. The extended Kalman filter may be regarded as incorporating a gain which changes the estimate of a parameter based on the quality of its previous estimate. Recalling that the Kalman filter is a sequential estimator, it can be seen that an overly optimistic estimate of the parameter quality forces the filter gain to decrease and therefore the filter relies less on subsequent data.

As is shown in Appendix H, if initial estimates are unbiased, the bias of the extended Kalman filter estimates depends on the multiplicative effects of the system and measurement nonlinearities and the covariance of the estimate. As the entire data are processed by the extended Kalman filter, the variances of the final parameter estimates reduce from those of the initial estimates. One may thus be tempted to reuse the data all over to reduce the bias of the estimates. Two schemes of reusing the data have previously been tried and are shown in Figure 5-1. Both methods regard the first extended Kalman filter as the second initial estimator (the equations-of-motion method being the first initial estimator). However, the second extended Kalman in the first scheme uses the data in a forward manner; whereas the second filter in the second method uses the data in a backward fashion. It is apparent from the above discussion on the basic characteristics of the extended Kalman filter that the second scheme has the virtue of being able to appropriately use the last part of the data, if the variance of the parameter estimates at the end of the forward pass is "suitably" increased in some artificial way. However, a fundamental difficulty common to both schemes of reusing the data is the determination of how to adjust the variance of the parameter estimates from the first filter to start up the second filter.

Another major difficulty associated with identification of the VTOL aircraft parameters is the relative uncertainty in formulating the equations of motion due to the complex interaction of propulsive and aerodynamic forces and moments. Consequently, the identification technique must have the capability of detecting the modeling errors to facilitate an improvement of the model. As was discussed in Section III, the detection of modeling errors requires the estimation of the unknown forcing functions, which can be obtained only through data smoothing. Initially, we (and SCI's subcontract work) directed our efforts toward examining more or less exclusively the feasibility of applying fixed interval smoothing techniques to VTOL parameter identification. However, the fixed interval smoothing algorithms currently available either require an extremely large amount of storage for the filtered state and error covariance matrices or have computational difficulties.

Thus, our major efforts in the development of techniques for VTOL parameter identification have been to overcome and/or to alleviate the aforementioned difficulties. Specifically, the following tasks have been performed:

(1) Development of a locally iterated filter-smoother (multi-corrector) for better parameter estimation.

(2) Development of a fixed-point smoothing technique to facilitate the computation of the unknown forcing functions to aid in detecting modeling errors.

(3) Improvement of the variance computation to better predict the quality of the parameter estimates.

This section is organized as follows: Section 5.1 describes in detail the developed techniques; Section 5.2 presents the derivation of the locally iterated filter-smoother and the fixed-point smoothing algorithm; the computational algorithm for the unknown forcing functions is discussed in Section 5.3; and Section 5.4 discusses the improved covariance matrix computations. The results of numerical experiments are shown in Section VI.

5.1 Description of the Developed Techniques

After the extended Kalman filter computer program had been developed and selected as the major tool for VTOL aircraft parameter identification, subsequent efforts were directed toward improving the accuracy of the parameter estimates by developing a multi-corrector Kalman filter technique, developing a fixed-point smoothing technique to facilitate the computation of unknown forcing functions to detect modeling errors, and obtaining a better prediction of the quality of the estimate parameters. Figure 5-2 shows a schematic diagram of CAL's developed identification program. Details of each block in the figure are described in the following subsections.

5.1.1 Initial Estimator Program

As discussed in Section III, the initial estimator program is essentially a computer program using the equations-of-motion method. Using the measured data of inputs and outputs, this program produces a set of parameter estimates and a set of approximate variances of the estimates. When measurements are corrupted with noise, as is always the case in a practical situation, this method of parameter estimation produces biased estimates.

As the measurement noise to signal ratio increases, the bias increases. As a result of the bias, the variance computed from this initial estimator program (3.3d) poorly represents the true quality of the estimation error. Depending on the level of the measurement noise, or more precisely the noise-to-signal ratio, the computed variance can be grossly optimistic, i.e., the computed variance is too small in comparison with the square of the actual estimation error. As a result, variances from the initial estimator are too small to properly "start up" the multi-corrector filter program. Therefore, in all previous identification runs, either generated data or flight test data, it was necessary to use engineering judgment to adjust the initial covariance matrix $P(0)$.

Experience has shown that an increase in the computed covariance from the initial estimator program by a factor of ten produced the best results. However, the best factor to use in each particular situation is not known, since it is strongly dependent upon the control input and noise levels present. Thus, a more automatic and preferable way to start up the multi-corrected filter is to calculate $P(0)$ by a different scheme. Discussions of this and related problems will be given later. In the following, we shall first describe the multi-corrected extended Kalman filter, the fixed-point smoother, and the computation of the unknown forcing functions.

5.1.2 Multi-Corrected Extended Kalman Filter

Previously we discussed the fact that the extended Kalman filter is a biased estimator in the presence of nonlinearities, which are inherent in parameter identification problems. One way to correct for system and measurement nonlinearities is to include higher-order terms in the Taylor series expansion about the reference trajectory (References 38 and 53). This leads to computationally unwieldy correction terms in the filtering algorithms. The other approach is to use some "local iteration" algorithm based on the extended Kalman filter in conjunction with the use of one stage optimal smoothing. By local we mean iteration at a data point at time t_{k+1} , or in an interval $[t_k, t_{k+1}]$. The purposes of the iteration is to improve the reference trajectory and thus the estimate in the presence of nonlinearities. A schematic diagram of the locally iterative process is shown in Figure 5-3.

The algorithm is obtained by linearizing to a first order the system and measurements around the best estimate at each data point. For example, starting at t_k with $\hat{x}_{k|k}$ and P_k, the estimate and covariance given the data up to time t_k respectively, we linearize and predict to t_{k+1}, the time of the next data point and apply one iteration of the extended Kalman filter. Based on this new estimate, we smooth back to t_k (one stage smoothing). The smoothing closes the loop, providing an improved reference for prediction to t_{k+1}, and the extended Kalman filter is again applied at data point t_{k+1} after recalculating the extrapolated covariance and gain. The iteration terminates when there is no significant difference between consecutive iterations, or after a prespecified number of iterations. Experience has indicated rapid convergence of the algorithm: rarely have more than two additional iterations been required.

Analysis has shown (Appendix H) that this scheme can significantly reduce the bias inherent in the extended Kalman filter, thereby improving the parameter estimate as well as the calculated variance of the estimation error. Because of these improvements, reuse of the entire data is not required after a complete pass is finished, thereby eliminating the engineering judgment inherent in increasing the variance of the parameter estimation error to recycle the data. A detailed derivation of the multi-corrector extended Kalman filter algorithm is given in Section 5.2. For the sake of easy reference we summarize the algorithm below. Notations are shown in the list of symbols.

The first iteration is the extended Kalman filter and the one-stage smoothing algorithm:

$$
\begin{aligned}
\hat{x}_{t|t} &= \hat{x}_{t|t-1} + \psi_t \left(y_t - h(\hat{x}_{t|t-1})\right) \\
\hat{x}_{t|t-1} &= g_t\left(\hat{x}_{t-1|t-1}\right) \\
\psi_t &= P_{t|t-1} H_t^T \left(H_t P_{t|t-1} H_t^T + R_t\right)^{-1} \\
P_{t|t-1} &= \Phi_{t,t-1} P_{t-1} \Phi_{t,t-1}^T + Q_t \\
P_t &= \left(I - \psi_t H_t\right) P_{t|t-1} \\
x_{t-1|t} &= \hat{x}_{t-1|t-1} + P_{t-1} \Phi_{t,t-1}^T \left(I - \psi_t H_t\right)^T H_t^T R_t^{-1} \left(y_t - h(\hat{x}_{t|t-1})\right)
\end{aligned}
\tag{5.1}
$$

Denoting $\hat{x}^{(1)}_{t/k} = \hat{x}_{k/k}$ and $\hat{x}^{(1)}_{k-1/k} = \hat{x}_{k-1/k}$, the second iteration and iterations thereafter (i = 2, 3....) are given by:

$$
\begin{aligned}
\hat{x}^{(i)}_{t|t} &= \hat{x}^{(i)}_{t|t-1} + \psi_t^{(i)} \left[y_t - h_t\left(x^{(i-1)}_{t|t}\right) - H_t\left(x^{(i-1)}_{t|t}\right)\left(\hat{x}^{(i)}_{t|t-1} - \hat{x}^{(i-1)}_{t|t}\right)\right] \\
\hat{x}^{(i)}_{t|t-1} &= g_t\left(\hat{x}^{(i-1)}_{t-1|t}\right) + \Phi_{t,t-1}\left(\hat{x}^{(i-1)}_{t-1|t}\right)\left(\hat{x}_{t-1|t-1} - \hat{x}^{(i-1)}_{t-1|t}\right) \\
\psi_t^{(i)} &= P^{(i)}_{t|t-1} H_t^{(i)T} \left(H_t^{(i)} P^{(i)}_{t|t-1} H_t^{(i)T} + R_t\right)^{-1} \\
P^{(i)}_{t|t-1} &= \Phi^{(i)}_{t,t-1} P_{t-1} \Phi^{(i)}_{t,t-1} + Q_t \\
P_t^{(i)} &= \left(I - \psi_t^{(i)} H_t^{(i)}\right) P^{(i)}_{t|t-1} \\
\hat{x}^{(i)}_{t-1|t} &= \hat{x}_{t-1|t-1} + P_{t-1} \Phi^{(i)T}_{t,t-1} \left[I - \psi_t^{(i)} H_t^{(i)}\right] H_t^{(i)T} R_t^{-1} \\
&\quad \cdot \; y_t - h_t\left(\hat{x}^{(i-1)}_{t|t}\right) - H_t\left(\hat{x}^{(i-1)}_{t|t}\right)\left(\hat{x}^{(i)}_{t|t-1} - \hat{x}^{(i-1)}_{t|t}\right)
\end{aligned}
\tag{5.2}
$$

5.1.3 Fixed-Point Smoothing

We have discussed modern data smoothing in Section III. In contrast to the filtering discussed above, the data smoothing is concerned with the estimate of the augmented state at some time in the past given data up to the present. Since the response caused by the unknown forcing function exerted on the system at time t will be contained in the measurements at time $t_d > t$ further "down stream" of t, it is obvious that, by smoothing, the augmented state estimate can be improved and, further, the unknown forcing function can be estimated.

Data smoothing can be classified into three classes: fixed-interval smoothing, fixed-lag smoothing, and fixed-point smoothing. Fixed-interval smoothing is concerned with the estimation of the state at some time t between the initial time t_0 and the final time t_f given all the data up to t_f; fixed-lag smoothing is concerned with the estimation of the state at some time t given data up to $t+T$ for some fixed value T; and the fixed-point smoothing is concerned with the estimation of the initial augmented state, that is, at t_0, given data up to some time t.

The fixed-interval smoothing algorithm for a linear system was first developed in the early sixties by Bryson (Reference 1), Rauch (References 39 and 40) and others. Subsequently, there was some work on the applications of their algorithms to problems of engineering significance (References 41 and 54). In view of the past experience, in the early stages of this project we directed our efforts toward examining more or less exclusively the feasibility of applying the fixed interval smoothing techniques to VTOL parameter identification. Our major interest was to see if it is feasible to improve the model of the VTOL aircraft dynamics by examining the unknown forcing function that can be obtained from smoothing techniques. It was found (Reference 55), however, that the fixed interval smoothing algorithms currently available require either extremely large amounts of storage for the filtered state and the error covariance matrices, or have computational difficulties.

Subsequently, in a further search for some practical ways of estimating the unknown forcing functions, we re-examined the entire set of smoothing techniques, and it is our belief that the fixed-point smoothing technique is the most suitable technique for estimating the initial state and the parameters, and from them to start the estimation of the unknown forcing functions.

In contrast to fixed interval smoothing, which requires a complete filtering pass before it can proceed with its smoothing pass backwards, the fixed-point smoother obtains its smoothed estimate as the filter proceeds forward. A schematic diagram is shown in Figure 5-4. The detailed development of the fixed-point smoothing algorithm is given in Section 5.2. The basic features of the algorithm are that no storage for the filtered state and the error covariance matrices is required, as the algorithm works in conjunction with the multi-corrected extended Kalman filter. Furthermore, there are no computational difficulties associated with this algorithm. Also, the computation of the unknown forcing functions can proceed with the completion of the entire pass of the fixed-point smoothing estimate. Consequently, previous difficulties associated with fixed interval smoothing are avoided.

For convenience, the fixed-point smoothing algorithm is given below.

$$\hat{x}(0/t_{k+1}) = \hat{x}(0/t_k) + B_{k+1} H_{k+1}{}^T R_{k+1}^{-1} \cdot [\text{RESIDUAL}]$$

$$B_{k+1} = B_k \phi_k^T \left[I - \psi_{k+1} H_{k+1}\right]^T, \quad B_0 = P_0 \tag{5.3}$$

where

B = dummy variables

ψ = gain matrix of the last local iteration

ϕ = transition matrix of the last local iteration

H = output matrix of the last local iteration

R = measurement error covariance matrix

P_0 = initial estimation error covariance matrix

Residual $= y_{k+1} - h_{k+1}\left(\hat{x}^{(f)}_{k+1|k+1}\right) - H^{(f)}_{k+1}\left(\hat{x}^{(f)}_{k+1|k} - \hat{x}^{(f)}_{k+1|k+1}\right)$

and the superscript "(f)" denotes the last local iteration.

5.1.4 Computation of Unknown Forcing Functions

To achieve the goal of employing the best possible mathematical model of the X-22A in transition or at fixed operating point (FOP), we need some means of evaluating the errors in the models. If we have the capability of determining this error from the identification process, then it is expected that having the form of the error in a given model will help in selecting terms that are missing and thereby help to improve the model.

For the sake of analytical simplicity, we regard the error in the assumed model as a white, stationary random process with covariance Q. We estimate this error (called unknown forcing function) after the completion of the fixed-point smoothing part of the analysis for the initial state and parameters. This procedure is, from a computational point of view, better than the conventional approach of using fixed-interval smoothing.

The derivation of the algorithm for computing the unknown forcing function is given in Section 5.3. Here, we simply list the computational algorithm for it.

$$\hat{w}_{k|N} = G_k \left(\hat{x}_{k-1|N} - \hat{x}_{k-1|k-1} \right) \quad \text{for } k = 1, \ldots, N$$

where

$\hat{w}_{k|N}$ - vector of forcing functions

$\hat{x}_{k|N}$ = $g(\hat{x}_{k-1|k}) + \Phi_{k,k-1} \left(\hat{x}_{k-1|N} - \hat{x}_{k-1|k} \right) + \hat{w}_{k|N}$
with initial condition $\hat{x}_{0|N}$

$\hat{x}_{0|N}$ - fixed point smoothing estimate

$g(\hat{x}_{k-1|k})$ - represents nonlinear integration from t_{k-1} to t_k
with initial condition $\hat{x}_{k-1|k}$

G_k = $\left[I - Q_k P_{k|k-1}^{-1} \right]^{-1} Q_k P_{k|k-1} \Phi_{k,k-1}$
which is the smoother gain matrix stored on a forward filter pass

$P_{k|k-1}$ - extrapolated filter covariance matrix

$\hat{x}_{k|k}$ - filtered estimate

$\hat{x}_{k-1|k}$ - one stage smoothed estimate for x_{k-1}

This computation is performed at the completion of a forward filter pass and the fixed-point smoothing computation. G_k, $\hat{x}_{k|k}$ and $\hat{x}_{k-1|k}$ are computed and sorted during the filter pass.

5.1.5 Better Prediction of the Quality of the Estimated Parameters

A very desirable feature of an identification technique is to be able to predict, with reasonable confidence, the accuracy of the estimated parameters. In the identification technique developed for the VTOL parameter identification program, three ways are used to judge the quality of a set of parameters and each individual parameter of that set. These are:

(a) Transient response matching to measured data.

(b) Identification consistency check using the predicted residual sequence (measured data minus the predicted value) during an identification run.

(c) Variance computation of estimated parameters.

A discussion of each check follows:

<u>(a) Transient Response Matching.</u>

One test of the validity of an identified model is its ability to reproduce the measured responses (within the measurement accuracy) from which the parameters were originally identified, where the identified model includes the estimated unknown forcing term. If the random forcing function is truly zero and the form of the model is correct, then the model should also match other measurement data with any control input.

In practice, it has been found that if the measured responses are insensitive to a group of parameters being identified, then these parameters are likely to be inaccurately identified even though a model using these parameters could match a particular measured response very well. Thus, a good input design (Appendix F) and transient response matching to data with different inputs is very important.

(b) Residual Consistency Tests

Another independent measure of the identification technique performance is to perform statistical tests on the predicted measurement residuals. The residuals are the differences between the actual measurements and predicted measurements. If the assumed noise and dynamical models are fairly accurate, these residuals should be small, random, zero mean and should possess statistical properties consistent with their calculated statistics. For example,

$$E\{\tilde{y}_k\} = E\left\{y_k - h_k\left(\hat{x}^{(f)}_{k|k}\right) - H^{(f)}_k\left(\hat{x}^{(f)}_{k|k-1} - \hat{x}^{(f)}_{k|k}\right)\right\} = 0 \tag{5.4a}$$

$$P_{\tilde{y}_k \tilde{y}_k} = H^{(f)}_k P^{(f)}_{k|k-1} H^{(f)^T}_k + R_k \tag{5 4b}$$

where $\tilde{y}_k$ is the predicted measurement residual, E is the expectation operation, and $P_{\tilde{y}_k \tilde{y}_k}$ is the covariance of $\tilde{y}_k$. We can then plot the square root of the diagonal terms on the righthand side of (5.4b) against the actual residual sequence to see if the filter performs as it predicts.

(c) Improved Variance Computation

Start-up procedure for the locally iterated filter-smoother

To obtain a quantitative measure of the quality of each parameter estimated, the variance of the parameter is computed. As discussed previously, the initial estimator is a biased estimator. Also, the variances of the parameter estimates are computed by the initial estimator based on classical linear regression theory with nonstochastic regressor for use in the initial covariance matrix, P_0 . As measurement errors are always present, the regressor is in actuality stochastic, and the variances computed for the parameter estimates are only an approximation.

From experience using computer generated data, where the noise levels are known, it has been observed that the variances of the parameter estimates from the initial estimates are in most cases too small to correctly represent the accuracy of the parameter estimates. Best results were obtained by increasing the computed variances by a factor of from 1 to 10 equally for all the parameters. This increase is necessary to account for the bias of the initial parameter estimates, as it forces the filter to place less weight on these estimates. Although the variance of each individual parameter could be increased by different factors, the computer time required to obtain the best combination of factors by experimentation would be formidable. Furthermore, the best factor to use in each particular situation is not known in general, since it is strongly dependent on the control input and noise levels present. In view of the erroneous variance computation, it is doubtful that equally increasing the variances by the same factor is appropriate. It seems more appropriate, therefore, to first more correctly compute the variances of the estimated parameters and then increase them equally to keep their magnitudes in the proper proportion.

A better scheme to start up the Kalman filter from initial parameter estimates is to calculate P_0 for the parameters by an independent technique. If the initial parameter estimates are produced from an efficient estimator, then the covariance matrix, P_0 , for the initial parameter estimates can be shown to approach the Cramer-Rao lower bound, CR . Therefore, the following equation can be employed in the calculation of the improved start-up covariance P_0 . Here, the matrices $\Phi_{i,i-1}$ and H_i are evaluated along the trajectory using the initial estimated parameters.

$$CR = \left[\sum_{i=1}^{N} Z_i^T H_i^T R_i^{-1} H_i Z_i \right]^{-1} \tag{5.5}$$

where

$$Z_i = \Phi_{i,i-1} Z_{i-1} \; , \quad Z_o = I$$

Since the inverse of CR is the sensitivity matrix, which is useful for input design, the initial covariance computation has also been coded as shown in Figure 5-2 into a separate subprogram for input design purposes.

Variance of Fixed-Point Estimated Parameters

The covariance matrix for the fixed-point smoothed estimate is shown in Section 5.2 to be

$$P_{x_o|Y(N)} = P_{x_o|Y(N-1)} - B_N H_N^{(f)T} R_N^{-1} H_N^{(f)} \Phi_N^{(f)} B_{N-1}^T \tag{5.6}$$

where B_k is given by

$$B_k = B_{k-1} \Phi_k^{(f)} \left[I - \psi_k^{(f)} H_k^{(f)} \right] , \; B_o = P_o \tag{5.7}$$

Since the locally iterated filter-smoother and fixed-point smoother employ a priori information, P_o , it would seem that the above equations could be employed for a final covariance computation. However, the a priori information for P_o in the case of parameter estimation is almost always unavailable and is usually produced from the same data given; in other words, P_o is obtained after processing the given data. As such, it is not a priori information in the true sense in that it is independent of the given data. Rather, the P_o obtained through using the data should be regarded as a means to start up the locally iterated filter-smoother. Consequently, it is appropriate to compute the covariance matrix of the fixed-point estimated parameters in an independent way that does not utilize the a priori information.

In deriving the fixed-point smoothing algorithm in Section 5.2, we have assumed that $x_o, Y(k)$, $1 \le k \le N$ are jointly Gaussian. This implies that both x_o and $x_o | Y(k)$ are normally distributed. We have, therefore,

$$f\left(Y(N)|x_o\right) = \frac{f\left(x_o|Y(N)\right) f\left(Y(N)\right)}{f(x_o)} \tag{5.8}$$

and, because both x_o and $x_o|Y(N)$ are Guassian,

$$\frac{\partial^2}{\partial x_o^2}\left[-\ln f\left(Y(N)|x_o\right)\right] = \frac{\partial^2}{\partial x_o^2}\left\{\frac{1}{2}\left\|x_o - E\left(x_o|Y(N)\right)\right\|^2_{P^{-1}_{x_o|Y(N)}}\right\}$$
$$-\frac{\partial^2}{\partial x_o^2}\ \frac{1}{2}\left\|x_o - \hat{x}_{o|o}\right\|^2_{P_o^{-1}} \tag{5.9}$$

Assuming that the fixed-point smoother is an asymptotically efficient estimator, then without use of a priori information, the covariance of the parameter estimate will approach the Cramer-Rao lower bound CR_N, which is given by

$$CR_N \triangleq \left\{\frac{\partial^2}{\partial x_o^2}\left[-\ln f\left(Y(N)|x_o\right)\right]\right\}^{-1} \tag{5.10}$$

From equation (5.9) it is readily shown that

$$CR_N = \left(P^{-1}_{x_o|Y(N)} - P_o^{-1}\right)^{-1} \tag{5.11a}$$

Equations (5.6), (5.7), and (5.11a) are the desired recursive formulas for computing the improved covariance matrix of the fixed-point smoothed estimate for parameters. It can be shown that, in the absence of process noise, equation (5.11a) reduces to

$$CR = \left[\sum_{i=1}^{N} Z_i^{(f)^T} H_i^{(f)^T} R_i^{-1} H_i^{(f)} Z_i^{(f)}\right]^{-1} \tag{5.11b}$$

where

$$Z_i^{(f)} = \Phi_{i,i-1}^{(f)} Z_{i-1}^{(f)},\quad Z_o^{(f)} = I$$

In the next three sections, detailed mathematical developments are given for the locally iterated filter-smoother and fixed-point smoothing algorithm, unknown forcing function computation, and the improved computation for the variances of the estimated parameters. Readers who are not interested in the mathematics can, without loss of continuity, skip these sections and go directly to Section VI, in which the results of the numerical experiments are presented.

5.2 Derivation of Locally Iterated Filter-Smoother and Fixed-Point Smoothing Algorithm

In this section, a unified approach is taken to derive the locally iterated filter-smoother and fixed-point smoothing algorithm. For the readers who are not interested in the detailed mathematics, this section along with 5.3 and 5.4 may be skipped without loss of continuity in going directly to Section VI. The material presented in this section is purposely designed to be self-contained; the necessary mathematical preliminaries are given in Appendix G. For the sake of convenience, the problem as formulated in Section II is restated here; however, for notational simplicity, the subscript " a " in equation (3.9) is dropped.

Statement of the Problem

Consider the nonlinear continuous system

$$\dot{x} = f(x,t) + w(t) \tag{5.12}$$

driven by zero mean white Gaussian noise, $w(t)$, which can be characterized by the difference equation*

$$x_i = g_i(x_{i-1}) + w_i \tag{5.13}$$

and discrete noisy measurements

$$y_i = h_i(x_i) + v_i \tag{5.14}$$

where $g_i(x_{i-1})$ denotes the solution, at time t_i, to

$$\dot{z}(t) = f(z,t) \tag{5.15}$$

given the initial condition $z(t_{i-1}) = x_{i-1}$. The random vector sequences w_i and v_i are white Gaussian with zero mean and covariance matrices

$$E\{w_i w_j^T\} = Q_i \delta_{ij} \quad , \quad E\{v_i v_j^T\} = R_i \delta_{ij} \quad , \quad E\{v_i w_j^T\} = 0^{**}$$

---

* the usual rules of calculus apply (see, for instance, Reference 56)

** correlated noise is treated in Appendix I.

The process noise sequence, w_i, in (5.13) is a useful, although artificial, method of accounting for dynamical modeling errors and unknown forcing inputs. The choice of a normal distribution is for analytical simplicity. The initial condition $x(t) \triangleq x_0$ in (5.13) is a Gaussian random variable with mean $\bar{x}_0$ and covariance P_0, i.e., $f(x_0) \triangleq N(\bar{x}_0, P_0)$. The problem is to obtain best (efficient) estimates for x_0 and w_i, $i = 1, 2, \ldots, N$ using the measured data $Y(N) \triangleq (y_1^T, y_2^T, \ldots, y_N^T)^T$.

Fixed-Point Smoothing and Locally Iterated Filter-Smoother Algorithms

The problem stated above is a problem of fixed-point nonlinear data smoothing for x_0 and fixed-interval smoothing for w_i for which exact solutions are not yet available. Our objective is to seek an approximate solution to the above problem. To this end, we shall assume that $x_0, Y(k)$ are jointly normal and so are x_{k-1}, $Y(k)$, and x_k, $Y(k)$ for $1 \le k \le N$. Note that this assumption is true only if (5.13) and (5.14) are linear, thus, our basic assumption is only an approximation. It is shown in Appendix G that the conditional expectation $E\{x_j | Y(N)\}$, $j = 0, k-1, k$ are the efficient estimators (unbiased and minimum variance) for x_0, x_{k-1} and $x(k)$ given data $Y(N)$. Using equations (G.21) and (G.22) in Appendix G and noting that $Y(N) = (Y(N-1)^T, y_N^T)^T$, it is readily shown that

$$\left.\begin{aligned} E\{x_j | Y(k)\} &= E\{x_j | Y(k-1)\} + P_{x_j \tilde{y}_k} P^{-1}_{\tilde{y}_k \tilde{y}_k} \tilde{y}_k \\ P_{x_j | Y(k)} &= P_{x_j | Y(k-1)} - P_{x_j \tilde{y}_k} P^{-1}_{\tilde{y}_k \tilde{y}_k} P^T_{x_j \tilde{y}_k} \end{aligned}\right\} \; j = 0, k-1, k \tag{5.16}$$

where

$$\tilde{y}_k = y_k - E\{y_k | Y(k-1)\} \tag{5.17}$$

and the covariance matrixes $P_{x_j \tilde{y}_k}$, $P_{\tilde{y}_k \tilde{y}_k}$ are defined by

$$P_{x_j \tilde{y}_k} \triangleq E\left\{ \left[x_j - E(x_j)\right] \left[y_k - E\{y_k | Y(k-1)\}\right]^T \right\} \tag{5.18}$$

$$P_{\tilde{y}_k \tilde{y}_k} \triangleq E\left\{ \left[y_k - E\{y_k | Y(k-1)\}\right] \left[y_k - E\{y_k | Y(k-1)\}\right]^T \right\} \tag{5.19}$$

where E is the expectation operation. Note that we have used in the above expressions the fact that $E\left\{y_k - E\left(y_k \mid Y(k-1)\right)\right\} = 0$.

Before we proceed to obtain a suboptimal fixed-point smoothing algorithm from (5.16), we shall first use equation (5.16) with $j = k-1, k$ to derive a locally iterated filter-smoother algorithm.

Locally Iterated Filter-Smoother Algorithm*

A common approach is to employ the extended Kalman filter to perform the estimation for x_k. However, it is shown (Appendix H) that the extended Kalman filter is a biased estimator. The bias is due to the multiplicative effect of nonlinearities in g_i and h_i and the levels of noise present in equation (5.12). One may correct for system and measurement nonlinearities by including higher-order terms in the Taylor series expansion about the reference trajectory (References 38 and 53). However, the approach taken here is to use some local iteration algorithm based on the extended Kalman filter in conjunction with the use of one stage optimal smoothing. The purpose of the local iteration is to improve the reference trajectory and thus the estimate in the presence of nonlinearities. Indeed, it can also be shown formally that the bias is reduced by the local iteration (see Appendix H).

We now use (5.16) to first derive the locally iterated filter-smoother. In (5.16), $E\left\{x_{k-1} \mid Y(k)\right\}$ is the one-stage optimal smoothed estimate for x_{k-1} and $E\left\{x_k \mid Y(k)\right\}$ is the optimal filtering estimate of x_k. Their covariance matrices are $P_{x_{k-1}|Y(k)}$ and $P_{x_k|Y(k)}$, respectively. First, we shall obtain the filtered estimate $E\left\{x_k \mid Y(k)\right\}$. To do this, we need $E\left\{x_k \mid Y(k-1)\right\}$, $E\left\{y_k \mid Y(k-1)\right\}$, $P_{x_k \tilde{y}_k}$ and $P_{\tilde{y}_k \tilde{y}_k}$ in (5.16).

---

* An equivalent version of this algorithm has previously been derived and evaluated by Wishner (Reference 57).

(i) Determination of $E\{x_k | Y(k-1)\}$

Consider the time interval $t_{k-1} \le t \le t_k$. Let us choose a nominal trajectory $x^*(t)$, which is the solution of (5.15) with initial condition $x^*(t_{k-1}) = x^*_{k-1}$. To a first-order approximation,

$$E\{x_k | Y(k-1)\} = E\{g_k(x_{k-1}) + w_k | Y(k-1)\}$$
$$= E\{g_k(x_{k-1}) | Y(k-1)\} \tag{5.20}$$
$$\approx g_k(x^*_{k-1}) + \Phi_{k,k-1}(x^*_{k-1})(\hat{x}_{k-1|k-1} - x^*_{k-1})$$
$$\triangleq x^*_{k|k-1} \tag{5.21}$$

where $\Phi_{k|k-1}(x^*_{k-1})$ is the one step transition matrix along $x^*(t)$.

(ii) Determination of $E\{y_k | Y(k-1)\}$

We linearize (5.14) about $x^*_k \triangleq x^*(t_k)$. To a first-order approximation

$$y_k \approx h_k(x^*_k) + H_k(x^*_k)(x_k - x^*_k) + v_k \tag{5.22}$$

where

$$H_k(x^*_k) \triangleq \left.\frac{\partial h_k(x)}{\partial x}\right|_{x^*_k}$$

Hence, since

$$E\{v_k | Y(k-1)\} = 0,$$
$$E\{y_k | Y(k-1)\} \approx h_k(x^*_k) + H_k(x^*_k)(x^*_{k|k-1} - x^*_k) \tag{5.23}$$

(iii) Determination of $P_{x_k \tilde{y}_k}$, $P_{\tilde{y}_k \tilde{y}_k}$

Using (5.12), (5.22), (5.23), and (5.18),

$$P_{x_k \tilde{y}_k} \approx E\left\{\left[g_k(x_{k-1}) + w_k - E(g_k(x_{k-1}))\right]\left[H_k(x^*_k)(x_k - x^*_{k|k-1}) + v_k\right]^T\right\}$$

Linearizing $g_k(x_{k-1})$ about x^*_{k-1} and using $E(x_{k-1}) = \hat{x}_{k-1|k-1}$, we have:

$$g_k(x_{k-1}) - E[g_k(x_{k-1})] \approx \Phi_{k,k-1}(x^*_{k-1})(x_{k-1} - \hat{x}_{k-1|k-1})$$
$$x_k - x^*_{k|k-1} \approx \Phi_{k,k-1}(x^*_{k-1})(x_{k-1} - \hat{x}_{k-1|k-1}) + w_k \tag{5.24}$$

Hence, again to first order,

$$P_{x_k \tilde{y}_k} \approx E\left\{\left[\Phi^*_{k,k-1}\left(x_{k-1}-\hat{x}_{k-1|k-1}\right)+w_k\right]\left[H^*_k \Phi^*_{k,k-1}\left(x_{k-1}-\hat{x}_{k-1|k-1}\right)+H^*_k w_k+v_k\right]^T\right\} \tag{5.25}$$
$$= P^*_{k|k-1} H^{*T}_k$$

where
$$P^*_{k|k-1} = \Phi^*_{k,k-1} P_{k-1} \Phi^{*T}_{k,k-1} + Q_k$$
$$H^*_k \triangleq H_k(x^*_k)\,,\quad \Phi^*_{k,k-1} \triangleq \Phi_{k,k-1}(x^*_{k-1})$$
$$P_{k-1} \triangleq E\left\{\left[x_{k-1}-\hat{x}_{k-1|k-1}\right]\left[x_{k-1}-\hat{x}_{k-1|k-1}\right]^T\right\} \tag{5.26}$$

assuming $\hat{x}_{k-1|k-1} = E(x_{k-1})$. Similarly,

$$P_{\tilde{y}_k \tilde{y}_k} \approx H^*_k P^*_{k|k-1} H^{*T}_k + R_k \tag{5.27}$$

We have, therefore,

$$P_{x_k \tilde{y}_k} P^{-1}_{\tilde{y}_k \tilde{y}_k} \approx P^*_{k|k-1} H^{*T}_k \left(H^*_k P^*_{k|k-1} H^{*T}_k + R_k\right)^{-1} \tag{5.28}$$
$$\triangleq \psi^*_k$$

Thus, based on the chosen trajectory $x^*(t),\, t_{k-1} \le t \le t_k$, with end points x^*_{k-1}, x^*_k, the filtered estimate $\hat{x}^*_{k|k}$ is

$$E\{x_k | Y(k)\} \approx \hat{x}^*_{k|k}$$
$$= x^*_{k|k-1} + \psi^*_k\left[y_k - h_k(x^*_k) - H^*_k\left(x^*_{k|k-1} - x^*_k\right)\right] \tag{5.29}$$

where

$$x^*_{k|k-1} = g_k(x^*_{k-1}) + \Phi^*_{k,k-1}\left(\hat{x}_{k-1|k-1} - x^*_{k-1}\right) \tag{5.30}$$

and ψ^*_k is given in (5.28). From the second equation in (5.16), the variance of the estimate $x^*_{k|k}$ is

$$P^*_k = P^*_{k|k-1} - P^*_{k|k-1} H^{*T}_k \left(H^*_k P^*_{k|k-1} H^{*T}_k + R_k\right)^{-1} H^*_k P^*_{k|k-1}$$
$$= \left(I - \psi^*_k H^*_k\right) P^*_{k|k-1} \tag{5.31}$$

Figure 5-5 shows the reference trajectory $x^*(t)$, its end points x^*_{k-1}, x^*_k, and the filtered estimate $\hat{x}^*_{k|k}$ based on this reference trajectory. Shown also is the reference trajectory for the standard extended Kalman filter which utilizes the reference trajectory with end points $\hat{x}_{k-1/k-1}$ and $\hat{x}_{k/k-1}$ where

$$\hat{x}_{k/k-1} = g_k(\hat{x}_{k-1/k-1})$$

With this choice of reference trajectory it is readily seen that (5.26), (5.29), and (5.31) reduce to the extended Kalman filter:

$$\left.\begin{aligned} \hat{x}_{k/k} &= \hat{x}_{k/k-1} + \psi_k\left[y_k - h_k(\hat{x}_{k/k-1})\right] \\ \psi_k &= P_{k/k-1}H_k^T\left(H_k P_{k/k-1}H_k^T + R_k\right)^{-1} \\ P_{k/k-1} &= \Phi_{k,k-1}P_{k-1}\Phi_{k,k-1}^T + Q_k \\ P_k &= (I - \psi_k H_k)P_{k/k-1} \end{aligned}\right\} \qquad (5.32)$$

We now proceed to find the one-stage smoothed estimate $E\{x_{k-1}/Y(k)\}$ using the same reference trajectory $z^*(t), t_{k-1} \le t \le t_k$. Denote this estimate by $x^*_{k-1/k}$. From (5.16)

$$x^*_{k-1/k} = \hat{x}_{k-1/k-1} + P_{\tilde{x}_{k-1}\tilde{y}_k} P^{-1}_{\tilde{y}_k\tilde{y}_k}\tilde{y}_k \qquad (5.33)$$

Following the same approach as above, it is easy to see that to a first-order approximation

$$P_{x_{k-1}\tilde{y}_k} \approx P_{k-1}\Phi^{*T}_{k,k-1}H^*_k \qquad (5.34)$$

and thus

$$\begin{aligned} x^*_{k-1/k} = \hat{x}_{k-1/k-1} + P_{k-1}\Phi^{*T}_{k,k-1}H^*_k\left(H^*_k P^*_{k/k-1}H^{*T}_k + R_k\right)^{-1}\Big[&y_k - h_k(x^*_k) \\ &- H^*_k\left(x^*_{k/k-1} - x^*_k\right)\Big] \end{aligned} \qquad (5.35)$$

or, equivalently,

$$\begin{aligned} x^*_{k-1/k} = \hat{x}_{k-1/k-1} + P_{k-1}\Phi^{*T}_{k,k-1}\left(I - \psi^*_k H^*_k\right)^T H^{*T}_k R^{-1}_k\Big[&y_k - h_k(x^*_k) \\ &- H^*_k\left(x^*_{k/k-1} - x^*_k\right)\Big] \end{aligned} \qquad (5.36)$$

The smoothed estimate $x^*_{k-1/k}$ is shown in Figure 5-5. The covariance matrix for $x^*_{k-1/k}$ is, from (5.16):

$$P^*_{k-1/k} = P_{k-1} - P_{k-1}\,\Phi^{*T}_{k/k-1} H^{*}_{k} \left(H^*_k P^*_{k/k-1} H^{*T}_k + R_k\right)^{-1} H^{*T}_k \Phi^*_{k/k-1} P_{k-1} \qquad (5.37)$$

We are now in a position to discuss the procedure of the locally iterated filter-smoother. First, before processing the data y_k, we choose the initial reference trajectory with end points $\hat{x}_{k-1/k-1}$, $\hat{x}_{k/k-1}$. With the choice of this reference trajectory, we obtain the filtered estimate $\hat{x}_{k/k}$ by the extended Kalman filter (Reference 18) and the smoothed estimate $\hat{x}_{k-1/k}$ by (5.38),

$$\hat{x}_{k-1/k} = \hat{x}_{k-1/k-1} + P_{k-1}\,\Phi^T_{k,k-1}\left(I - \psi_k H_k\right)^T H^T_k R^{-1}_k \left[y_k - h_k\left(\hat{x}_{k/k-1}\right)\right] \qquad (5.38)$$

which is obtained from (5.36) by replacing x^*_{k-1} and x^*_k by $\hat{x}_{k-1/k-1}$ and $\hat{x}_{k/k-1}$, respectively. Now, after the data y_k is processed, the estimate $\hat{x}_{k-1/k}$ and $\hat{x}_{k/k}$ should be more near the true trajectory. Thus, we choose $\hat{x}_{k-1/k}$ and $\hat{x}_{k/k}$ as the end points of the second trajectory as shown in Figure 5-6. Denote $\hat{x}_{k-1/k}$, $\hat{x}_{k/k}$ by $\hat{x}^{(1)}_{k-1/k}$, $\hat{x}^{(1)}_{k/k}$. We then proceed to obtain the second set of estimates $\hat{x}^{(2)}_{k/k}$ and $\hat{x}^{(2)}_{k-1/k}$ using equations (5.29), (5.30), and (5.36). In doing so, of course, x^*_{k-1} and x^*_k are replaced by $\hat{x}^{(1)}_{k-1/k}$ and $\hat{x}^{(1)}_{k/k}$ respectively. This procedure is continued for the third set of estimates $\hat{x}^{(3)}_{k-1/k}$ and $\hat{x}^{(3)}_{k/k}$ and so on, until the successive estimates of x_k are "close enough". Experience has indicated rapid convergence of the algorithm: rarely have more than two additional iterations been required.

The fixed-point smoothing algorithm is discussed next.

Fixed-Point Smoothing Algorithm

We are now in a position to derive the desired approximate fixed-point smoothing algorithm. Once again from (5.16),

$$\left.\begin{aligned} E\{x_0|Y(k)\} &= E\{x_0|Y(k-1)\} + P_{x_0\tilde{y}_k} P^{-1}_{\tilde{y}_k\tilde{y}_k} \tilde{y}_k \\ P_{x_0|Y(k)} &= P_{x_0|Y(k-1)} - P_{x_0\tilde{y}_k} P^{-1}_{\tilde{y}_k\tilde{y}_k} P^T_{x_0\tilde{y}_k} \end{aligned}\right\} \quad (5.39)$$

where

$$\tilde{y}_k = y_k - E\{y_k|Y(k-1)\}$$

Observe that the term $P^{-1}_{\tilde{y}_k\tilde{y}_k}\tilde{y}_k$ in (5.39) is identical to that in the filter-smoother case (5.16). Thus, it is necessary to evaluate only the term $P_{x_0\tilde{y}_k}$ in (5.39).

As in the case of the locally iterated filter-smoother, a proper choice of reference trajectory is required for better linearization of g_k and h_k in (5.12). It is logical to choose the final trajectory used in the locally iterated filter-smoother for each time interval $t_{k-1} \le t \le t_k$, $0 \le k \le N$. Denote the final trajectory by f and define

$$\Phi^{(f)}_{k,k-1} \triangleq \Phi_{k,k-1}\left(\hat{x}^{(f)}_{k-1|k}\right)$$

$$H^{(f)}_k \triangleq H_k\left(\hat{x}^{(f)}_{k|k}\right) \qquad \text{etc.}$$

Then, for $k = 1$,

$$\begin{aligned} P_{x_0\tilde{y}_1} &= E\left\{\left(x_0 - E(x_0)\right)\left(y_1 - E(y_1|Y(0))\right)^T\right\} \\ &\approx E\left\{\left(x_0 - \hat{x}_{0|0}\right)\left[H_1^{(f)}\Phi^{(f)}_{1,0}\left(x_0 - \hat{x}_{0|0}\right) + H_1^{(f)}w_1 + v_1\right]^T\right\} \\ &\approx P_0\,\Phi^{(f)T}_{1,0} H_1^{(f)} \end{aligned}$$

The "gain" for fixed-point smoothing at $k = 1$ can be readily obtained from (5.27) as

$$P_{x_0\tilde{y}_1} P^{-1}_{\tilde{y}_1\tilde{y}_1} = P_0\,\Phi^{(f)T}_{1,0} H_1^{(f)}\left(H_1^{(f)} P^{(f)}_{1|0} H_1^{(f)T} + R_1\right)^{-1}$$

or, equivalently,

$$P_{x_0\tilde{y}_1} P^{-1}_{\tilde{y}_1\tilde{y}_1} = B_1 H_1^{(f)T} R_1^{-1}$$

where

$$B_1 = P_0\,\Phi^{(f)T}_{1,0}\left(I - \psi_1^{(f)} H_1^{(f)}\right)^T$$

For $k = 2$,

$$P_{x_0\tilde{y}_2} = E\left\{(x_0 - E(x_0))\left[y_2 - E(y_2|Y(1))\right]^T\right\}$$
$$\approx E\left\{(x_0 - \hat{x}_{0|0})(x_1 - \hat{x}_{1|1})^T \Phi_{2,1}^{(f)^T} H_2^{(f)^T}\right\}$$

Since

$$x_1 \approx g_1(\hat{x}_{0|1}^{(f)}) + \Phi_1^{(f)}(x_0 - \hat{x}_{0|1}^{(f)}) + w_1$$
$$\hat{x}_{1|1} \approx g_1(\hat{x}_{0|1}^{(f)}) + \Phi_1^{(f)}(\hat{x}_{0|0} - \hat{x}_{0|1}^{(f)}) + \psi_1^{(f)}(y_1 - E(y_1|Y(0)))$$

we have

$$P_{x_0\tilde{y}_2} \approx P_0 \Phi_1^{(f)^T}\left[I - \psi_1^{(f)} H_1^{(f)}\right]^T \Phi_2^{(f)^T} H_2^{(f)^T}$$

and

$$P_{x_0\tilde{y}_2} P_{\tilde{y}_2\tilde{y}_2}^{-1} = B_2 H_2^{(f)^T} R_2^{-1}$$

where

$$B_2 = B_1 \Phi_2^{(f)^T}\left[I - \psi_2^{(f)} H_2^{(f)}\right]^T$$

In general, for any $k \geq 1$,

$$P_{x_0\tilde{y}_k} P_{\tilde{y}_k\tilde{y}_k}^{-1} = B_k H_k^{(f)T} R_k^{-1} \tag{5.40}$$

where

$$B_k = B_{k-1} \Phi_k^{(f)^T}\left[I - \psi_k^{(f)} H_k^{(f)}\right]^T, \quad B_0 = P_0$$

Thus, we have the following suboptimal fixed-point smoothing algorithm:

$$\hat{x}_{0|k} = \hat{x}_{0|k-1} + B_k H_k^{(f)^T} R_k^{-1}\left[y_k - h_k(\hat{x}_{k|k}^{(f)}) - H_k^{(f)}(\hat{x}_{k|k-1}^{(f)} - \hat{x}_{k|k}^{(f)})\right]$$
$$B_k = B_{k-1} \Phi_k^{(f)^T}\left[I - \psi_k^{(f)} H_k^{(f)}\right]^T, \quad B_0 = P_0 \tag{5.41}$$

From (5.41) we see that the fixed-point smoothed estimate is again computed in a recursive manner using a combination of old estimates and new data. The residual sequence is identical to $y_t - h_t(\hat{x}^{(i)}_{t|t}) - H^{(i)}_t(\hat{x}^{(f)}_{t|t-1} - \hat{x}^{(i)}_{t|t})$ which is the final residual sequence in the locally iterated filter-smoother, and the fixed-point smoothing gain is a function of the filter gain. The fixed-point smoothing algorithm (5.41) can therefore be easily mechanized to work in conjunction with the locally iterated filter-smoother in an "on-line" fashion.

After all the data $Y(N)$ has been processed, we obtain the fixed-point smoothed estimate $\hat{x}_{0|N}$. Using this estimate and the filtered estimates, an estimate of the unknown forcing term w_t can be made. The computational algorithm is discussed in the next section.

5.3 Computations of the Unknown Forcing Function

From the results of the fixed-point smoother, $\hat{x}_{0|N}$, the filtered estimate $\hat{x}_{t|t}$ and the constraint equation of the system (5.12), it is relatively straightforward to derive an approximate algorithm for estimation of the unknown forcing term, w_t , in (5.12). This estimate will be called $\hat{w}_{t|N}$ here. However, it is necessary to use the equation for the fixed-interval smoother, $\hat{x}_{t|N}$, defined but not derived above. A short derivation, using the results of the one-stage smoothed estimate, follows.

Using a well-known matrix identity, ψ^*_t , in (5.28) can be written as

$$\psi^*_t = P^*_t H^{*T}_t R^{-1}_t \tag{5.42}$$

where all symbols were defined previously. Employing (5.42), (5.29), (5.31), and (5.36), and after lengthy algebraic manipulations, the one-stage smoothed estimate may also be expressed by

$$\hat{x}_{t-1|t} = \hat{x}_{t-1|t-1} + P_{t-1}\Phi^T_t P^{-1}_{t|t-1}\left[\hat{x}_{t|t} - \hat{x}_{t|t-1}\right] \tag{5.43}$$

where the $*$ and f superscripts have been dropped for convenience.

We shall now make use of (5.43) in a sequential manner to obtain the fixed-interval smoother. Suppose that we have already obtained $\hat{x}_{k-1/k}$ via (5.43). It represents the best estimate we have concerning the state at $k-1$ given data up to k. Now, consider the smoothing problem of a single-stage transition between the state at $k-1$ and $k-2$ and reapply (5.43). This yields:

$$\hat{x}_{k-2/k} = \hat{x}_{k-2/k-2} + P_{k-2}\,\phi^T_{k-1}\,P^{-1}_{k-1/k-2}\left[\hat{x}_{k-1/k} - \hat{x}_{k-1/k-2}\right] \tag{5.44}$$

where $\hat{x}_{k-2/k}$ and $\hat{x}_{k-1/k}$ have replaced $\hat{x}_{k-1/k}$ and $\hat{x}_{k/k}$, respectively, in (5.43).

Therefore, the fixed-interval smoother becomes

$$\hat{x}_{k-1/N} = \hat{x}_{k-1/k-1} + P_{k-1}\,\phi^T_k\,P^{-1}_{k/k-1}\left[\hat{x}_{k/N} - \hat{x}_{k/k-1}\right] \quad , 1 \le k \le N \tag{5.45}$$

which is a backward recursion starting with the filter estimate $\hat{x}_{N/N}$.

To obtain the estimate $w_{k/N}$ for the unknown forcing function applied to the system at time t_k, we need the constraint equation for (5.45). To find the constraint equation, let us consider (5.12)

$$x_k = g_k(x_{k-1}) + w_k \qquad \begin{matrix}(5.12)\\ \text{(repeat)}\end{matrix}$$

Then:

$$\hat{x}_{k/N} \triangleq E\left\{x_k \,|\, Y(N)\right\} = E\left\{\left[g_k(x_{k-1}) + w_k\right] \,\Big|\, Y(N)\right\} \tag{5.46}$$

Now, as usual, expand $g_k(x_{k-1})$ about the final one stage smoothed estimate $\hat{x}_{k-1/k}$ (note that the superscript f has been dropped), which yields:

$$g_k(x_{k-1}) \approx g_k(\hat{x}_{k/k-1}) + \Phi_{k,k-1}(x_{k-1} - \hat{x}_{k-1/k})$$

Substituting the above equation into (5.46), we have the desired constraint equation for the fixed-interval smoothing:

$$\hat{x}_{t|N} = g(\hat{x}_{t-1|t}) + \Phi_{t,t-1}(\hat{x}_{t-1|N} - \hat{x}_{t-1|t}) + \hat{\omega}_{t|N} \tag{5.47a}$$

or

$$\hat{\omega}_{t|N} = \hat{x}_{t|N} - g_t(\hat{x}_{t-1|t}) - \Phi_t(\hat{x}_{t-1|N} - \hat{x}_{t-1|t}) \tag{5.47b}$$

Making use of (5.45), (5.30), and (5.47b), it can readily be shown that

$$\hat{\omega}_{t|N} = Q_t P^{-1}_{t|t-1}(\hat{x}_{t|N} - \hat{x}_{t|t-1}) \tag{5.48}$$

Notice that the form of (5.48) is identical to that of the linear case (Reference 30). However, it should be pointed out that $P_{t|t-1}$ and $x_{t|t-1}$ in (5.48) are the final values in the locally iterated extended Kalman filter. Notice also that if $\hat{x}_{t|N}$ is available for all t, (5.48) will suffice to estimate the unknown forcing function. However, at the completion of the fixed-point smoothing we have only $\hat{x}_{0|N}$, and the constraint equation (5.47b) and (5.48) must be reused. We have, therefore,

$$\hat{\omega}_{t|N} = \left[I - Q_t P^{-1}_{t|t-1}\right]^{-1} Q_t P^{-1}_{t|t-1} \left\{ g(\hat{x}_{t-1|t}) - \hat{x}_{t|t-1} + \Phi_{t,t-1}(\hat{x}_{t-1|N} - \hat{x}_{t-1|t}) \right\} \tag{5.49}$$

Once again, using (5.30), we have

$$g(\hat{x}_{t-1|t}) - \hat{x}_{t|t-1} = -\Phi_{t,t-1}(\hat{x}_{t-1|t-1} - \hat{x}_{t-1|t})$$

Then (5.49) finally becomes

$$\hat{\omega}_{t|N} = G_t(\hat{x}_{t-1|N} - \hat{x}_{t-1|t-1}) \tag{5.50a}$$

where

$$G_t = \left[I - Q_t P^{-1}_{t|t-1}\right]^{-1} Q_t P^{-1}_{t|t-1} \Phi_{t,t-1} \tag{5.50b}$$

Note that the gain matrix G_t can be precomputed and stored along with $\hat{x}_{t|t}$ in the locally iterated filter-smoothing pass.

Equations (5.50) and (5.47a) form a pair of difference equations which are recursively solved for $\hat{\omega}_{k/N}$, starting with $\hat{x}_{0/N}$.

5.4 Improved Covariance Computation

Variances for Fixed-Point Estimated Parameters

The covariance matrix for the fixed-point smoothed estimate can be readily obtained from equations (5.39) and (5.40) as:

$$P_{x_0|Y(N)} = P_{x_0|Y(N-1)} - B_N H_N^{(i)'} Q_N^{-1} H_N^{(i)} \Phi_N^{(i)'} B_{N-1}^T \tag{5.51}$$

where B_N is given by the second equation of (5.41).

Since the locally iterated filter-smoother and fixed-point smoother employ a priori information, P_0 , it would seem that equation (5.51) could be employed for a final covariance computation. However, as will be discussed in the next section, the a priori information for P_0 in the case of parameter estimation is almost always unavailable and is usually produced from the same given data; in other words, P_0 is obtained after processing the given data. As such, it is not a priori information in the true sense in that it is independent of the given data. Rather, the P_0 obtained through using the data should be regarded as a means to start up the locally iterated filter-smoother. Consequently, it is appropriate to compute the covariance matrix of the fixed-point estimated parameters in an independent way that does not utilize the a priori information.

Recall that in deriving the fixed-point smoothing algorithm we have assumed that x_0 , $Y(k), 1 \le K \le N$ are jointly Gaussian. This implies that both x_0 and $x_0|Y(k)$ are normally distributed. We have, therefore,

$$f\left(Y(N)/x_0\right) = \frac{f(x_0|Y(N))\, f\left(Y(N)\right)}{f(x_0)} \tag{5.52}$$

and, because both x_0 and $x_0|Y(N)$ are Gaussian,

$$\frac{\partial^2}{\partial x_0^2}\left[-\ln f\left(Y(N)|x_0\right)\right]=\frac{\partial^2}{\partial x_0^2}\left\{\frac{1}{2}\left\|x_0-E\left(x_0|Y(N)\right)\right\|^2_{P^{-1}_{x_0|Y(N)}}\right\}$$
$$-\frac{\partial^2}{\partial x_0^2}\ \frac{1}{2}\left\|x_0-\hat{x}_{0|0}\right\|^2_{P_0^{-1}} \tag{5.53}$$

Assuming that the fixed-point smoother is an asymptotically efficient estimator, then without use of the a priori information, the covariance of the parameter estimate will approach the Cramer-Rao lower bound CR_N (Reference 19) which is given by

$$CR_N \triangleq \left\{\frac{\partial^2}{\partial x_0^2}\left[-\ln f\left(Y(N)|x_0\right)\right]\right\}^{-1} \tag{5.54}$$

From equation (5.53), it is readily shown that

$$CR_N=\left(P^{-1}_{x_0|Y(N)}-P_0^{-1}\right)^{-1} \tag{5.55}$$

Equations (5.55), (5.51) and the second equation of (5.41) are the desired recursive formulae for computing the improved covariance matrix of the fixed-point smoothed estimate for parameters. It can be shown that with $w_i = 0$, i.e., $Q_1 = Q_2 = \ldots = 0$, equation (5.55) reduces to

$$CR=\left[\sum_{i=1}^{N} Z_i^{(f)T} H_i^{(f)T} R_i^{-1} H_i^{(f)} Z_i^{(f)}\right]^{-1} \tag{5.56}$$

where

$$Z_i^{(f)}=\Phi^{(f)}_{i,i-1}\ Z^{(f)}_{i-1}\ ,\ Z_0^{(f)}=I$$

Start-Up Procedure for Locally Iterated Filter Smoother

When employing the equations-of-motion estimator as the initial start-up procedure for the Kalman filter on computer generated data (see Section VI), it has been observed that the variances of the parameter estimates, which are used as the diagonal elements for P_0 computed for this estimator were not consistent with the parameter estimates. In most cases, the variances were much too small to indicate the accuracy of the parameters estimated. However this was expected, since the equations-of-motion estimator is a simple least squares technique (equation error method) with unity weighting; and we have shown in Section III that this estimator gives asymptotically biased estimates when measurement errors are present. We recall also that, in Section 3.1, the variances of the parameter estimates were computed based on the classical linear regression theory with non-stochastic regressor. Since in actuality the regressor is stochastic, the variances computed in the equations-of-motion method are only an approximation.

From experience using computer generated data, where the noise levels are known, best results were obtained by increasing the computed variances by a factor of from 1 to 10 equally for all the parameters. This increase was necessary to account for the bias of the initial parameter estimates by forcing the filter to place less weight on these estimates. Although the variance of each individual parameter could be increased by different factors, the computer time required to obtain the best combination of factors by experimentation would be formidable. Further, the best factor to use in each particular situation is not known since it is strongly dependent on the control input and noise levels present. However, in view of the erroneous variance computation, it is doubtful that equally increasing the variances with the same factor is appropriate. It seems more appropriate, therefore, to first more correctly compute the variances of the estimated parameters and then increase them equally to keep their magnitudes in the proper proportion.

Thus, a better scheme to start up the Kalman filter from initial parameter estimates is to calculate P_0 for the parameters by an independent technique. Assuming that the initial parameter estimates are produced from an efficient estimator, then the covariance matrix, P_0, for the initial parameter estimates can be shown to approach the Cramer-Rao (CR) lower bound. Thus, equation (5.56) can be employed in the calculation of the improved start-up covariance P_0. Here, of course, the matrices $\Phi_{i,i-1}$ and H_i are evaluated along the trajectory using the initial estimated parameters, i.e.,

$$CR \propto \left[\sum_{i=1}^{N} Z_i^T H_i^T R_i^{-1} H_i Z_i \right]^{-1} \qquad (5.57)$$

where

$$Z_i = \Phi_{i,i-1} Z_{i-1} \quad , Z_0 = I$$

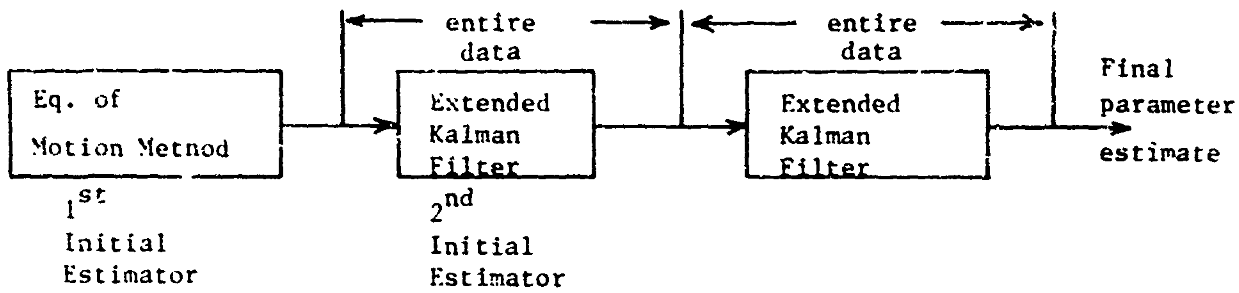

Figure 5-1a A Systematical Recycling Scheme

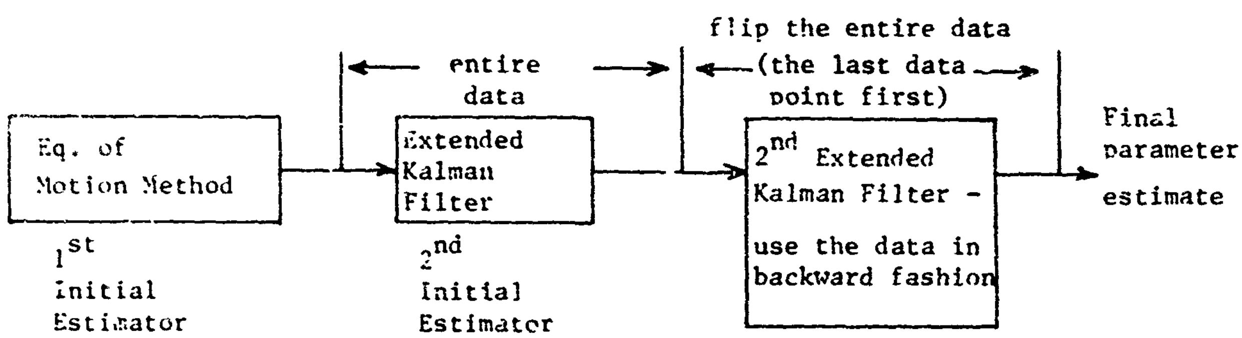

Figure 5-1b An Alternate Recycling Scheme -
SCI's Forward-Backward Filtering

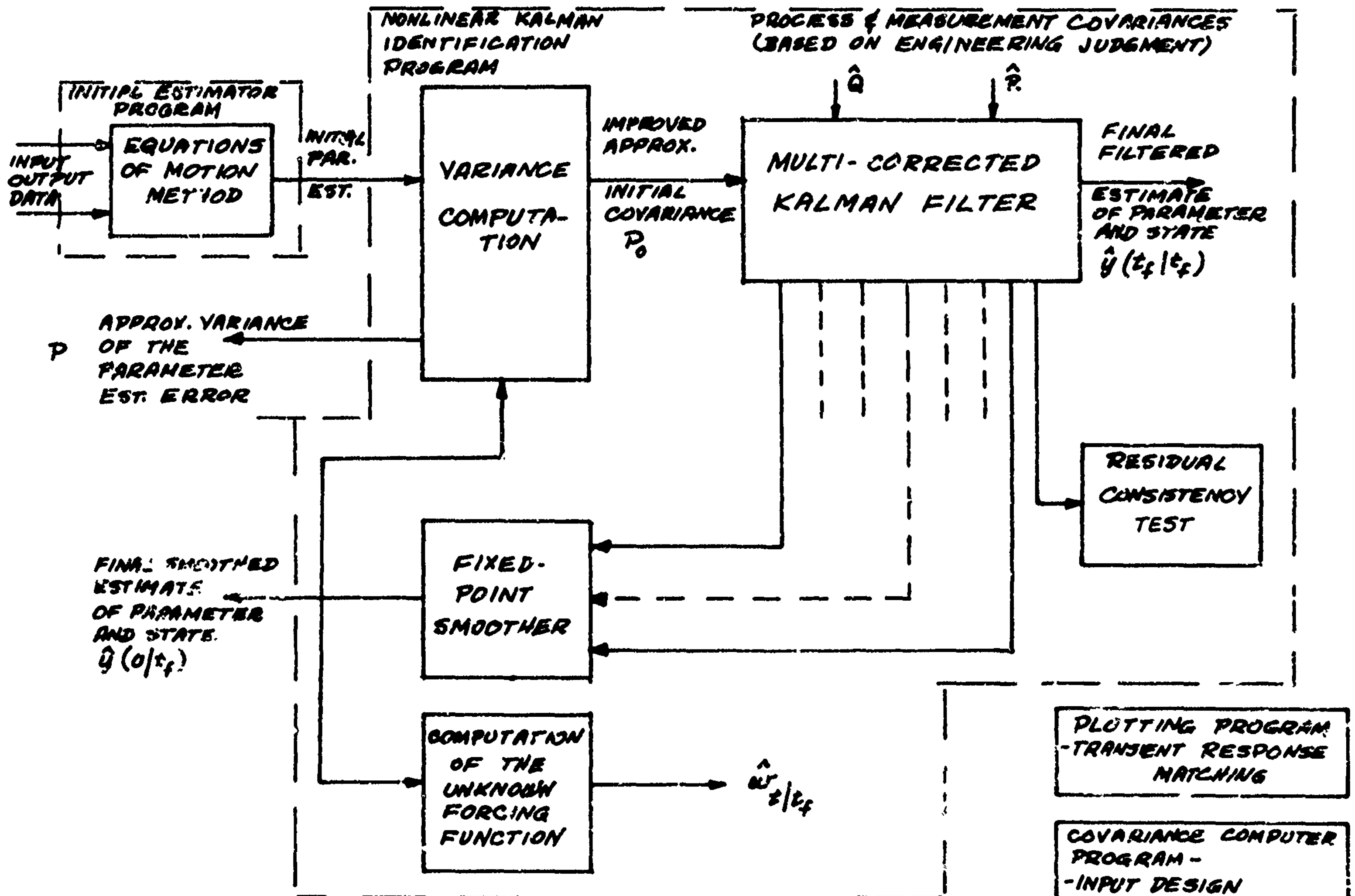

Figure 5-2 Block Diagram of the CAL Identification Program

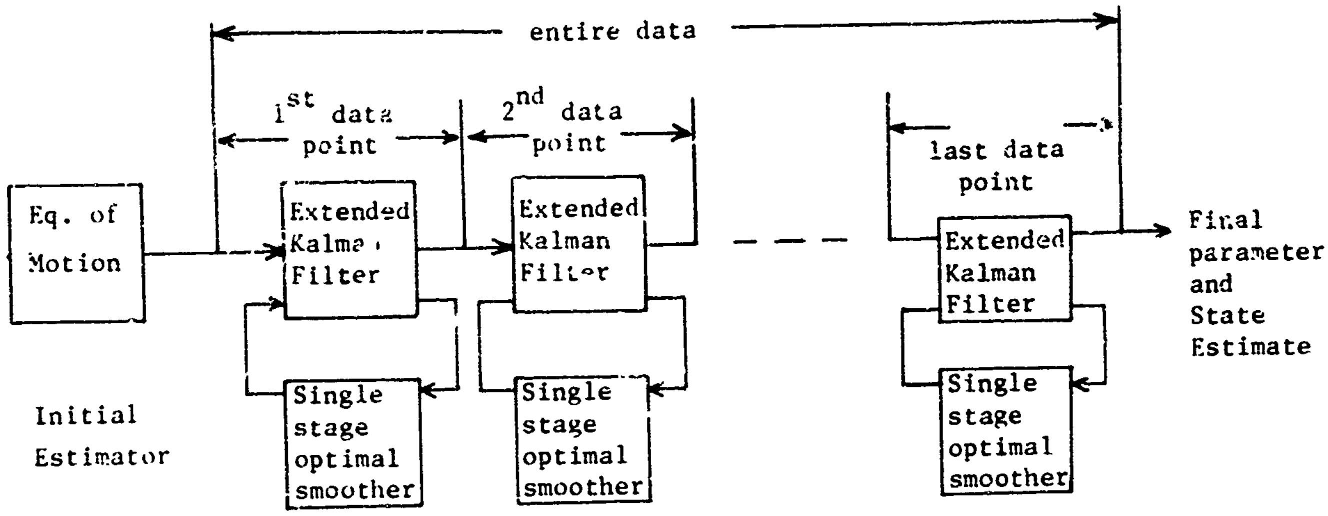

Figure 5-3 Local Iterative Filter-Smoother (The Multi-Correction Scheme)

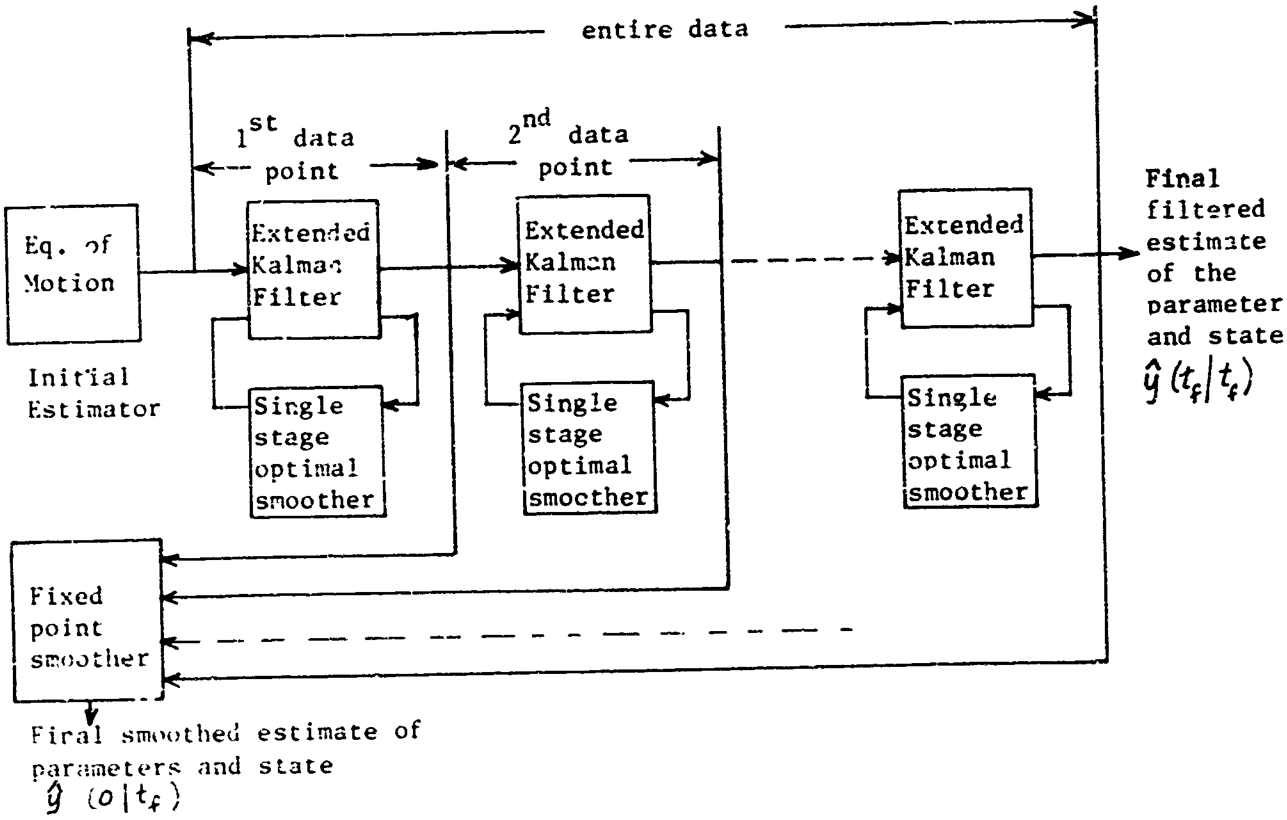

Figure 5-4 Fixed-Point Smoother Working in Conjunction With Local Iterative Filter-Smoother

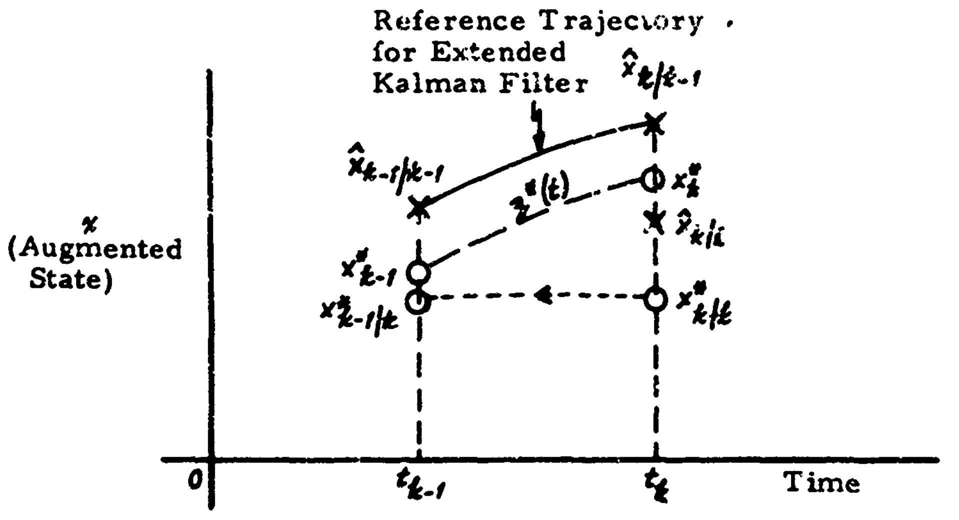

Figure 5-5 Reference Trajectory

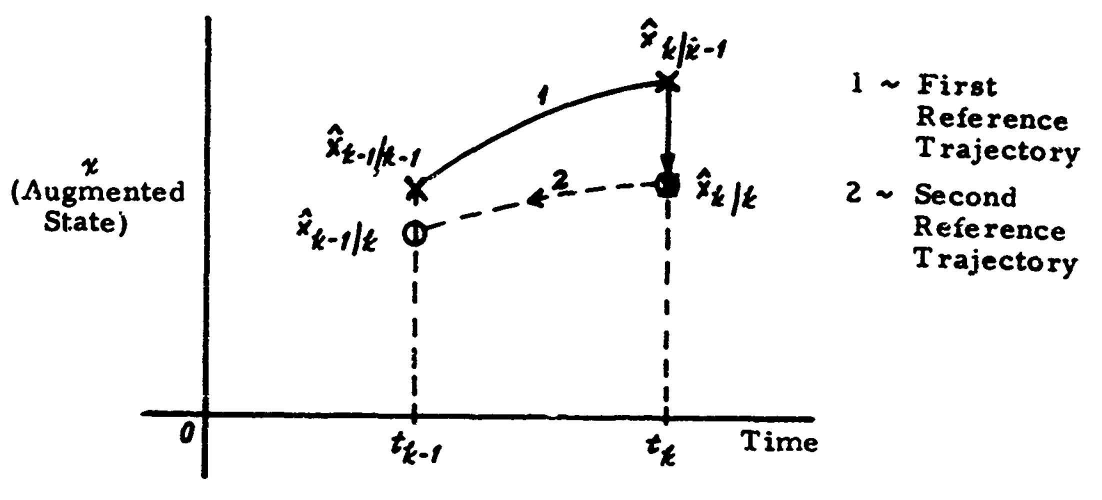

Figure 5-6 Updating of Reference Trajectory

SECTION VI

NUMERICAL VERIFICATION OF ADVANCED TECHNIQUES

To prove the concepts and to verify the accuracy of the developed identification techniques, computer-generated data were used. In this section we shall describe the generation of the data that were used. We will then discuss the results of applying the technique to these data, and indicate the effects of using acceleration measurements, the effects of reusing the data, the effects of the multi-correction and fixed-point smoothing, the effects of a different start-up procedure, and finally the effects of the noise covariances $\mathcal{R}$ and $\mathcal{Q}$. In lieu of exhaustive Monte Carlo simulation to fully evaluate the performance of the technique, which would be very costly for this identification problem, the criteria of performance used here are: 1) the accuracy of the parameters estimated, and 2) transient response matching to measured data.

6.1 Data Generation

Appendix D describes the computer-generated data employing the linearized equations of motion and Gaussian noise sequences. The flight conditions were chosen to be at a fixed-duct incidence of 30°, and the resulting data were designated as 1A, 1B, 1C, and 1D, depending on the noise levels and on whether or not process noise was present. Since the equations of motion that best describe the X-22A aircraft are nonlinear as discussed in Section II, more data were subsequently generated to study in greater depth the effects of nonlinearities and a larger number of parameters on the accuracy of the developed technique. Again, as in the linear case, independent white Gaussian random noise sequences with zero mean and appropriate variances were added to the outputs of the state variables and the accelerations, simulating measurement noise. In addition, the same type of noise sequences was added to the vehicle representation in the equations of motion to simulate process noise.

Data 2A-1, 2C-1, and 2D-1, as shown in Table 6-1a, were generated using an input (single pulse) in the longitudinal stick deflection alone. Again, the flight conditions were chosen at the duct incidence of 30°. The flight conditions, noise levels, and the true parameters used for data generation are all shown in Table 6-1a. In Table 6-1a, we also see the characteristics of the set of data 2A-2 through 2D-2 using a better conditioned input (multi-pulses) in the longitudinal stick deflection.

To aid in the evaluation of the improved techniques, and particularly the improved start-up procedure, and to serve as a basis for application of the identification technique to flight test data at FCP (Fixed-Operating-Point), two additional sets of computer-generated data were generated. These cases, called 3C-1 and 3D-1, are shown in Table 6-1b, and were generated without and with process noise, respectively. The noise level used is also shown in the table. The model in each case employed linear aerodynamics with slightly modified "global" values at $\lambda = 45°$. However, in these cases, process noise was considered to represent equation error and not gust effects as in the previous cases (2A-1 through 2D-1, 2C-2 and 2D-2 above). Thus, the process noise effectiveness matrix, $\mathcal{G}_1$, in (2.15), is simply $\mathcal{G}_1 = I_4$. A realistic longitudinal stick input, taken from Flight 2F198 of the MPE II data (Reference 58) was used. Detailed descriptions of the MPE II data will be given in Section VII.

The measurement noise levels used were obtained by observing the oscillograph records of the MPE II data. As will be explained in Section VII, these levels are very high. In addition, the standard deviation of the process noise was chosen as approximately 10% of the RMS (root mean square) value of the acceleration measurements, thus causing a very high value for $\sigma_{\dot{w}}$.

In all cases, the data were generated on the computer employing a fourth-order Runge-Kutta integration technique with a fixed step size (Δt) of 0.05 seconds. For derivative evaluations between data points, linear interpolation was used for the control inputs, but the process noise inputs, $w(t)$, were held constant. Since Δt is sufficiently small, the process noise can effectively be interpreted as forcing the dynamical equations through a sample and hold network, the output of which is a white Gaussian sequence whose covariance is approximately reduced by a factor of Δt from the covariance of the input noise. Following this interpretation, the process noise standard deviations given in Table 6-1 are those prior to sampling and holding. Due to the discrete formulation of the identification algorithm, no ambiguity exists for the measurement error. Refer to Appendix D for a more detailed explanation.

As a representative case, and to observe the effects of the defined level of process noise on the measured responses, data generated for 3C-1 and 3D-1 are shown in Figures 6-1 and 6-2, respectively. Responses for $\dot{u}$, $\dot{w}$, and $\dot{q}$ (labeled as u^*, w^*, and q^*), although not used as measurement sources, are shown along with the simulated measurements - q, θ, u, w, n_x, n_z, and $\dot{q}$.

6.2 Effects of Using Acceleration Measurements

Longitudinal acceleration measurements $\dot{q}$, n_x, and n_z contain additional information concerning the excitation and motions of the aircraft. The parameters identified using the acceleration measurements in addition to the state variable measurements would therefore be expected to be more accurate than those identified using only the state variable measurements.

Table 6-2 shows a comparison of the results obtained from the extended Kalman filter with and without acceleration measurements on data case 2D-2. The initial parameter estimates were from the equations-of-motion estimator, and the initial variances of these estimates (which were calculated from the equations-of-motion estimator using (3.3d)) were multiplied by a factor of 10 to initialize the Kalman filter. In both identification runs on data 2D-2 with and without acceleration measurements, the initial conditions for the aircraft states (q, θ, u, and w) were set equal to the first point in the measurements, and their initial covariances were set equal to the measurement noise present on these sensors. (Note:

this procedure was followed for all identification runs in this section.) Notice that the parameter estimates are, in general, closer to the correct values for the runs with acceleration measurements than for those without. The improvement in accuracy is not drastic, however, which perhaps is a result of conditioned input and the fact that the total noise level present on the acceleration measurements (which includes the contribution added by the process noise) is large relative to the noise level in the other state measurements.

Unfortunately, introducing acceleration measurements into the extended Kalman filter increases the computational load by a large amount, because the size of the matrix required for inversion at each data point is equal to the number of time histories used and also because the measurements now become nonlinear functions of the aircraft state and parameters. Using acceleration measurements in addition to the state variable measurements, the number of time histories increases from 4 to 7, which requires, among other things, inverting a 7 x 7 matrix instead of a 4 x 4 matrix at each data point. Proper scaling of the variables and parameters is also required to avoid ill-conditioned numerical situations (large differences in order of magnitude). It was found that the best combination of units was ft/sec^2 for n_x and n_z and degrees for all angular units.

The transient responses computed from these two sets of identified parameters (Table 6-2) matched very well with the measurements. These responses are shown in Figure 6-3 for the case in which acceleration measurements were used; those of cases without acceleration measurements were essentially identical. Due to the very high signal to noise ratio (which, incidentally, is very unrealistic and cannot be obtained in flight because of the large excursions of the aircraft motion), the transient responses computed using the initial estimated parameters (from the equations-of-motion method) also match very well.

6.3 Effects of Reusing Data

Since the parameter identification of a VTOL aircraft is a post-flight data analysis problem, it is possible, of course, to reuse the same flight data. Further, since the extended Kalman filter is a biased estimator for parameter identification problems (see Appendix H), it is desirable to reuse the same data all over to reduce the bias of the estimate. In our early development of identification techniques employing the extended Kalman filter, we were therefore forced to utilize a recycling scheme to improve the parameter estimates. This scheme essentially considered the first pass through the extended Kalman filter as the second initial estimator (the equations-of-motion method being the first initial estimator) for the second pass of the extended Kalman filter, which then refiltered the data in a forward fashion (t_0 to t_f). An alternate way of reusing the data is backward filtering. Again, we may consider the forward pass as the second initial estimator for the second extended Kalman filter (the backward filter), which filters the data from t_f to t_0 . These two schemes of repeatedly using the extended Kalman filter are shown in Figure 5-1. It is important to point out that both second filters are extended Kalman filters, and, therefore, the second filter is again a biased estimator just as the first filter. As we have discussed, the locally iterated filter-smoother subsequently developed circumvents this difficulty of needing to reuse the data.

Table 6-3 shows a comparison of typical computer runs of the two schemes of reusing the data, both using acceleration measurements. The data used are multi-pulses in δ_{ES} , with both moderate process and measurement noise (data 2D-2). From this table, it can be seen that the second filter, either forward or backward, does not substantially improve the parameter estimates. This fact may be partly attributable to the fact that the initial estimator has already given a good parameter estimate for this type of input.

6.4 Effects of Multi-Corrections - The Use of Locally Iterated Filter-Smoother

Table 6-4a shows a comparison of the parameter estimates resulting from the above schemes of reusing the data in the extended Kalman filter with the results of a simple version of the locally iterated (or multi-corrected) extended Kalman filter on data case 2D-2. In these computer runs, as before, acceleration measurements were utilized. The last column in Table 6-4a is case $F_{10}^{*}(1)$, in which a simplified multi-corrector + (no optimal one-stage smoothing, only one additional local iteration) was used. From Table 6-4a we see that the parameter estimates are slightly more accurate than the two schemes of reusing the data. From Tables 6-3 and 6-4a, a comparison can also be made between this simple version, $F_{10}^{*}(1)$, and the extended Kalman filter, F_{10}, with no recycling. Again, the differences are very small, indicating the initial parameter estimates are accurate enough to require little or no improvement in the reference trajectory from the additional correction. Again, all transient responses are equivalent to those in Figure 6-3.

The effects of the multi-correction can be seen more clearly from Table 6-4b. The data used here are not well-conditioned (single pulse in δ_{es} with moderate measurement noise). Further, because of the fact that the data have no process noise added (case 2C-1), the simplified version of multi-correction is identical to a better version which incorporates optimal one-stage smoothing. From this table it is seen that the results of two additional local iterations improve significantly the estimate of the parameters. It can also be seen that improvements can be made with different choices of P_0, the initial covariance matrix of the estimated parameters. Typical transient responses are shown in Figure 6-4.

\+ This simplified version of multi-correction was programmed for the case where process noise was absent. One-stage smoothing then becomes backward prediction, which is simply an integration of the dynamical equations backward one data point from the filtered estimate.

The same comparison is made in Table 6-4c for data case 2D-1 employing the correction with one-stage smoothing. As shown, no improvement is obtained for this data set; however, it is again noted that the parameter estimates are very sensitive to P_0. Transient responses, representative of all three sets of parameter estimates, are given in Figure 6-5. Results of the fixed-point smoothing algorithms working in conjunction with the locally iterated filter will be discussed below.

Table 6-5 shows the effects of multi-correction for data case 3D-1. The acceleration measurements were used and the multi-corrector used was the one with optimal one-stage smoothing. The results show that one additional correction improves the parameter estimates. Transient response matching to data case 3D-1 is shown in Figure 6-6. The improvement in response matching over the time histories computed using the parameters estimated from the equations-of-motion method is clearly indicated in this figure.

From Tables 6-4b and 6-4c, it is evident that the parameter estimates using the locally iterated filter-smoother are very sensitive to the choice of the initial covariance matrix P_0. Evaluation of a better choice of P_0 as discussed in Section 5.4 is given in the next subsection.

6.5 Effects of Different Start-Up Procedures

From the preceding discussions and tables associated with evaluating the locally iterated filter, it is apparent that the final parameter estimates are very sensitive to the initial covariance matrix P_0. This fact can be seen in Table 6-4b for data case 2C-1, where three sets of parameter estimates are obtained from the locally iterated filter by increasing equally all the variances of the initial parameter estimates (from the equations-of-motion estimator) by factors of 1, 10 and 100. The results obtained from using a factor of 10 are better in the X and Z derivatives than those from using 1, but are not as good in the moment derivatives. Clearly, no uniformly better set of parameters is obtained by increasing all of the initial variances computed from (3-3d) by the same factor*. Furthermore, the proper amount of increase for each parameter is dependent on the control input and noise levels present. These numerical results confirm the desirability of employing the proposed start-up procedure discussed in Section 5.4.

Since the CR lower bound given in equation (5.57) is computed in the quasilinearization identification algorithm, which has been previously evaluated (see Section 3.2), this algorithm was used to evaluate the proposed new start-up procedure on data 3C-1 and 3D-1, which have a smaller number of parameters than data 2C-1 and 2D-1. A comparison is made in Table 6-6a between σ_{EM} (from equations-of-motion estimator), σ_{CR} (CR lower bound standard deviation), and the absolute estimation error for data 3C-1 and 3D-1. Here the absolute estimation error is the absolute difference between the true parameter value and the parameter estimate from the initial estimator. The CR bound was computed in the quasilinearization program and increased by a factor of 20. As is evident, the absolute estimation error is generally within the $2\sigma_{CR}$ value, which demonstrates that this method of computing the initial variances gives a better indication of the initial parameter estimate quality than does the equations-of-motion estimator.

Results presented in Table 6-6b are for data case 3D-1. Here the lower bound, CR, was computed as given by (5.57). Included in the table is a comparison between the extended Kalman filter (F_1) and the locally iterated filter ($F_1(1)$) with one iteration, starting with $\hat{P}_0$ for the parameters from the equations-of-motion estimates. This comparison has already been discussed and shown in Table 6-5 and thus will not be dwelled upon further.

---

* The same situation can be seen from Table 6-4c, which utilized data set 2D-1, and Table 6-5, which utilized data set 3D-1.

Also shown are the results from the fixed-point smoothing algorithm, for both the initial aircraft states and the parameters employing the improved start-up procedure with a factor of 20. The fixed-point smoother was working in conjunction with the locally iterated filter using one iteration. A final variance computation for these estimates as discussed in Section 5.4 and computed by (5.57), is given by $\sigma = \sqrt{CR_u}$ (standard deviation).

The results are very impressive. Comparing the smoothed parameter estimate with the locally iterated filter, we see a substantial improvement.* The filtered parameter estimates are shown as a function of time in Figure 6-7. Transient response matching to measured data is equivalent to the case in Figure 6-6. The final variance computation for these estimates also agrees very well with the error in the estimates. In most cases, the magnitude of the absolute estimation error is within the 2σ value obtained from the final variance computation.

Improved accuracy may be possible by equally increasing the initial variances from the CR computation by a different factor to form P_0. The best factor to use could be obtained by additional experimentation; however, time constraints did not permit further development of the start-up procedure.

6.6 Fixed-Point Smoothing Results

The fixed-point smoothing algorithm developed in Section 5.2 has been applied to data cases 2D-1 and 3D-1. The results, as indicated on Tables 6-4b and 6-6c, have shown that the smoothed parameter estimates and filtered parameter estimates are approximately the same. A close examination reveals that this weak "smoothability" of the parameters is attributable to the low ratio of process noise to measurement noise considered in these cases. An augmented state is considered smoothable if smoothing

* This comparison can be made because the parameters are only slightly smoothable (see next section).

of the data yields an estimate of the state which is different from that which would be obtained by integrating the final filtered state estimate (at t_f) backward in time (Reference 41). For the parameter identification problem, the parameters to be identified are considered constant states, and therefore the filtered and smoothed parameter estimates will be equal only if the parameters are not smoothable.

From the equations for the fixed-point smoothing algorithm or the fixed-interval smoothing algorithm, which are given in Sections 5.2 and 5.3, and the form of the state transition matrix between data points, it can be shown that the improvement which smoothing gives over filtering is strongly dependent upon the ratio of the levels of process noise to measurement noise present although the proof of this observation is by no means trivial. As an intuitive example, however, let us look at the relative magnitudes of the process noise to measurement noise present in data set 3D-1. Since the measurement system is discrete whereas the dynamics are continuous, the comparison is properly made by comparing the magnitude of the elements of Q, for a <u>discrete</u> process noise sequence, to the elements of R, the measurement noise covariance matrix which includes the effects of process noise in the acceleration measurements.

From Table 6-1b, we have

$$Q = (\Delta t)^2 \left[\begin{array}{cccc|c} .16 & 0 & 0 & 0 & \\ 0 & 0 & 0 & 0 & 0 \\ 0 & 0 & .01 & 0 & \\ 0 & 0 & 0 & 10.24 & \\ \hline & & 0 & & 0 \end{array}\right]$$

$$= \left[\begin{array}{cccc|c} 4\times 10^{-4} & 0 & 0 & 0 & \\ 0 & 0 & 0 & 0 & 0 \\ 0 & 0 & 2.5\times 10^{-5} & 0 & \\ 0 & 0 & 0 & 2.56\times 10^{-2} & \\ \hline & & 0 & & 0 \end{array}\right]$$

and

$$R = \begin{bmatrix} 4.84 \times 10^{-2} & & & & & & 0 \\ & 8.1 \times 10^{-3} & & & & & \\ & & 6.76 & & & & \\ & & & 1.0 & & & \\ & & & & .1593 & & \\ & 0 & & & & 12.83 & \\ & & & & & & 5.45 \end{bmatrix}$$

Judging from the magnitude of the elements of R and Q, then, the parameters are expected to be only slightly smoothable for data case 3D-1; as confirmed by numerical results. The same situation applies for data case 2D-1, except here the analysis is more complicated because the process noise is not stationary.

6.7 Residual Consistency Test

An essential feature of an identification technique is to be able to predict, with reasonable confidence, the accuracy of the estimated parameters. If more than one set of parameter estimates are available, either from the same measurement data or different measurement data with different control inputs, then a judgment is required to determine which parameter set is the most accurate, or which combination of these parameter sets would give the most accurate set.

As a means of evaluating the accuracy of the estimates, transient response matching to measured data and an improved final covariance computation for the parameter estimates have been employed. Also, an improved start-up procedure for calculating P_0 has been proposed in order to obtain more accurate parameter estimates. This start-up procedure has had limited evaluation on computer generated data where the measurement noise and process noise levels are known.

However, when using the locally iterated filter and fixed-smoothing technique on actual flight data, the actual values of R and Q to use in the algorithm must be determined by engineering judgment. R can usually be obtained readily from the measured data but Q is not as easily chosen. Since the improved start-up procedure, the final covariance computation and, of course, the final parameter estimates - either indirectly through the computation of P_0 or the sensitivity of the estimates to R and Q (see Appendix K) - depend upon the selected values for R and Q, a performance measure to aid in the selection of these matrices is very important.

A measure of the identification technique performance can be made by performing statistical tests on the predicted measurement residuals (innovation sequences), which are the differences between the actual measurements and predicted measurements during the filter operation. These residuals are defined as $\tilde{y}_k$ in Section 5.2 for the locally iterated filter. From equations (5.17), (5.27), and (5.29), we have

$$\tilde{y}_k = y_k - h_k(x_k^*) - H_k^*(x_{k|k-1}^* - x_k^*)$$

$$E\{\tilde{y}_k\} = 0$$

$$P_{\tilde{y}_k \tilde{y}_k} = H_k^* P_{k|k-1}^* H_k^{*T} + R_k$$

Thus, if the assumed noise covariances (R and Q) and dynamical model are fairly accurate, these residuals should be small, random, zero mean and should possess statistical properties <u>consistent</u> witn their calculated statistics, $P_{\tilde{y}_k \tilde{y}_k}$. Although the residual sequence provides a convenient way of adaptively estimating Q and R as filtering proceeds (Reference 31), the approach taken here is to use them to provide an indicator for determining if the R and Q were set properly. If not, R and Q can be readjusted and another identification run made.

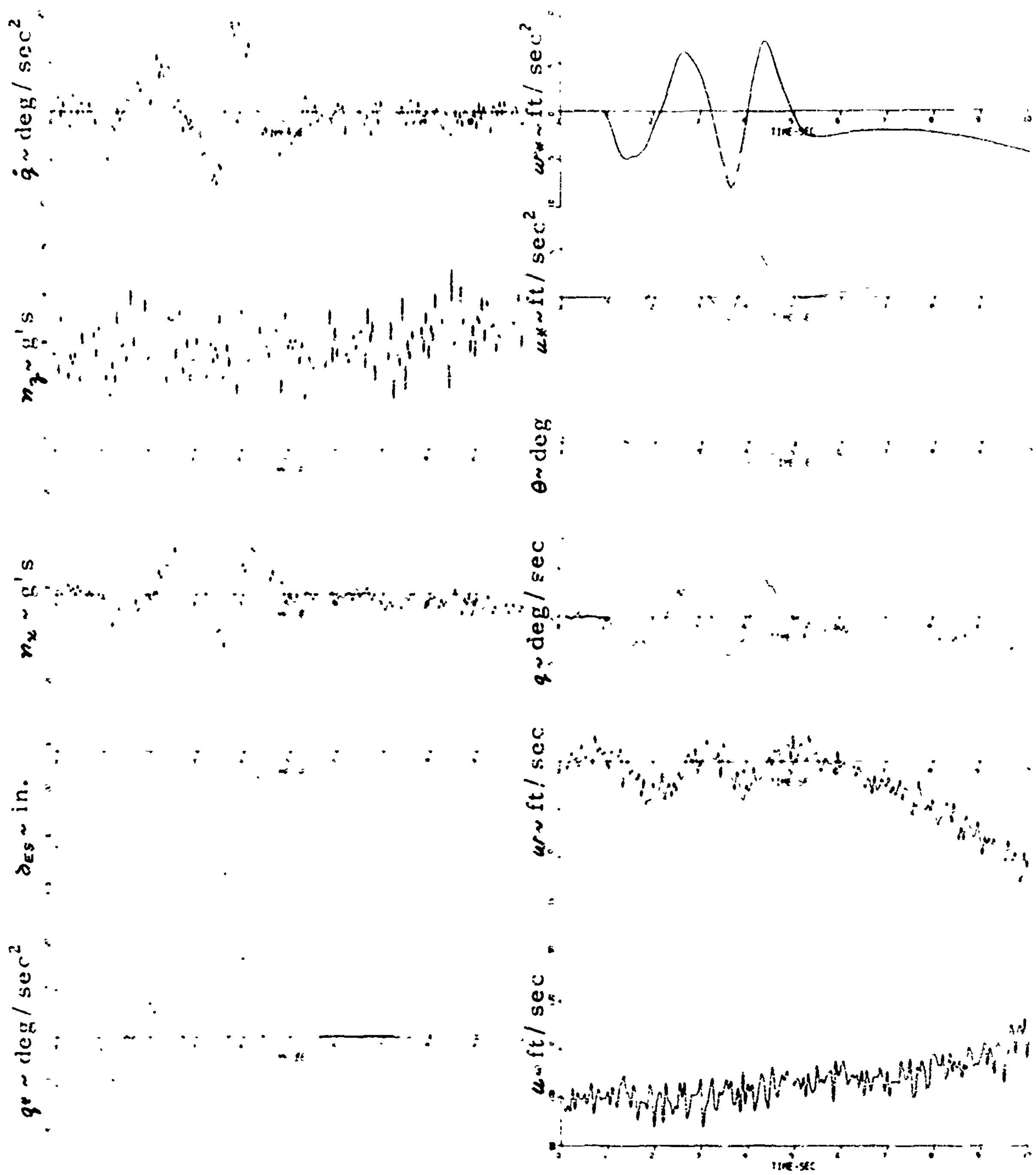

Figure 6-1 Computer Generated Data 3C-1

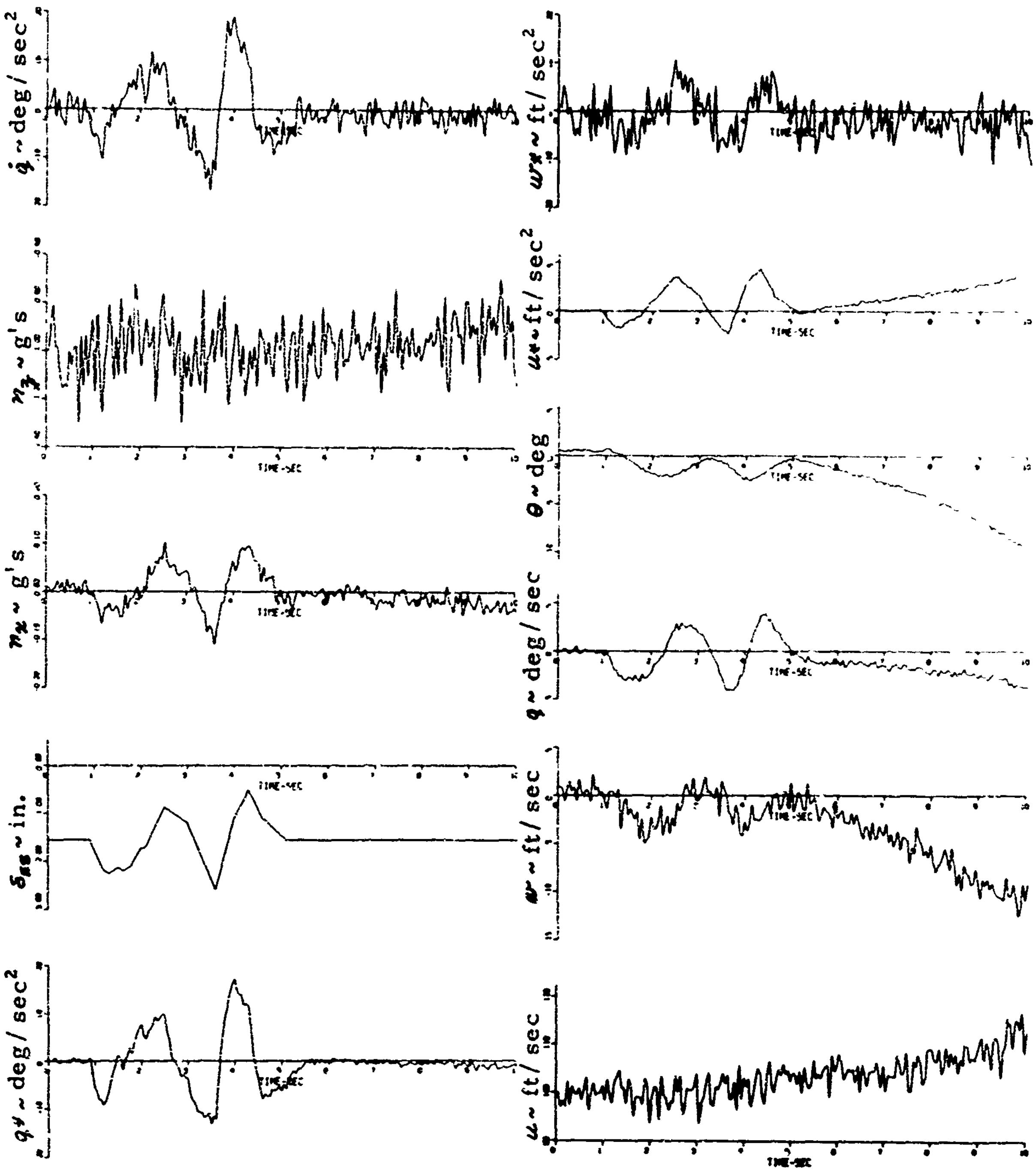

Figure 6-2 Computer Generated Data 3D-1

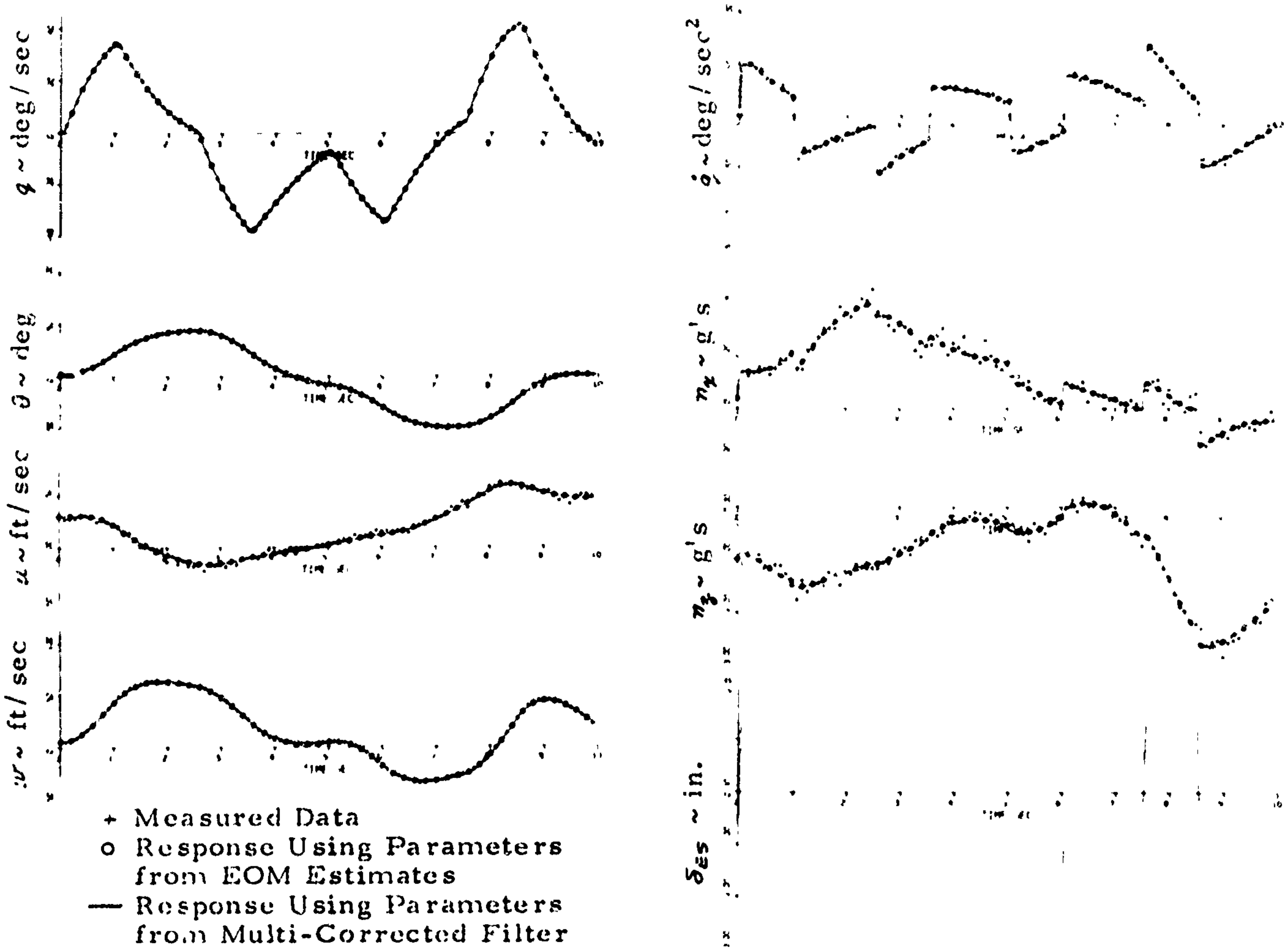

Figure 6-3 Transient Response Matching to Data 2D-2, Typical Kalman

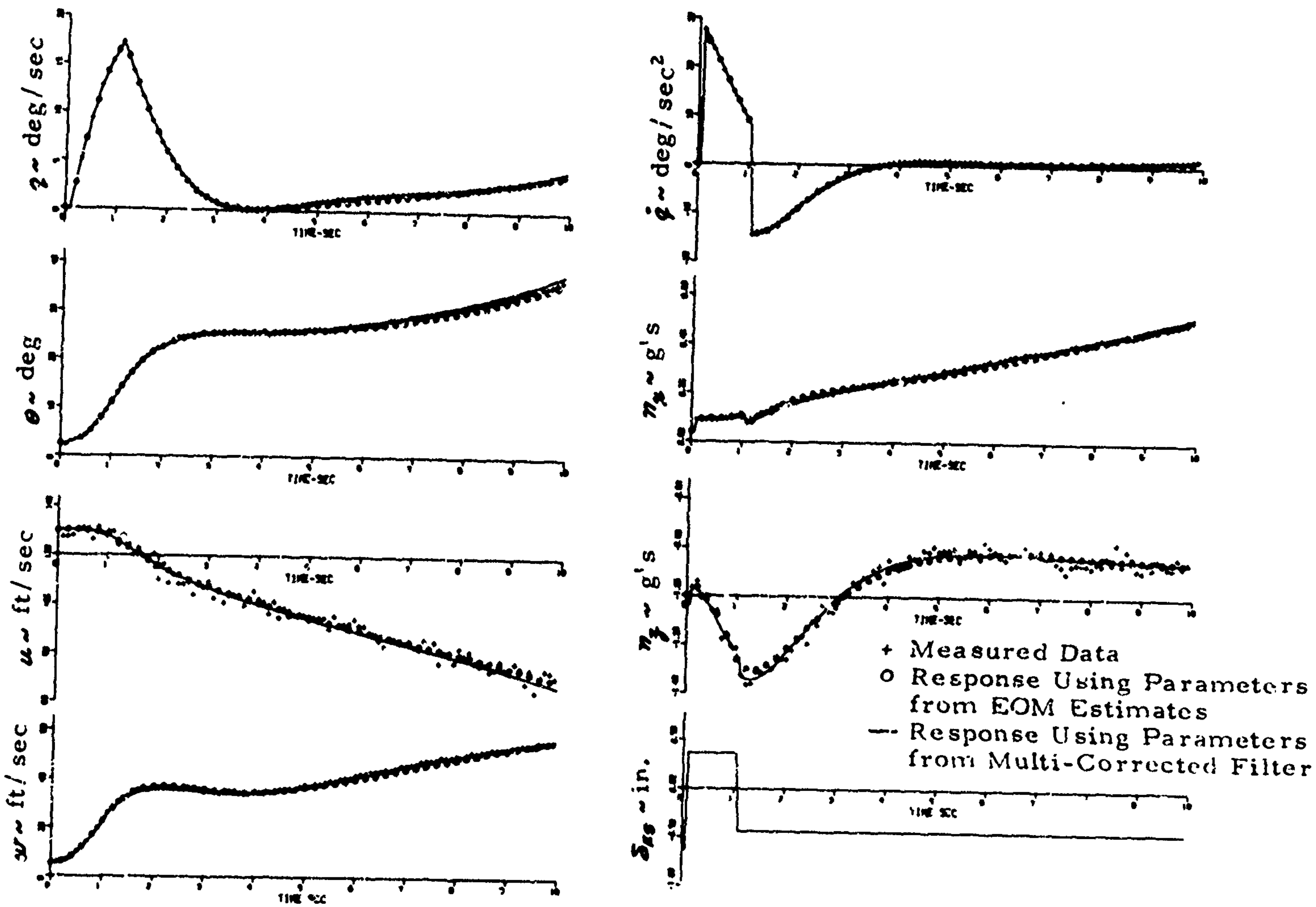

Figure 6-4 Transient Response Matching to Data 2C-1, Typical Kalman

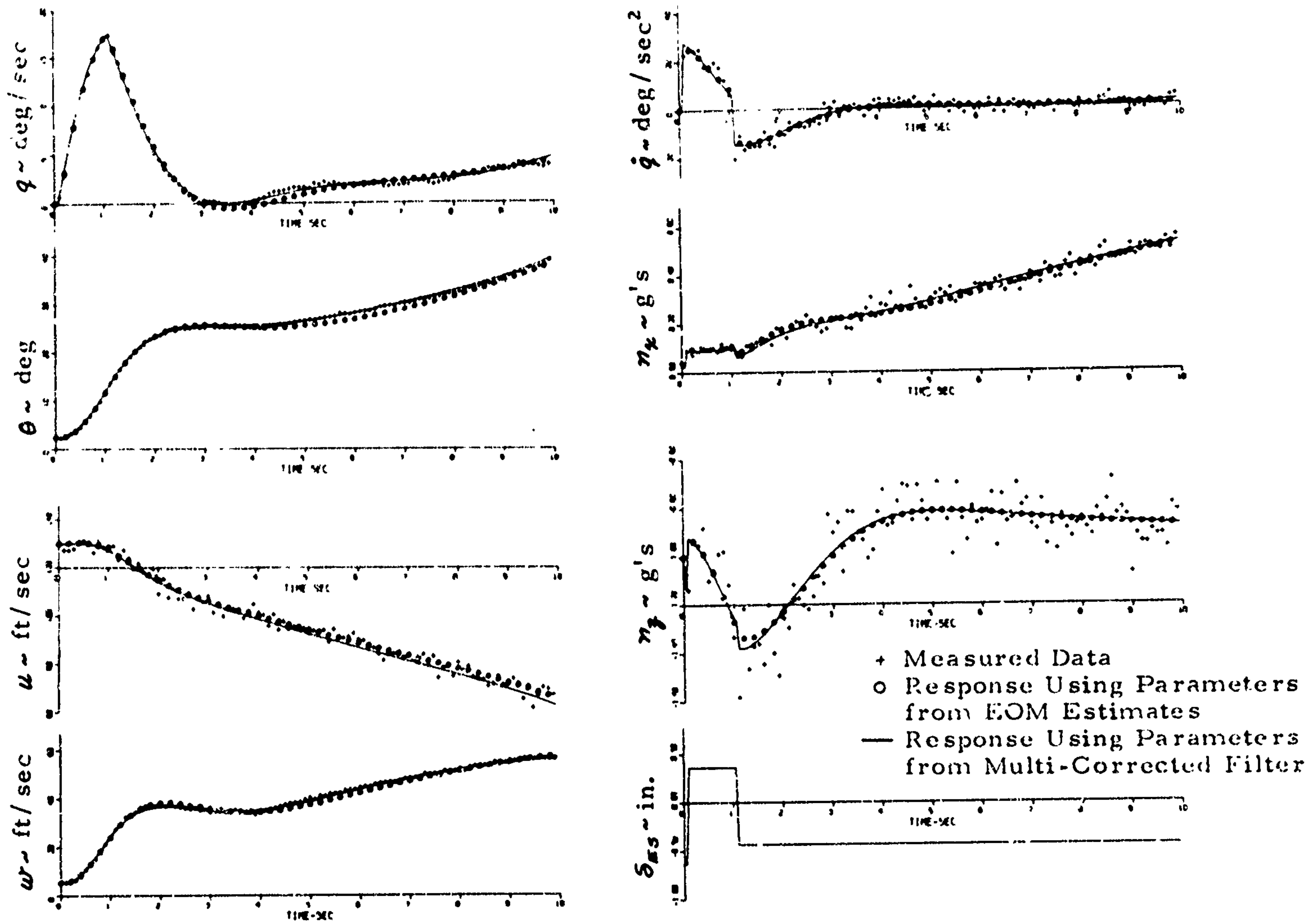

Figure 6-5 Transient Response Matching to Data 2D-1, Typical Kalman

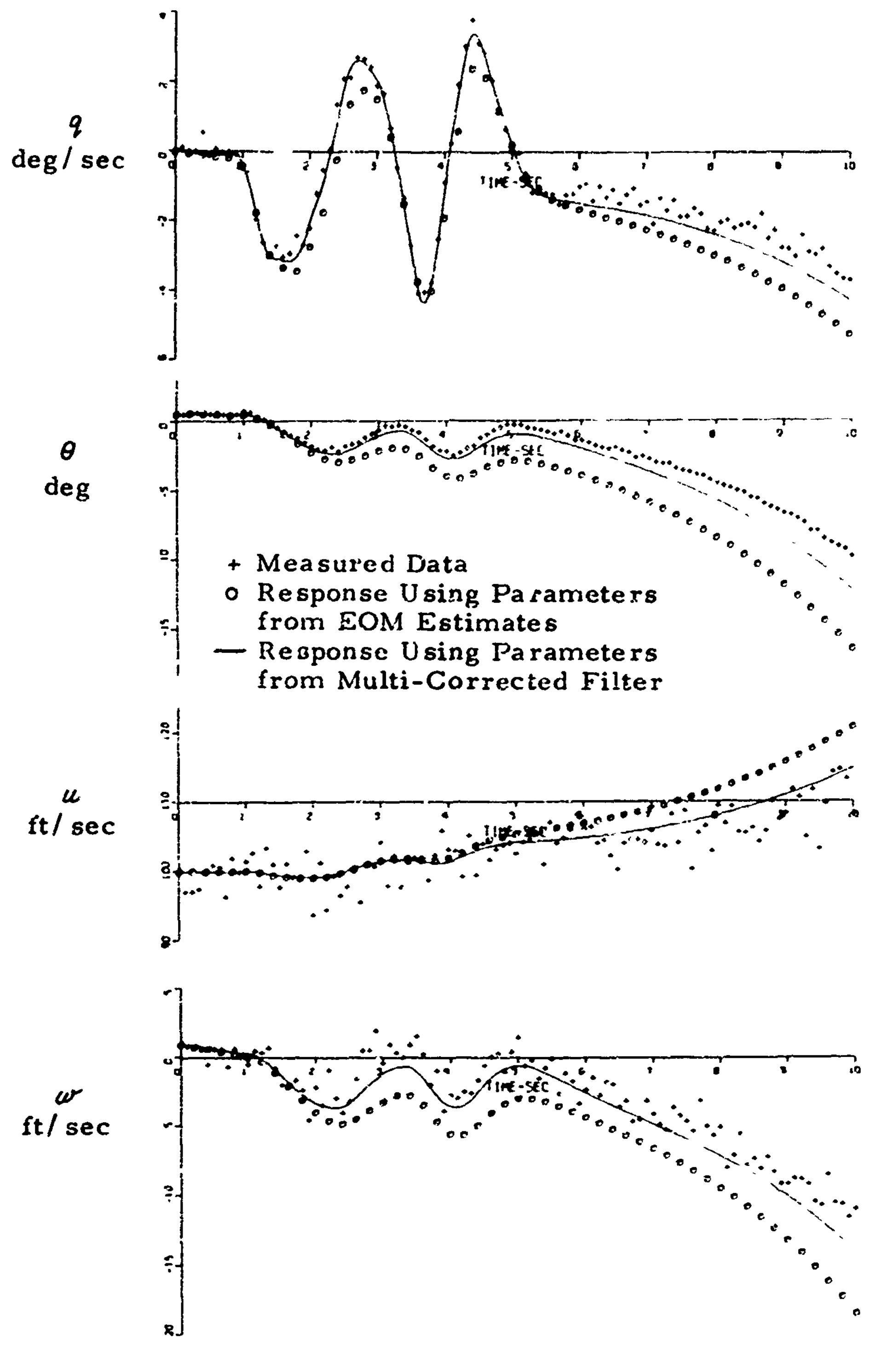

Figure 6-6 Transient Response Matching to Data 3D-1, $F_1(1)$ Filter

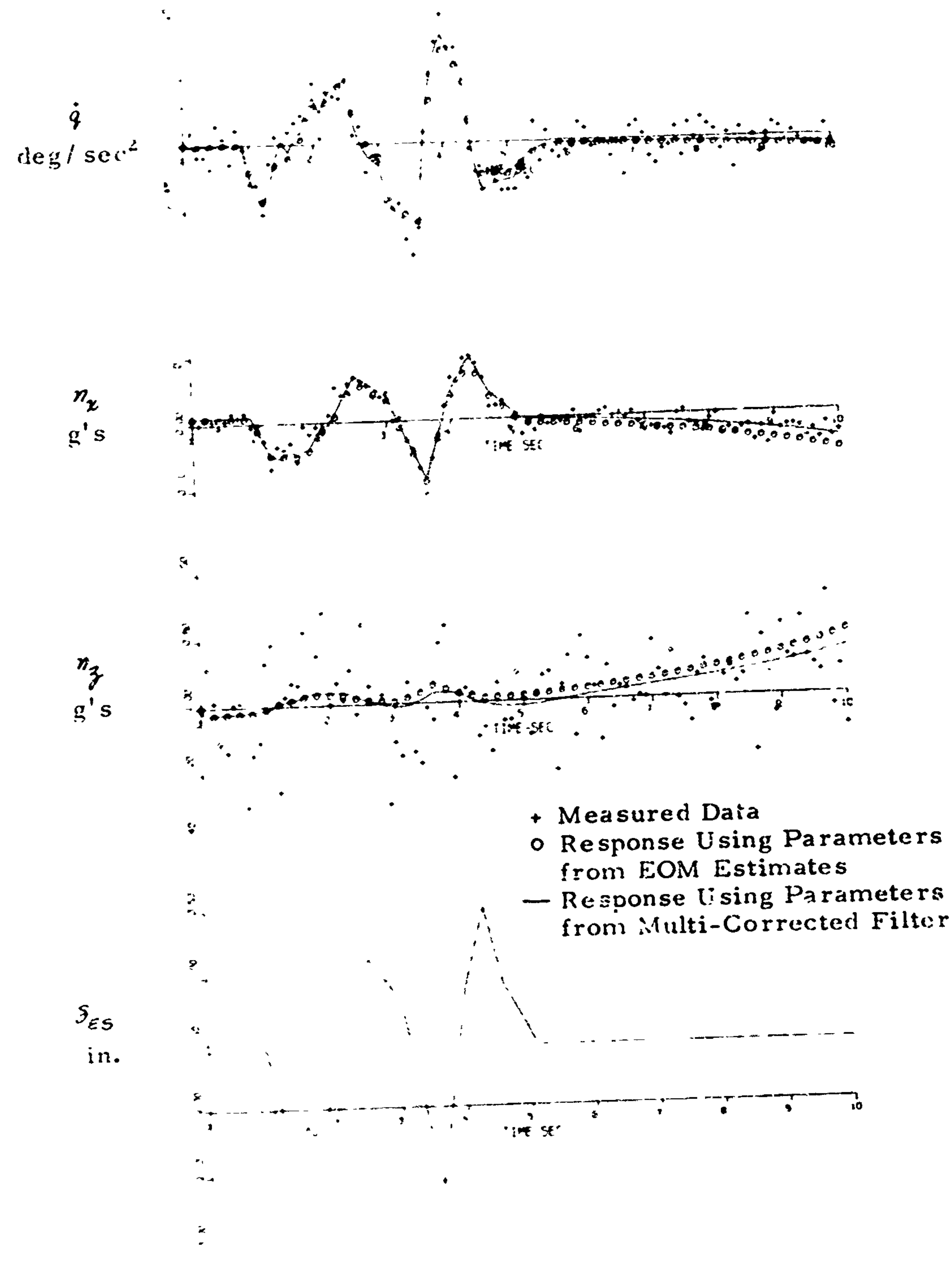

Figure 6-6 (continued)

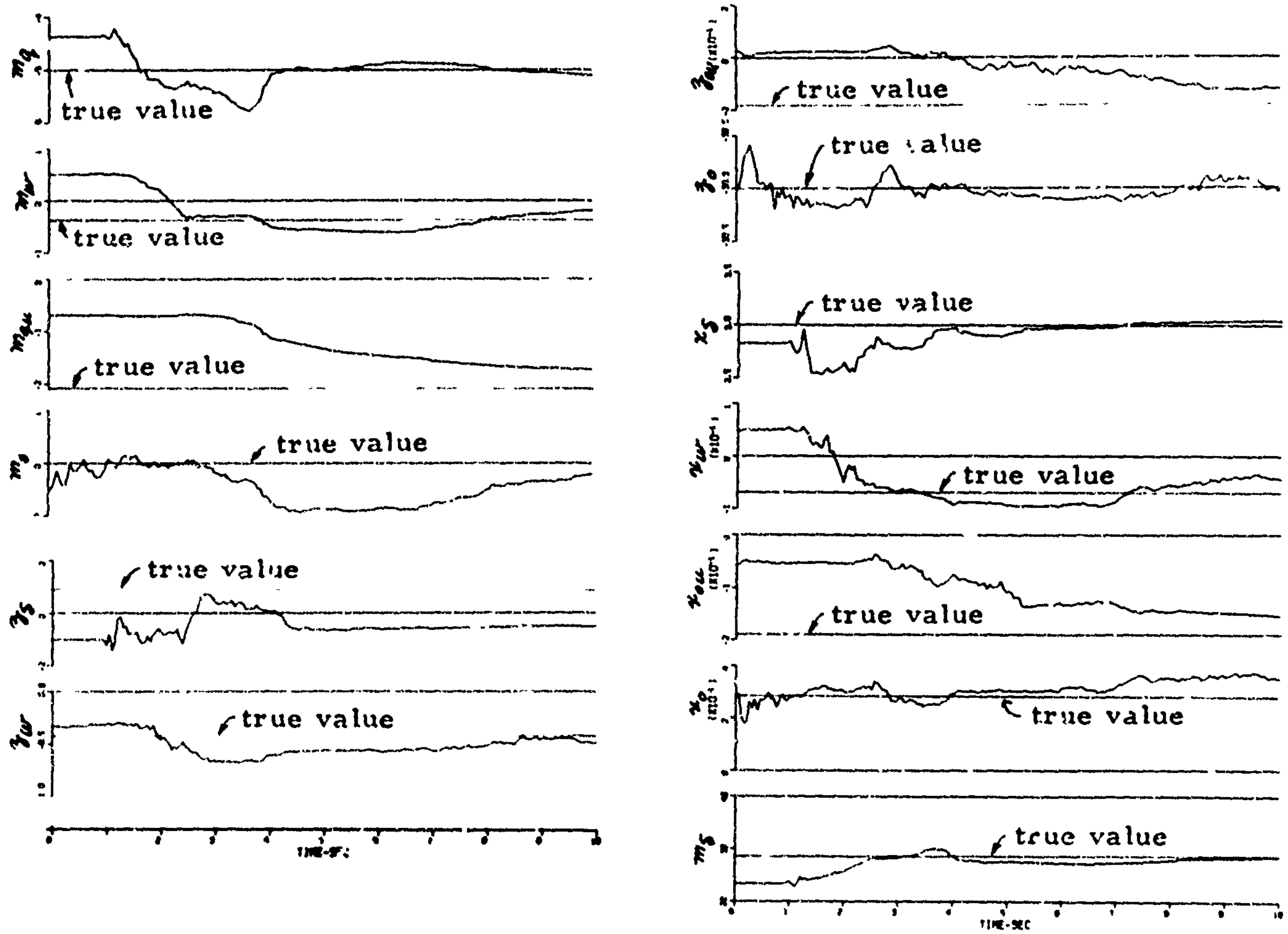

Figure 6-7 Filtered Estimates (States and Parameters) Data 3D-1, $F_{CR}(1)$ Filter

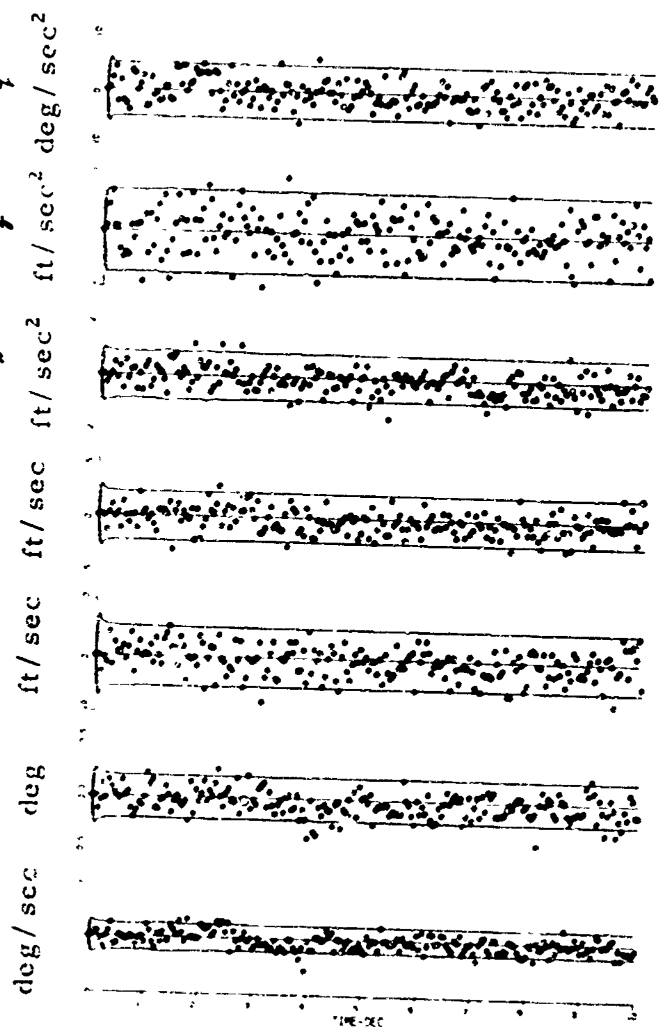

Figure 6-8 Residual Sequence for R and Q True Data 3D-1, $F_{CR}(1)$ Filter

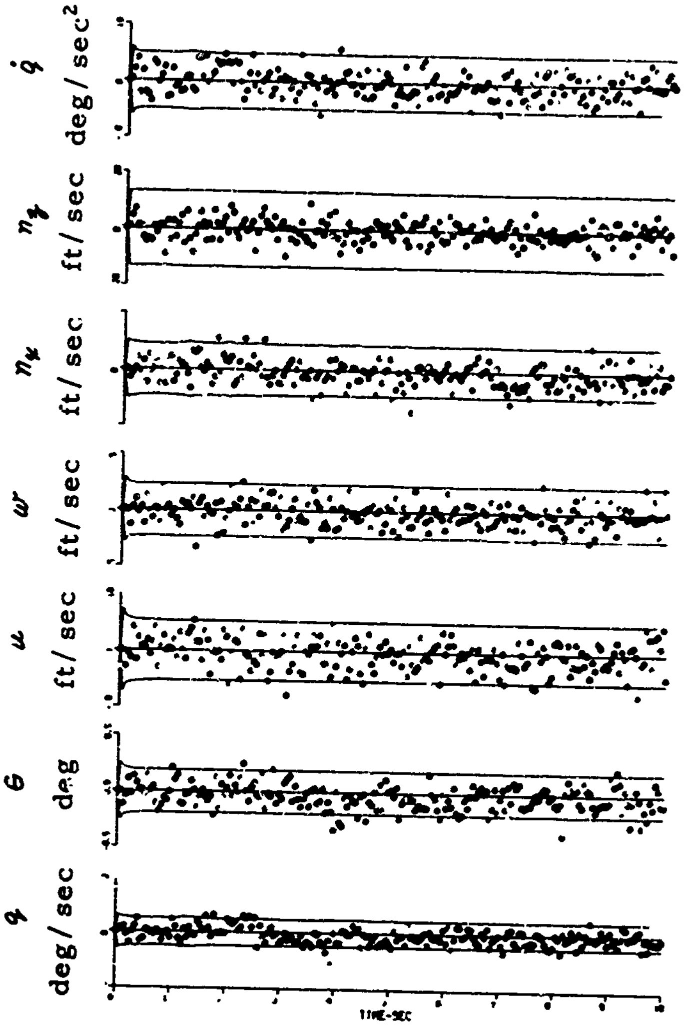

Figure 6-9 Residual Sequence for True R and 4Q, Data 3D-1, $F_{CR}(1)$ Filter

TABLE 6-1a: Computer-Generated Data Characteristics for Data 2A-1, 2B-1, 2C-1, 2D-1 and 2A-2 Through 2D-2

True Parameters

COMBINED PARAMETER		$m_o(u)$	$m_w(u)$	$m_q(u)$	$m_{\delta_{es}}(u)$	$x_o(u)$	$x_w(u)$	$x_{\delta_{es}}(u)$	$z_o(u)$	$z_w(u)$	$z_{\delta_{es}}(u)$
COMBINED DIMENSION		$1/SEC^2$		1/SEC	$1/IN.-SEC^2$	FT/SEC^2		$FT/IN.-SEC^2$	FT/SEC^2		$FT/IN.-SEC^2$
COEFFICIENTS OF THE POLYNOMINAL IN u	u^0	.50518	-.001747	-.497	.3275	18.30	.2211	-.778	-32.17	-.2939	-.3507
	u^1	-.00308	-.0000553	-.00103	.001167	-.09187	-.001587	.0185	.91	-.00287	.01667
	u^2	-.0000062	-	-	-	-.0003	-	-	-.007	-	-
	u^3	-	-	-	-	-	-	-	-	-	-

Noise Levels

		STANDARD DEVIATION	
		LOW	MODERATE
GUSTS (PROCESS NOISE)	u_g	1.0 FPS	5.0 FPS
	w_g	1.0 FPS	5.0 FPS
	θ_g	0.2 DEG/SEC	1.0 DEG/SEC
MEASUREMENT NOISE	u	0.5 FPS	2.5 FPS
	w	0.075 FPS	0.375 FPS
	θ	0.03 DEG	0.15 DEG
	$\dot{\theta}$	0.01 DEG/SEC	0.05 DEG/SEC
	n_x	0.001 g	0.005 g
	n_z	0.005 g	0.025 g
	$\dot{q}$	$0.0025\ DEG/SEC^2$	$0.0125\ DEG/SEC^2$

COEFFICIENTS ARE 1st ORDER FUNCTION OF u EXCEPT $m_o(u)$, $x_o(u)$ AND $z_o(u)$ BEING 2nd ORDER	MEASUREMENT NOISE ONLY	LOW	2-A
		MODERATE	2-C
	MEASUREMENT NOISE PLUS "GUST" NOISE	LOW	2-B
		MODERATE	2-D

True Parameters - Gust Effectiveness

COMBINED PARAMETER		$m_u(u)$	$x_u(u)$	$z_u(u)$
COMBINED DIMENSION		1/FT-SEC	1/SEC	1/SEC
COEFFICIENTS OF THE POLYNOMINAL IN u	u^0	.1308	2.066	3.243
	u^1	-.0031	-.05491	-.07327
	u^2	.0000232	.000445	.00052
	u^3	$-.569\times10^{-7}$	$-.1187\times10^{-5}$	$-.1236\times10^{-5}$

TABLE 6-1a (con't.)

Computer-Generated Data Characteristics for Data 2A-1 Through 2D-1 and 2A-2 Through 2D-2

Flight Conditions

λ	= 30°		
u_0	= 130 fps	w_0	= 5.362 fps
β_0	= 17.26°	q_0	= 0
δ_{ES_0}	= -.637 in.		
G.W.	= 14,364 lb	Altitude: Sea Level STD	

Control Inputs

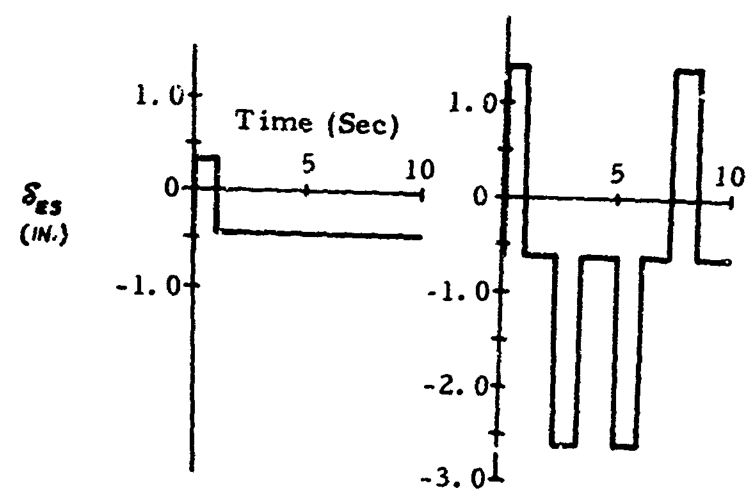

2-A-1
2-B-1
2-C-1
2-D-1

2-A-2
2-B-2
2-C-2
2-D-2

TABLE 6-1b

Computer-Generated Data Characteristics for

Data 3C-1 (Measurement Noise Only) and

3D-1 (Both Process and Measurement Noise)

Noise Levels

MEASUREMENT NOISE	
SENSOR	STANDARD DEVIATION σ
q	.22 deg/sec
θ	.09 deg
u	2.6 ft/sec
α_V	.15 deg
n_x	.012g
n_z	.05g
$\dot{q}$	2.3 deg/sec^2
w	1.0 ft/sec

PROCESS NOISE	
NOISE	VALUE
$\sigma_{\dot{q}}$	.4 deg/sec^2
$\sigma_{\dot{u}}$	.1 ft/sec^2
$\sigma_{\dot{w}}$	3.2 ft/sec^2

- Measurement Noise is any random fluctations and/or uncertainty in a measurement output (white or correlated).

- Process noise is used here to approximate unknown driving forces and to account for inaccuracy in modeling the dynamics of the aircraft.

TRUE PARAMETERS*

Parameter	M_0	M_u	M_w	M_q	M_δ	M_β	X_c	X_u	X_w	X_δ	X_β	Z_c	Z_u	Z_w	Z_δ	Z_β
Value	0.0	-.036	-.00644	-5.0	.50	.043	.2861	-.19	-.0675	3.0	.727	-32.199	-.180	-.430	.90	-180

* Perturbed, Radians

TABLE 6 -1b (con't.)

Computer-Generated Data Characteristics for
Data 3C-1 (Measurement Noise Only) and
3D-1 (Both Process and Measurement Noise)

Control Input

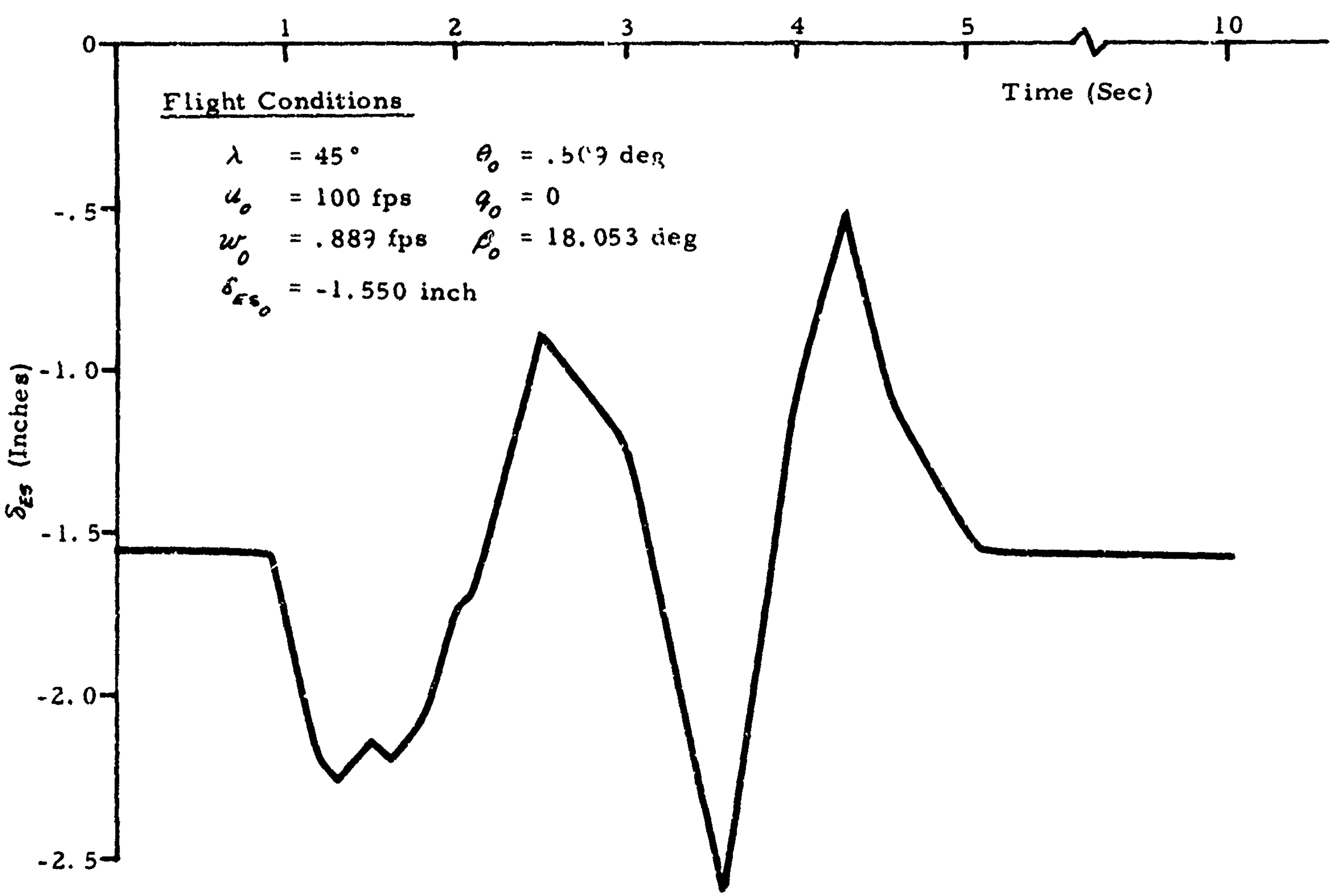

TABLE 6-2

Kalman Filter Estimates With and Without Acceleration Measurements

Parameter		True Value*	Data 2D-2: Multi-Step δ_{ES} With Process Noise		
			Equations of Motion	With Accelerations F_{10}	Without Accelerations F_{10}
M_0	1	.50518	.30828	.40586	.39796
	u	-.00308	.000884	-.000589	-.000391
	u^2	-6.2×10^{-6}	-2.467×10^{-5}	-.00001961	-2.057×10^{-5}
M_w	1	-.001747	-.00271	-.002955	-.003088
	u	-5.53×10^{-5}	-4.97×10^{-5}	-.00004714	-4.64×10^{-5}
M_q	1	-.497	-.5924	-.57211	-.58733
	u	-.00103	4.684×10^{-5}	-.000197	-.0000203
M_δ	1	.3275	.33012	.31575	.32378
	u	.001167	.001131	.001273	.001218
X_0	1	18.30	17.899	18.427	18.340
	u	-.09[illegible]67	-.0872	-.09353	-.09466
	u^2	-.0003	-.000306	-.0002976	-.000268
X_w	1	.2211	.20523	.21955	.17575
	u	-.001587	-.001455	-.001560	-.001185
X_δ	1	-.778	-.4563	-.71386	-.78528
	u	.0184	.01604	.01841	.01843
Z_0	1	-32.17	-31.14	-37.2157	-32.78
	u	.910	.9081	1.0336	.9451
	u^2	-.007	-.007008	-.007664	-.00722
Z_w	1	-.2939	-.36993	-.3660	-.3457
	u	-.00287	-.002316	-.002302	-.00252
Z_δ	1	-.3507	-1.2589	-1.9496	-1.0546
	u	.01667	.023506	.031203	.02467

* Perturbed value; moment derivatives in rad/sec^2

TABLE 6-3

Kalman Filter Estimates for Different Recycling Techniques With Acceleration Measurements

Parameter		True Value	Eqs. of Motion	Data 2D-2 : Multi-Step δ_{es} With Process Noise & Measurement Noise			
				1st Filter		2nd Filter	
				F_{10} *	F_1	$F_{10} \to F_{10}$	$F_{10} \to B_{10}$ **
M_0	1	28.9	17.974	23.036	23.514	22.975	22.637
	u	-.176	.0458	-.03047	-.04541	-.026347	-.0165
	u^2	-.000355	-.001394	-.001134	-.001034	-.0011673	-.00122
M_w	1	-.100	-.1562	-.1687	-.1636	-.17567	-.17796
	u	-.00317	-.002842	-.002705	-.00276	-.002652	-.00268
M_q	1	-.497	-.5901	-.57227	-.5797	-.570296	-.58445
	u	-.00103	-.0000415	-.000191	-.000126	-.0002101	-.0000238
M_δ	1	18.7	18.975	18.172	18.623	17.9098	17.9687
	u	.0669	.064103	.07212	.06756	.074777	.07372
X_0	1	18.30	17.906	18.529	19.097	18.5807	18.502
	u	-.09167	-.08722	-.09511	-.101613	-.095805	-.09176
	u^2	-.0003	-.0003067	-.000292	-.000236	-.0002902	-.000316
X_w	1	.2211	.20503	.2191	.2151	.218277	.2104
	u	-.001587	-.001452	-.001557	-.00153	-.0015543	-.00151
X_δ	1	-.778	-.45212	-.7076	-.63189	-.72659	-.8884
	u	.0184	.0160179	.01838	.01747	.018551	.01982
Z_0	1	-32.17	-31.485	-37.24	-33.27	-38.1777	-40.103
	u	.910	.90954	1.033	.9511	1.05321	1.0813
	u^2	-.007	-.0070144	-.00766	-.007226	-.0077637	-.007845
Z_w	1	-.2939	-.370313	-.3624	-.35174	-.37043	-.3447
	u	-.00287	-.002309	-.00233	-.002458	-.002272	-.00258
Z_δ	1	-.3507	-1.2187	-1.9321	-1.133	-2.22405	-2.2487
	u	.01667	.02321	.0311	.02287	.034006	.03395

* F_{10}: the 1st forward pass with the variances of parameters obtained from the equations of motion method multiplied by 10.

** B: backward filtering

TABLE 6-4a

Kalman Filter Estimates for Different Recycling Techniques and Multi-Correction Technique With Acceleration Measurements

Parameter		True Value	Data 2D-2 : Multi-Step $\hat{S}_{fs}$ With Process Noise			
			Eqs. of Motion	Forward-Forward $F_{10} \to F_{10}$	Forward-Backward $F_{10} \leftrightarrow F_{10}$	Multi-correction* $F_{10}(1)$*
M_0	1	28.9	17.974	22.975	22.637	24.3068
	u	-.176	0.158	-.026347	-.0[illegible]65	-.00673
	u^2	-.000355	-.001394	-.0011673	-.00122	-.0009078
M_w	1	-.100	-.1562	-.17567	-.17796	-.19281
	u	-.00317	-.002842	-.002652	-.00268	-.00254
M_q	1	-.497	-.5901	-.570296	-.58445	-.56778
	u	-.00103	-.0000415	-.0002101	-.0000238	-.0002686
M_δ	1	18.7	18.975	17.9098	17.9687	17.3155
	u	.0669	.064103	.074777	.07372	.07995
X_0	1	18.30	17.906	18.5807	18.502	21.213
	u	-.09167	-.08722	-.095805	-.09176	-.1442
	u^2	-.0003	-.0003067	-.0002902	-.000316	-.00006432
X_w	1	.2211	.20503	.218277	.2104	.20484
	u	-.001587	-.001452	-.0015543	-.00151	-.0014979
X_δ	1	-.778	-.45212	-.72659	-.8884	-.7845
	u	.0184	.0160179	.018551	.01982	.01860
Z_0	1	-32.17	-31.485	-38.1777	-40.103	-28.0749
	u	.910	.90954	1.05321	1.0813	.8319
	u^2	-.007	-.0070144	-.0077637	-.007845	-.0065889
Z_w	1	-.2939	-.370313	-.37043	-.3447	-.33118
	u	-.00287	-.002309	-.002272	-.00258	-.002823
Z_δ	1	-.3507	-1.2187	-2.22405	-2.2487	-2.84206
	u	.01667	.02321	.034006	.03395	.039515

* Simple version of local iteration - one addition correction

TABLE 6-4b

Effects of the Multi-Correction for Case 2C-1 *

Data: 2C-1 (single pulse in δ_{ES} with only moderate measurement noise)

Parameter		True Value	Eqs. of Motion	Simple extended Kalman		Simple version of multi-correction (2 additional corrections)		
				F	F_{10}	F(2)	$F_{10}(2)$	$F_{100}(2)$
M_o	1	28.9	-73.4	42.9	39.34	29.061	26.692	30.665
	u	-.176	1.258	-.418	-.367	-.1822	-.1483	-.2243
	u^2	-.000355	-.00533	.000665	.000492	-.00033	-.000447	-.000102
M_w	1	-.100	1.181	-.223	-.168	-.11092	-.07796	-.1235
	u	-.00317	-.0131	-.00203	-.00248	-.00308	-.00338	-.00301
M_q	1	-.497	-2.85	-.635	-.760	-.4961	-.5761	-.5646
	u	-.00103	.0176	-.000117	.000850	-.00102	-.000400	-.000559
M_δ	1	18.7	21.55	19.3	19.231	19.799	21.003	25.166
	u	.0669	.0383	.0625	.0632	.0588	.04912	.01655
X_o	1	18.3	-15.88	10.7	13.93	8.253	18.63	17.57
	u	-.0917	.433	.0241	-.0297	.0663	-.0955	-.0838
	u^2	-.0003	-.00232	-.000749	-.000523	-.00093	-.000299	-.00033
X_w	1	.221	.617	.309	.257	.3279	.2133	.2213
	u	-.00159	-.0046	-.00229	-.00189	-.00246	-.001529	-.00161
X_δ	1	-.778	-21.39	-4.78	1.584	-4.696	-1.3865	.3253
	u	.0184	.178	.0502	.000191	.04969	.02328	.00979
Z_o	1	-32.2	-30.45	6.82	-47.99	-5.450	-31.268	-27.458
	u	.910	0.991	.349	1.146	.5517	.9063	.8272
	u^2	-.007	-.0078	-.00512	-.00796	-.00597	-.00716	-.00679
Z_w	1	-.294	.00973	-.607	-.148	-.49881	-.31007	-.32695
	u	-.00287	-.00459	.000153	-.0039	-.000718	-.00238	-.00229
Z_δ	1	-.351	-138.56	-44.9	.533	-47.779	-12.47	-7.8219
	u	.0167	1.084	.373	.01507	.39792	.1212	.08597

* with acceleration measurements

TABLE 6-4c

EFFECTS OF MULTI-CORRECTION

Data 2D-1 (i) Pulse δ_{es}
(ii) Process and Measurement Noise
(iii) With Accel. Meas.

PARAMETER		TRUE VALUE	EQUATIONS OF MOTION	EXTENDED KALMAN	MULTI-CORRECTION * (TWO ADDITIONAL CORRECTIONS)	
				F_1	$F_1(2)$	$F_{10}(2)$
M_0	1	28.9	-37.28	27.259	23.415	106.43
	U	-.176	1.126	.11753	.1909	-1.254
	U^2	-.000355	-.00647	-.00247	-.00278	.00317
M_w	1	-.100	.610	-.09351	-.0451	-.833
	U	-.00317	-.0102	-.00438	-.0051	.00249
M_q	1	-.497	-1.256	-.85188	-.673	-3.01
	U	-.00103	.0077	.003155	.0017	.0202
M_δ	1	18.7	-41.3	-33.287	-35.9	25.79
	U	.0669	.521	.4598	.484	.0272
X_0	1	18.3	-18.88	-5.671	-9.36	56.25
	U	-.0917	.4752	.2408	.328	-.626
	U^2	-.0003	-.0025	-.0015	-.0019	.0015
X_w	1	.221	.689	.447	.516	-.088
	U	-.00159	-.0052	-.0032	-.0039	.0044
X_δ	1	-.778	-28.14	7.115	-3.72	-36.9
	U	.0184	.2312	-.0369	.0463	.314
Z_0	1	-32.2	11.71	2.514	2.819	-11.99
	U	.910	.477	.6301	.63	.9295
	U^2	-.007	-.0064	-.007	-.0072	-.0089
Z_w	1	-.294	-.5119	-.6462	-.6221	-.673
	U	-.00287	.00065	.00032	.00011	.00068
Z_δ	1	-.351	-150.6	-99.59	-105.4	-82.16
	U	.0167	1.19	.812	.863	.7286

*Smoothed parameter estimates are approximately the same.

Table 6-5 Effects of Multi-Correction for Case 3D-1*

Data 3D-1: (i) Process Noise (iii) Linear Aero.
(ii) Realistic δ_{ES} Input (iv) $\lambda = 45°$

PARAMETER	TRUE PARAMETER	E.O.M. INITIAL ESTIMATE	KALMAN P(0) - E.O.M. VARIANCES	
			F_1	$F_1(1)$ **
M_0	0.0	-.00908	-.00851	-.00803
M_u	-.036	-.01166	-.0288	-.0288
M_w	-.00644	.00899	-.00143	-.00152
M_q	-5.0	-4.368	-5.279	-5.261
M_δ	.50	.408	.506	.5045
M_β				
X_0	.2861	.2907	.4537	.3545
X_u	-.19	-.0566	-.0899	-.0891
X_w	-.0675	.0489	.02065	.0212
X_δ	3.0	2.826	2.917	2.917
X_β				
Z_0	-32.199	-33.01	-32.954	-32.954
Z_u	-.180	.0257	-.0625	-.0637
Z_w	-.413	-.329	-.4189	-.419
Z_δ	.90	-1.011	-.8111	-.787
Z_β				

*Using acceleration measurements.
**Indicates one additional correction and one stage optimal smoothing.

TABLE 6-6a

Variance Comparison [P (0)] For Different Start Up Procedures

PARAMETER	TRUE VALUE*	CASE 3C-1 (NO PROCESS NOISE)			CASE 3D-1 (PROCESS NOISE)		
		ABSOLUTE ESTIMATION ERROR	E.O.M. σ_{EM}	START UP $\sqrt{20}\ \sigma_{CR}$ **	ABSOLUTE ESTIMATION ERROR	E.O.M. σ_{EM}	START UP $\sqrt{20}\ \sigma_{CR}$ **
M_0	0.0	.01998	.0068	.00564	.0091	.0074	.0076
M_u	-.036	.0233	.0015	.0031	.024	.00154	.00308
M_w	-.00644	.0102	.0026	.0035	.015	.00275	.0041
M_q	-5.0	.246	.42	.42	.632	.403	.491
M_δ	.50	.136	.03	.029	.092	.031	.036
M_β							
X_0	.2861	.0924	.048	.424	.0046	.052	.791
X_u	-.19	.1235	.01	.116	.113	.011	.158
X_w	-.0675	.0999	.013	.175	.116	.0295	.271
X_δ	3.0	.14	.10	3.26	.174	.10	3.194
X_β							
Z_0	-32.199	.0993	.157	.427	.811	.392	.667
Z_u	-.180	.1712	.035	.129	.206	.082	.144
Z_w	-.413	.1808	.043	.188	.084	.102	.230
Z_δ	.900	.7102	.33	1.8	1.91	.750	1.76
Z_β							

* Perturbed, Radians

** Note that the term $\partial h/\partial p$ was neglected in Eq. (3.19). when the acceleration measurements were used.

TABLE 6-6b

Parameter Estimates Employing Different Start-Up Procedures and an Improved Final Variance Computation

Data 3D-1

	Initial State and Parameters	True Value -Perturbed Degrees	Data: 3D-1						
			Initial Estimates	Initial P_0 from Initial Estimator			Improved Start-Up Procedure for P_0		
				Initial Variances	Filter Estimates F_1 Extended Kalman	Filter Estimates $F_1(I)$ Local Iteration	Initial[1] Variances $k = 20$	Smoothed Estimates[2]	Final $\sigma = \sqrt{CR_{ii}}$
Aircraft States at t_0	q_0	0.0	0.0	.0484	NA	NA	.0484	-.093	.173
	θ_0	.509	.509	.0081	NA	NA	.0081	.484	.035
	u_0	100	100.0	6.76	NA	NA	6.76	99.93	.21
	w_0	.889	.889	1.0	NA	NA	1.0	.393	.274
Constant Parameters	M_0	0.0	-.5202	.1814	-.4871	-.460	.5456	-.2042	.359
	M_u	-2.06	-.6683	.0078	-1.649	-1.650	.0094	-1.724	.043
	M_w	-.369	.5153	.0249	-.0822	-.0871	.034	-.1774	.049
	M_q	-5.0	-4.368	.1623	-5.279	-5.261	.194	-5.098	.118
	M_δ	28.65	23.39	3.16	28.99	28.906	3.675	28.64	.504
	X_0	.2861	.2907	.0028	.3537	.3545	.0508	.346	.05
	X_u	-.190	-.0566	.00012	-.0899	-.0891	.0028	-.1547	.012
	X_w	-.0675	.0489	.00019	.0206	.0212	.0046	-.0458	.014
	X_δ	3.0	2.826	.010	2.917	2.917	.1405	3.048	.024
	Z_0	-32.199	-33.01	.154	-32.95	-32.95	.418	-33.03	.123
	Z_u	-.180	.0257	.0067	-.0625	-.0637	.015	-.125	.047
	Z_w	-.413	-.329	.0105	-.4189	-.4196	.040	-.495	.059
	Z_q	.90	-1.011	.563	-.8111	-.7874	2.91	-.524	.43

1. Variances from CR lower bound were multiplied by a factor of 20.
2. Filtered parameter estimates are approximately the same.

TABLE 6-7

Sensitivity of Parameter Estimates to Variations In Q

Data: 3D-1

Parameter	True Value - Perturbed (deg)	Initial Parameter	Parameter Estimates Locally Iterated Filter P_0 - Start-Up *	
			True R & Q	True R 4Q
M_0	0.0	-.5202	-.2042	-.225
M_{0_u}	-2.06	-.6683	-1.724	-1.67
M_w	-.369	.5153	-.1774	-.1276
M_q	-5.0	-4.368	-5.098	-5.086
M_δ	28.65	23.39	28.64	28.49
X_0	.2861	.2907	.346	.352
X_{0_u}	1.9	-.0566	-.1547	-.1548
X_w	-.0675	.0489	-.0438	-.0414
X_δ	3.0	2.826	3.048	3.053
Z_0	32.199	-33.01	-33.03	-33.03
Z[illegible]	-.180	.0257	-.125	-.0447
Z_w	-.413	-.3290	-.495	-.427
Z_δ	.90	-1.011	-.524	-.5397

* Parameter Variances from C R lower bound multiplied equally by 20

SECTION VII

APPLICATION OF ADVANCED TECHNIQUES TO EXPERIMENTAL DATA

7.1 Application to Princeton Data

The Princeton Dynamic Model Track (PDMT) of Princeton University is a facility designed expressly for the dynamic testing of scaled, powered V/STOL models in and near hovering flight. The design of the test apparatus is such that the data generated should not be directly interpreted via conventional airplane/helicopter rigid body equations of motion; modifications must be incorporated in the equations to account for the apparatus. In order to ensure a familiarity with the differences between PDMT test data and full-scale flight data, we shall first review briefly the test apparatus at the PDMT and the type of data that this generates. We will then discuss the modifications of the identification programs necessary to analyze the PDMT data. Finally, the analysis of the data will be presented.

7.1.1 Test Apparatus and Coordinate Transformation

A full description of the PDMT is given in Reference 59; for our purposes, a summary will suffice. The PDMT consists of a 750-foot monorail track enclosed within a 30-foot by 30-foot building. A servo-driven carriage rides this track; for dynamic testing in the plane of symmetry (longitudinal degrees of freedom), the carriage incorporates a boom which allows ± 5 feet of vertical motion relative to the track. A powered, dynamically scaled model is attached to the boom by horizontal and vertical error links; relative motion of the model with respect to the boom is measured by the links and used to command the carriage to follow horizontal motion, and the vertical boom to follow vertical motion. The model is attached to the error links through a pivot about which it is free to rotate in the plane of symmetry. The error-link commands, therefore, allow the pivot point to move such that the model flies "free" -- its motion is not mechanically constrained. Linear velocities and accelerations, parallel and perpendicular to the track, are measured, as are angular position, rate, and acceleration at the pivot point. The measured quantities are telemetered and recorded in analog form; an analog-digital converter then records them in digital form (along with some scaling), and CAL received them in this form.

The CAL computer programs for V/STOL identification have been written to be compatible with flight test data, and the state variables are therefore written with respect to a body axis system with the origin at the center of gravity. Since the PDMT data are measured with respect to a space-fixed, or inertial, axis system at the pivot, they must be transformed to body axis variables.

The transformation is a straightforward translation and rotation (see Figure 7-1), and the results are:

$$
\begin{aligned}
\theta_B &= \theta_S \\
u_B &= u_S \cos\theta_S - w_S \sin\theta_S + q_S Z_{cg} \\
w_B &= w_S \cos\theta_S + u_S \sin\theta_S - q_S (X_{cg} - r) \\
q_B &= q_S \\
\dot{u}_B &= \dot{u}_S \cos\theta_S - \dot{w}_S \sin\theta_S - u_S q_S \sin\theta_S - w_S q_S \cos\theta_S + \dot{q}_S Z_{cg} \\
\dot{w}_B &= \dot{w}_S \cos\theta_S + \dot{u}_S \sin\theta_S - w_S q_S \sin\theta_S + u_S q_S \cos\theta_S - \dot{q}_S (X_{cg} - r) \\
\dot{q}_B &= \dot{q}_S
\end{aligned}
$$

where the subscripts S and B are for inertial and body axis systems respectively, and Z_{cg} and $(X_{cg} - r)$ denote the vertical and horizontal distances, respectively, between the pivot point and c.g. (See Figure 7-1).

7.1.2 Equations of Motion for PDMT Quad Duct Test Model

In addition to the data transformations necessary to adapt the PDMT measurements to CAL identification programs, the equations of motion employed in these programs must themselves be modified to account for a difference between the model dynamics and those from a full-scale flight test which arises from the effect of the error linkages. A schematic sketch is shown in Figure 7-2; from this may be seen the essential fact that a dynamic test on the PDMT involves three masses:

(1) The quad model itself (M) which is free to rotate about the pivot and translate horizontally and vertically.

(2) The vertical error link (M_v), which may translate horizontally and vertically in the inertial reference frame but which does not rotate.

(3) The horizontal error link (M_h), which may translate only horizontally in the inertial reference frame, and which does not rotate.

As we have explained, these links provide the position error signals of the model motion, and are carried by the model; although aerodynamic forces on them may generally be neglected, their inertial effects should be included. In essence, the "reference masses" which are accelerated by external forces are different in horizontal, vertical, and rotational motions:

Horizontal:	$M + M_v + M_h$
Vertical:	$M + M_v$
Rotational:	M (or I_{cg})

The full development of of the equations of motion, under only the assumption that c.g. position and I_{cg} may be considered constant, is given in Appendix L; the resulting, nonlinear equations, in a body axis system, are summarized below:

$$
\begin{aligned}
&-\dot{u}_B - w_B q - g\sin\theta + \mu\left\{Z_{cg}\left[\left(1+\frac{\xi}{\mu}\right)\cos^2\theta + \frac{1}{\sigma}\sin^2\theta\right]\right. \\
&\left.+ (X_{cg}-r)\left(\frac{1}{\sigma} - 1 - \frac{\xi}{\mu}\right)\sin\theta\cos\theta\,\dot{q}\right\} + \mu\left\{Z_{cg}\left(\frac{1}{\sigma} - 1 - \frac{\xi}{\mu}\right)\sin\theta\cos\theta\right. \\
&\left.- (X_{cg}-r)\left[\left(1+\frac{\xi}{\mu}\right)\cos^2\theta + \frac{1}{\sigma}\sin^2\theta\right]\right\}q^2 + \left[\sin^2\theta + \sigma\cos^2\theta\right]X_{aero_B} \qquad (7.2a) \\
&-\left[(1-\sigma)\sin\theta\cos\theta\right]Z_{aero_B} \\
&= 0
\end{aligned}
$$

$$
\begin{aligned}
&-\dot{w}_B + u_B q + g\cos\theta - \frac{\mu}{\sigma}\left\{(X_{cg}-r)\left[\cos^2\theta + \left(1+\frac{\xi}{\mu}\right)\sigma\sin^2\theta\right]\right. \\
&\left.+ Z_{cg}\left[1-\left(1+\frac{\xi}{\mu}\right)\sigma\right]\sin\theta\cos\theta\right\}\dot{q} + \frac{\mu}{\sigma}\left\{(X_{cg}-r)\left[1\left(1+\frac{\xi}{\mu}\right)\sigma\right]\sin\theta\cos\theta\right. \\
&\left.- Z_{cg}\left[\cos^2\theta + \left(1+\frac{\xi}{\mu}\right)\sigma\sin^2\theta\right]\right\}q^2 + \left[\cos^2\theta + \sigma\sin^2\theta\right]Z_{aero_B} \qquad (7.2b) \\
&-\left[(1-\sigma)\sin\theta\cos\theta\right]X_{aero_B} \\
&= 0
\end{aligned}
$$

Note: Z_{aero_B} and X_{aero_B} are the aerodynamic forces along the body axes divided by $M + M_V$.

$$
\begin{aligned}
&-\dot{q}\left\{I_{cg} + (X_{cg}-r)^2\left[M_h\sin^2\theta + M_V\right] + Z_{cg}^2\left[M_h\cos^2\theta + M_V\right]\right. \\
&\left.- 2M_h(X_{cg}-r)Z_{cg}\cos\theta\sin\theta\right\} - M_h\left[-(X_{cg}-r)\sin\theta + Z_{cg}\cos\theta\right] \\
&\cdot\left\{(\dot{u}_B + q w_B)\cos\theta + (\dot{w}_B - q u_B)\sin\theta + q^2\left[(X_{cg}-r)\cos\theta + Z_{cg}\cos\theta\right]\right\} \qquad (7.2c) \\
&+ M_V\left\{(X_{cg}-r)(g\cos\theta + \dot{w}_B - q u_B) - Z_{cg}(\dot{u}_B + q w_B - g\sin\theta)\right\} + M_{aero_B} \\
&= 0
\end{aligned}
$$

where:

$$\sigma = \frac{M+M_v}{M+M_v+M_h}$$

$$\mu = \frac{M_v}{M+M_v+M_h}$$

$$\xi = \frac{M_h}{M+M_v+M_h} = 1-\sigma$$

For the quad model, the values of the above parameters are:

M	= 47.4 lb	σ	= 0.90
M_v	= 4.1 lb	μ	= 0.072
M_h	= 5.6 lb	ξ	= 0.1

These equations for the model are considerably more complex than those for the full-scale machine. The effect of the error links and the c.g. offset have introduced additional functions of the usual state variables into the equations, and have also added functions of q^2. Although these changes could be implemented into the CAL computer programs, it would be preferable to employ an existing program. With this in mind, some simplifications are made. Since the c.g. offset, $\vec{l} = 0$, at the midpoint of the duct angle range ($\lambda = 60°$), it is reasonable to consider the largest possible value these terms could have and compare their orders of magnitude with the other terms in the equation. Based on known geometric characteristics of the PDMT quad model (References 60 and 61), the maximum possible values of c.g. offset may be found to be:

$$(X_{cg}-r)_{max} = 0.03 \text{ feet}$$

$$z_{cg_{max}} = 0.075 \text{ feet}$$

(It should be noted that these values occur at different values of λ, but for order-of-magnitude estimations we use the maximum values regardless of this discrepancy.) Using these values, and limiting pitch angle to $0° < \theta < 30°$, it was found that the maximum values of the coupling terms in the force equations are:

Horizontal force:	$\dot{q}$ term is order of 0.06 ft/sec^2
	q^2 term is order of 0.02 ft/sec^2
Vertical force:	$\dot{q}$ term is order of 0.04 ft/sec^2
	q^2 term is order of 0.03 ft/sec^2

Although these approximate values were obtained using model-scale values, their dimensions are linear acceleration; they may therefore be compared directly to full-scale linear accelerations (see Reference 60), and can be seen to be negligible.

Also, in the moment equation, the center-of-gravity offset terms multiplying $\dot{q}$ appear to the second power and may be neglected, as they are small compared to I_{cg}; similarly the q^2 term is multiplied by offset terms to the second power and may be neglected. The terms involving linear accelerations, however, may be significant compared to $I_{cg}\dot{q}$, and must be retained.

The approximate equations are therefore (utilizing the simplification resulting from the fact that $X_{aero_B} << Z_{aero_B}$):

$$-\dot{u}_B - w_B q - g\sin\theta + \left[\sin^2\theta + \sigma\cos^2\theta\right] X_{aero_B} - \left[(1-\sigma)\sin\theta\cos\theta\right] Z_{aero_B} = 0$$

$$-\dot{w}_B - u_B q + g\cos\theta + \left[\cos^2\theta + \sigma\sin^2\theta\right] Z_{aero_B} = 0 \tag{7.3}$$

$$-\dot{q} - \frac{M_h}{I_{cg}}\left[-(X_{cg}-r)\sin\theta + Z_{cg}\cos\theta\right]\left[(\dot{u}_B + q w_B)\cos\theta + (\dot{w}_B - q u_B)\sin\theta\right]$$

$$+\frac{M_v}{I_{cg}}\left[(X_{cg}-r)(g\cos\theta + \dot{w}_B - q u_B) - Z_{cg}(\dot{u}_B + q w_B - g\sin\theta)\right] + M_{aero_B} = 0$$

Subsequently, more simplifications were made when the PDMT Quad Model test data were made available to CAL (Reference 61). It was found that for the tests conducted, which were fixed-operating point tests at the duct incidence of 45 deg, 60 deg, and 75 deg, the actual values of the c.g. offset were as follows:

Duct Incidence $\lambda \sim$ deg		45	60	75
c.g. offset	Horizontal $X_{cg} - r$	0.0052 ft	0	-0.0111 ft
	Vertical Z_{cg}	0.0071 ft	0	-0.0005 ft

Notice that the values of the actual c.g. offset were negligibly small as compared to the maximum possible values in the preceding order-of-magnitude estimations. Also, it was found that, by examining the test data, the pitch attitude excursion was well within ± 15°. With these observations, Equations (7.3) were further simplified to (7.4)

$$\begin{aligned} \dot{u}_B + w_B q + g\cos\theta &= X_{aero_B} - (1-\sigma)\sin\theta\cos\theta \; Z_{aero_B} \\ \dot{w}_B - u_B q - g\cos\theta &= Z_{aero_B} \\ \dot{q} &= M_{aero_B} \end{aligned} \tag{7.4}$$

for the analysis of these test data. Comparing (7.4) to our nonlinear equations of motion for the full-scale X-22A, we see that there is an extra term $-\left[(1-\sigma)\sin\theta\cos\theta\right] Z_{aero_B}$ which was regarded as a process noise later in the parameter identification process.

In Appendix L, a linearization of the complete nonlinear equations (7.2) was also performed with the assumption that a small perturbation was valid for fixed-duct tests. The resulting linearized Equations (L.14) and (L.15) are extremely complicated. However, after evaluation of the terms in these equations using the quad duct mass parameters, $\sigma = 0.90$, $\mu = 0.72$, $\xi = 0.1$, moment of inertia $I_{cg} = 2.30$ slug-ft^2, and the actual values of c.g. offset, along with the usual assumption that $X_{\dot{w}} = Z_{\dot{w}} = M_{\dot{w}} = 0$, equation (L. 15) may be simplified to

$$\begin{bmatrix} \dot{u} \\ \dot{w} \\ \dot{\theta} \\ \dot{q} \end{bmatrix} = \begin{bmatrix} X'_u & X'_w & -g\cos\theta_o & -w_o \\ Z'_u & Z'_w & -g\sin\theta_o & u_o \\ 0 & 0 & 0 & 1 \\ M_u & M_w & 0 & M_q \end{bmatrix} \begin{bmatrix} u \\ w \\ \theta \\ q \end{bmatrix} + \begin{bmatrix} X'_B & X'_{\delta_{ES}} \\ Z'_B & Z'_{\delta_{ES}} \\ 0 & 0 \\ M_B & M_{\delta_{ES}} \end{bmatrix} \begin{bmatrix} \Delta B \\ \Delta\delta_{ES} \end{bmatrix} \qquad (7.5)$$

where the variables are perturbation values, and the body derivatives X_i, Z_i $(i = u, w, B, \delta_{ES})$ are related to X'_i, Z'_i, by

$$\left.\begin{aligned} X_i &= \frac{f_6 X'_i + f_2 Z'_i}{f_1 f_6 + f_2^2} \\ Z_i &= \frac{f_1 Z'_i + f_2 X'_i}{f_1 f_6 + f_2^2} \end{aligned}\right\} \quad i = u, w, B, \delta_{ES} \qquad (7.6)$$

where f_j, $j = 1, 2, 6$ are functions of the trim pitch attitude θ_0 :

$$f_1 = \sin^2\theta_o + 0.9\cos^2, \quad f_2 = 0.1\sin\theta_o\cos\theta_o, \quad f_6 = \cos^2\theta_o + 0.9\sin^2\theta_o$$

The values of these functions for the tested conditions are listed in the following table.

λ-deg	45			60			75		
θ_0-deg	-5	0	5	-5	0	5	-5	0	5
f_1	no test data	.9	.9004	.9004	0.9	.9004	.9004	0.9	0.9004
f_2		0	.00868	-.00868	0	.00868	-.00868	0	.00868
f_3		1.0	.99884	.99884	1.0	.99884	0.99884	1.0	.99884

One may proceed directly to linearize the simplified nonlinear equations of motion (7.4). The resulting linear equations are slightly simpler as shown in equation (7.7).

$$\begin{bmatrix} \dot{u} \\ \dot{w} \\ \dot{\theta} \\ \dot{q} \end{bmatrix} = \begin{bmatrix} X'_u & X'_w & -\sigma g \cos\theta_o & -w_o \\ Z_u & Z_w & -g \sin\theta_o & u_o \\ 0 & 0 & 0 & 1 \\ M_u & M_w & 0 & M_q \end{bmatrix} \begin{bmatrix} u \\ w \\ \theta \\ q \end{bmatrix} + \begin{bmatrix} X'_B & X'_{\delta_{ES}} \\ Z_B & Z_{\delta_{ES}} \\ 0 & 0 \\ M_B & M_{\delta_{ES}} \end{bmatrix} \begin{bmatrix} \Delta B \\ \Delta\delta_{ES} \end{bmatrix} \quad (7.7)$$

where $X_i = X'_i + (1-\sigma)\sin\theta_o Z_i \; , \; i = u, w, B, \delta_{ES}$

7.1.3 Conversion of Princeton Test Data to Identification Computer Program Data Format

The PDMT test data were received by CAL from Princeton University in April, 1970. The data include the digital tapes, the analog traces, the test conditions, and the data conversion factors. There are 29 runs at a duct incidence of 75°; 54 runs at 60° and 44 runs at 45°. As described earlier, all the data were measured with respect to the space-fixed axis system. Data measured were θ_S, q_S, $\dot{q}_S$, u_B, $\dot{u}_B$, w_B, $\dot{w}_B$, n_x, n_z, δ_{ES}, and B. The inputs used in these runs were longitudinal stick deflection with or without collective inputs. The longitudinal stick inputs were doublets with periods of two seconds; all the collective inputs were step inputs. Various levels of rate feedback, depending on duct incidence, were used in all the test runs. The differential elevon deflections, $\Delta\delta_f$, were linearly proportional to the differential collection commands ΔB with the following mixing ratios:

$\lambda \sim$ deg	75	60	45
$\Delta f / \Delta B \sim$ deg/deg	5	1.0	2.0

The pitch acceleration data were quite noisy and very inconsistent with pitch rate measurements; the data were taken using two displaced linear accelerometers. Apparently, the pitch accelerometer originally installed was not up to specifications. More detailed descriptions of the data are given in Reference 61.

Using the conversion factors supplied by PDMT, the nine-track digital data of Princeton were transcribed to a CAL tape in their correct dimensional form (e.g., ft/sec, deg/sec^2, etc.). These data were further transformed from the PDMT measurement axis system to a body-fixed axis system using equation (7.1). Because the linear accelerometers were mounted with a slight inclination to the reference body axis system of the model, necessary corrections on the measured n_x and n_z were made. However, no transformations were required for δ_{ES} and B .

Since the data were in model scale, the stability and control derivatives identified from these data will, of course, be in model scale. To convert the values of the model-scale derivatives to those of full-scale derivatives, the conversion factors can be derived from Reference 60. The results are listed in Table 7-3. This, then, is the final conversion: the stability and control derivatives are now full-scale, the body-axis values, and may be compared to other available data. We shall next discuss the results of identification runs on the PDMT data.

7.1.4 Identification Results Using Princeton Data

The Princeton data were initially analyzed with the linear Kalman filter program without using acceleration measurements, since the nonlinear computer program had not reached the final form described in Section V. Data analysis was begun with λ = 75° data. Six runs at λ = 75° were chosen for consideration; they are listed below with their inputs:

Run No.	δ_{ES} doublet input	B step input	θ_0 degrees	u_0 fps
55	.5	.3	-1.215	17.26
58	-.5	.3	-1.526	17.33
68	-.5	.15	5.968	9.935
71	.5	.3	6.111	9.82
76	.5	.6	-5.57	21.15
79	.25	0	-6.147	21.44

The λ = 75° data were chosen for initial identification attempts because the length of data runs is longest at this flight condition. Because of the low trim velocity at this flight condition, the small perturbation assumption on velocity is not valid, as we shall see later. Nonetheless, these data were analyzed using the linear equations in order to check the computer results against available PDMT results, which were generally derived using linearized equations.

A sample of early identification results is shown in Tables 7-1 and 7-2. Table 7-1 shows the results of a linear Kalman run on data No. 55 using the equations-of-motion method to obtain initial estimates. The measurement noise statistics were estimated from the data and are shown in the following table.

Measurement Noise at λ = 75 Deg

Motion Variables	Measurement Noise Standard Deviation
q ~ deg/sec	.25
θ ~ deg	.15
u ~ deg	.10
w ~ deg	.15

The transient response computed using the parameters identified in Table 7-1 matches very well with the data as shown in Figure 7-4. Table 7-2 shows the results of using the same data (No. 55) with the initial estimates obtained by scaling down parameter values obtained from the global aerodynamic program (Reference 1). However, as shown in Figure 7-5, the response computed from the global values matches very poorly with the data, although the time histories computed from the parameters identified using the linear Kalman program again match well with the data.

From Tables 7-1 and 7-2, it is seen that the parameters identified using the two different sets of initial estimates are considerably different. This may be partly attributable to the following reasons:

(i) Initial covariance matrix. The variances of the parameter estimates computed from the equations-of-motion program were used for the Kalman program initialization for both sets of initial estimates. As was discussed in Section V, these variances are too small to indicate the dispersion of the estimation error. In a sense, the early versions of the Kalman filter may be regarded as attaching a "confidence level" to the initial estimate of a parameter based on its variance. If the variance is small, this indicates a high confidence level, and the filter will not adjust the parameter value much from its initial estimate. Tables 7-1 and 7-2 give evidence that this was the case.

(ii) Acceleration measurements. Acceleration measurements were not used in these runs. It was discussed in Section VI that the acceleration measurements contain additional information. Use of this additional information should further alleviate the nonuniqueness problem.

Unfortunately, as described earlier, neither the improved start-up procedure nor the use of acceleration measurements were included in the linear Kalman program. Thus, the results of the early applications of the technique to the Princeton data were not conclusive.

Several ancillary results, however, were indicated by this application. For example, from Figure 7-4, it is clear that the global parameters do not represent well the model dynamics. Furthermore, it was found that the linearized equations (7-4) poorly represent the dynamics of the PDMT model at $\lambda = 75°$. Indeed, a sample calculation using run No. 55 revealed that the neglected kinematic terms in the linearization of the X and Z equations, $q\,\Delta w$ and $q\,\Delta u$, were the same order of magnitude as $X_w \Delta w$, and $X_u \Delta u$, $Z_u \Delta w$, where the values of the derivatives X_w, X_u, Z_u, Z_w were taken from global or available PDMT values as shown in Table 7-1. Clearly then, the linearized equations (7.4) are inadequate to represent the $\lambda = 75°$ data.

We also found that the trim definition of the PDMT model is not entirely satisfactory for identification purposes. Initially, the initial data point was used as the trim value, a procedure which may lead to inconsistent trim values. In addition, the addition of a collective input at the $\lambda = 75°$ cases frequently was necessary to maintain level flight path angle (rather than the expected climb), a fact which might indicate improper initial trim. The use of incorrect trim values in the equations of motion can lead to erroneous results.

The trim anomaly can be avoided if one performs the linearization of the nonlinear equations about some accelerated reference conditions (rather than trim conditions). If this is done, we have, in lieu of equation (7.5), the following linearized equations:

$$\begin{bmatrix} \dot{u} \\ \dot{w} \\ \dot{\theta} \\ \dot{q} \end{bmatrix} = \begin{bmatrix} X'_u & X'_w & -g\cos\theta_R & -w_R \\ Z'_u & Z'_w & -g\sin\theta_R & u_R \\ 0 & 0 & 0 & 1 \\ M_u & M_w & 0 & M_q \end{bmatrix} \begin{bmatrix} u \\ w \\ \theta \\ q \end{bmatrix} + \begin{bmatrix} x'_0 & x'_B & x'_{\delta_{ES}} \\ z'_0 & z'_B & z'_{\delta_{ES}} \\ 0 & 0 & 0 \\ m_0 & m_B & m_{\delta_{ES}} \end{bmatrix} \begin{bmatrix} 1 \\ \Delta B \\ \Delta\delta_{ES} \end{bmatrix} \quad (7.8)$$

where the variables are perturbation values from their reference values u_R, w_R, q_R, θ_R, $\dot{u}_R$, $\dot{w}_R$. If q_R is chosen to be zero, then x'_0, z'_0 and m'_0 become constants. This equation, with the primes removed, was later used in the initial application of the techniques to the X-22A flight test data. Since in our nonlinear program the reference values are used in representing the aerodynamic terms as described in Section II, the trim problem does not exist.

We now present the results of data analysis using the nonlinear identification program. Data analyzed are cases at duct incidences of 45° and 75°. The flight conditions, inputs, and reference values of these cases are shown in Table 7-4 and the noise levels of these data are shown in Table 7-5.

It is to be recalled that, due to the inertia effects of the error linkages, the general nonlinear equations of motion derived by CAL for the Princeton dynamic model are very complicated as shown in equation (7.2). Further simplifications were subsequently made using the actual data furnished by Princeton. Equation (7.4) shows the simplified nonlinear equations of motion. It is seen that the X-equation has an extra term which is not present in the equations of motion for the full-scale X-22 aircraft. Without modifying the computer program, this term was treated as a modeling error which can be considered as process noise ($\sigma_{\dot{u}}$) as shown in Table 7-5.

The results of the computer runs are shown in Tables 7-6, 7-7, and 7-8. The transient response matching for the four runs on Table 7-6 is shown in Figures 7-6 through 7-9. It is seen from these figures that the parameters identified using acceleration measurements and using modeling error simulation result in a better match to the data. Figure 7-10 shows the time histories computed using the parameters identified from No. 154 (the parameter set in the column next to the last on Table 7-6) and the input of No. 157; the data plotted are those of No. 157; and the responses computed from the initial estimates of No. 157 are also shown in this figure. Table 7-9 shows a comparison of the effects of linearized and nonlinear kinematic coupling for run No. 55, and Figure 7-11 shows the transient response matching for the parameter set shown in the last column of Table 7-9. Notice that the data length used in the nonlinear runs for No. 55 is 10 seconds instead of the total length of approximately 14 seconds used in the linear Kalman runs (see Figure 7-4). From Table 7-9, it is seen that the most significant change in the parameters identified appears to be in the control derivatives.

From these computer runs, it may be seen that the identified derivatives in the pitching moment equation are fairly consistent. In fact, a sensitivity computation shows that the inputs for these runs analyzed (doublet in δ_{ES} and step in B) is adequate for the identification of pitching moment derivatives; but the inputs do not give sufficient sensitivity for X_δ, X_B, Z_δ, Z_B. It appears that a collective input other than a simple step is desirable. Thus, it is recommended that the experimental input design method discussed in Appendix F, which uses sensitivity as the criterion to determine the input, should be employed prior to any future PDMT test to determine an input which would enable the extraction of better quality parameter estimates.

As we mentioned earlier, the angular acceleration measurements are inconsistent with the pitch rate measurements. Clearly, the present method used at the PDMT of using two linear accelerometers to replace the $\dot{q}$ sensor is inadequate for the identification requirement. Also, the missing terms in the X force equation due to the error linkage inertia coupling were compensated by considering it as process noise; however, since it is a deterministic function, the missing terms in the X force equation should be programmed into the computer equations in the future.

7.2 Application to X-22A Flight Data

Application of the identification technique to actual flight test data obtained from the Phase II Military Preliminary Evaluation (MPE II) of the X-22A variable stability aircraft is presented in this section (Reference 58). Identification results for two cases each at fixed duct incidences of $\lambda = 30°$ and $\lambda = 45°$ are given, employing both the linear version (equation D.2) of the extended Kalman filter and the nonlinear locally iterated filter (5.1 and 5.2). Due to the limited availability of transition data, results are presented for only one slow transition.

7.2.1 Data Selection and Digitization

The MPE II of the X-22A aircraft consisted of eleven test flights, labelled 2F195 through 2F205, conducted from 31 March to 11 April 1969 for the purpose of "qualitatively" evaluating the state of development and potential of the X-22A VSS (Reference 58). Although the evaluation was qualitative in nature, data were recorded in flight on a 50-channel oscillograph. These flight data were the only available data for the X-22A for the purpose of parameter identification during this project. Consequently, each flight plan, flight log and oscillograph record were carefully scrutinized to obtain flight data which could possibly be used in the identification of stability and control derivatives in the longitudinal plane at fixed duct incidence and slow ($\dot{\lambda} \approx \pm 1.5$ deg/sec) and fast ($\dot{\lambda} \approx \pm 4$ deg/sec) transition. The main criteria used for selection were:

(a) little lateral-directional motion.

(b) large longitudinal maneuvers (large signal to noise ratio),

(c) variable stability system (VSS) in operation (if possible), and

(d) equivalent flight conditions (weight, altitude, etc.).

All four criteria were considered very important from the standpoint of identification, as well as, of course, accurate measurements. VSS operation was considered important because the equations of motion were written considering the longitudinal stick position, δ_{ES} as a control input rather than the individual elevons and blades. Since the feedforward system is in operation in the VSS mode, control system nonlinearities, which are not modeled, are therefore reduced. Thus, when in the VSS mode, the δ_{ES} measurements at the actual longitudinal stick position can directly be used for identification.

All the required measurement sources, with the exception of w, were available on the oscillograph traces. Since α_V is a function of w, the α_V (alpha vane) measurements were used in place of w. This, of course, precluded data selection at low speed operation. Unfortunately, not being able to design the experiments (the flight tests) a priori for our specific purpose, data could not be found which simultaneously satisfied all four criteria. The best data available were selected for data reduction.

Once a flight record was selected, the measured responses were manually digitized at a sampling frequency high enough to avoid consistent bias errors. However, the recorder speed allowed a minimum sampling time of .1 seconds. Without channel filters, the n_x, n_z and $\dot{q}$ traces were so corrupted with high frequency noise (especially the n_x and n_z traces) that it was necessary to manually fair ("smooth") a line through these measurements prior to sampling. Consequently, the n_x and n_z measurement accuracy is very questionable. Since .1 seconds is slightly coarse, the sample interval was reduced to .05 seconds by linear interpolation of the digitized data. Fairing of all other measurements was done where necessary. In general, in addition to the poor quality of the oscillograph recordings, it was found the data had relatively low signal-to-noise ratio and consequently were not very desirable for parameter identification.

Four fixed-duct incidence cases were selected and digitized from the oscillograph records. The two cases at $\lambda = 30°$ are 2F197 and 2F203 and those at $\lambda = 45°$ are 2F195 and 2F198. Time-in-flight and aircraft operating points are given in Table 7-10. Motion variables measured were q, θ, u, α_V, n_x, n_z and $\dot{q}$. The control input, δ_{ES}, was measured at the R.H. pitch stick, and, in actuality, $\sin\theta$ is the measurement source and not θ. However, due to the small perturbation in θ, $\sin\theta \approx \theta$.

Three equivalent cases for slow accelerated transition ($\dot{\lambda} = -1.5$ deg/sec) were also selected from the MPE II data. Time-in-flight and operating points for these cases are given in Table 7-10. The case from 2F197 was manually digitized from the oscillograph recorder and the other two were used to define the reference trajectories necessary for the parameter identification of the first case. However, no useful high rate transition cases could be found.

Motion variables measured were the same as those for the fixed-duct incidence cases. However, during transition, the X-22A was in the fly-by-wire (FBW) mode, and thus the feedforward loop was not operational. Consequently, in order to circumvent control system nonlinearities, the individual elevon and propeller pitch settings were digitized and equivalent longitudinal stick positions were found using the static calibration data from References 62, 63, and 64. Duct angle, λ, and collective pitch stick, β_c inputs were also digitized from the recorded traces of these variables.

7.2.2 Selection of Noise Levels

The measurement noise and process noise levels estimated from the flight records are given in Table 7-11. Since the effects of process noise can be observed in the acceleration measurements, two sets of measurement noise levels are given for the acceleration measurements, depending on whether process noise is assumed present or not.

Although all high frequency noise was removed by manually fairing each response prior to discretization as explained above, the standard deviations of the measurement noise were taken as the peak-to-peak noise level present divided by 4. These values were then checked to make sure they agreed with the absolute rms accuracy which could be expected from the respective sensor and recording system, including the "human telereading"* of the responses. In this way, the filter will be able to properly interpret the accuracy of the data it receives.

The selection of Q (the process noise covariance matrix) from flight test data is much more difficult. Here, process noise is primarily construed as uncertainty in the mathematical model or unknown forcing inputs. With this interpretation, it is obvious that the process noise statistics are nonstationary with nonzero mean. However, the process noise is characterized as a stationary random process with zero-mean in the filter model. Therefore, some means of a priori estimating its value (on the average) must be used. The approach taken here was to assume modeling errors in the aerodynamic representation of the aircraft. Since these errors are observable in the acceleration measurements, σ for the process noise were defined as 10% of the square root of the average power in the acceleration measurements -- called the rms (root mean square) value. For example, σ for $\dot{q}_g$ was calculated as

$$\sigma_{\dot{q}_g} = .1 \sqrt{\frac{1}{N} \sum_{i=1}^{N} (\dot{q}_i)^2}$$

where N is the number of data points and $\dot{q}_i$ is the acceleration measurement of $\dot{q}$ at the i^{th} point. Since n_z is always approximately 1 g, a factor of 4% was used instead of 10% for this measurement. Results, which are approximately representative for all five flight records, are given in Table 7-11.

* The analog oscillograph records are manually digitized by employing a Telereader.

It should be noted that, when process noise is used in the filter model, the noise levels in the n_x, n_z and $\dot{q}$ acceleration measurements are reduced accordingly. In the results presented below, the process noise (when used) was assumed to enter the dynamics through a sample and hold as explained in Section VI. This interpretation is not exactly correct for flight data, since the dynamical representation of the aircraft is continuous.

7.2.3 Results at Fixed-Duct Incidence

The flight conditions and reference values employed for all four cases at fixed-duct incidence angle are given in Table 7-12. Equivalent reference values were selected for flights at equal duct incidence for ease in comparing the parameter estimates obtained.

From the results of applying the technique to computer generated data 3C-1 and 3D-1 as well as the PDMT data, it was found that, for the inputs used in these flight tests, the X and Z derivatives were relatively insensitive and therefore difficult to identify, although the sensitivity of the pitching moment derivatives appears to be adequate for good parameter identification of the M derivatives. In all identification runs in this section, the initial estimates for the aircraft states (q_o , θ_o , u_o and w_o) were chosen to be the first measured data point and the variances for these estimates (for components of $\hat{v}$) were the measurement noise on their respective sensors. Since there is no w sensor, an equivalent noise level was computed for this signal, using first-order approximations.

Prior to the development of the locally-iterated filter employing the nonlinear model for the X-22A, preliminary identification results were obtained on data 2F197 and 2F203 (λ =30°) using the linear version of the extended Kalman filter (linear model, equation D.2) without acceleration measurements. Results for each case are presented in Table 7-13. Since the linear version of the extended Kalman filter was not programmed with an α_V measurement source, a w measurement was obtained by calculating

w from the α_V , q , and u measurements. Similarly, n_x and n_z measurements were transferred to $\dot{u}$ and $\dot{w}$ for use in the equations-of-motion estimator. The filter was started using the variances (multiplied equally by a factor of 10) from the equations-of-motion estimator and systematically recycled three times forward. Process noise was assumed zero. As explained in Section 7.1, X_0 , Z_0 and M_0 were used to eliminate trim uncertainties.

The results for these cases are impressive. Transient response matching to measured data is shown in Figure 7-12 and 7-13 for 2F 197 and 2F203, respectively. Close response matching to the state measurements is noted. Clearly, the linearized equations characterize the X-22A very well for this case.

Using the nonlinear program and the simple version of the locally iterated filter (the version in which process noise is assumed zero, i.e., in (5.1) and (5.2) set Q = 0), identification was performed on 2F197 and 2F203 with nonlinear aerodynamics (23 parameters) and linear aerodynamics (13 parameters) without acceleration measurements. Results are given in Tables 7-14 and 7-15.

Because of the small airspeed change (a maximum speed change of 5 or 6 fps) in both cases, the correct nonlinearities of the derivatives with respect to u in the 23-parameter cases were not expected; however, upon evaluating these derivatives at the average airspeed of 138 fps, the two 23-parameter cases were somewhat consistent with their corresponding 13-parameter cases as shown in Table 7-16. For all the cases run, the moment derivatives appeared to be fairly consistent; the Z and the X derivatives did not. This is attributable to the fact that the aircraft had little motion in both u and w in these two cases. Transient response matching to measured data (Figure 6-14, flight 2F197) employing 23 and 13 parameters to represent the aerodynamics, where the parameter estimates are from the equations-of-motion estimator, indicates that the 13-parameter case is the best. Although not shown, the computer printouts of the transient responses from the Kalman filter also verify that the 13-parameter model is better. Thus, the linear aerodynamic representation in (2.9) was used for further identification purposes.

From Tables 7-13 and 7-16 the effects of linearizing the nonlinear kinematic coupling term in the linear model can be observed. In general, if the contribution of a stability derivative to the aerodynamic force or moment is of the same order of magnitude as $q\Delta u$ and $q\Delta w$ (representative of the neglected kinematics in linearization), then the stability derivative would be expected to be affected. Such is the case for the M_u and X_w derivatives.

Results of parameter identification in 2F197 and 2F203 without and with acceleration measurements are given in Table 7-17. In all cases P_0 was formed by multiplying the equations-of-motion parameter variances equally by a factor of 10 and two iterations were employed in the locally iterated filter. Transient response matching to measured data using the parameters identified is given in Figures 7-15 through 7-17. It is seen that the responses matched very well, especially for those computed from the parameters identified using acceleration measurements. The exceptions are the n_x and n_z measurements. However, since these measurements were so highly corrupted with noise prior to manually fairing, particularly n_z, this was expected. Note that matching is within the measurement accuracy defined for these measurements. As expected, the moment derivatives identified appeared to be consistent, but the X and Z derivatives were not. It should also be noted that the initial estimator used a w-measurement and not α_V. Thus a transformation was required.

Another test of the accuracy of the parameters estimated is to match the transient responses computed employing the parameters identified from one set of data to other sets of measured data with a different control input. This was done for the parameters estimated from 2F197 and 2F203 with acceleration measurements. Results are shown in Figures 7-18 and 7-19. Figure 7-18 shows data from 2F203 matched against the transient responses generated using the parameters identified from 2F197 for both the initial parameter estimates from the equations of motion and the locally iterated filter. Figure 7-19 gives the opposite case. Results are very good (within the measurement noise levels present) even though the initial conditions of the aircraft states were taken as the first measured data point and thus could be in error.

The results also tend to verify the low sensitivities of the X and Z parameters. That is, although the X and Z derivatives were not too consistent between the two sets of parameter estimates from the different flight data, the responses matched very well, thereby verifying that the measured responses were not very sensitive to these derivatives for the control inputs employed and the noise levels present. No identification runs were made for which process noise was assumed present.

Results for flight data 2F195 and 2F198 are given in Tables 7-17 through 7-19. Transient response matching for all cases except $F_1(1)$ on data 2F198 are shown in Figures 7-20 through 7-24. Acceleration measurements were used in all cases.

At the time of these parameter identification runs, the improved start-up procedure (Section 5.4) was in the preliminary stages of development. Table 7-18 gives a comparison of the equations of motion σ's (σ_{EM}) to the lower bound σ's (σ_{CR}) multiplied by $\sqrt{20}$. These σ_{CR} were computed via equation (3.19) with the $\partial h/\partial p$ term neglected. However, they are presented here since results utilizing the σ_{CR}'s on 2F198 are given.

Tables 7-19 and 7-20 show the results for both data 2F195 and 2F198 when process noise is assumed absent and present, respectively. Due to the poor input, (δ_{ES}), somewhat poor results were obtained for data 2F195 in all cases. For data 2F198, which has a better input than 2F195, better results were obtained for the case in which process noise was assumed present. This is indicated by the improvement in transient response matching for this case over the other two (compare Figure 7-22, in which process noise was assumed present, with Figures 7-20 and 7-21 where $Q = 0$). However, from Figures 7-20 and 7-21, transient response matching is better for the case using the new start-up procedure even when the term $\partial h/\partial p$ in equation (3.19) is neglected. Again, it should be noted that the moment derivatives identified were consistent, but that the X and Z derivatives were not.

Although the states and parameters are not smoothable when process noise is assumed zero, the fixed-point smoothing algorithm can still be employed to obtain a better estimate of the initial conditions of the aircraft states; this estimate will be the same as backward prediction of the final filtered state estimate to time t_0 . Table 7-21 depicts the results of the fixed-point smoothing estimates of the initial states for all four flight records. In each case, the equations-of-motion variances were multiplied, equally, by a factor of 10 to form P_0 . The initial estimates, in all instances, were very close to the smoothed estimates, except for q_0 of flight 2F195, which is different by approximately 1 deg/sec.

A comparison between the parameters identified at $\lambda = 45°$ from Princeton data No. 154 and flight 2F198 is given in Table 7-22. The Princeton results here have been transformed from the model to full scale. Recall that the Princeton data were analyzed without modifying the computer program to account for the additional term in the X equation (which is an inertia coupling term from the Z equation). Despite this inadequacy in the model representation, and inconsistency in the other parameters such as c.g. location, gross weight, model scaling, etc., it is seen that the moment derivatives compare very favorably.

Unfortunately, all of the results presented here for the identification runs at fixed-duct incidence were completed before the improved start-up procedure, final variance computation and filter consistency test were programmed. Also, additional experiments with different noise levels, especially process noise (Q) with the continuous interpretation, may have been helpful. However, due to the poor quality of the MPE II data, additional experimentation was considered to be unwarranted.

From the limited results of employing the identification technique at fixed-duct incidence it can be concluded that the MPE II flight test data is inadequate for consistent parameter identification of the X and Z derivatives. Although the M derivatives were identified consistently, there was insufficient excitation by the δ_{ES} inputs, for the noise levels present, to identify the X and Z parameters accurately.

From the standpoint of instrumentation, more accurate n_x and n_z measurements are required for proper identification of the X and Z parameters. Use of the existing channel filters may prove to be sufficient. In general, if the flight tests are set up a priori, the present X-22A instrumentation, with possible simple modification of the n_z sensor (i.e., a shock mount), appears to be adequate for identification at fixed-duct incidence of 45° to 0°. A w-sensor (LORAS) or another way to measure w is required for lower speed operation. Clearly, a digital recording system is desirable from the standpoint of economical post-flight data handling when large amounts of data are to be analyzed.

7.2.4 Results in Slow Transition

Due to the absence of good transition data from the MPE II flight tests, only limited parameter identification has been tried on one slow transition case ($\dot{\lambda}$ = -1.[illegible] deg/sec) from flight 2F197. The reference trajectories for q, λ , w , δ_{ES} and θ were obtained as the [illegible]age of the responses for this flight and that of an equivalent flight, 2F205. These references are shown in Table 7-23. Data for this flight are shown in Figure 7-25. A total of 26 parameters was used to represent the model. The M_0 , X_0 , and Z_0 derivatives were represented by second-order polynomials in u to compensate for inadequacy in the reference trajectory. Using the results of Reference 1 for an accelerated transition at $\dot{\lambda}$ = 3 deg/sec and those of equilibrium transition, it was considered adequate to represent all other derivatives as first-order polynomials or constants. Noise models employed were the same as those used for fixed-duct identification at $\lambda = 30°$ and are given in Table 7-11. Process noise was always assumed present. To conserve computer time, the transformed ω measurement was used in place of the α_v measurement.

Parameter identification results employing the locally iterated filter with one iteration are shown in Table 7-24. It was found that the transient responses generated using the equations-of-motion parameter estimates could not be integrated beyond three seconds without computer overflows. Although it is not shown, the same situation occurred when 35 parameters were used to represent the aerodynamics. Thus, the improved start-up procedure could not be used initially. However, results employing the locally iterated filter on 5 seconds of data using the equations-of-motion variances for P_0 were much better. Transient responses generated for this parameter set could be obtained for the full 5 seconds, although accurate response matching was not obtained. Since these parameter estimates were better than the equations-of-motion estimates, they were used as the initial estimates for a 10 second filter pass. The final parameter covariances from the 5 second filter, calculated by equation (5.56)*, were used to form P_0.

Transient response matching to measured data using the parameters estimated from the 10 second filter pass are shown in Figure 7-26. The residual sequences and a few selected filtered parameter estimates are also shown. The residual sequences indicate that the filter followed the data very well. However, improvement in the noise models could be made.

It is expected that better results could be obtained by a "boot-strapping" procedure whereby the parameter estimates from the 10 second filter are used as initial estimates for another filter pass. P_0 would be calculated by the improved start-up procedure without a priori information, and increased by an appropriate factor for best results. Adjustment of the noise covariance matrices (R and Q) should also be considered.

---

* A priori information was employed in this calculation for the lower bound.

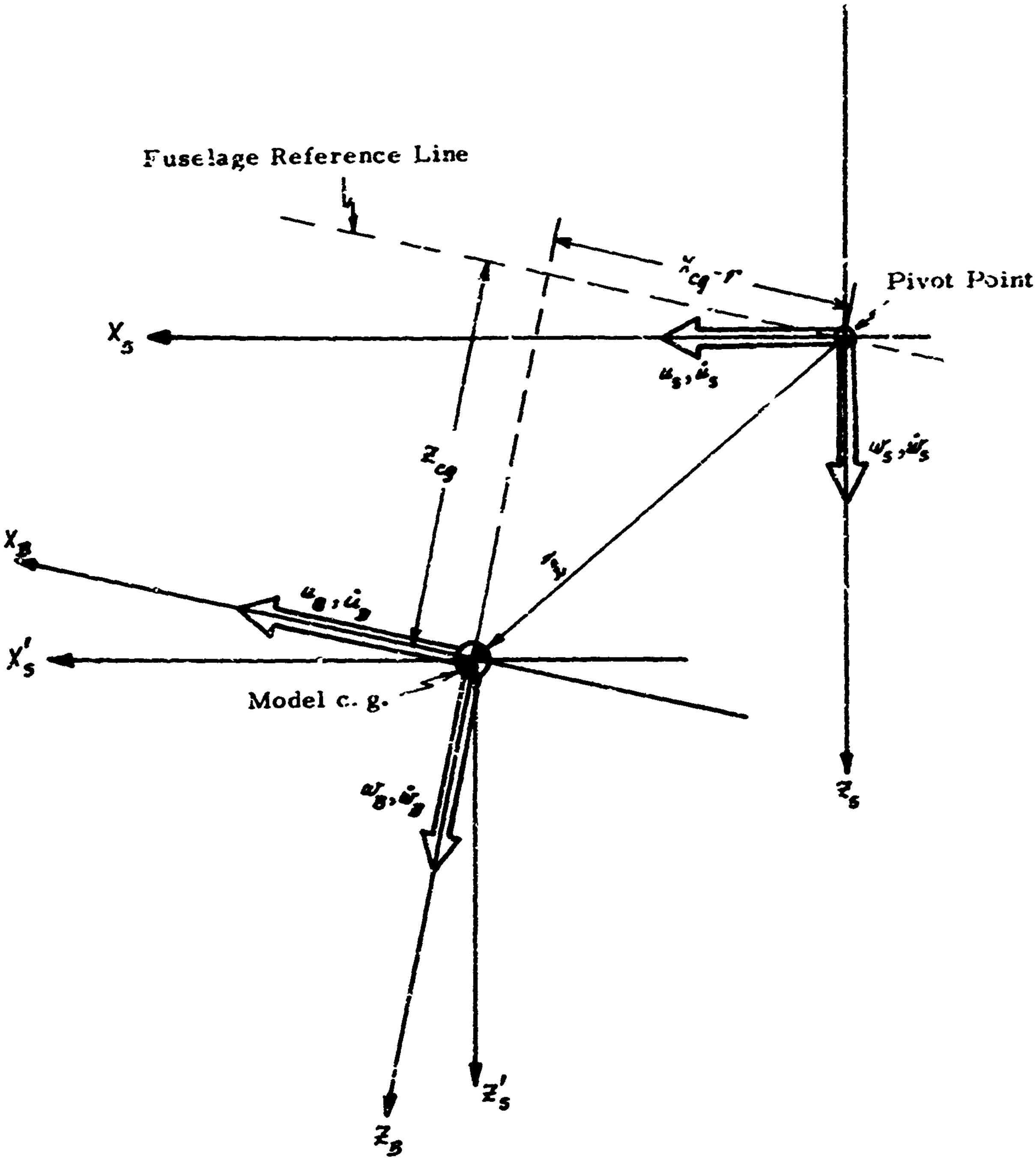

Figure 7-1 Space-Fixed and Body-Fixed Axis Systems

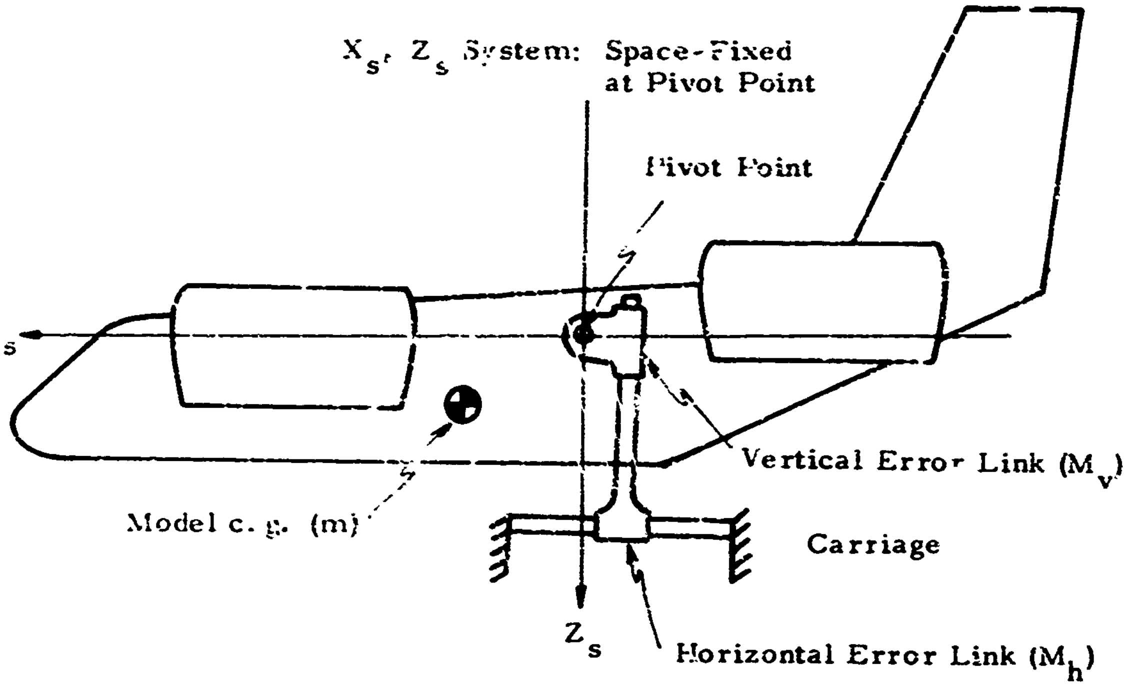

Horizontal Mass: $M + M_v + M_h$

Vertical Mass: $M + M_v$

Rotating Mass: M (I_{cg})

Figure 7-2 Model and Error Link Mass Arrangement

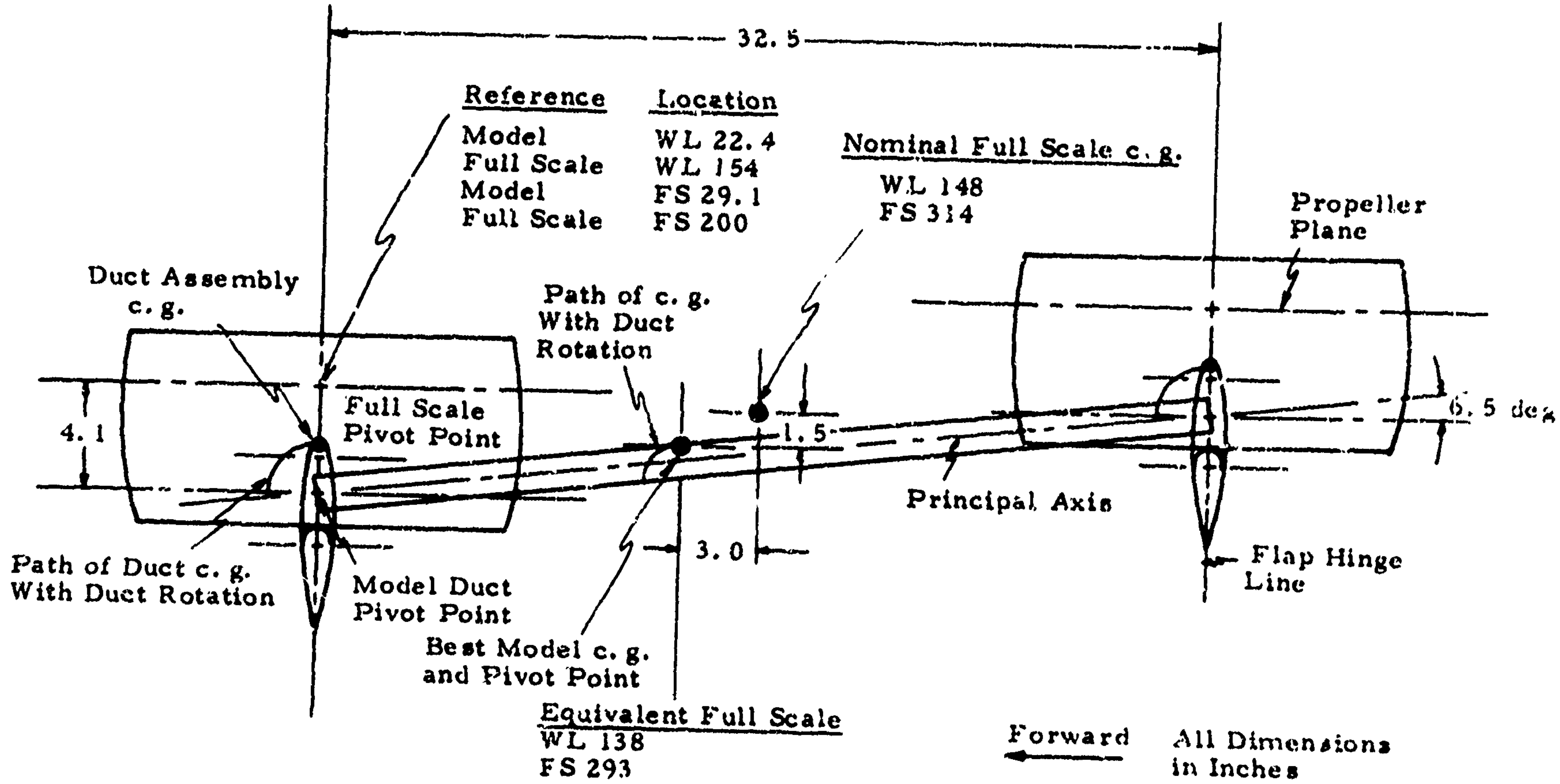

Figure 7-3 Princeton Dynamic Model Track Quad Model Geometry (taken from Reference 60)

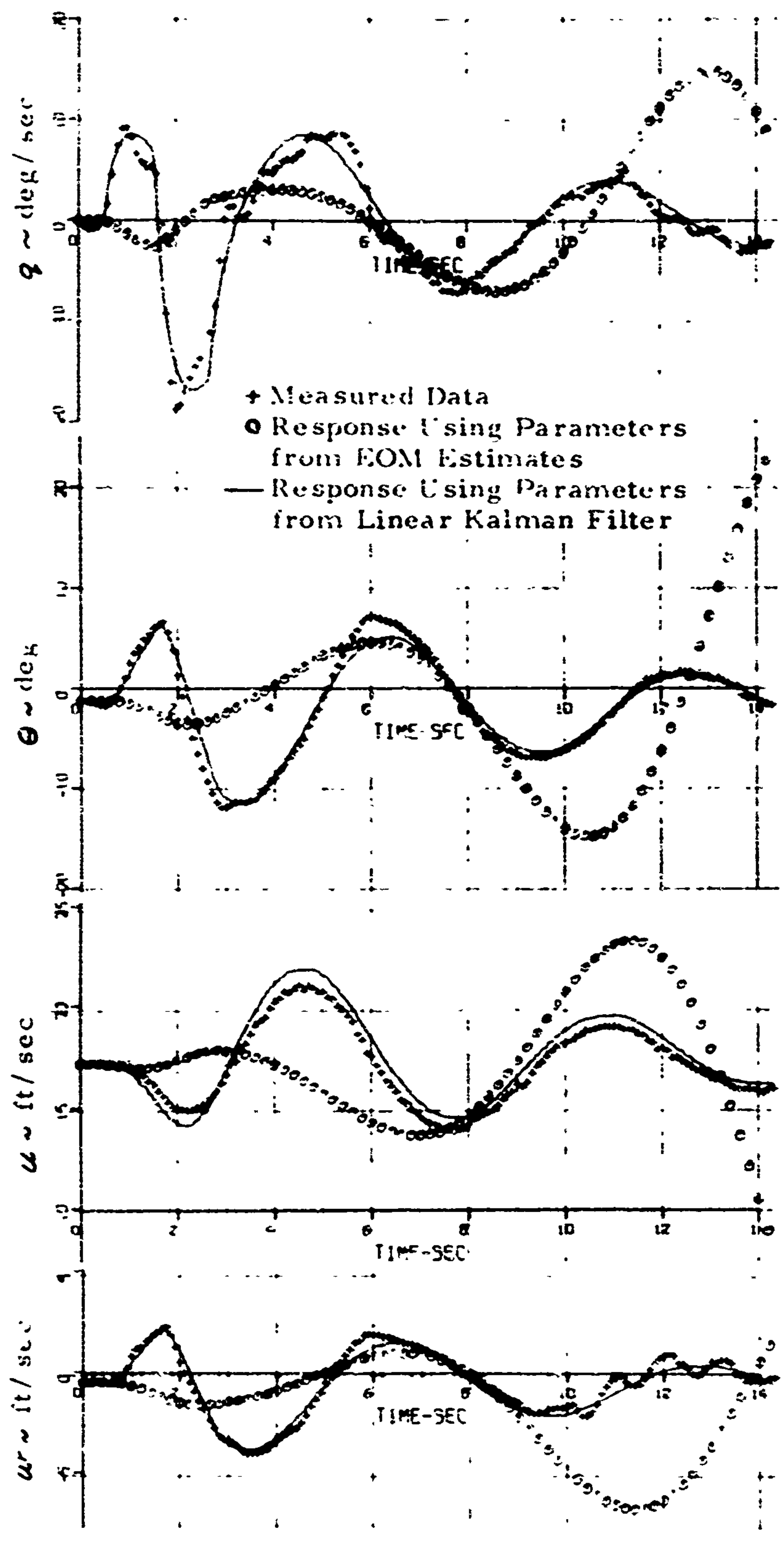

Figure 7-4 Transient Response Matching to Princeton Data #55
Linear Kalman Without Acceleration, Initial Estimate: EOM

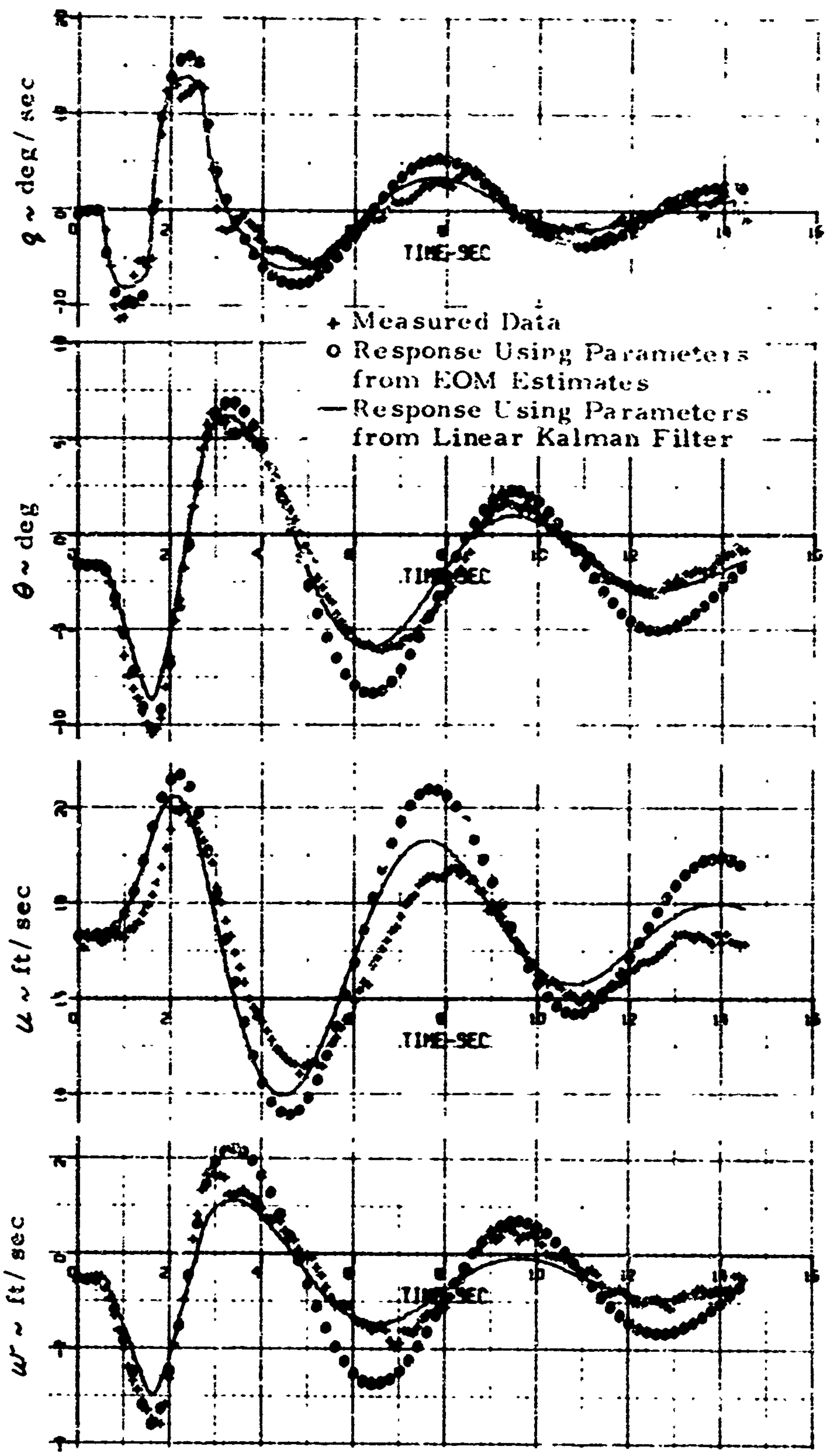

Figure 7-5 Transient Response Matching to Princeton Data #55
Linear Kalman Without Acceleration, Initial Estimate: Global

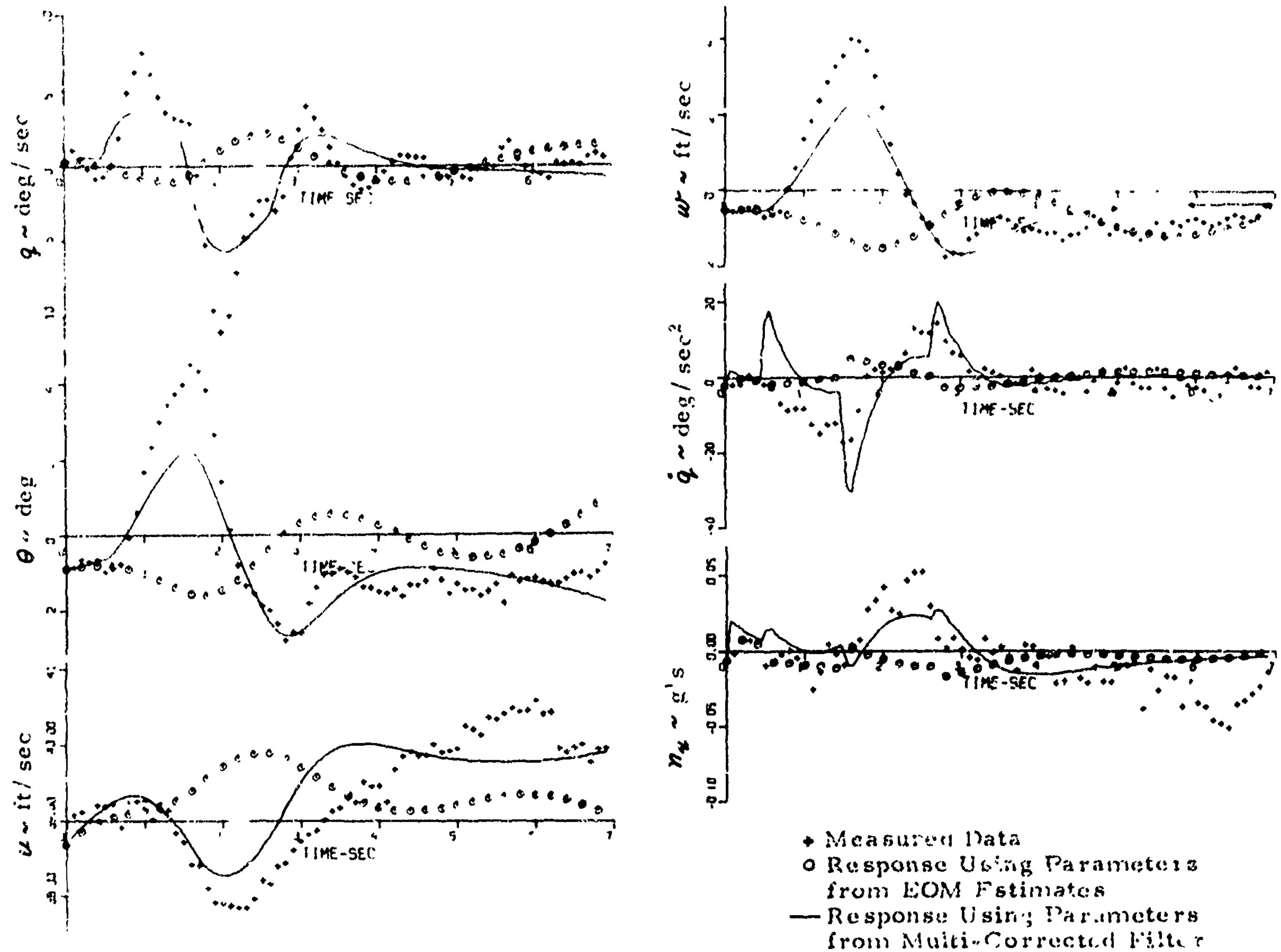

Figure 7-6 Transient Response Matching to Princeton Data #154 With Acceleration Measurements and Modeling Error, $F_{CR}(1)$

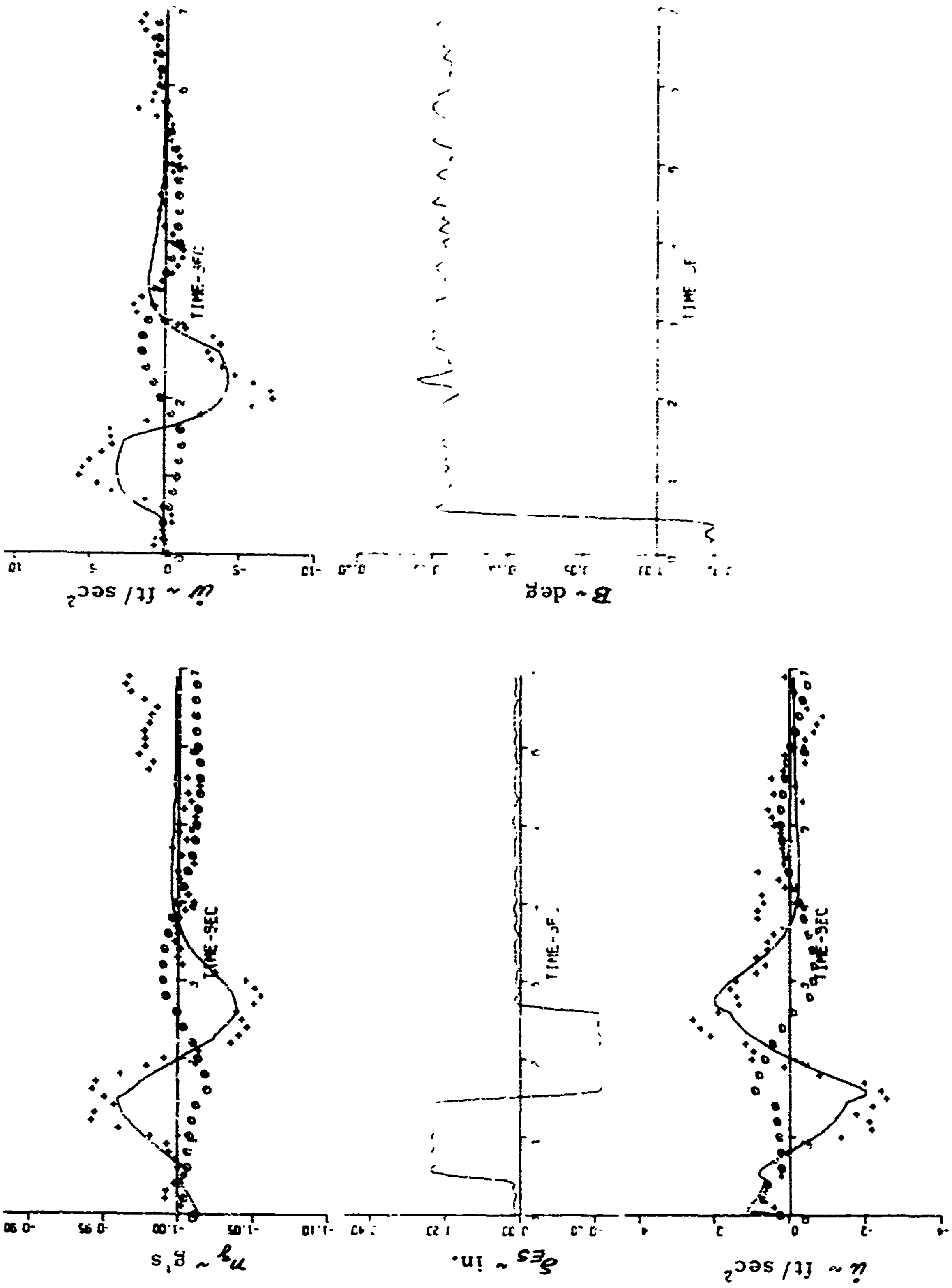

Figure 7-6 (continued)

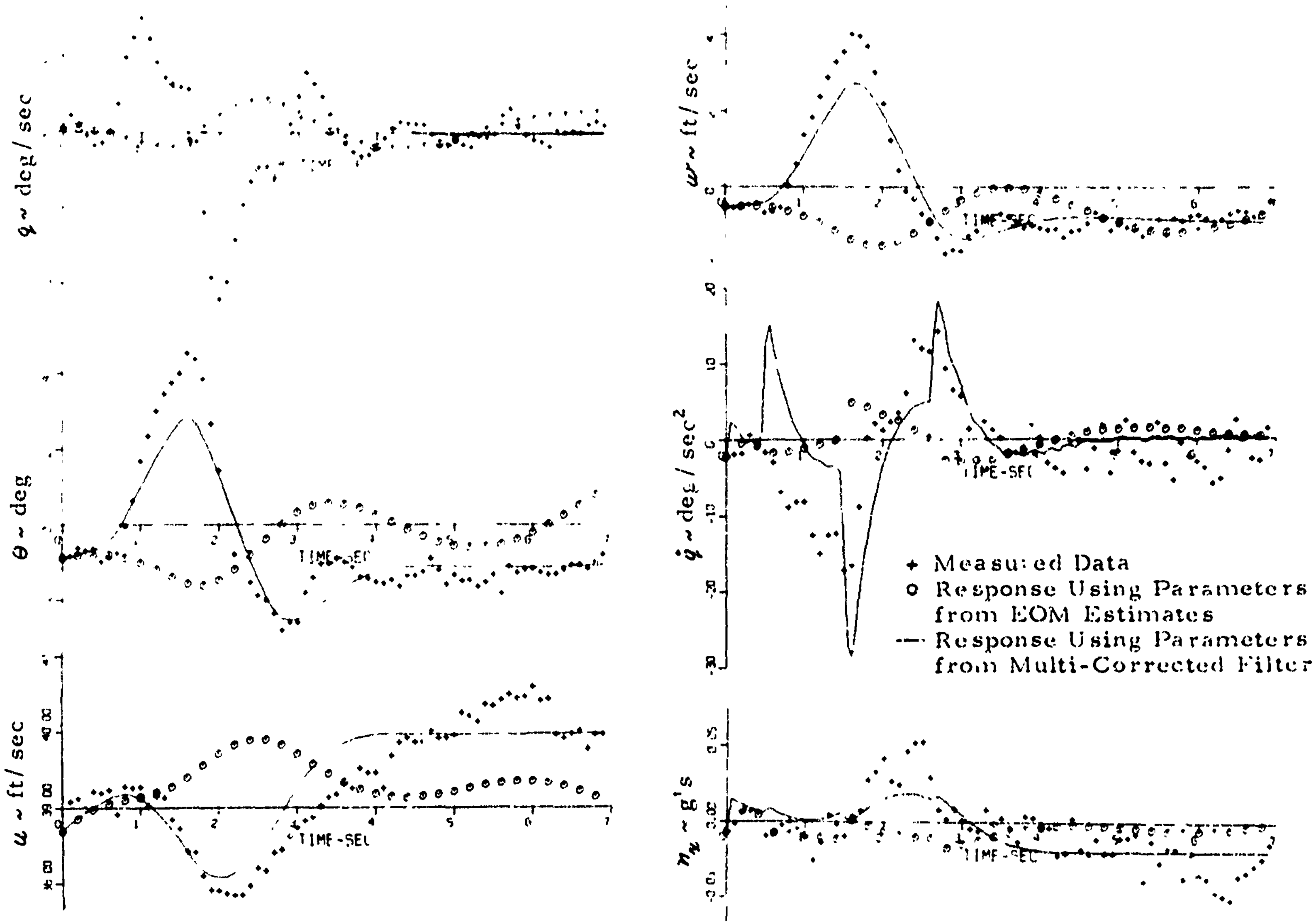

Figure 7-7 Transient Response Matching to Princeton Data #154 With Acceleration Measurements and Modeling Error, $F_1(1)$

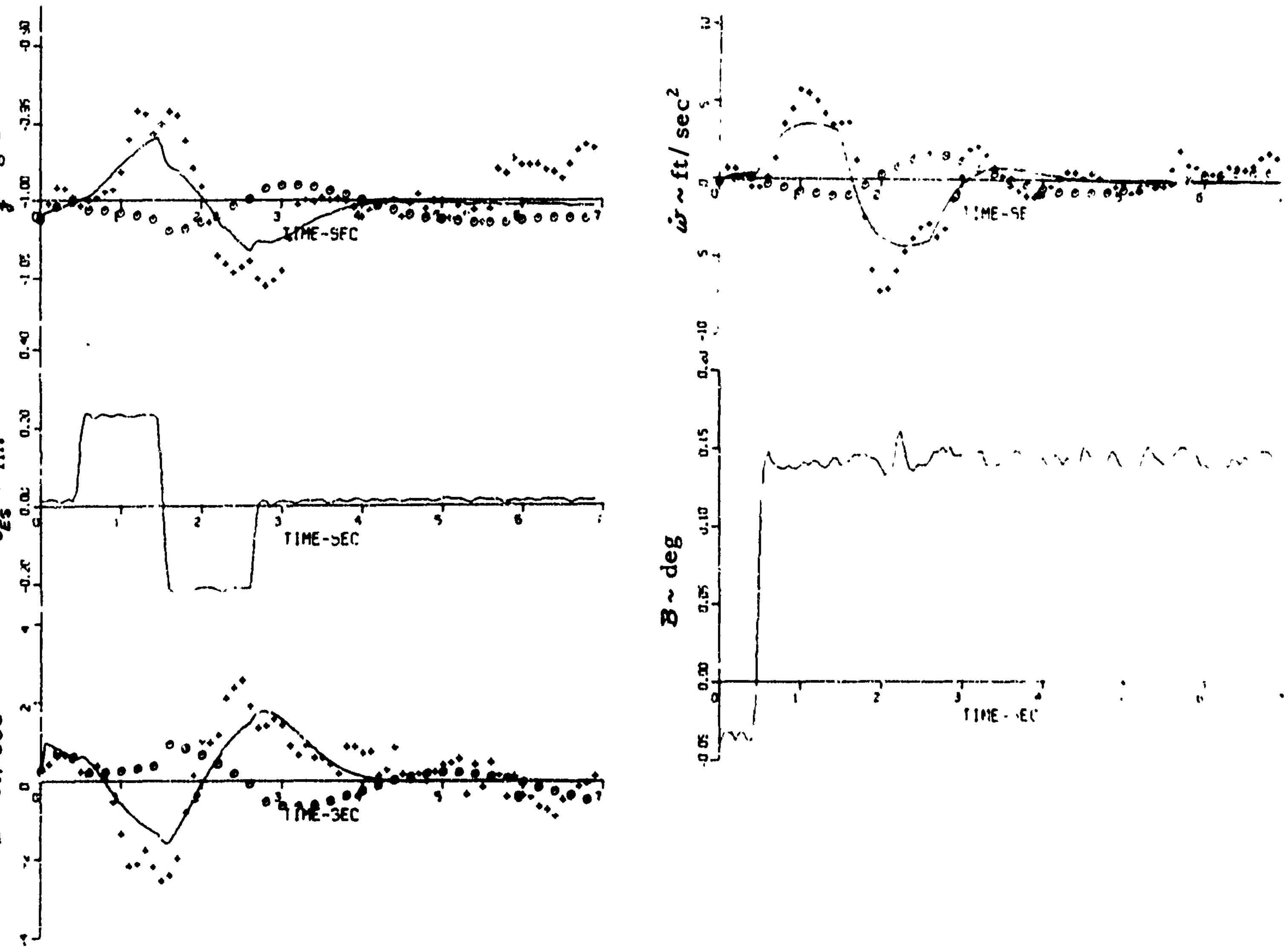

Figure 7-7 (continued)

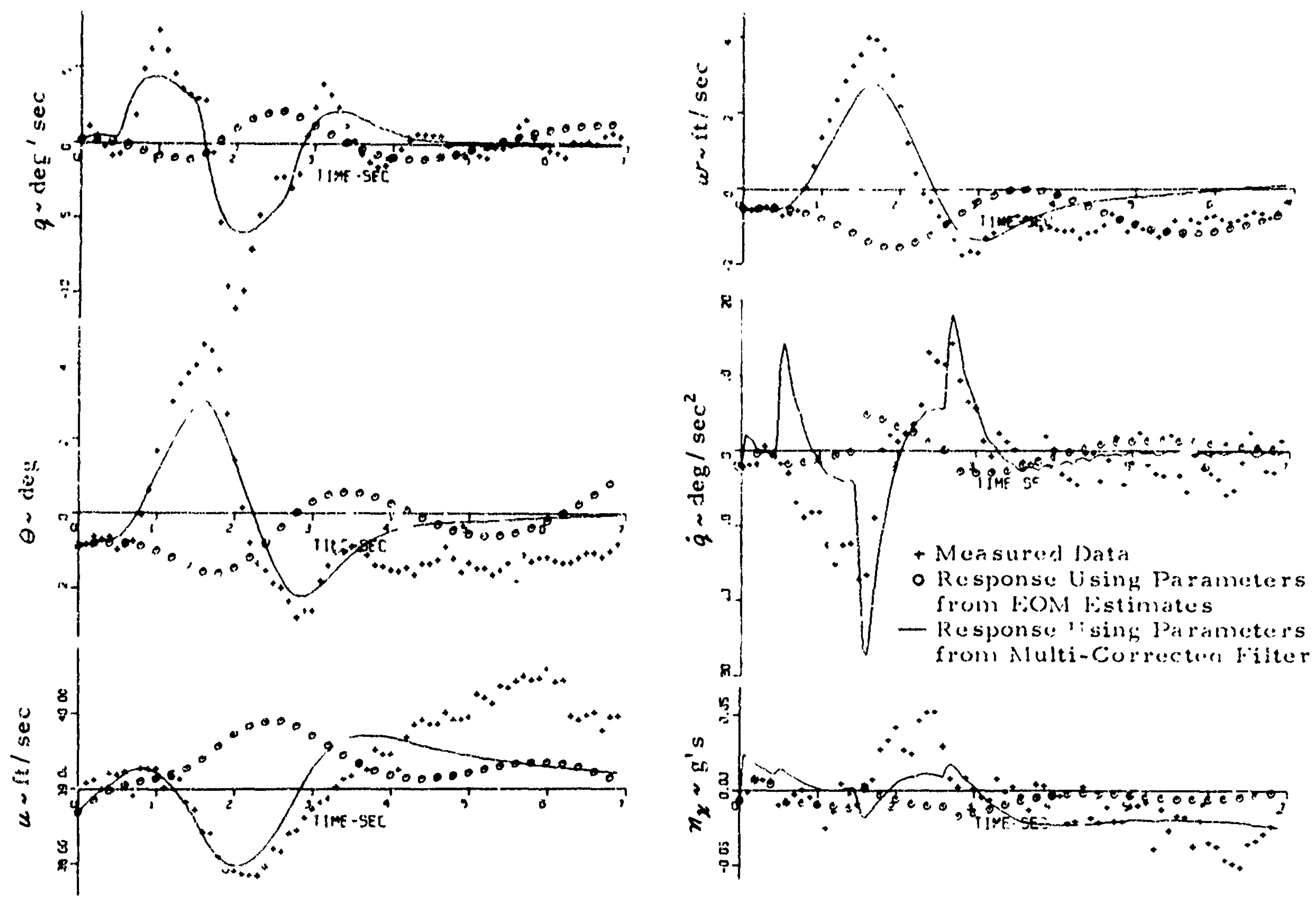

Figure 7-8 Transient Response Matching to Princeton Data #154 With Acceleration Measurement, No Modeling Error, $F_{10}(1)$

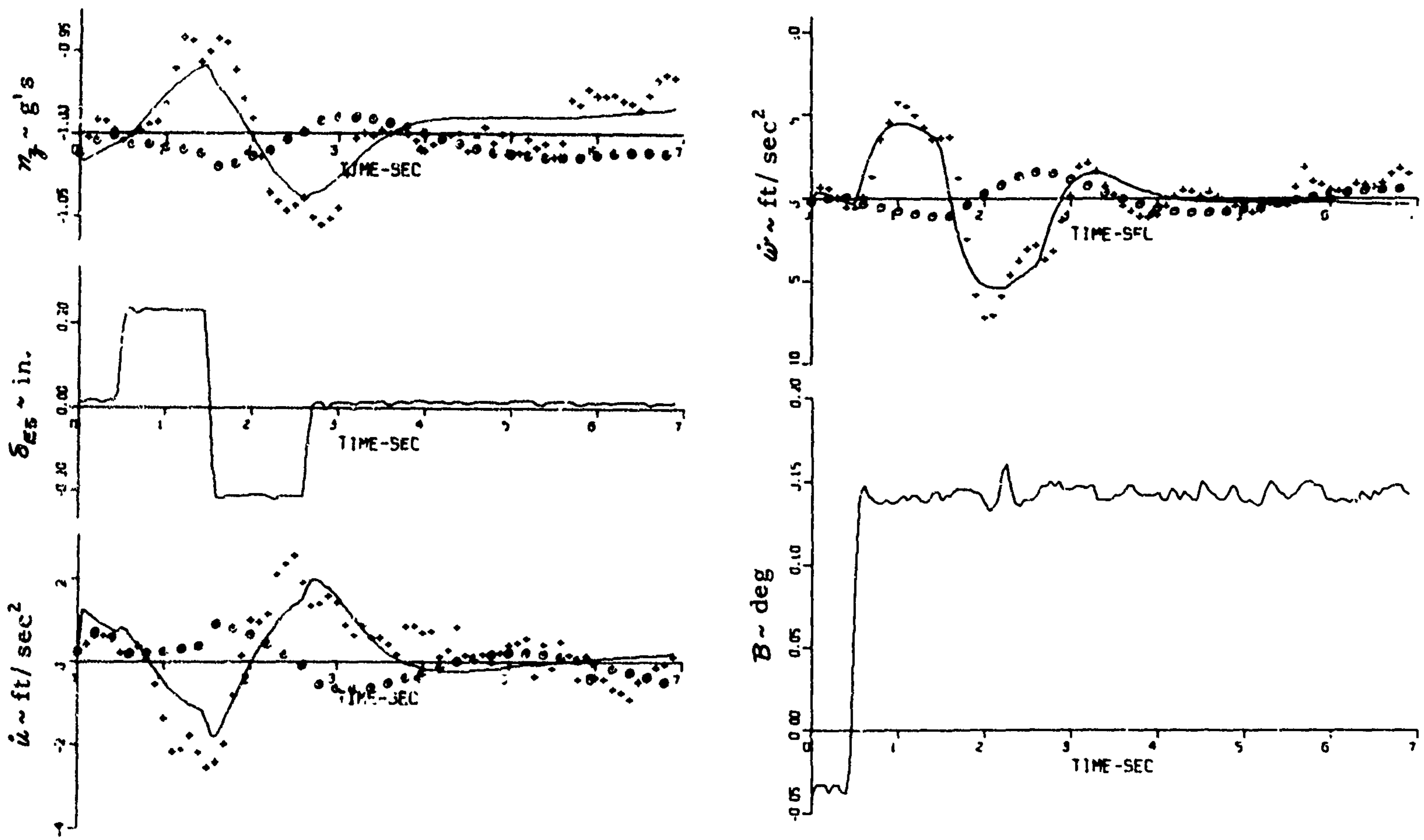

Figure 7-8 (continued)

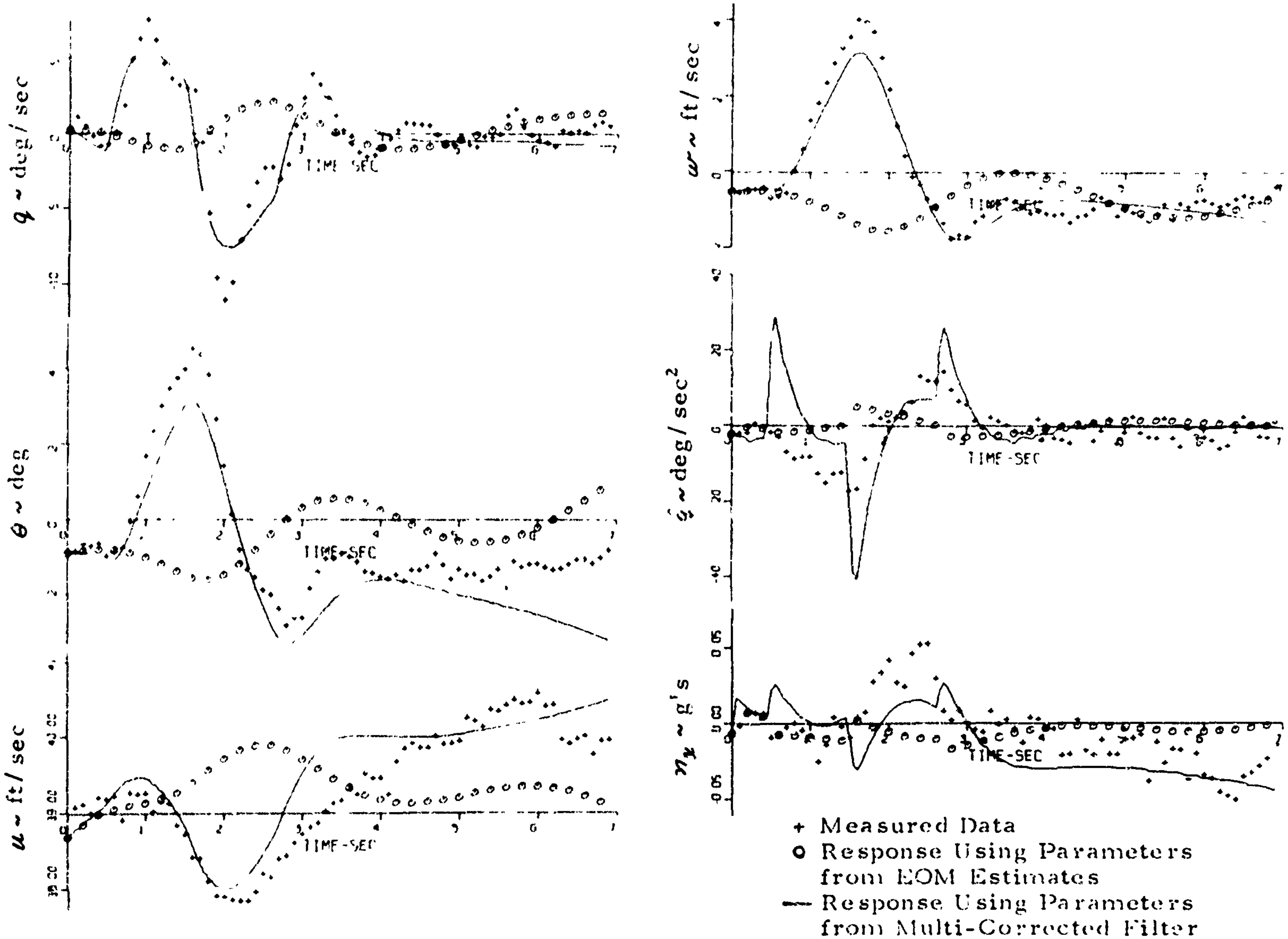

Figure 7-9 Transient Response Matching to Princeton Data #154 Without Acceleration Measurements, No Modeling Error, $F_{10}(1)$

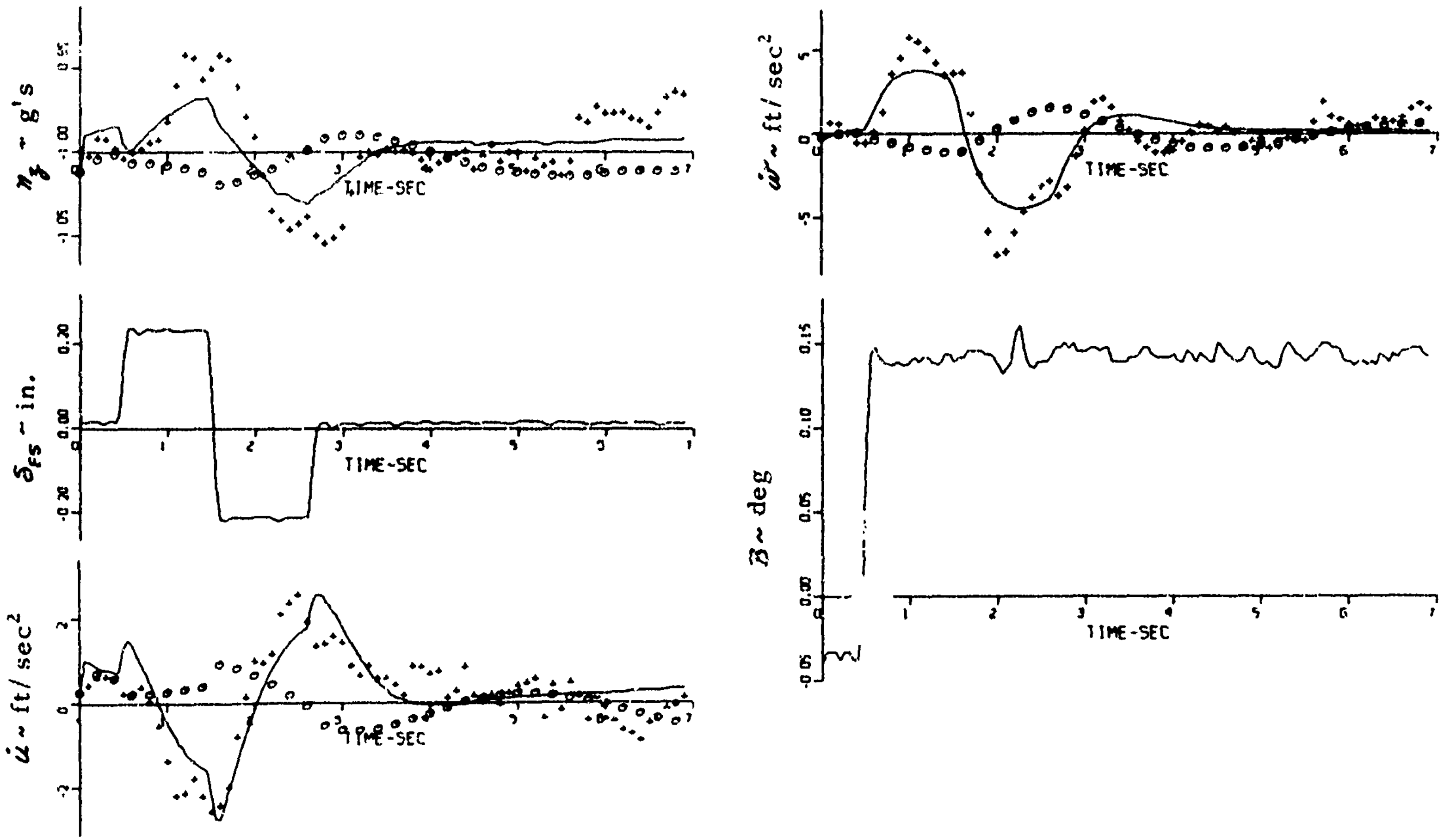

Figure 7-9 (continued)

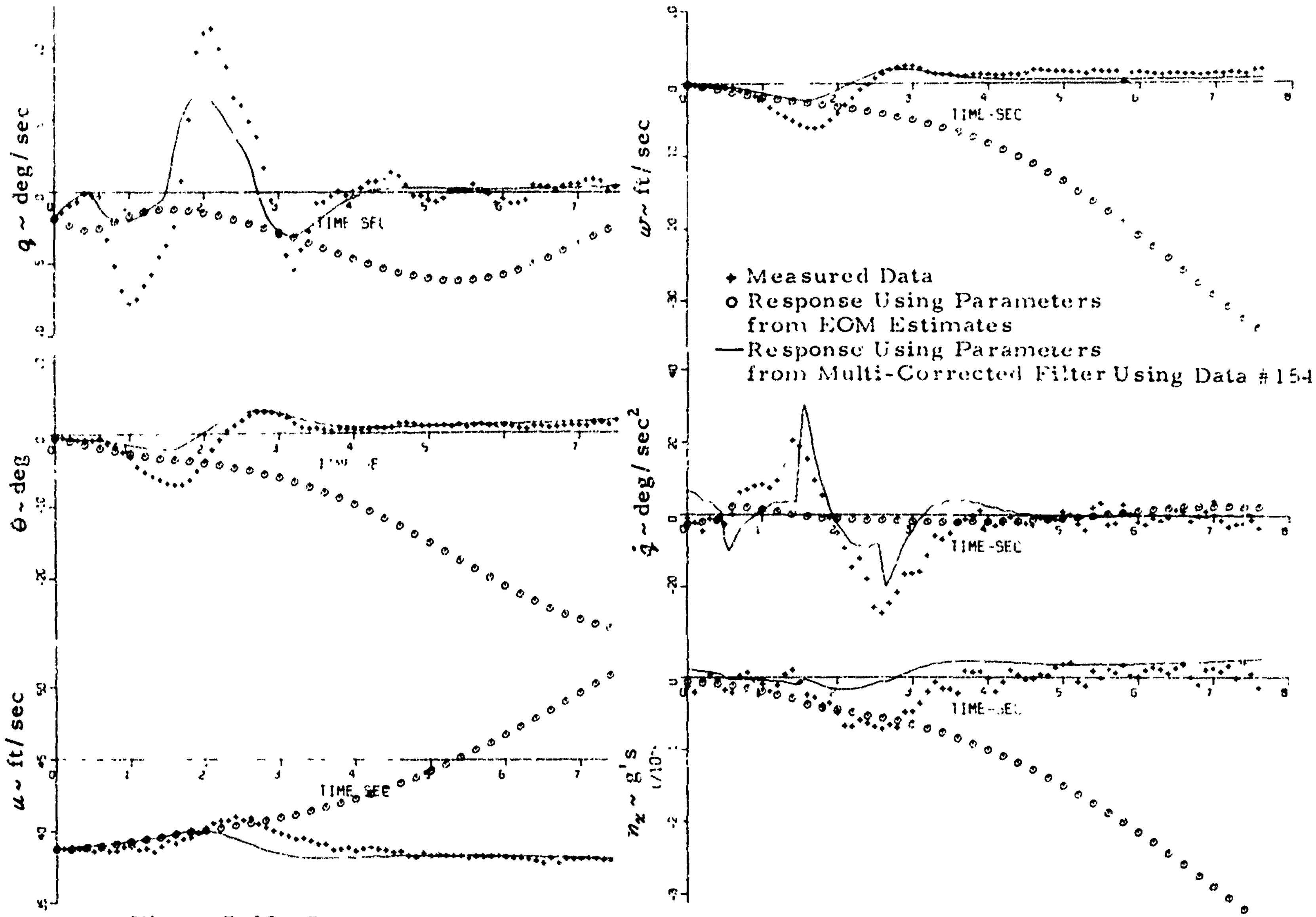

Figure 7-10 Transient Response Matching to Princeton Data #157
Using Parameter Identified From #154 ($F_1(1)$ with Accel. & Q)

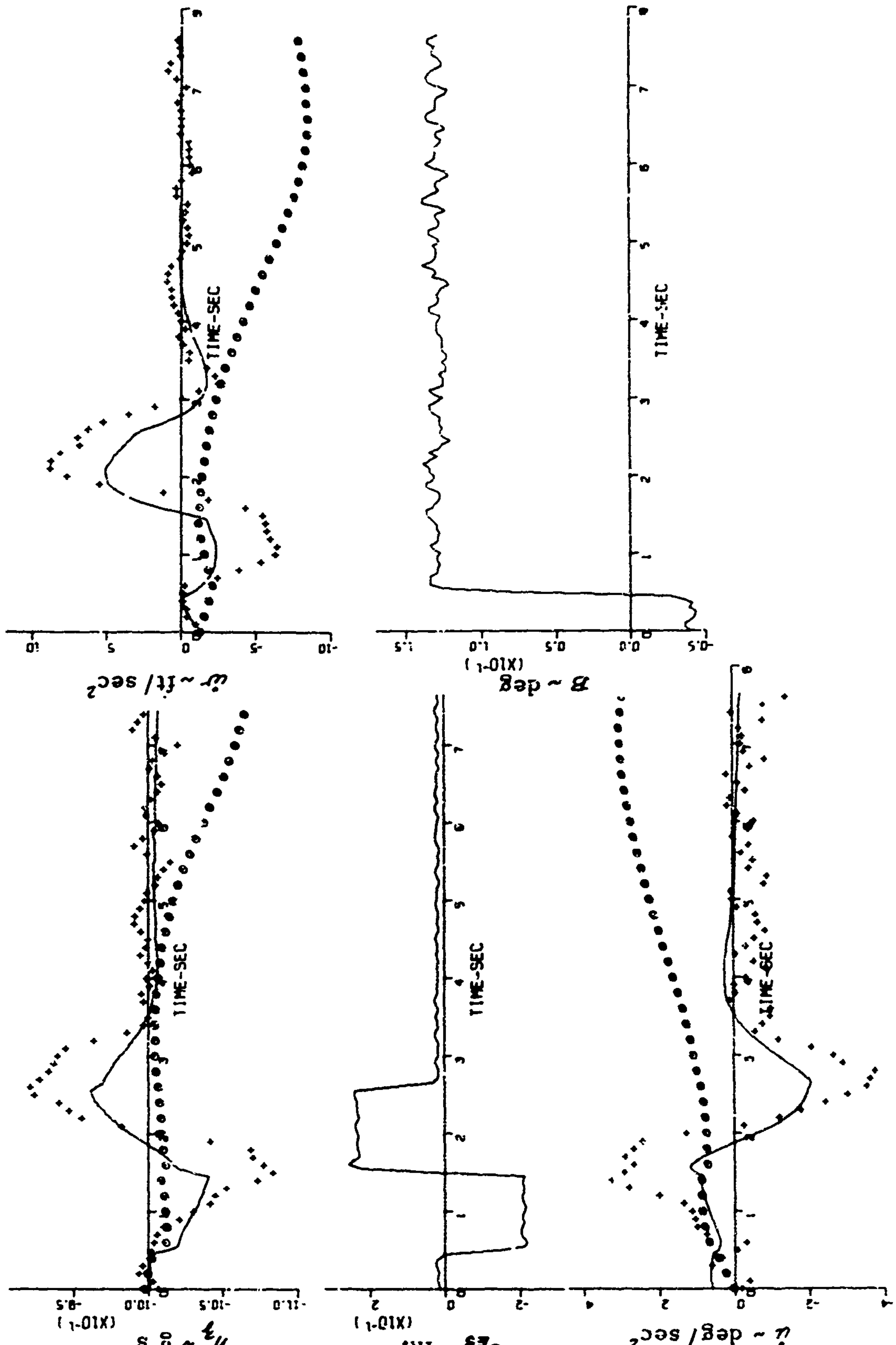

Figure 7-10 (continued)

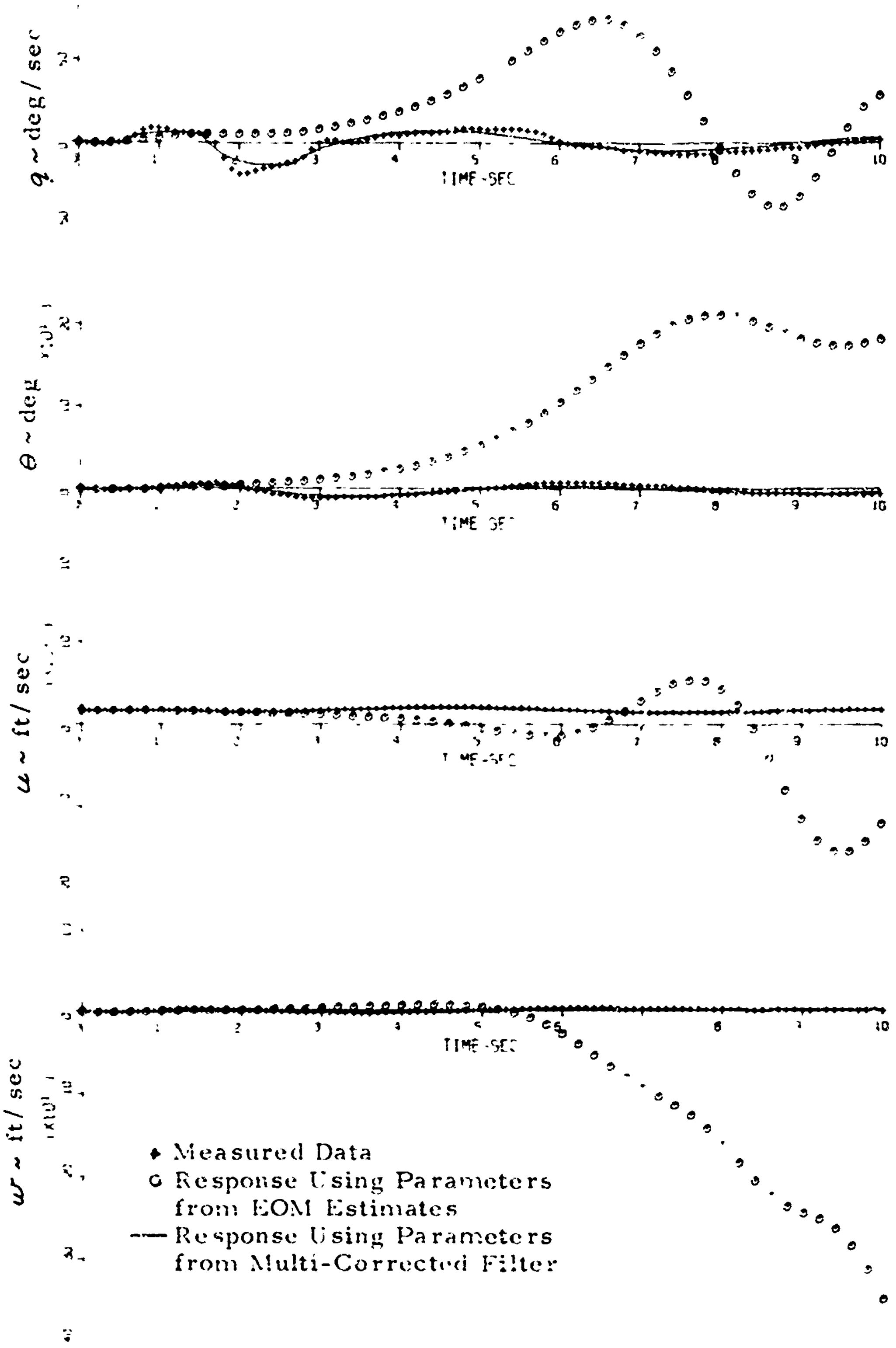

Figure 7-11 Transient Response Matching to Princeton Data #55 With Acceleration Measurements and Model Error

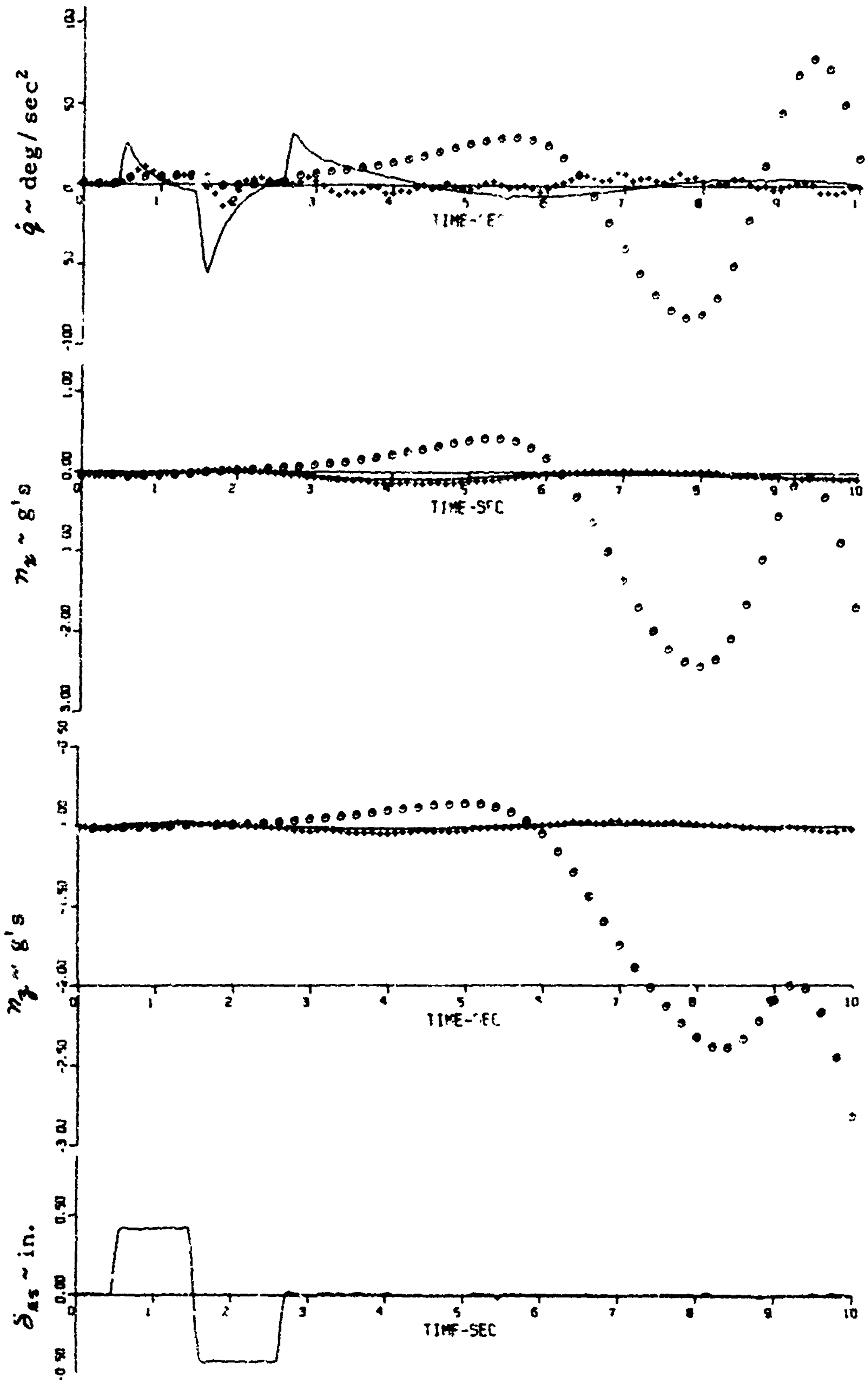

Figure 7-11 (continued)

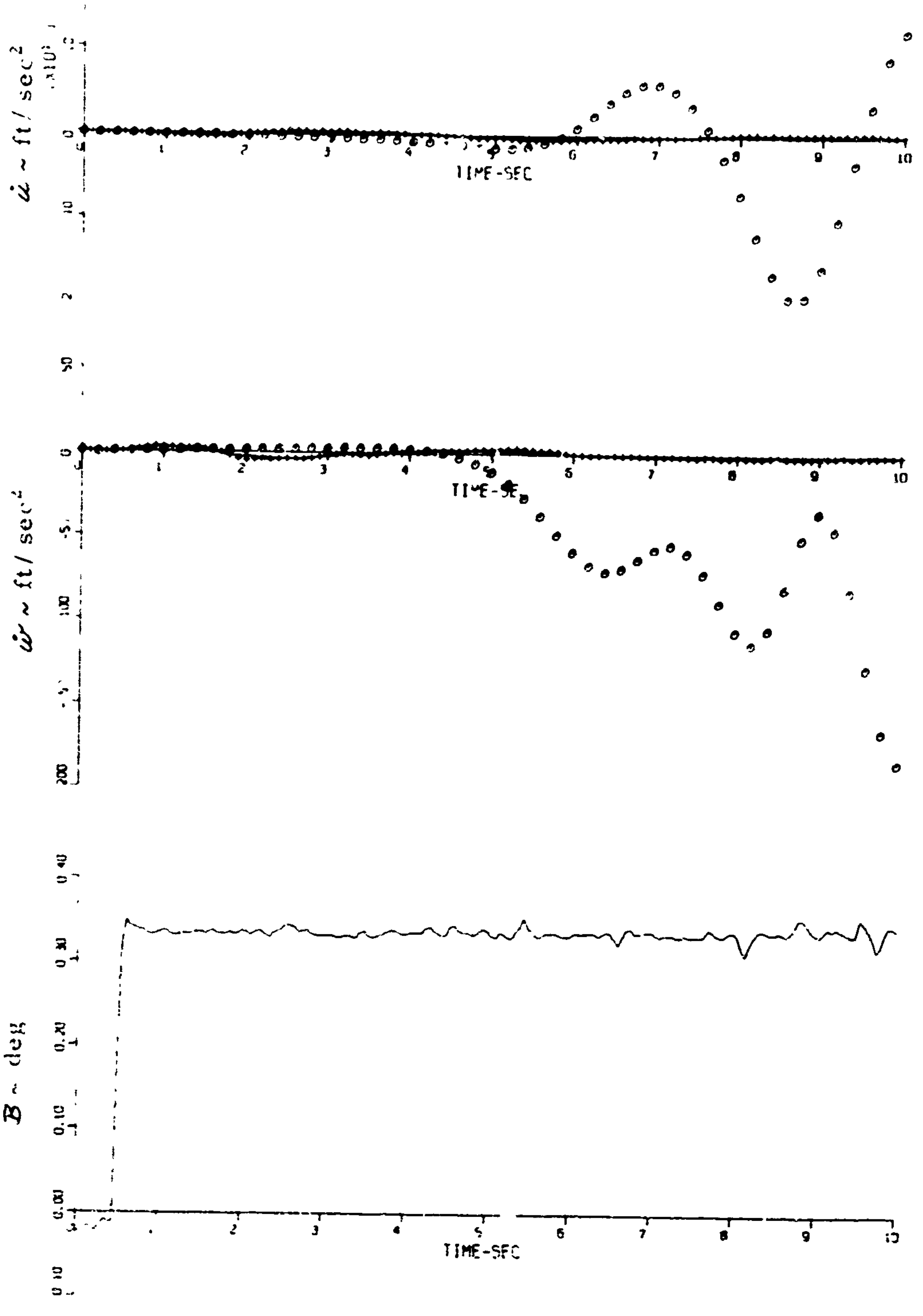

Figure 7-11 (continued)

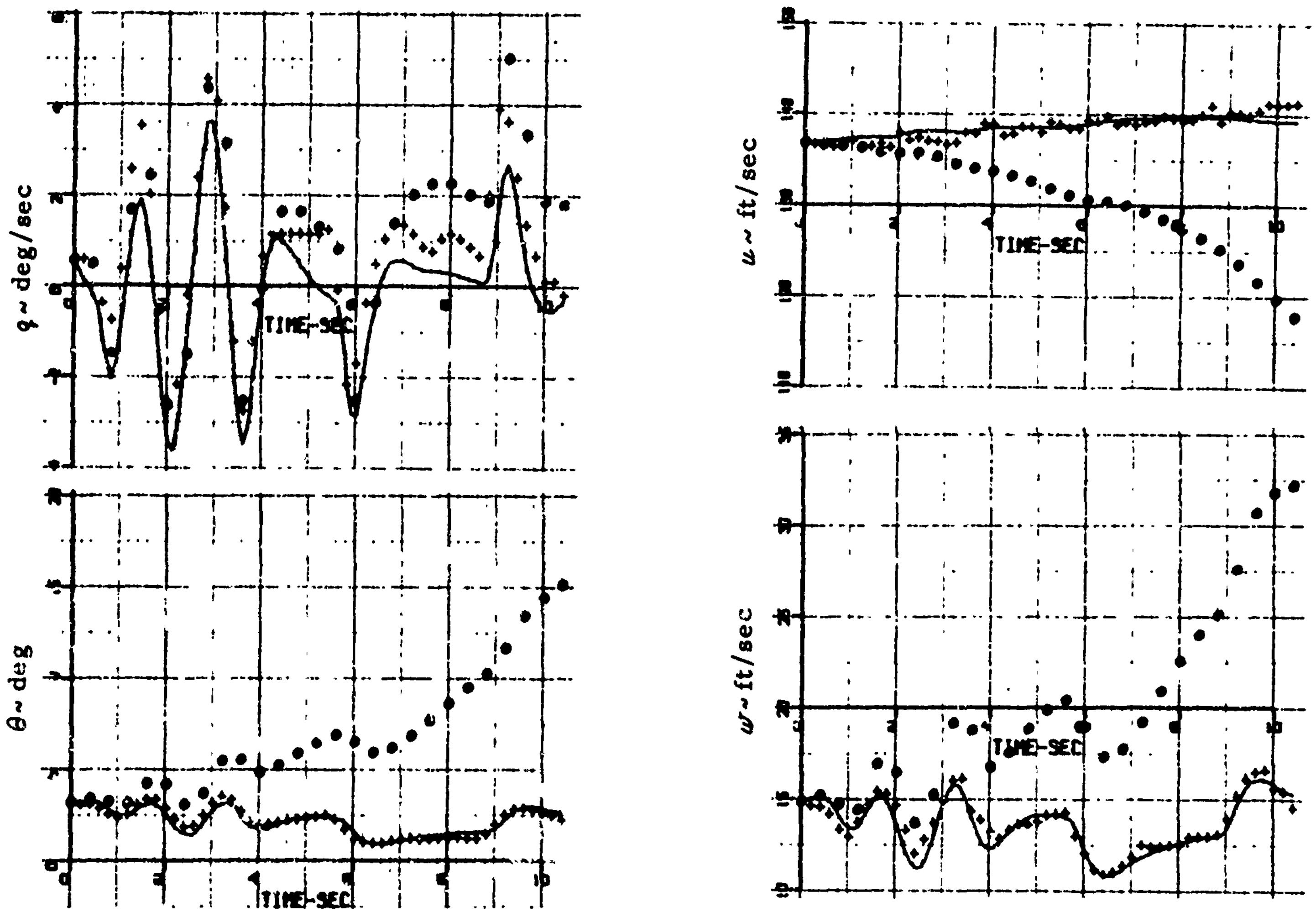

Figure 7-12 Transient Response Matching to Flight Data 2F197, Linear Kalman

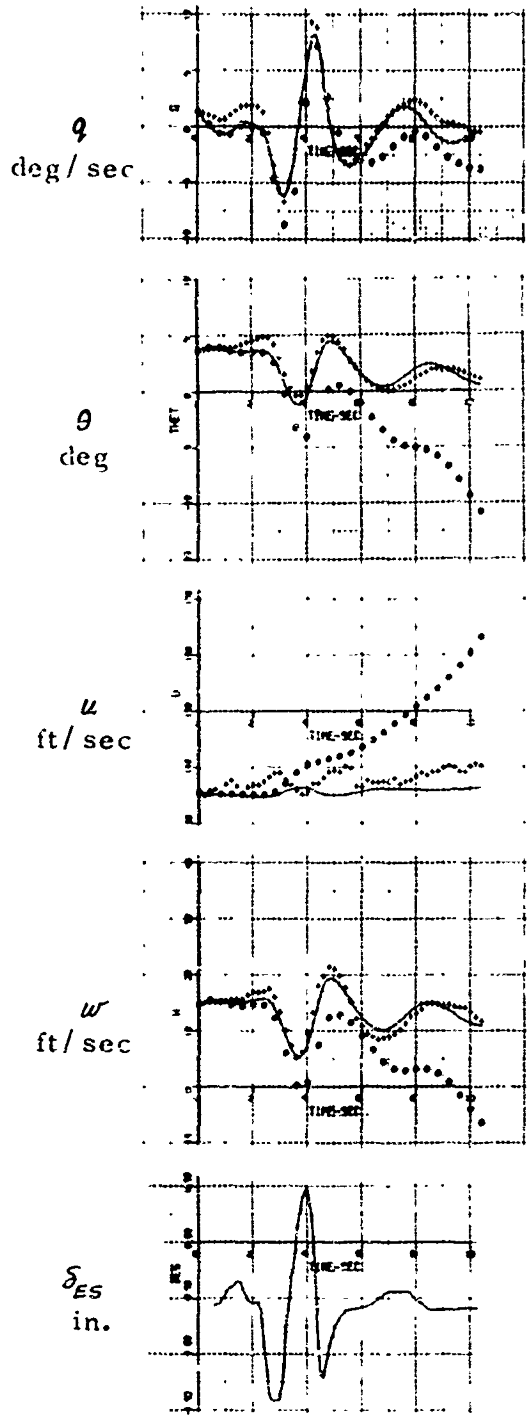

Figure 7-13 Transient Response Matching to Flight Data 2F203, Linear Kalman

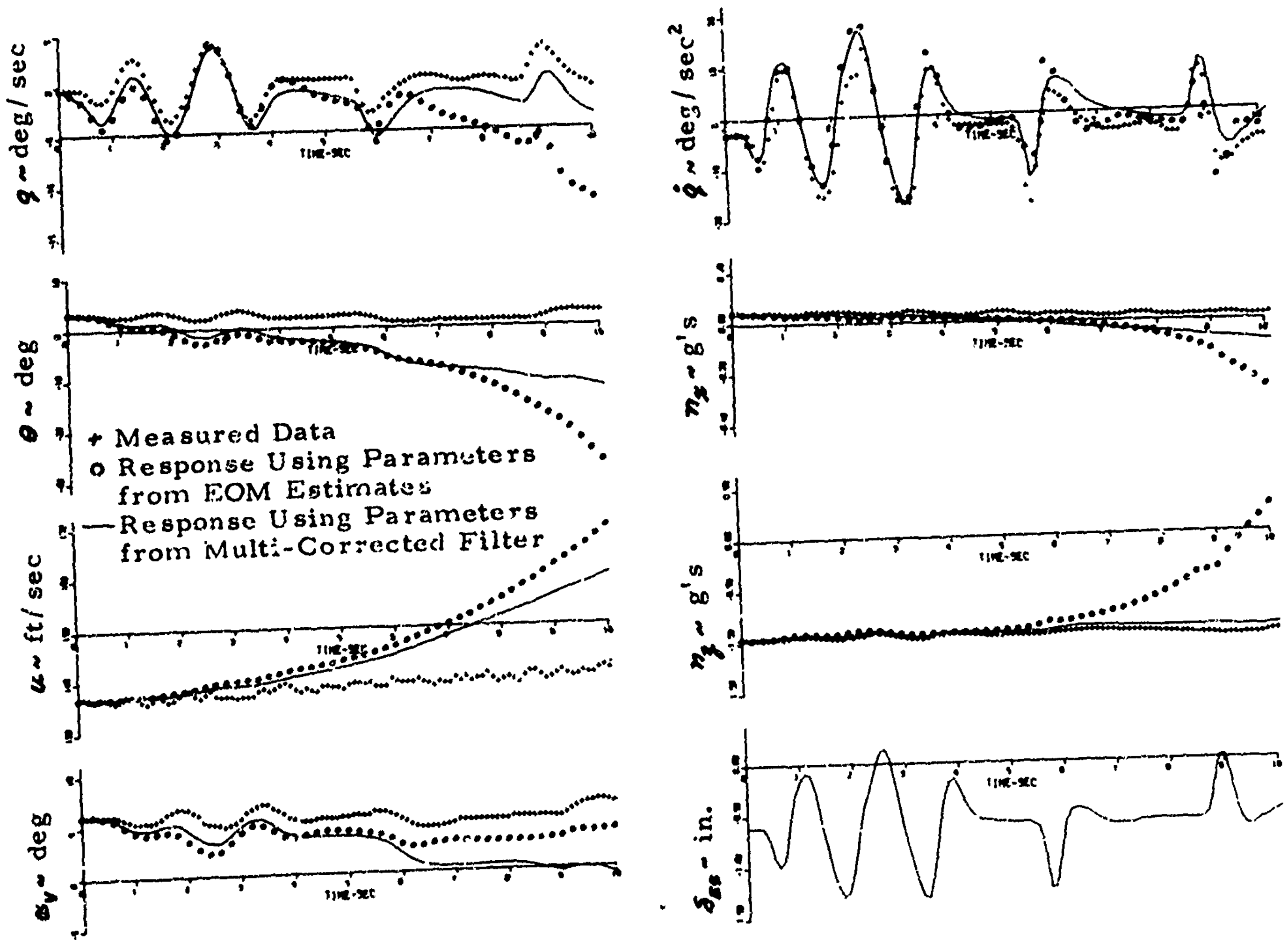

Figure 7-14 Transient Response Matching to Flight Data 2F197, E. O. M. 23 vs. 13 Parameter Model

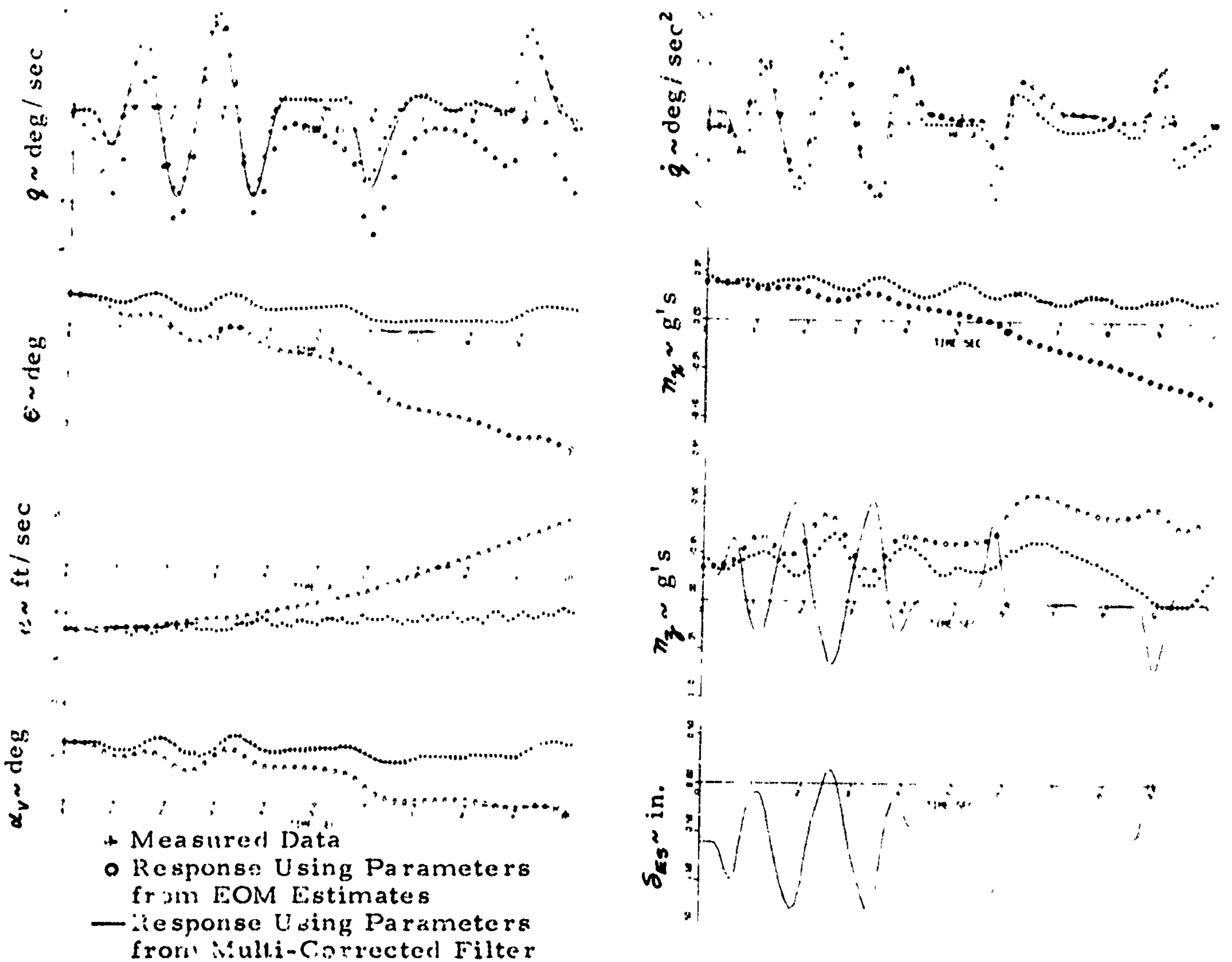

Figure 7-15 Transient Response Matching to Flight Data 2F197, $F_{10}(2)$ Without Acceleration Measurements

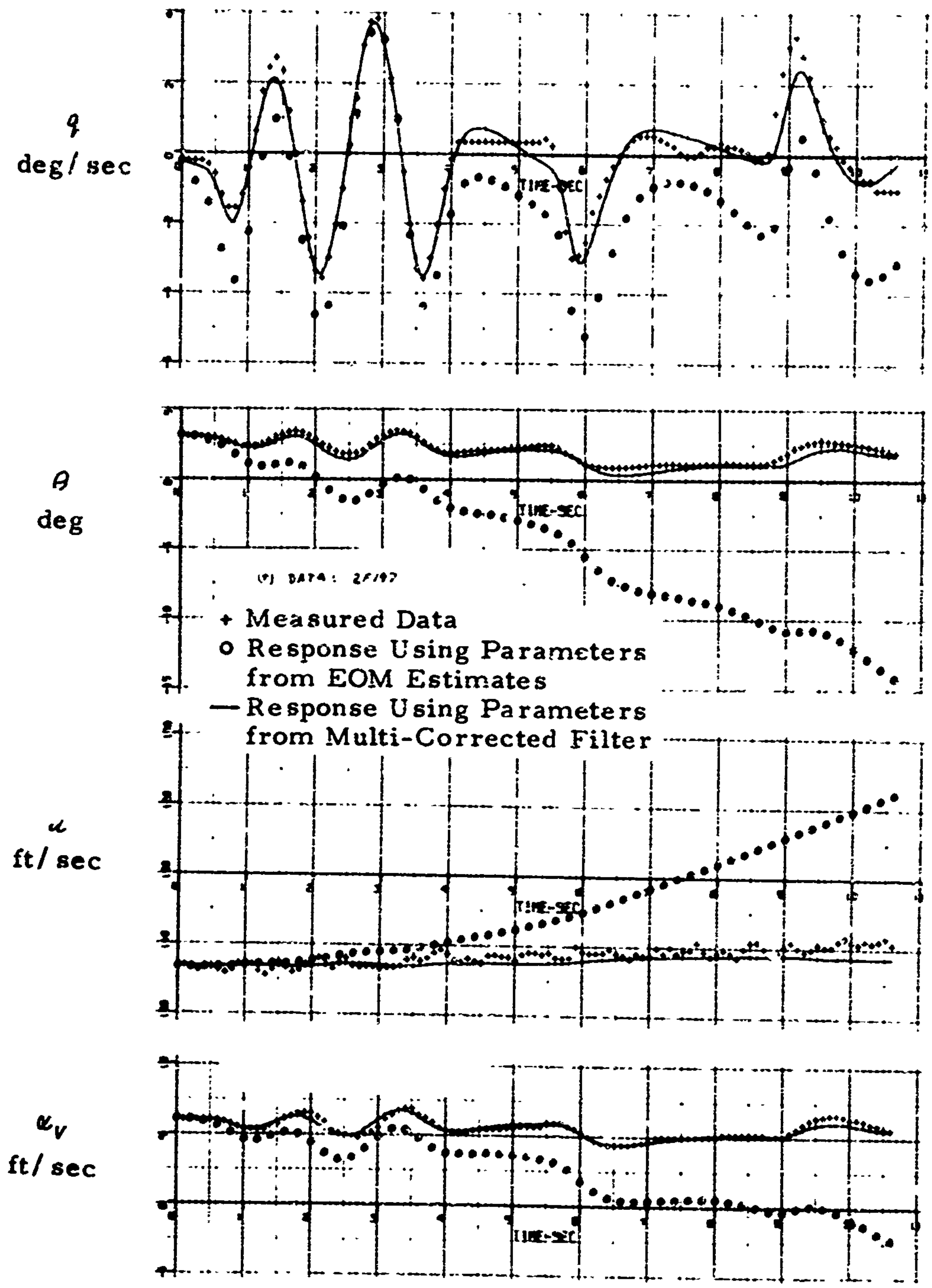

Figure 7-16 Transient Response Matching to Flight Data 2F197, $F_{10}(2)$ With Acceleration Measurements

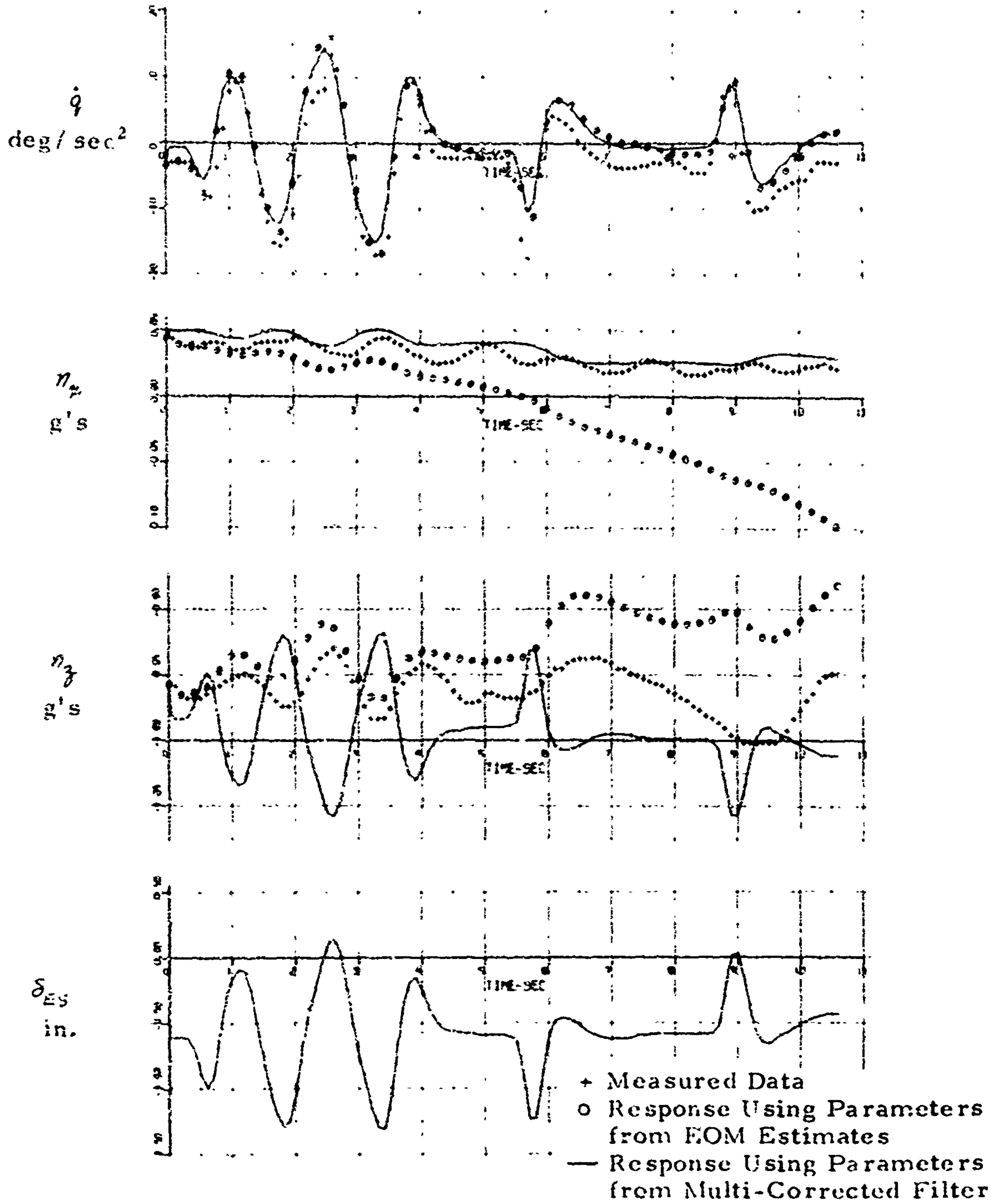

Figure 7-16 (continued)

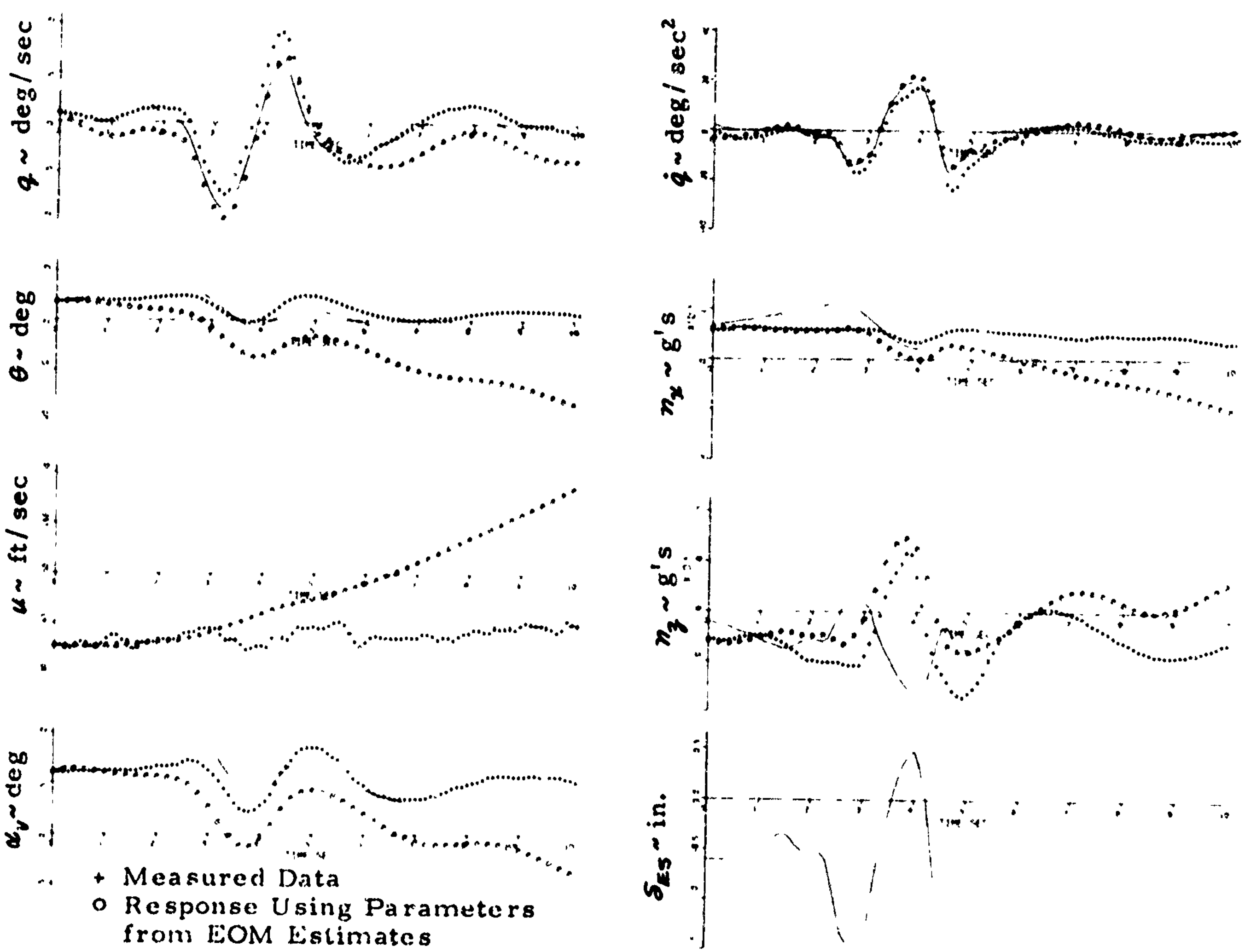

Figure 7-17 Transient Response Matching to Flight Data 2F203, $F_{10}(2)$ With Acceleration Measurements

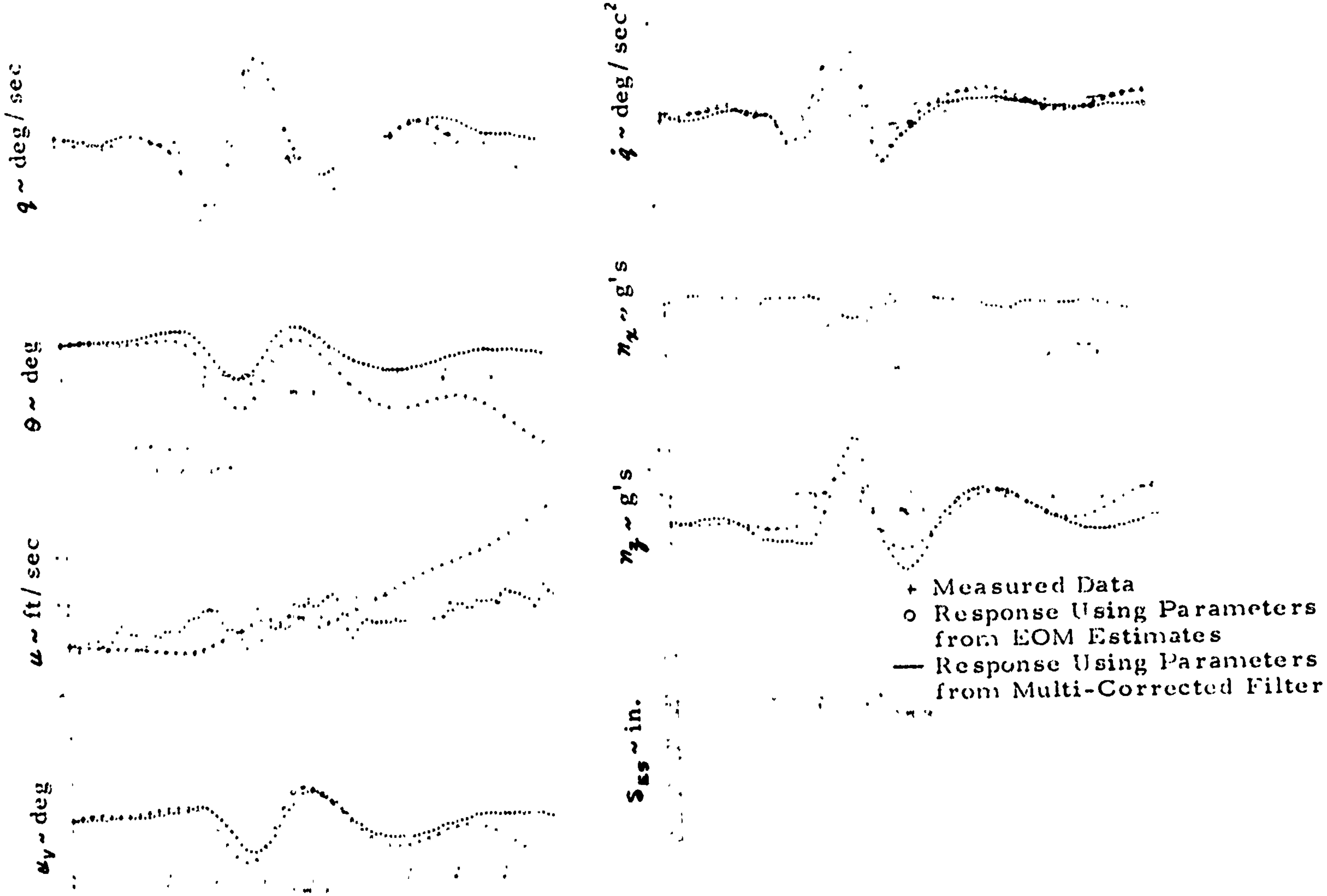

Figure 7-18 Transient Response Matching to Flight Data 2F203, Parameter Estimate from 2F197

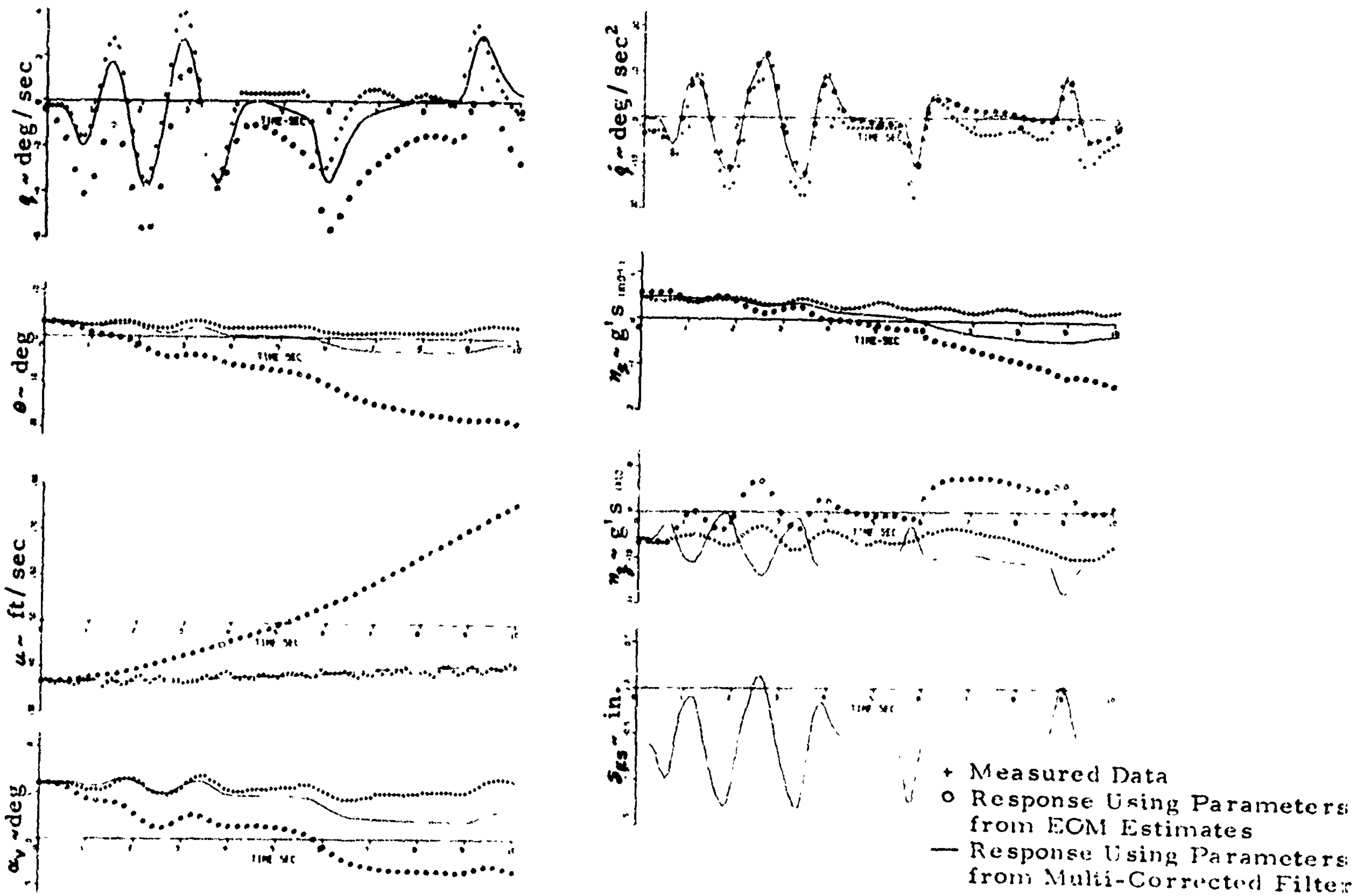

Figure 7-19 Transient Response Matching to Flight Data 2F197, Parameter Estimates from 2F203

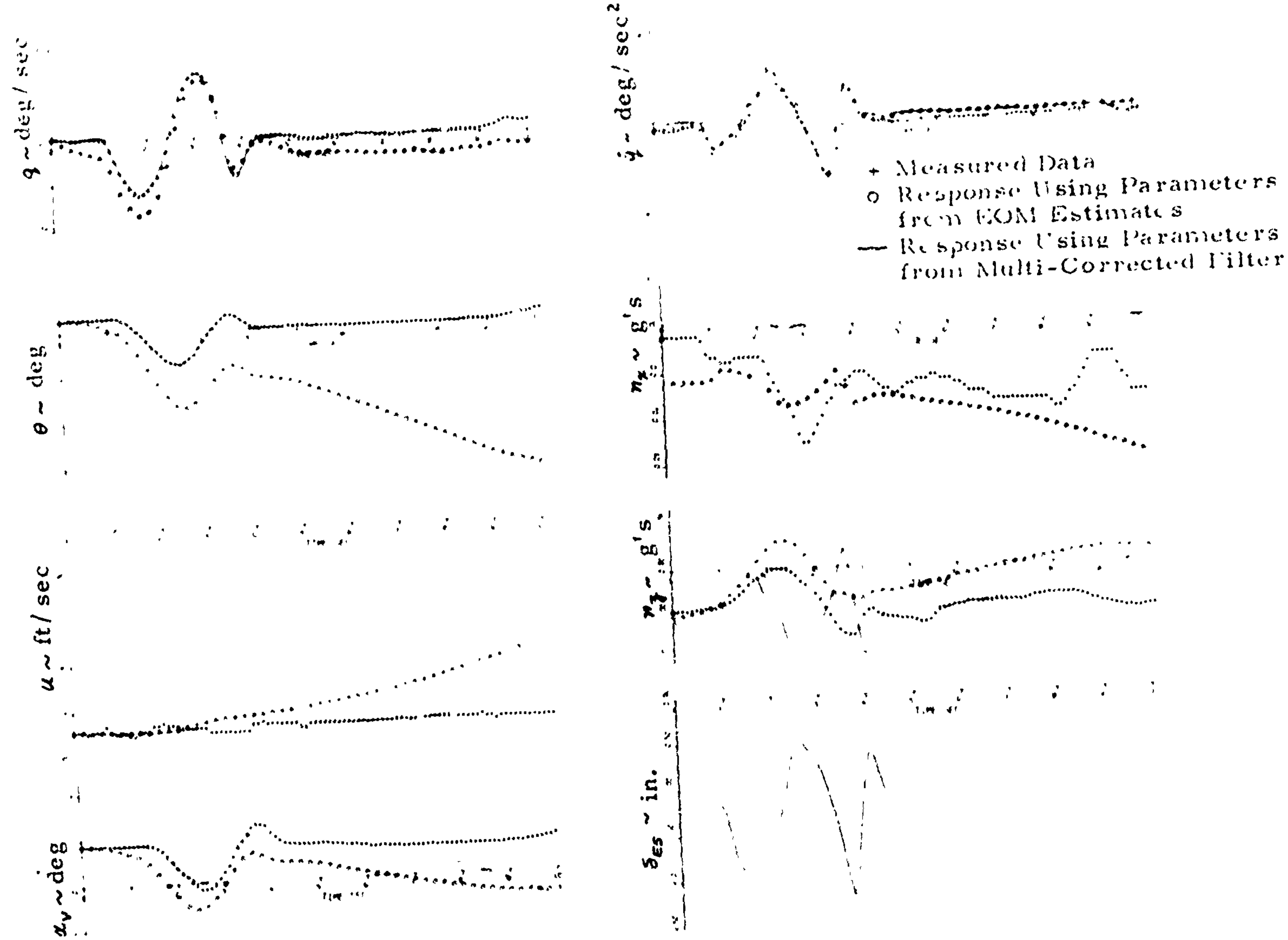

Figure 7-20 Transient Response Matching to Flight Data 2F198, $F_{10}^{(1)}$

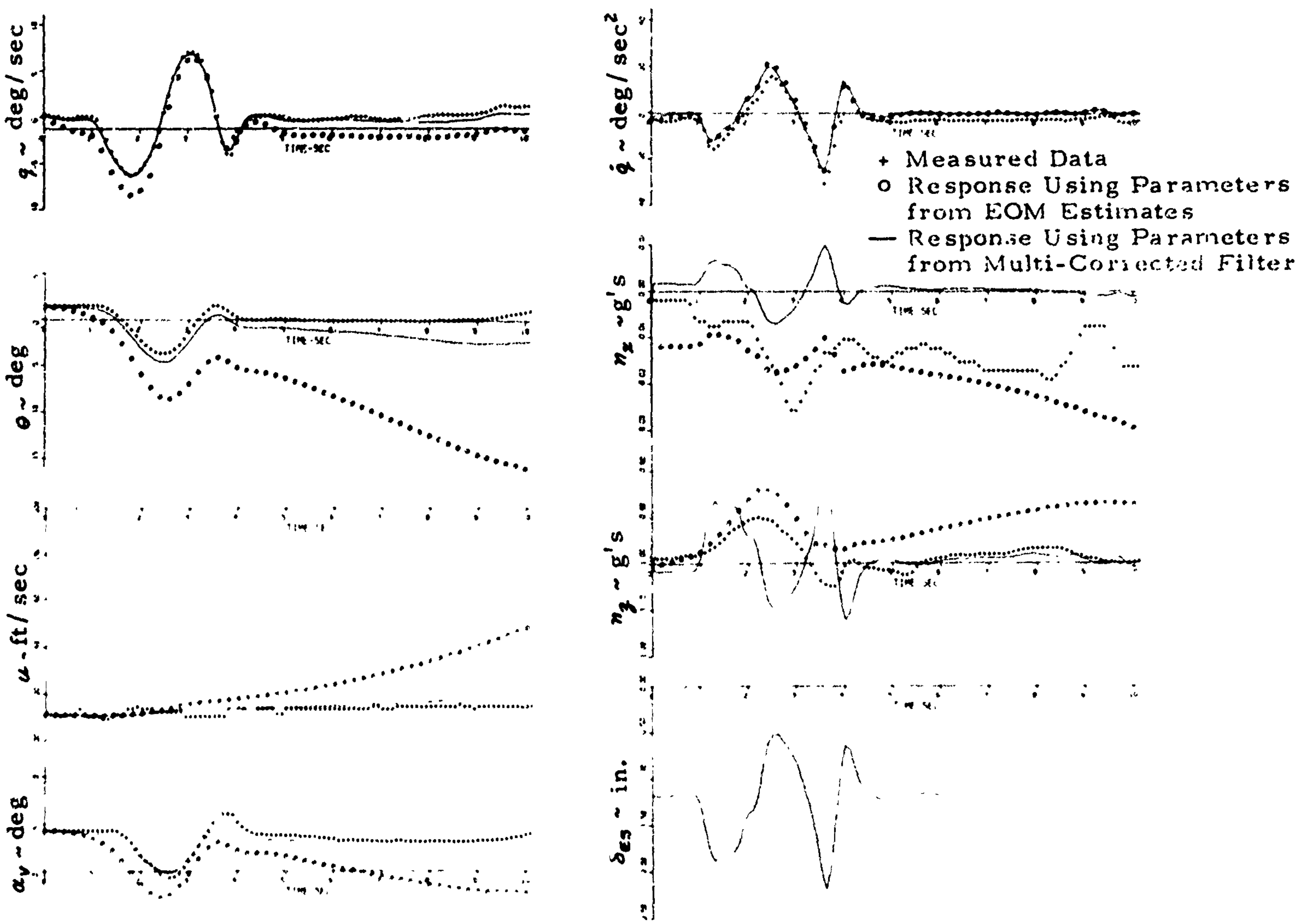

Figure 7-21 Transient Response Measurement to Flight Data 2F198, $F_{CR}(1)$

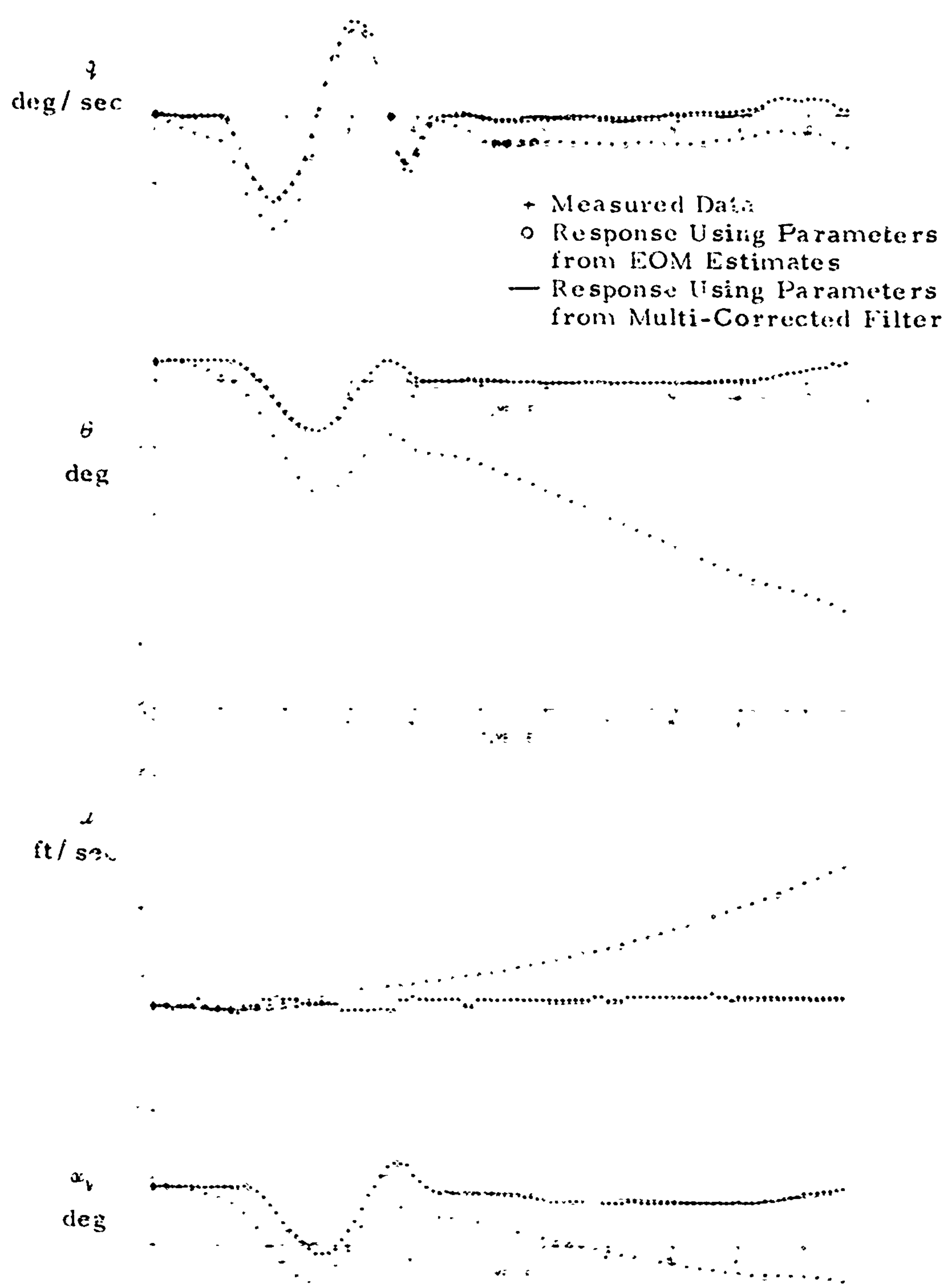

Figure 7-22 Transient Response Measurement to Flight Data 2F198, $F_1(1)$

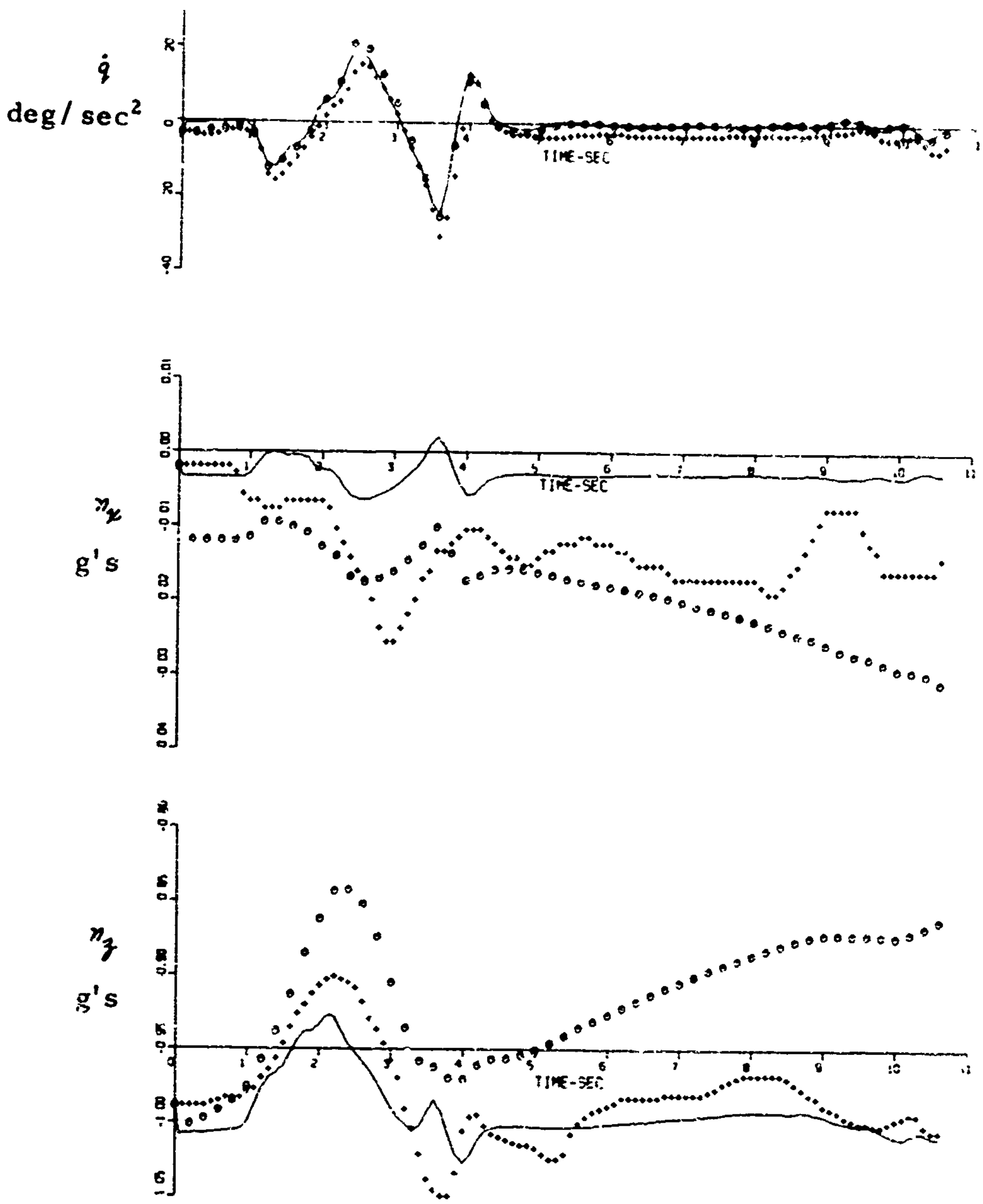

Figure 7-22 (continued)

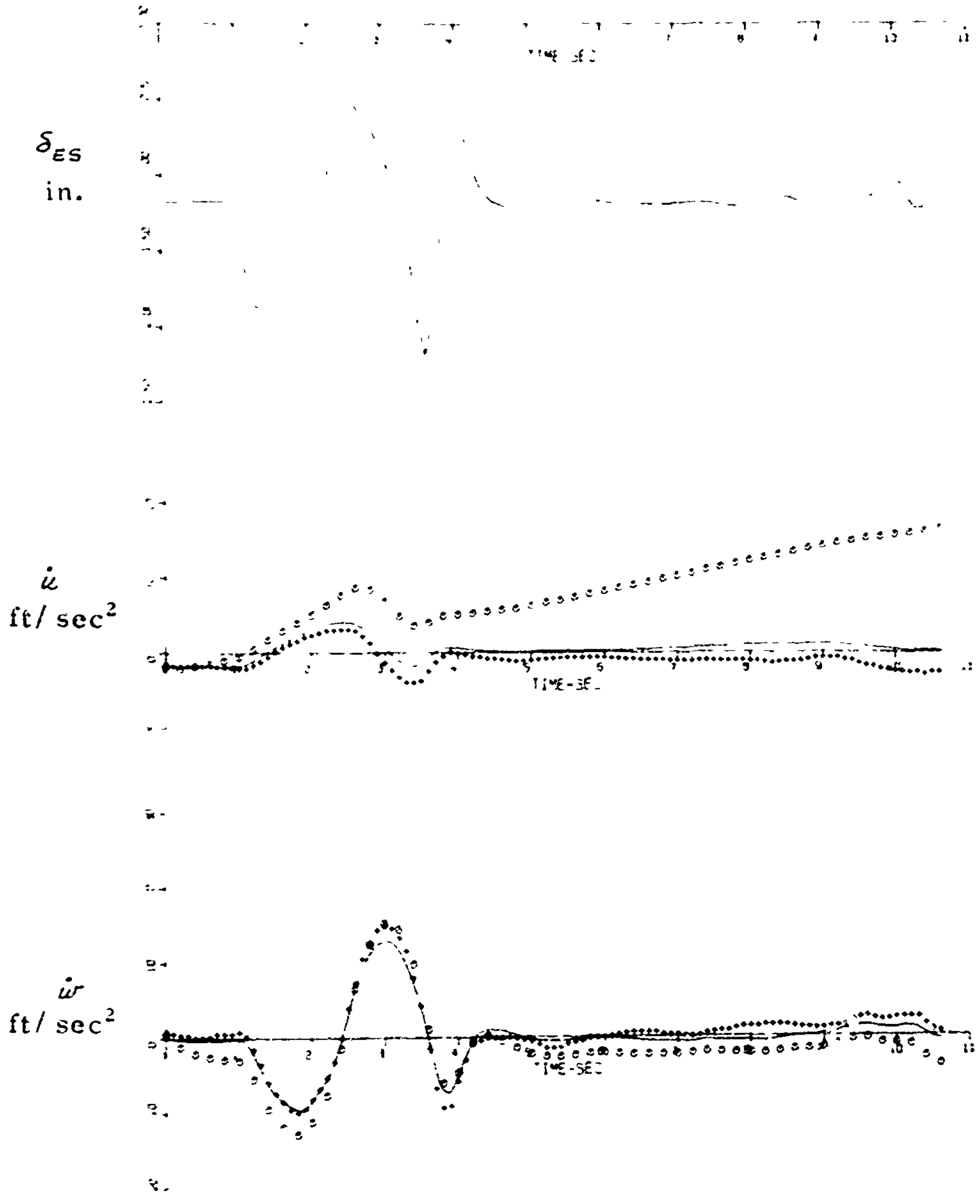

Figure 7-22 (continued)

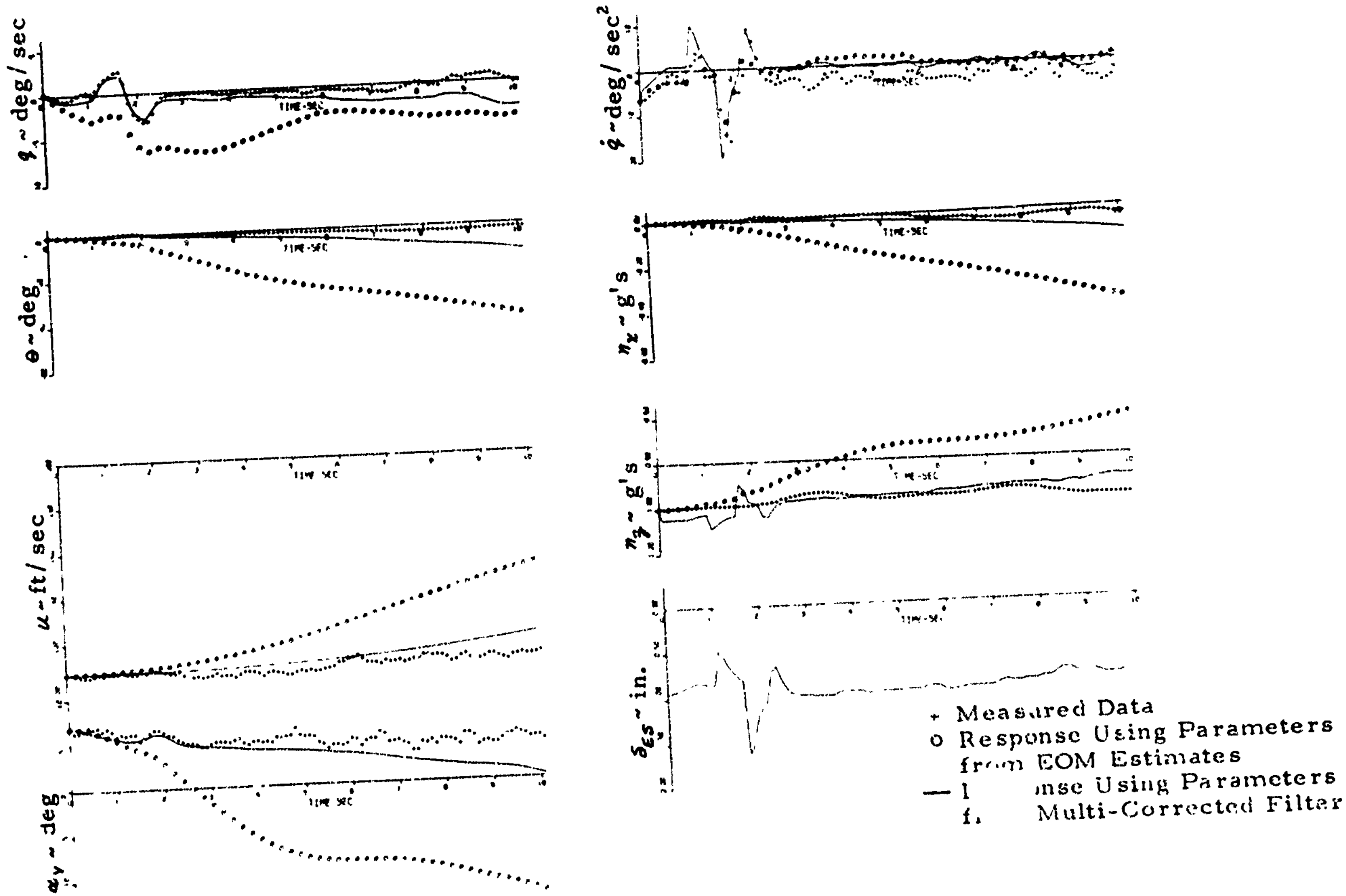

Figure 7-23 Transient Response Measurement to Flight Data 2F195, F_{10}(1)

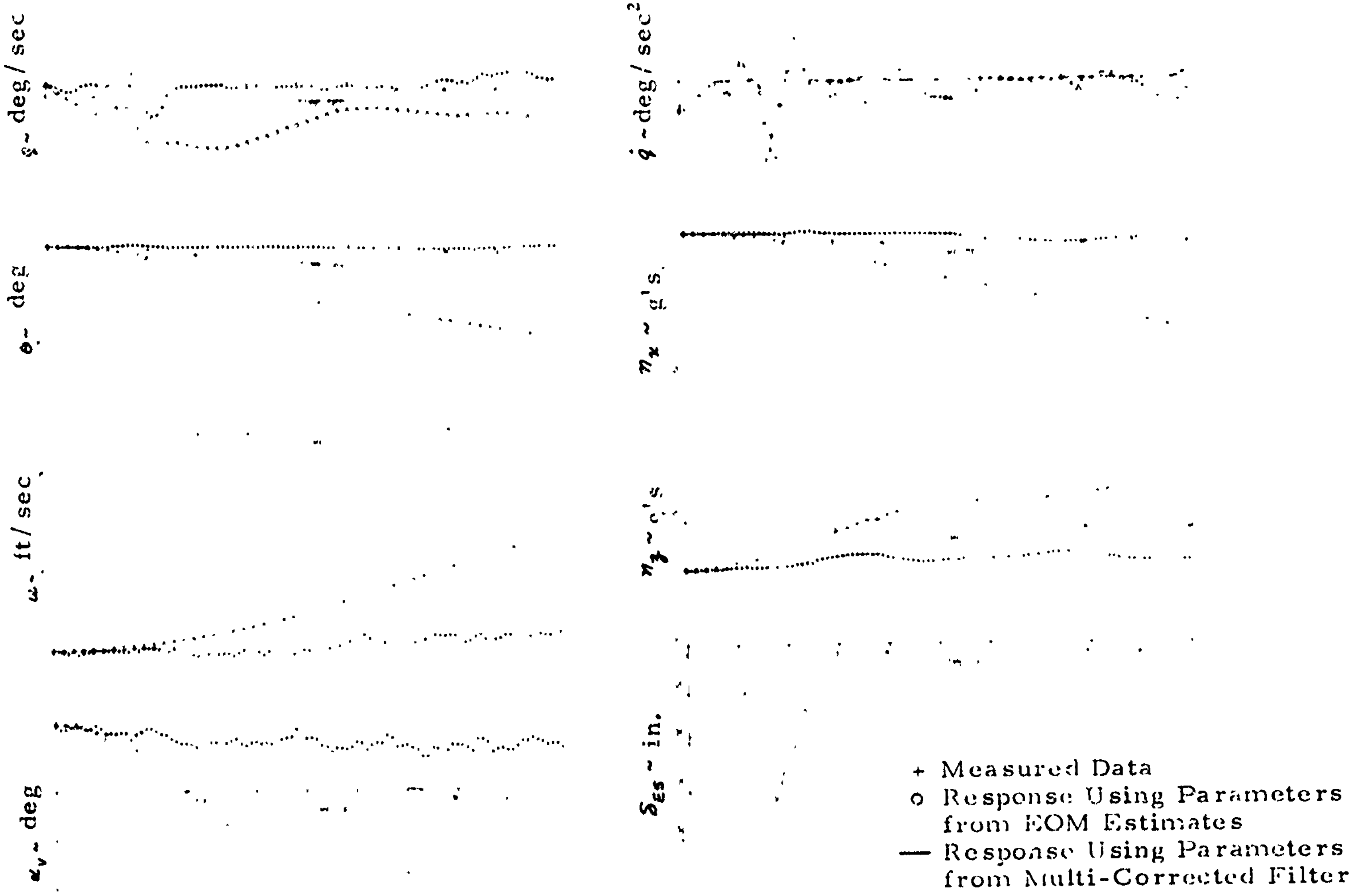

Figure 7-24 Transient Response Measurement to Flight Data 2F195, $F_1(1)$

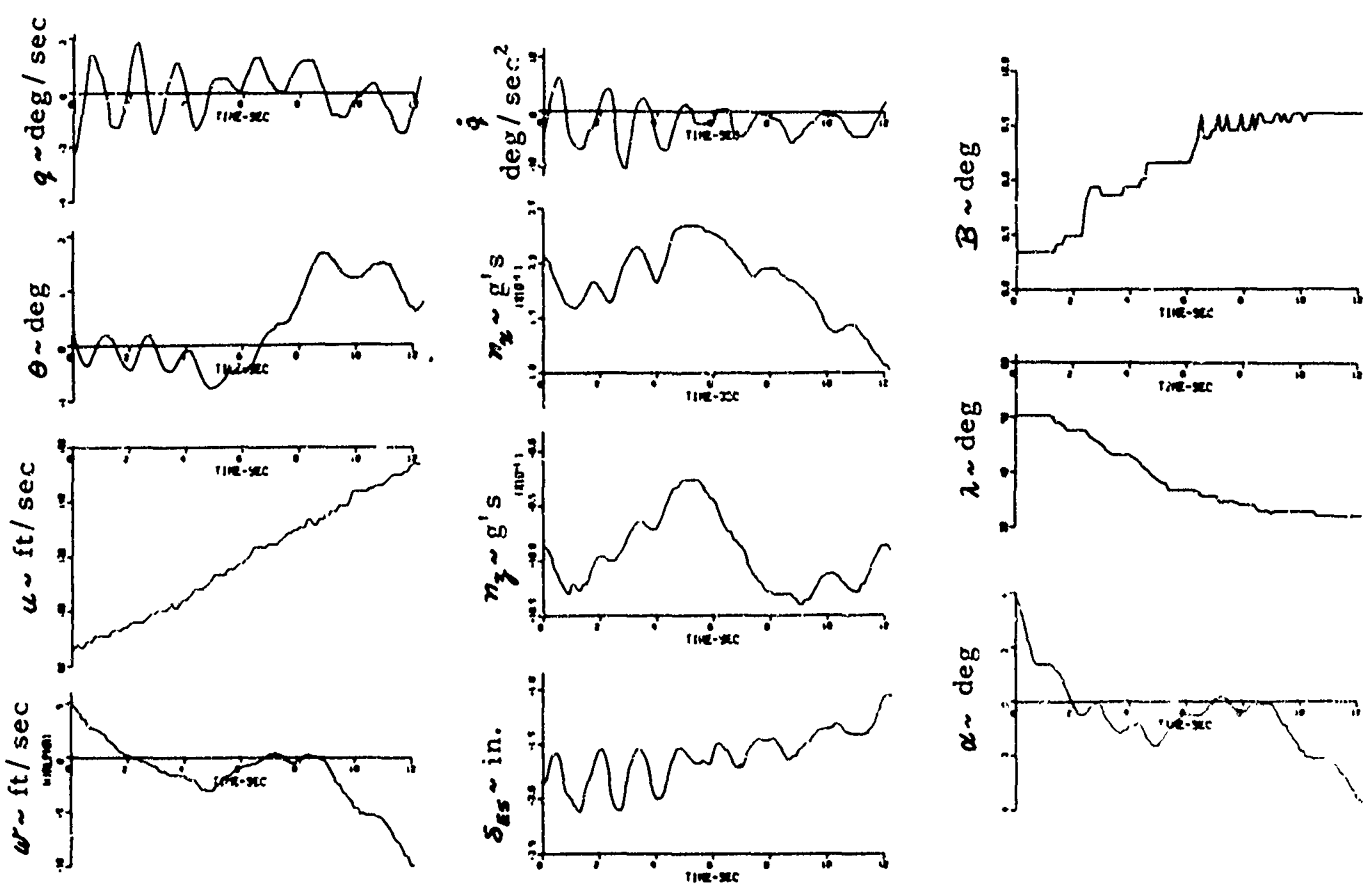

Figure 7-25 Slow Transition Flight Data 2F197

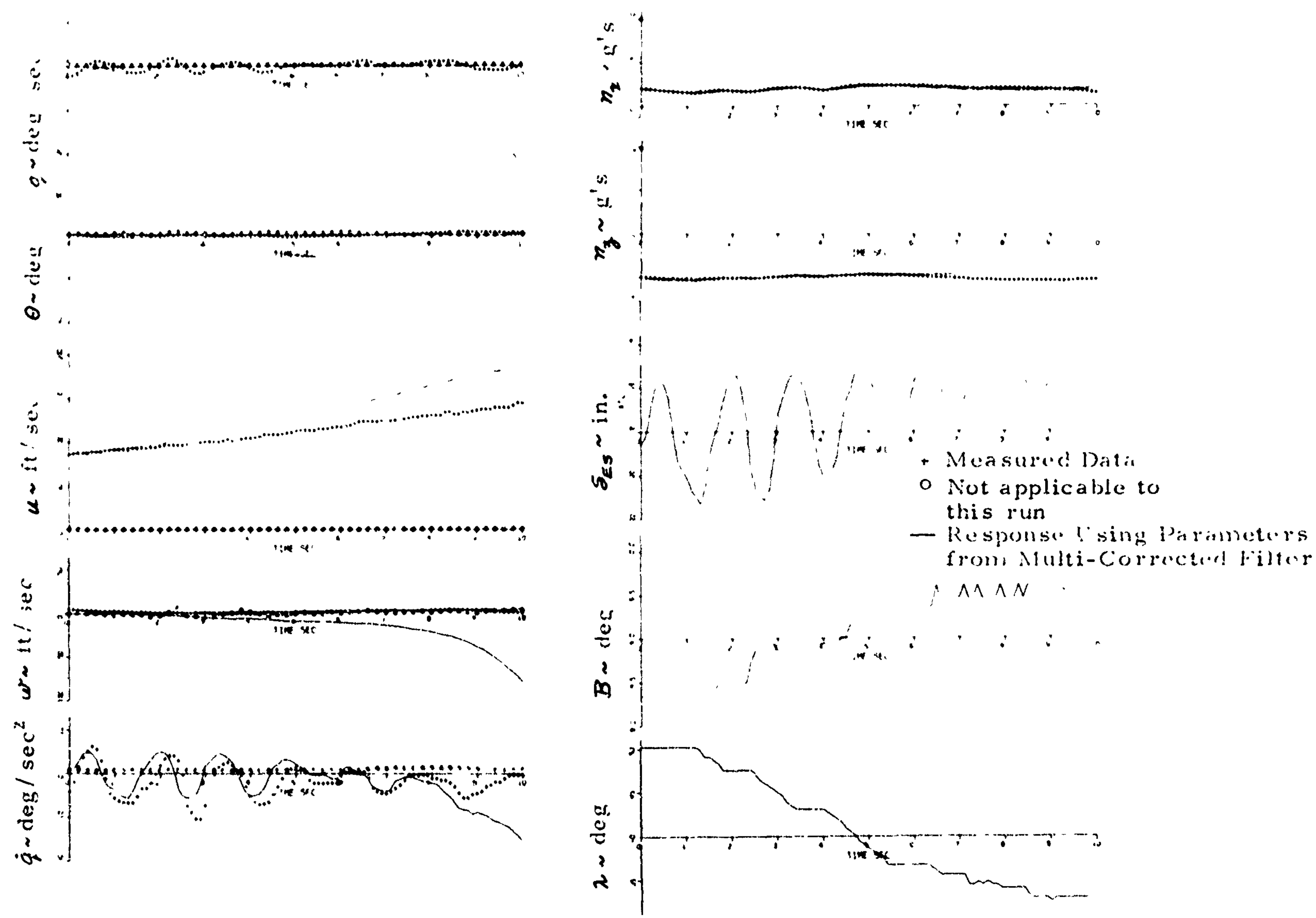

Figure 7-26a Transient Response Measurement to Flight Data 2F197 in Transition

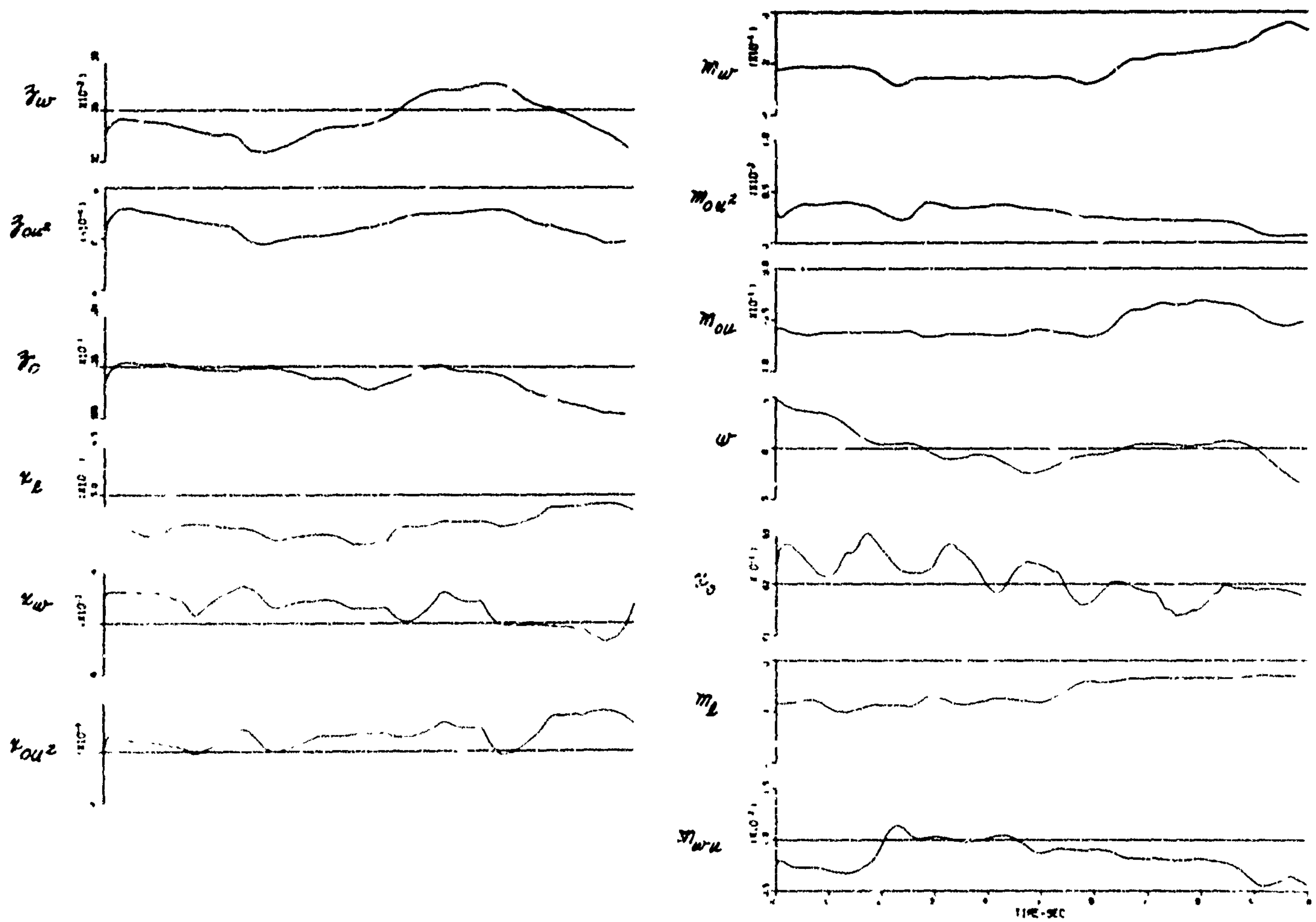

Figure 7-26b Selected Filter Estimates, Flight Data 2F197 in Transition

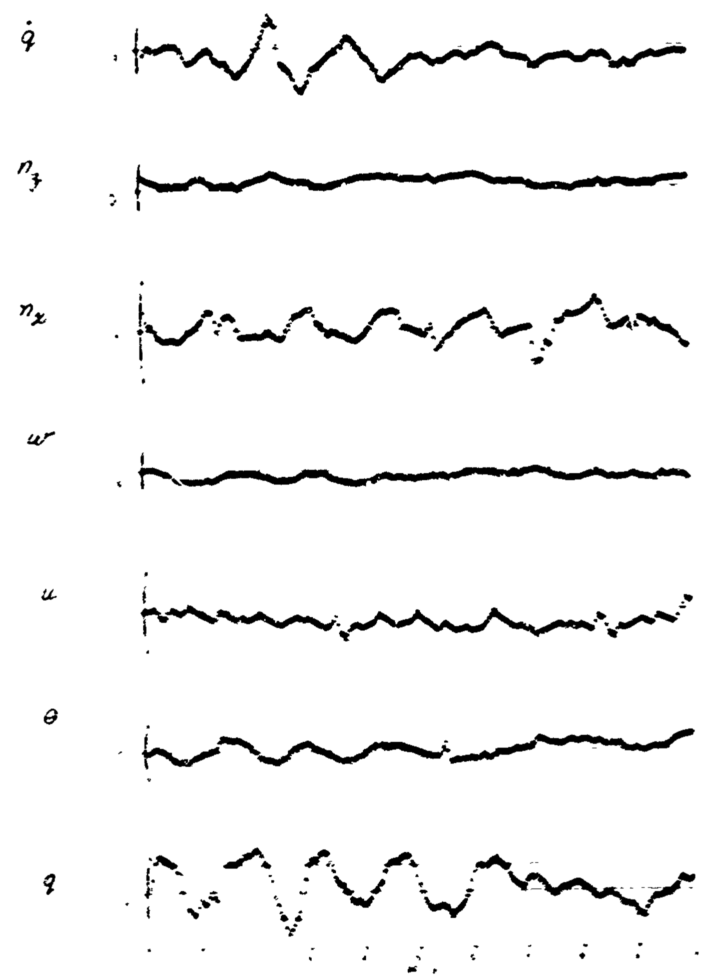

Figure 7-26c Residual Sequences, Flight Data 2F197 in Transition

Table 7-1: Linear Kalman Run on Data #55 Using Equations-of-Motion Method as Initial Estimator

$\lambda = 75°$
$\theta_{trim} \approx 0°$

(i) Full Scale Value
(ii) Linear Aero.
(iii) Linearized Kinematic

PARAMETER	GLOBAL VALUE	EQUATIONS OF MOTION	KALMAN NO ACCEL.	PDMT (APPROX.)
M_u	.0275	.00111	.00856	.027
M_w	.0175	-.00014	-.00156	.016
M_q	-4.6*	-.0378	-1.81	NA
M_δ	.461	-.0199	.312	NA
M_β	.0209	.00322	-.0174	NA
X_o				
X_u	-.230	-.222	-.155	-.22
X_w	-.0534	.152	.028	NA
X_δ	.300	.667	-.918	NA
X_β	.500	-.443	-.529	NA
Z_o				
Z_u	-.0273	-.0398	.0234	-.036
Z_w	.1468*	.0745	.0312	-.027
Z_δ	.07825	.292	.7104	NA
Z_β	-2.00	-.248	.0231	NA

* approximate value
NA: not available

Table 7-2: Linear Kalman Run on Data #55 Using Global Values as Initial Estimates

$\lambda = 75°$ (i) Full Scale Value
$\theta_{trim} \approx 0°$ (ii) Linear Aero (iii) Linearized Kinematic

PARAMETERS	GLOBAL	PDMT (APPROX.)	KALMAN NO ACCEL.
M_u	.0275	.027	.0256
M_w	.0175	.016	.01405
M_q	-4.6*		-4.0516
M_B	.0209		.0184
$M_{\delta_{es}}$	.461		.6341
X_u	-.230	-.22	-.3395
X_w	-.0053		-.04975
X_B	.500		-1.0238
$X_{\delta_{es}}$	.300		-1.2284
Z_u	-.0273	-.036	.0230
Z_w	.1468*	-.027	.01184
Z_B	-2.00		.07375
$Z_{\delta_{es}}$	.0783		.550

* approximate value

TABLE 7-3

Scale Factors for Converting
Model Values to X-22A Values
K = .1453

X-22A =	Scale Factor X.	Model
$M_0 \begin{pmatrix} 1 \\ u \\ u^2 \\ u^3 \end{pmatrix}$	$\begin{matrix} K \\ K^{1.5} \\ K^{2.0} \\ K^{2.5} \end{matrix}$	$M_0 \begin{pmatrix} 1 \\ u \\ u^2 \\ u^3 \end{pmatrix}$
$M_w \begin{pmatrix} 1 \\ u \\ u^2 \\ u^3 \end{pmatrix}$	$\begin{matrix} K^{1.5} \\ K^{2.0} \\ K^{2.5} \\ K^{3.0} \end{matrix}$	$M_w \begin{pmatrix} 1 \\ u \\ u^2 \\ u^3 \end{pmatrix}$
$M_q \begin{pmatrix} 1 \\ u \\ u^2 \\ u^3 \end{pmatrix}$	$\begin{matrix} K^{0.5} \\ K^{1.0} \\ K^{1.5} \\ K^{2.0} \end{matrix}$	$M_q \begin{pmatrix} 1 \\ u \\ u^2 \\ u^3 \end{pmatrix}$
$M_\delta, M_\beta, M_\lambda \begin{pmatrix} 1 \\ u \\ u^2 \\ u^3 \end{pmatrix}$	$\begin{matrix} K \\ K^{1.5} \\ K^{2.0} \\ K^{2.5} \end{matrix}$	$M_\delta, M_\beta, M_\lambda \begin{pmatrix} 1 \\ u \\ u^2 \\ u^3 \end{pmatrix}$
$\begin{matrix} X_0, Z_0 \\ X_\delta, Z_\delta \\ X_\beta, Z_\beta \\ X_\lambda, Z_\lambda \end{matrix} \begin{pmatrix} 1 \\ u \\ u^2 \\ u^3 \end{pmatrix}$	$\begin{matrix} K^0 \\ K^{0.5} \\ K^{1.0} \\ K^{1.5} \end{matrix}$	$\begin{matrix} X_0, Z_0 \\ X_\delta, Z_\delta \\ X_\beta, Z_\beta \\ X_\lambda, Z_\lambda \end{matrix} \begin{pmatrix} 1 \\ u \\ u^2 \\ u^3 \end{pmatrix}$
$X_w, Z_w \begin{pmatrix} 1 \\ u \\ u^2 \\ u^3 \end{pmatrix}$	$\begin{matrix} K^{0.5} \\ K^{1.0} \\ K^{1.5} \\ K^{2.0} \end{matrix}$	$X_w, Z_w \begin{pmatrix} 1 \\ u \\ u^2 \\ u^3 \end{pmatrix}$

TABLE 7-4

Flight Conditions and Reference Values of Princeton Data Runs

PRINCETON DATA ANALYZED BY NONLINEAR PROGRAM

RUN NO.	DUCT INCIDENCE λ (DEG)	$\Delta\delta_{es}$ DOUBLET INPUT (IN.)	ΔB STEP INPUT (DEG)	APPROXIMATE TRIM ATTITUDE Θ_o (DEG)	APPROXIMATE TRIM SPEED u_o (FPS)	DATA LENGTH (SEC)
154	45	.25	.15	0	39	7.0
157		-.25	.15	0	39	7.6
55	75	.5	.30	0	17	10.0
58		-.5	.30	0	17	10.0

REF. CONDITIONS

λ (DEG)	q_R	θ_R	u_R	w_R	$\Delta\delta_{es_R}$	ΔB_R
45	0	0	39 ft/sec	0	0	-.02 deg
75	0	0	17.5 ft/sec	0	0	-.05 deg

TABLE 7-5

Noise Levels for Princeton Data Runs

NOISE MODELS

MEASUREMENT NOISE FOR $\lambda = 45°$ and 75°

MOTION VARIABLES	MEASUREMENT NOISE STANDARD DEVIATION
q	.25 deg/sec
θ	.15 deg
u	.10 deg
w	.15 deg
n_x	.0075g
n_z	.0075g
$\dot{q}$	1.5 deg/sec^2

PROCESS NOISE MODEL

PROCESS NOISE STAND. DEV. σ	$\lambda = 45°$ No. 154 and 157		$\lambda = 75°$ No. 55 and 58	
	COMPENSATION FOR X-FORCE EQUATION	10% OF AERO FORCES AND MOMENT	COMPENSATION FOR X-FORCE EQUATIONS	10% OF AERO FORCES AND MOMENT
$\sigma_{\dot{q}}$	0	.4 deg/sec^2	0	.4 deg/sec^2
$\sigma_{\dot{u}}$	.05 ft/sec^2	.1 ft/sec^2	.20 ft/sec^2	.2 ft/sec
$\sigma_{\dot{w}}$	0	3.22 ft/sec^2	0	3.22 ft/sec^2

TABLE 7-6

Parameter Estimation From Nonlinear Program for

Princeton Data No. 154

$\lambda = 45°$

$\theta_{trim} \approx 0°$

(i) Linear Aero

(ii) Full Scale Value

PARAMETER	GLOBAL VALUE	EQUATIONS OF MOTION			MULTI-CORRECTED FILTER/FIXED PT. SMOOTHER			
		PARA. EST.	σ_{EQ}	σ_{CB}	ACCEL., Q AND START UP [1]	ACCEL., Q [2]	ACCEL. [3]	NO ACCEL.
M_u	-.036	-.00342	.000391	.0037	-.00680	-.00751	-.00904	-.0119
M_w	-.00644	-.00316	.00188	.00029	-.00736	-.00652	-.00747	-.0081
M_q	-.644	-.1777	.0442	.07	-1.262	-1.132	-1.160	-1.077
M_δ	.500	-.0278	.00803	.0058	.184	.197	.206	.280
M_β	.043	.0211	.014	.01	.0527	.0570	.0888	.208
X_o								
X_u	-.190	-.274	.0204	.05	-.431	-.358	-.496	-.530
X_w	-.0675	-.0149	.0098	.049	-.115	-.0695	-.128	-.122
X_δ	3.06	-1.111	.304	.751	1.892	.721	1.594	3.443
X_β	.727	-.506	.734	2.156	-1.028	-.0198	.256	.949
Z_o								
Z_u	-.180	.2998	.0185	.072	.361	.221	.392	.226
Z_w	-.413	.2178	.00893	.072	.265	.216	.271	.139
Z_δ	.900	.4778	.276	1.01	.826	1.477	.625	.966
Z_β	-1.80	-1.793	.665	2.44	-1.120	-1.848	-2.28	-4.46

1. $F_{CR}(1)$
2. $F_1(1)$
3. $F_{1v}(1)$

TABLE 7-7

Parameter Estimation From Nonlinear Program for

Princeton Dat No. 154 and No. 157

(i) Full Scale Value
(ii) Linear Aero.

$\dot{\lambda} = 45°$
$\theta_{trim} \approx 0°$

PARAMETER	GLOBAL VALUE	NO. 154			NO. 157	
		EQUATIONS OF MOTION	ACCEL., Q [1]	ACCEL., Q AND START UP [2]	EQUATIONS OF MOTION	ACCEL., Q [1]
M_u	-.036	-.00342	-.00751	-.00680	-.00729	-.0103
M_w	-.00644	-.00316	-.00652	-.00736	-.00279	-.00461
M_q	-.644	-.1777	-1.132	-1.262	-.154	-.806
M_δ	.500	-.0278	.197	.184	-.00165	.262
M_β	.043	.0211	.0570	.0527	.0497	.114
X_0						
X_u	-.19	-.274	-.358	-.431	-.334	-.410
X_w	-.0675	-.0149	-.0695	-.115	-.00576	-.010
X_δ	3.00	-1.111	.721	1.892	-.3143	3.407
X_β	.727	-.506	-.0198	-1.028	-.2301	.609
Z_0						
Z_u	-.180	.2998	.221	.361	.3567	.90
Z_w	-.413	.2178	.216	.265	.1562	.173
Z_δ	.900	.4778	1.477	.826	-.3122	.826
Z_β	-1.80	-1.793	-1.843	-1.120	-1.922	-1.744

1. $F_1'(1)$
2. $F_{CR}(1)$

TABLE 7-8

Parameter Estimation From Nonlinear Program for

Princeton Data No. 55 and No. 58

$\lambda = 75°$

$\theta_{r,m} \approx 0°$

(i) Full Scale Value
(ii) Linear Aero.

PARAMETER	GLOBAL VALUE	NO. 55				NO. 58
		EQUATIONS OF MOTION	MULTI-CORRECTED FILTER/FIXED PT. SMOOTHER			EQUATIONS OF MOTION
			NO ACCEL. [1]	ACCEL. [1]	ACCEL. & Q [2]	
M_u	0.0275	-.00952	.00982	.00753	.00778	-.00231
M_w	0.0175	.00033	-.00437	-.00371	-.00353	-.00044
M_q	-4.6**	.0194	-1.865	-1.415	-1.351	.1698
M_δ	.461	.0216	.314	.195	.195	.00384
M_β	.0209	.00157	.0733	.0199	.0071	.00317
X_0						
X_u	-.230	-.223	-.0995	-.0975	-.160	-.201
X_w	-.0534	.144	.104	.151	.142	.159
X_δ	.300	-.507	1.568	.0302	.117	-.673
X_β	.500	-.465	.891	.5684	-.116	-.995
Z_0						
Z_u	-.0273	-.0657	-.0342	-.00097	-.0425	-.0732
Z_w	.1468	.0892	.0055	.0922	.0712	.0822
Z_δ	.07825	.196	4.83	1.971	1.0067	-.0254
Z_β	-2.00	.120	1.56	.6755	.547	.0983

** with feedback

1. F_{10} (1)

2. F_1 (1)

TABLE 7-9

COMPARISON OF THE EFFECTS OF LINEAR AND NONLINEAR
KINEMATIC COUPLING FOR NO. 55

$\lambda = 75°$ (i) Full Scale Value

$\theta_{trim} \approx 0°$ (ii) Linear Aero

PARAMETER	GLOBAL VALUE	LINEARIZED KINEMATIC		NONLINEAR KINEMATIC			
		EQUATIONS OF MOTION	KALMAN NO ACCEL.	EQUATIONS OF MOTION	MULTI-CORRECTED FILTER/FIXED PT. SMOOTHER		
					NO ACCEL.[1]	ACCEL.[1]	ACCEL. Q[2]
M_u	.0275	.00111	.00856	-.000952	.00982	.00753	.00778
M_w	.0175	-.00014	-.00156	.00033	-.00437	-.00371	-.00353
M_q	-4.6 *	-.0378	-1.81	.0194	-1.865	-1.415	-1.351
M_δ	.461	-.0199	.312	.0216	.314	.195	.195
M_β	.0209	.00322	-.0174	.00157	.0733	.0199	.0071
X_0							
X_u	-.230	-.222	-.155	-.223	-.0975	-.0975	-.160
X_w	-.0534	.152	.028	.144	.104	.151	.142
X_δ	.300	.667	-.918	-.507	1.568	.0302	.117
X_β	.500	-.443	-.529	-.465	.891	.568	-.116
Z_0							
Z_u	-.0273	-.0398	.0234	-.0657	-.0342	-.00097	-.0425
Z_w	.1468	.0745	.0312	.0892	.0055	.0922	.0712
Z_δ	.07825	.292	.7104	.196	4.83	1.971	1.0067
Z_β	-2.00	-.248	.0231	.120	1.56	.6755	.547

*with feedback

1 $F_{10}(1)$

2 F_1 (1)

TABLE 7-10

Flight Conditions for X-22A Flights

A. Fixed-Duct Operating Points

Case 1:	2F195, Time: 38:15	MPE II Flight Test
	1. 2200 ft 2. $\lambda \approx 45°$ 3. 2150 lb F.R.	VS Card #27
Case 2:	2F197, Time: 44:30	MPE III Flight Test
	1. 5000 ft 2. $\lambda \approx 30°$ 3. 2000 lb F.R.	VS Card #38
Case 3:	2F203, Time: 37:00	MPE Phase III Flight Test
	1. Altitude: ? 2. $\lambda \approx 30°$ 3. 2100 lb F.R.	VS Card #37, no SAS
Case 4:	2F198, Time: 38:00	MPE Phase II Flight Test
	1. Altitude 2000 ft 2. $\lambda \approx 45°$ 3. 1900 lb F.R.	VS Card #27

B. Transition $45° \longrightarrow 30°$ @ $\dot{\lambda} \approx -1\ 1/2°/sec$

Case 1:	2F197, Time: 1:20:12	MPE Phase II Flight Test
	1. 850 lb F.R. 2. Altitude: ?	FBW
Case 2:	2F203, Time: 1:29:15	MPE Phase III Flight Test
	1. Altitude: ? 2. 600 lb F.R.	FBW
Case 3:	2F205, Time: 38:55	MPE Flight Test, Composite
	1. Altitude: ? 2. 1850 lb F.R.	FBW

TABLE 7-11

NOISE STATISTICS FROM FLIGHT RECORDS

MEASUREMENT NOISE		
SENSOR	STANDARD DEVIATION σ	
	WITHOUT Q	WITH Q
q	.22 deg/sec	.22 deg/sec
θ	.09 deg	.09 deg
u	2.6 ft/sec	2.6 ft/sec
α_V	.15 deg	.15 deg (1)
n_p	.012g	.011g
n_z	.05g	.03g
$\dot{q}$	2.3 deg/sec^2	2.26 deg/sec^2
w (3)	1.0 ft/sec	1.0 ft/sec

PROCESS NOISE (2)	
NOISE	VALUE
$\sigma_{\dot{q}}$	.4 deg/sec^2
$\sigma_{\dot{u}}$	.1 ft/sec^2
$\sigma_{\dot{w}}$	1.3 ft/sec^2

(1) .35° for 2F 195

(2) $\sigma \approx$ % RMS, e.g. $\sigma_{\dot{q}} \approx .1 \left[\frac{1}{N} \sum_{i=1}^{N} (\dot{q}_i)^2 \right]^{1/2}$

(3) Equivalent noise if α_V measurement is transformed to w measurement with σ_{α_V} = .15 deg

TABLE 7-12

Flight Conditions and Reference Values for X-22A Fixed-Duct Flight Data

FIXED DUCT OPERATING POINTS

FLIGHT	λ DEGREES	ALTITUDE - FT	FUEL REMAINING - LB	TIME IN FLIGHT	VS CARD NO.
2F197	≈30	5000	2000	44:30	38
2F203	≈30	?	2100	37:00	37
2F195	≈45	2200	2150	38:15	27
2F198	≈45	2000	1900	38:15	27

REFERENCE VALUES

FLIGHT	λ_r DEG	β_r DEG	δ_{ES_r} INCH	u_r FT/SEC	w_r FT/SEC	q_r DEG/SEC
2F197	30	≈2.8	-.6	135	14	0.0
2F203	30	≈2.8	-.6	135	14	0.0
2F195	49.7	≈3.6	-1.0	108	10	0.0
2F198	47.6	≈5.6	-1.0	108	10	0.0

TABLE 7-13

Previous Results Using Linear Kalman Program Using Recycling (Without Acceleration Measurements)

Parameter	Global Value	Flight 2F (197)		Flight 2F (203)	
		E.O.M. $w(\alpha_v)$	Linear Kalman* $w(\alpha_v)$	E.O.M. $w(\alpha_v)$	Linear Kalman* $w(\alpha_v)$
M_u	=-0.0042	-.01503	-.0074	-.00749	-.0255
M_w	-.008	-.01815	-.0174	-.0107	-.0202
M_q	-.624	-.5175	-1.785	-.267	-.839
M_δ	.505	.3483	.3447	.2836	.263
X_u	=-.155	-.1886	-.3382	-.0778	-.5905
X_w	.01	-.0443	.0745	-.0125	.112
X_δ	1.50	-.05904	-.239	-.899	-.444
Z_u	=-.218	-.1049	-.187	-.1836	-.907
Z_w	-.66	-.2573	-.161	-.3469	-.223
Z_δ	1.75	.252	.556	1.394	.431

* Recycling 3 times (F-F-F)

TABLE 7-14

Parameter Estimation From Nonlinear Kalman Without Acceleration Measurements With and Without Nonlinear Aerodynamics Data: 2F197 (i) α_γ (ii) $Q = 0$ (iii) $\lambda = 30°$

Parameter		Global* True Value Radians	Nonlinear Aero: 23 Parameters		Linear Aero: 13 Parameters	
			E.O.M.	Iterated Filter F_{10} (2)	E.O.M.	Iterated Filter F_{10} (2)
M_0	1	.50518	-39.3355	221.81	2.0346	2.1746
	u	-.00308	.58245	-3.196	-.015192	-.01576
	u^2	-6.2×10^{-6}	-.0021582	.0115104		
M_w	1	-.001747	.3790	-.6855	-.01819	-.021841
	u	-5.53×10^{-5}	-.0028365	.004765		
M_q	1	-.497	43.252	107.488	-.524796	-1.3821
	u	-.00103	-.31752	-.791478		
M_δ	1	.3275	-1.31203	-7.002	.34838	.3248
	u	.001167	.012172	.053079		
X_0	1	18.30	-121.82	-1149.15	19.4824	24.3466
	u	-.09167	1.90917	17.0607	-.13336	-.164108
	u^2	-.0003	-.00738	-.0632198		
X_w	1	.2211	2.8211	12.6279	.04779	.14253
	u	-.001587	-.019665	-.09462		
X_δ	1	-.778	-1.9562	26.8192	-.026871	.039519
	u	.0104	.0145965	-.20323		
Z_0	1	-32.17	87.716	1225.98	-14.659	-18.3101
	u	.910	-13.007	-18.2349	-.11997	-.09632
	u^2	-.007	.04656	.0661011		
Z_w	1	-.2939	-.822988	-2.68205	-.27205	.1181
	u	-.00287	.003772	.0215422		
Z_δ	1	-.3507	31.7097	97.3043	.18935	-3.4097
	u	.01667	-.22946	-.748971		

* Reference Values: u_0 = 130 fps, w_0 = 5.36 fps, q_0 = 0, δ_{es} = -0.637"

TABLE 7-15

Parameter Estimation From Nonlinear Kalman Without Acceleration Measurements With and Without Nonlinear Aerodynamics Data: 2F203 (i) α_v (ii) $Q = 0$ (iii) $\lambda = 30°$

Parameter		Global* True Value Radians	Nonlinear Aero: 23 Parameters E.O.M.	Nonlinear Aero: 23 Parameters Iterated Filter F_{10} (2)	Linear Aero: 13 Parameters E.O.M.	Linear Aero: 13 Parameters Iterated Filter F_{10} (2)
M_0	1	.50578	-37.056	-393.788	.97644	5.73274
	u	-.00308	.54556	5.8516	-.007544	-.0418785
	u^2	-6.2×10^{-6}	-.0020107	-.021735		
M_w	1	-.001747	.41310	.231278	-.01706	-.0172007
	u	-5.53×10^{-5}	-.0030704	-.001848		
M_q	1	-.497	13.9943	82.985	-.269699	-.827912
	u	-.00103	-.104744	-.61257		
M_δ	1	.3275	1.7233	-13.6617	.28355	.314784
	u	.001167	-.010472	.102515		
X_0	1	18.30	-194.33	505.698	19.9484	58.4284
	u	-.09167	2.9755	-7.1247	-.13284	-.416967
	u^2	-.0003	-.0112706	.02512		
X_w	1	.2211	-1.51809	2.18399	.040294	.0308756
	u	-.001587	.011318	-.0151183		
X_δ	1	-.778	-12.445	-44.743	-.431389	-.578513
	u	.0184	.087422	.310408		
Z_c	1	-32.17	577.836	3185.27	-6.57158	66.845
	u	.910	-8.6737	-47.120	-.17788	-.715661
	u^2	-.007	.030869	.172556		
Z_w	1	-.2939	-2.7769	2.0688	-.36346	-.242373
	u	-.00287	.0175188	-.013381		
Z_δ	1	-.3507	34.6815	-89.748	1.[illegible]969	-4.49796
	u	.01667	-.24500	.62825		

* Reference Values: u_0 = 130 fps, w_0 = 5.36 fps, q_0 = 0, δ_{es_0} = -.637"

TABLE 7-16

Parameter Estimate From Nonlinear Kalman Without Acceleration Measurements (Evaluated at u = 138 fps)

Parameter	Global Value	Flight Data 2F197		Flight Data 2F203	
		$F_{10}(2)$-23 Par.	$F_{10}(2)$-13 Par.	$F_{10}(2)$-23 Par.	$F_{10}(2)$-13 Par.
M_u	-0.0042	-.0191	-.01576	-.147	-.041878
M_w	-.008	-.0275	-.021841	-.02372	-.0172007
M_q	-.624	-1.736	-1.3821	-1.55	-.827912
M_δ	.505	.323	.3248	.4853	.314784
X_u	-.155	-0.388	-0.1641	-.1916	-.41697
X_w	.01	-.4301	.14253	.09799	.030876
X_δ	1.50	-1.2268	.039519	-1.907	-.578513
Z_u	-.218	0.009	-.09632	0.5004	-.71566
Z_w	-.66	.29095	.1181	.2218	-.24237
Z_δ	1.75	-6.0537	-3.4097	-3.049	-4.49796

TABLE 7-17

Parameter Estimation From Nonlinear Kalman

X-22A Data at $\lambda = 30°$ (i) α_V (ii) No Q (iii) Linear Aero. (iv) $10\ \sigma^2_{EM}$

Parameter	Global Values*	Test Data: 2F 197 - $F_{10}(2)$			Test Data: 2F 203 - $F_{10}(2)$		
		Equations of Motion	Nonlinear Kalman $F_{10}(2)$		Equations of Motion	Nonlinear Kalman $F_{10}(2)$	
			Using Accel. Meas.	Without Using Accel. Meas.		Using Accel. Meas.	Without Using Accel. Meas.
M_0	.580	2.0346	3.4634	2.175	.9764	5.163	5.733
M_u	-.0042	-.01519	-.02534	-.01576	-.00754	-.03773	-.041878
M_w	-.008	-.0182	-.02584	-.02184	-.01071	-.01466	-.0172007
M_q	-.624	-.5248	-1.2719	-1.3821	-.2697	-.9288	-.827912
M_δ	.505	.3485	.3142	.3248	.2834	.3079	.314784
M_β							
X_0	21.885	19.482	39.33	24.347	19.948	73.18	58.428
X_u	-.155	-.1334	-.2761	-.1641	-.1328	-.5243	-.41697
X_w	.01	.04779	.0742	.14253	.0403	.08139	.030876
X_q	1.50	-.0269	.01265	.039519	-.4314	.08294	-.578513
X_β							
Z_0	-2.12	-14.66	-6.831	-18.31	-6.572	97.694	66.85
Z_u	-.218	-.1191	-.18174	-.09632	-.1779	-.9395	-.71566
Z_w	-.66	-.2721	.0240	.1181	-.3635	-.200	-.24237
Z_δ	1.75	.1894	-3.011	-3.4097	1.2697	-3.194	-4.49796
Z_β							

* Nonperturbed, Radians.

TABLE 7-18

Comparison of Initial Variances [P (0)] For Different Start-Up Procedures

X-22A Data at $\lambda = 45°$

PARAMETER	TEST DATA: 2F 195			TEST DATA: 2F 198		
	E.O.M. ESTIMATE*	σ_{EM}	$\sqrt{20}\,\sigma'_{CE}$ **	E.O.M. ESTIMATE*	σ'_{EM}	σ_{CE}
M_0	-.0812	.0032	.0061	.00418	.0095	.0048
M_u	-.0061	.0012	.00029	-.00509	.00141	.0005
M_w	-.0067	.0017	.00032	-.0129	.00084	.00067
M_q	.0073	.167	.111	-.6777	.053	.106
M_δ	.272	.0177	.0275	.3784	.009	.011
M_β						
X_0	-.387	.0195	1.45	-.3577	.051	2.08
X_u	-.173	.0069	.137	-.0130	.008	.085
X_w	.1224	.01	.125	.0040	.0048	.297
X_δ	.207	.106	10.4	-.1375	.045	6.07
X_β						
Z_0	-31.35	.034	.965	-32.81	.137	.904
Z_u	-.025	.012	.86	-.039	.0218	.043
Z_w	-.290	.018	.077	-.387	.013	.131
Z_δ	-.701	.187	7.20	-.592	.123	2.56

* Perturbed (Radians)

** Note that the term $\partial h/\partial p$ was neglected in Eq. (3.19) when the acceleration measurements were used.

TABLE 7-19

Parameter Estimation From Nonlinear Kalman

X-22A Data at $\lambda = 45°$ (i) α_V (iii) Linear Aero.
(ii) Q = 0 (iv) With Accel. Meas.

PARAMETER	GLOBAL VALUES*	TEST DATA: 2F 195			TEST DATA: 2F 198		
		EQUATIONS OF MOTION	NONLINEAR KALMAN		EQUATIONS CF MOTION	NONLINEAR KALMAN	
			$10\,\sigma^2_{EM}$			$10\,\sigma^2_{EM}$	START UP σ_{CF}
M_0	3.60	.57708	2.484		.554	4.021	.978
M_u	-.036	-.006095	-.0236		-.0051	-.0358	-.00857
M_w	-.00644	-.00671	-.02198		-.0129	-.0165	-.0159
M_q	-.644	.007312	-.9716		-.6777	-1.024	-1.161
M_δ	.500	.2723	.4299		.378	.4133	.385
M_β							
X_0	19.286	18.252	21.025		1.0495	-.0362	.125
X_u	-.190	-.1726	-.1976		-.01303	.00076	-.00082
X_w	-.0675	.1224	.0864		.00401	.00336	.01341
X_δ	3.00	.2069	.3026		-.1375	-.0707	-.2449
X_β							
Z_0	-14.1987	-28.661	-38.22		-28 60	-57.70	-40.51
Z_u	-.180	-.02487	.0577		-.03899	.2144	.056
Z_w	-.413	-.29018	-.4229		-.3873	-.1552	-.2064
Z_δ	.900	-.70066	-5.804		-.5925	-4.999	-6.77
Z_β							

*Nonperturbed, Radians.

TABLE 7-20

Parameter Estimation From Nonlinear Kalman

X-22A Data at $\lambda = 45°$ (i) α_V (iii) Linear Aero
(ii) With Accel. Meas.

PARAMETER	GLOBAL VALUES*	TEST DATA: 2F 195			TEST DATA: 2F 198		
		EQUATIONS OF MOTION	NONLINEAR KALMAN		EQUATIONS OF MOTION	NONLINEAR KALMAN	
			WITH Q $F_1(1)$	WITHOUT Q $F_{10}(1)$		WITH Q $F_1(i)$	WITHOUT Q $F_{10}(1)$
M_0	3.60	.57708	1.084	2.484	.554	1.272	4.021
M_u	-.036	-.006095	-.0173	-.0236	-.0051	-.011	-.0358
M_w	-.00644	-.00671	-.0175	-.02198	-.0129	-.0124	-.0165
M_q	-.644	.007312	-1.04	-.9716	-.6777	-1.078	-1.024
M_δ	.500	.2723	.369	.4299	.378	.389	.4133
M_β							
X_0	19.286	18.252	19.07	21.025	1.0495	-.92[illegible]	-.0362
X_u	-.19	-.1726	-.180	-.1976	-.01303	.0071	.00076
X_w	-.0675	.1224	.1098	.0864	.00401	-.000114	.00336
X_δ	3.00	.2069	.1737	.3026	-.1375	-.162	-.0707
X_β							
Z_0	-14.199	-28.66	-29.81	-38.22	-28.60	-23.93	-57.70
Z_u	-.80	-.02487	-.0152	.0577	-.03899	-.083	.2144
Z_w	-.413	-.29018	-.30	-.4229	-.3873	-.33	-.1552
Z_δ	.90	-.70066	-1.15	-5.804	-.5925	-1.35	-4.999

*Nonperturbed, radians

TABLE 7-21

Results of Fixed-Point Smoothing For Initial Aircraft States *

Fixed Duct Incidence λ = 30°

States	Data 2F197		Data 2F203	
	Initial Estimate	Smoothed Estimate	Initial Estimate	Smoothed Estimate
q_0 (deg/sec)	-.229	-.0914	.913	.390
θ_0 (deg)	3.19	3.12	3.69	3.78
u_0 (ft/sec)	136.8	137.4	135.5	141.29
w_0 (ft/sec)	14.52	13.67	14.46	14.59

Fixed Duct Incidence λ = 45°

States	Data 2F195		Data 2F198	
	Initial Estimate	Smoothed Estimate	Initial Estimate	Smoothed Estimate
q_0 (deg/sec)	.1461	1.197	.1412	.373
θ_0 (deg)	-.0542	-.2107	1.35	1.38
u_0 (ft/sec)	107	105.7	111.5	111.1
w_0 (ft/sec)	12.9	12.62	8.54	8.57

* Results are with $Q=0$ and P_0 formed from σ_{EM}^2 multiplied by 10

TABLE 7-22

Comparison of Parameter Estimates $\lambda = 45°$

Using Princeton Data and X-22A Data $\theta_{trim} \approx 0°$

Para	Global Value**	Princeton Data No. 154	X-22A Data 2F198
M_u	-.036	-.00751	-.011
M_w	-.00044	-.00652	-.0124
M_q	-.044	-1.132*	-1.078
M_δ	.500	.197	.389
M_β	.043	.057	
X_o			
X_u	-.190	-.358	.0071
X_w	-.0675	-.0695	-.00114
X_δ	3.00	.721	-.162
X_β	.727	-.0198	
Z_o			
Z_u	-.180	.221	-.083
Z_w	-.413	.216	-.33
Z_δ	.900	1.477	-1.35
Z_β	-1.80	-1.848	

* With pitch rate feedback

** Nonperturbed, Radians

TABLE 7-23

Reference Values Used for Slow Transition Identification

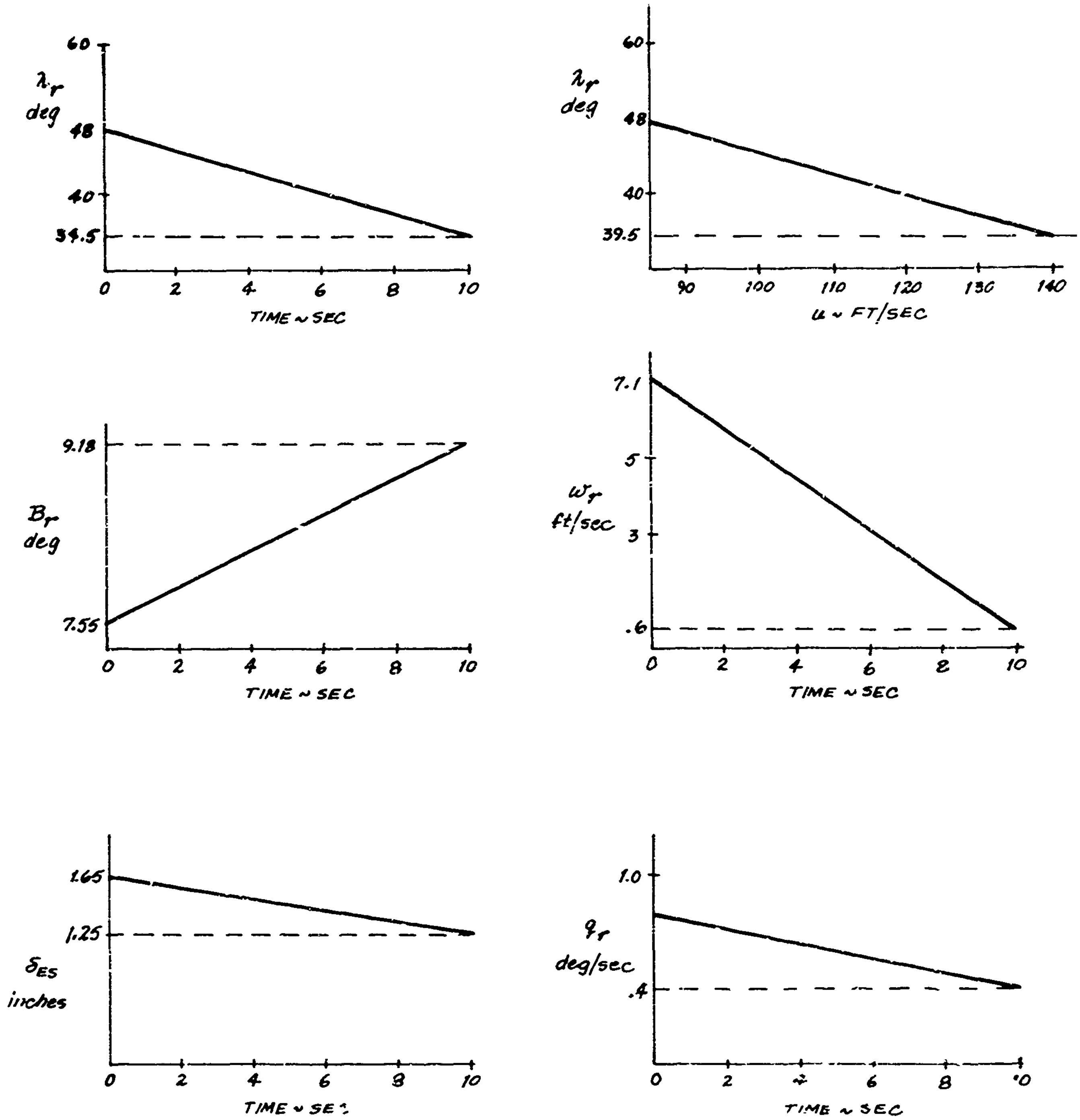

TABLE 7-24

Parameter Estimation on Slow Transition
Flight Data 2F197

$\dot{\lambda}$ = - 1 1/2 °/sec

Parameter	E.O.M. Estimate	Iterated Filter for 5 sec $F_1(1)$	Iterated Filter - 10 sec Par. & P_o from 5 sec Filter
M_0 (1)	53.49	54.07	19.08
M_0 (u)	-.8441	-.805	-.2363
M_0 (u^2)	.00325	.0031	.000773
M_w (1)	-.284	-1.13	-.739
M_w (u)	.00161	.007598	.00555
M_q	1.538	.2715	-.2481
M_θ	.902	-.1994	.3256
M_δ	14.46	15.86	18.33
M_λ	-.397	-.8224	-.2822
X_0 (1)	.778	.8193	1.871
X_0 (u)	.0935	.0917	.07224
X_0 (u^2)	-.00040	-.000388	-.000303
X_w	-.0375	-.0449	-.0449
X_β (1)	6.220	5.919	6.036
X_β (u)	-.0507	-.0472	-.0493
X_δ	.295	.334	.3592
X_λ	-.505	-.532	-.5167
Z_0 (1)	-9.31	-10.82	-11.27
Z_0 (u)	-.2717	-.258	-.2499
Z_0 (u^2)	.000656	.00063	.000588
Z_w	-.2971	-.2945	-.2983
Z_β (1)	-6.738	-8.36	-7.764
Z_β (u)	.059	.0706	.06475
Z_δ	-.558	-.531	-.5232
Z_λ (1)	-2.905	-2.902	-2.944
Z_λ (u)	.02012	.0200	.02037

* Nonperturbed, degrees

SECTION VIII

CONCLUSIONS

This study has shown that there are four major ingredients that constitute a successful identification of stability and control parameters of V/STOL aircraft from test data. These ingredients are: (1) a sound identification technique, (2) a properly designed input, (3) adequate and accurate measurements of aircraft motion variables, and (4) an adequate model.

1. Identification Technique Development

A study of three groups of available identification techniques shows that:

(i) Equation-error methods are asymptotically biased estimators in the presence of measurement errors, which always exist in practice. Consequently these methods are inadequate for identification of V/STOL aircraft parameters.

(ii) Measurement-error methods (or response-error methods) are asymptotically unbiased estimators in the absence of process noise (or modeling errors). However, in the presence of modeling errors, as is most likely to be the case for V/STOL aircraft, the response-error methods give asymptotically biased estimates if the dynamic system and/or measurement system are nonlinear; but the methods yield asymptotically unbiased estimates if both the dynamical system and measurement systems are linear. Since the V/STOL dynamics are nonlinear and modeling errors are most likely to exist, the measurement-error methods are clearly inadequate.

(iii) A study of methods that treat both measurement and process errors showed that the methods available at the start of this program were inadequate for the V/STOL identification problem featuring nonlinear dynamics represented by large numbers of parameters, significant modeling errors, and measurement errors. Thus, development of an advanced technique for the identification of V/STOL aircraft parameters from flight data was required.

With an understanding of the basic shortcomings of the available techniques, an advanced technique for the identification of V/STOL aircraft parameters was developed that is suitable to do the job. The technique is a suboptimal sequential fixed-point nonlinear smoothing algorithm working in conjunction with a locally iterated filter-smoother algorithm working in an "on-line" fashion to update the estimates of the initial state and the parameters as new measurement becomes available. A good procedure to start up the algorithm has also been developed. Applications of these techniques to computer-generated data and test data, both X-22A data and Princeton Dynamic Model Track test data, have shown that the technique is suitable for parameter identification of nonlinear systems having a large number of parameters and dynamical modeling errors.

When a priori information is lacking, as is frequently the case for parameter identification problems, an improved scheme for computing the variances of the fixed-point smoothed estimates has been developed. An algorithm for the estimation of the unknown forcing inputs has also been derived to work in a forward manner after all the data have been processed through the fixed-point smoother.

2. Input Design

From the study of parameter identifiability and the design of an appropriate input it was concluded that:

(i) Sensitivity of the aircraft motion to parameter variation is a good criterion for input design. An increase in sensitivity results in an increase in parameter identifiability.

(ii) An input design that simultaneously optimizes the identifiability of all the parameters using exact optimization techniques is not practical; however, suboptimal techniques appear to be feasible by grouping the parameters into several groups for the purpose of sequential identification of the group of parameters. Also, cut-and-try methods based on past experience and using sensitivity as the criteria have been demonstrated to be practical.

3. Adequacy and Accuracy of the Measurements

From the analytical study and the numerical experiments on the test data, it was concluded that

(i) At least one motion variable must be measured in each degree of freedom.

(ii) Accelerations contain additional information, and should therefore be measured and used in parameter identification.

SECTION IX

RECOMMENDATIONS

This identification program has been severely constrained by lack of well-conditioned X-22A data. The data that have been used were taken from the MPE II flight tests of the X-22A; these data were not obtained for identification purposes. Consequently, an accurate identification of the X-22A could not be achieved. Thus, in this identification project, primary emphasis has been placed on the development of the techniques capable of accurately identifying the parameters of the model chosen to represent the X-22A aircraft, using computer-generated data. Because of the inadequate flight data, meaningful correlation of the parameters identified from the MPE II flight data with those obtained from wind tunnel data (the global digital computer program) could not be satisfactorily done. Therefore, it is strongly recommended that, first of all, better conditioned X-22A flight data be obtained using the procedure recommended in the report and that the developed identification techniques be applied to these data for more extensive correlation with the wind tunnel data.

Also, during the course of this project, several problem areas associated with the developed identification techniques were not completely solved. These areas could be and should be further studied to improve the techniques and to enhance their general applicability to V/STOL aircraft. The major areas that are recommended for future work are listed below:

1. Completely check out the computer program for the estimation of the unknown forcing functions and perform numerical experiments to verify its capability of detecting the modeling errors.

2. Program the improved computational algorithm for the variances of the fixed-point smoothed estimates and perform numerical evaluation to verify the theoretically predicted results.

3. Improve the identification techniques developed by including the capability of simultaneously identifying the covariance functions of the process and measurement noise.

4. Modify the present identification computer program to allow inclusion of additional mathematical models of the X-22A, both fixed-operating point (FOP) and in transition, and to reflect the coordinate systems in which the data are recorded, and then apply the experimental data to these models to determine the most suitable dynamic models for FOP and for transition of the X-22A aircraft.

5. Program the complete equations of motion for the Princeton track model and apply the Princeton data to this model to identify the stability and control parameters of the model.

6. Conduct further study on input design.

7. Establish quantitative criteria for the accuracy of the measurement instruments (and sensors) required to achieve a prescribed accuracy of the estimated parameters.

APPENDIX A

LINEAR TIME-VARYING MATHEMATICAL MODEL FOR THE X-22A IN TRANSITION FLIGHT - AN ALTERNATE IDENTIFICATION MODEL

If the reference trajectory is chosen to be

$$u_R = f(\lambda_R),$$

where $\lambda_R = \lambda_R(t)$ and the corresponding set of references for state and control variables are $w_R(t)$, $q_R(t)$, $\theta_R(t)$, $\delta_{B_R}(t)$, and $\delta_{ES_R}(t)$, then it is readily shown in a straightforward manner that the first term in the x equation in equation (2.4) can be written as

$$x_0(u,\lambda) = \bar{x}_0(t) + \bar{x}_{0_u}(t)\Delta u + \bar{x}_{0_\lambda}(t)\Delta\lambda + \text{higher order terms} \tag{A.1}$$

where

$$\bar{x}_0(t) \triangleq x_0(u_R,\lambda_R) = x_0\left(f(\lambda_R),\lambda_R\right) = \bar{\bar{x}}_0(\lambda_R)$$

$$\bar{x}_{0_u}(t) \triangleq \frac{\partial x_0}{\partial u}(u_R,\lambda_R)$$

etc.

Similar expressions can be written for the other terms in (2.4). Then, to first order, equation (2.1) can be written as

$$\frac{d}{dt}\begin{pmatrix}\Delta q\\ \Delta\theta\\ \Delta u\\ \Delta w\end{pmatrix} = \begin{pmatrix} m_q(t) & 0 & m_u(t) & m_w(t)\\ 1 & 0 & 0 & 0\\ x_q(t)-w_R(t) & -g\cos\theta_R(t) & x_u(t) & x_w(t)-q_R(t)\\ z_q(t)+u_R(t) & -g\sin\theta_R(t) & z_u(t)+q_R(t) & z_w(t)\end{pmatrix}\begin{pmatrix}\Delta q\\ \Delta\theta\\ \Delta u\\ \Delta w\end{pmatrix}$$

$$+\begin{pmatrix} m_0(t) & m_B(t) & m_{\delta_{ES}}(t) & m_\lambda(t)\\ 0 & 0 & 0 & 0\\ x_0(t) & x_B(t) & x_{\delta_{ES}}(t) & x_\lambda(t)\\ z_0(t) & z_B(t) & z_{\delta_{ES}}(t) & z_\lambda(t)\end{pmatrix}\begin{pmatrix}1\\ \Delta B\\ \Delta\delta_{ES}\\ \Delta\lambda\end{pmatrix} \tag{A.2}$$

Preceding page blank

where

$$\Delta q = q(t) - q_R(t)$$

$$\Delta\theta = \theta(t) - \theta_R(t)$$

etc

and

$$x_o(t) = -q_R u_R - g \sin\theta_R + \left[\bar{x}_o(t) + \bar{x}_w(t) w_R + \bar{x}_{\delta_B}(t)\delta_{B_R} + \bar{x}_{\delta_{ES}}(t)\delta_{ES_R}\right]$$

$$z_o(t) = +q_R u_R + g \cos\theta_R + \left[\bar{z}_o(t) + \bar{z}_w(t) w_R + \bar{z}_{\delta_B}(t)\delta_{B_R} + \bar{z}_{\delta_{ES}}(t)\delta_{ES_R}\right]$$

$$m_o(t) = \left[\bar{m}_o(t) + \bar{m}_q(t) q_R + \bar{m}_w(t) w_R + \bar{m}_{\delta_B}(t)\delta_{B_R} + \bar{m}_{\delta_{ES}}(t)\delta_{ES_R}\right]$$

APPENDIX B

A STATISTICAL ANALYSIS OF THE ESTIMATES FROM THE EQUATION-ERROR METHODS

To begin with, we shall discuss the statistical properties of the estimates using the equations-of-motion error method. It has been discussed briefly in Reference 21 that, due to the fact that in practice the data are contaminated with measurement noise, the method will generally give only biased estimates. Here, we shall discuss in detail the estimate using this method and other initial estimators discussed in Section 3.1.

More specifically, we shall analyze how the bias and the variance of the estimate are affected by the noise level and the data length used.

Consider a general case in which the process uncertainty is present in equation (2.15). From (3.2)

$$z_2^o(N) = A_N^o p + w(N) \tag{B.1}$$

where $w(N) \triangleq \left[w_1(t_0), w_1(t_1), \cdots, w_1(t_N), \cdots, w_3(t_0) w_3(t_1), \cdots, w_3(t_N)\right]^T$, and $z_2^o(N)$ and A_N^o represent the results from the noise-free measurements and z_N and A_N are the corresponding actual measurements, i.e.,

$$\begin{aligned} z_N &= z_2^o(N) + v_2(N) \\ A_N &= A_N^o + \Delta A_N \end{aligned} \tag{B.2}$$

where $v_2(N) \triangleq \left[v_{21}(t_0), v_{21}(t_1), \cdots, v_{21}(t_N); \cdots; v_{23}(t_0), v_{23}(t_1), \cdots, v_{23}(t_N)\right]^T$ and ΔA_N are the errors due to the noisy measurements of the state. The estimator using (3.3) is

$$\hat{p} = (A_N^T A_N)^{-1} A_N^T z_N \tag{B.3}$$

Now pre-multiplying (B.1) by $\left[A_N^T A_N\right]^{-1} A_N^T$ and using (B.2) and (B.3) yields

$$\hat{p} = (A_N^T A_N)^{-1} A_N^T A_N^o p + (A_N^T A_N)^{-1} A_N^T \left(w(N) + v_2(N)\right) \tag{B.4}$$

Thus the error of the estimate becomes

$$\hat{p} - p = (A_N^T A_N)^{-1} A_N^T \left(w(N) + v_2(N) - \Delta A_N p\right) \tag{B.5}$$

The bias of the estimate is

$$E\left[\hat{p}-p\right] = -pE\left[(A_N^T A_N)^{-1} A_N^T \Delta A_N\right] \tag{B.6}$$

and the mean square of the estimate is

$$\begin{aligned} E & \left[(\hat{p}-p)(\hat{p}-p)^T\right] \\ & = E\left[(A_N^T A_N)^{-1} A_N^T (w(N)+v_z(N)-\Delta A_N p)(w(N)+v_z(N)-\Delta A_N p)^T \cdot \right. \\ & \quad \left. \cdot A_N (A_N^T A_N)^{-1}\right] \\ & = E\left[(A_N^T A_N)^{-1} A_N^T (W_N+U_N) A_N (A_N^T A_N)^{-1} \right. \\ & \quad \left. + (A_N^T A_N)^{-1} A_N^T \Delta A_N p p^T \Delta A_N^T A_N (A_N^T A_N)^{-1}\right] \end{aligned} \tag{B.7}$$

where W_N and U_N are the covariance matrices of $w(N)$ and $v_z(N)$ respectively.

From (B.6) and (B.7), it is evident that

(i) The estimate $\hat{p}$ is biased, even if the noise vector in the acceleration measurements $v_z(N)$, and error vector in the equations of motion, $w(N)$, have zero mean and are independent of A_N.

(ii) The bias of the estimate is affected solely by the error in the state variables' measurements as long as the errors in the acceleration measurements and in the equations of motion are zero mean.

(iii) The variance of the estimate is, however, affected by the noise level of all the measurements and by the equations-of-motion errors.

Qualitatively speaking, it is also evident from (B.6) that the percentage bias is dictated by the signal-to-noise ratio in the state variable measurements. Indeed, if the signal-to-noise ratio is infinite (i.e., no measurement errors in the state variables), there is no bias; if the signal-to-noise ratio is zero, then the parameter estimates become 100% biased.

Questions remain as to how the bias is affected by the data length for a given signal-to-noise ratio, i.e., does an increase in data length help reduce the bias? In other words, what is the asymptotical behavior of this bias? The answer to these questions has also been found. In the following analysis it is shown that

(i) The estimate is asymptotically biased. Thus, use of longer data records does not help reduce the bias.

(ii) The bias increases as the signal-to-noise ratio, x/σ_1, decreases. For single parameter cases, the percentage bias is given by $\dfrac{1}{1+(x/\sigma_1)^2} \times 100\%$ of the true value of the parameter. Similar results have also been obtained for n-parameter cases.

In order not to be bogged down by the complicated matrix algebra which tends to obscure the basic ideas, we shall consider a single scalar equation

$$\dot{x} = ax + w_1(t) \tag{B.8a}$$

with the measurements

$$y = x + v_1(t) \tag{B.8b}$$

$$z = \dot{x} + v_2(t) \tag{B.8c}$$

We shall later extend our results to the vector equations. Substituting (B.8a) and (B.8b) into (B.8c) there results

$$z = ay + (v_2 + w_1) - av_1 \tag{B.9}$$

Thus, from the viewpoint of classical linear regression, the combination of the equation-of-motion error w_1 and the error in the measurement of the acceleration v_2 is what is important. Consequently, there is no loss of generality to assume that $w_1 = 0$ and that

$$E\left[v_2\right] = E\left[v_1\right] = E\left[v_1 v_2\right] = 0 \tag{B.9a}$$

$$E\left[v_1^2\right] = \sigma_1^2 \tag{B.9b}$$

$$E\left[v_2^2\right] = \sigma_2^2 \tag{B.9c}$$

In other words, equation (B.8a) is deterministic; the measurement errors in the state variable and the time rate of the state variables are zero mean, independent, and with finite variance σ_1^2, and σ_2^2 respectively.

Upon an application of the classical linear regression to (B.9) there results a sequence of estimates $\{\hat{a}_i\}$ for the parameter a corresponding to the number of samples:

$$\hat{a}_1 = \frac{y_1 z_1}{y_1^2} \triangleq \frac{p_1}{q_1} \qquad \text{one data point} \tag{B.10a}$$

$$\hat{a}_2 = \frac{y_1 z_1 + y_2 z_2}{y_1^2 + y_2^2}$$

$$= \frac{\frac{1}{2}(y_1 z_1 + y_2 z_2)}{\frac{1}{2}(y_1^2 + y_2^2)} \triangleq \frac{p_2}{q_2} \qquad \text{two data points} \tag{B.10b}$$

— — — — — — — — — — — — — —

$$\hat{a}_n = \frac{\frac{1}{n}\sum_{i=1}^{n} y_i z_i}{\frac{1}{n}\sum_{i=1}^{n} y_i^2} \triangleq \frac{p_n}{q_n} \qquad n \text{ data points} \tag{B.10c}$$

First, we shall consider the one sample (one data point) case. We have

$$\hat{a}_1 = \frac{y_1 z_1}{y_1^2} = \frac{z_1}{y_1}$$

Since $v_1(t_i)$ and $v_2(t_i)$ are Gaussian random variables, i.e., have density functions

$$f(v_1) = N(0, \sigma_1^2) = \frac{1}{\sqrt{2\pi}\,\sigma_1} e^{-\frac{v_1^2}{2\sigma_1^2}}$$

$$f(v_2) = N(0, \sigma_2^2) = \frac{1}{\sqrt{2\pi}\,\sigma_2} e^{-\frac{v_2^2}{2\sigma_2^2}}$$

it is clear from (B.8a) and (B.10a) that y_1 and z_1 are also normal variables. In fact,

$$f(y_1) = N(x_1, \sigma_1^2) \tag{B.11a}$$

$$f(z_1) = N(a x_1, \sigma_2^2) \tag{B.11b}$$

Since $v_1(t_1)$ and $v_2(t_2)$ are independent, hence y_1 and z_1 e also independent, and hence y_1 and z_1 are jointly normal. It follows that (see, for instance, page 197 of Reference 65)

$$f(\hat{a}_1) = \int_0^{\infty} y_1 f_{zy}(\hat{a}_1 y_1, y_1)\, dy_1 - \int_{-\infty}^{0} y_1 f_{zy}(\hat{a}_1 y_1, y_1)\, dy_1$$

$$= \int_0^{\infty} y_1 f_y(y_1) f_z(\hat{a}_1 y_1)\, dy_1 - \int_{-\infty}^{0} y_1 f_y(y_1) f_z(\hat{a}_1 y_1)\, dy_1 \tag{B.11c}$$

Using (B.11) and a great deal of algebraic manipulations, it was found that

$$f(\hat{a}_1) = \frac{K}{\pi \sigma_1 \sigma_2}\left\{\sigma_3^2 e^{-\frac{m^2}{2\sigma_3^2}} + \sqrt{2\pi}\, m \sigma_3 \left[\Phi\left(\frac{m}{\sigma_3}\right) - \frac{1}{2}\right]\right\} \tag{B.12a}$$

where

$$K = \exp - \frac{x_1^2}{2\sigma_2^2}\left[\left(\frac{\sigma_2}{\sigma_1}\right)^2 + a^2 - \frac{(\sigma_2^2/\sigma_1^2 + a\hat{a}_1)^2}{\sigma_2^2/\sigma_1^2 + \hat{a}_1^2}\right]$$

$$\sigma_3^2 = \frac{\sigma_2^2}{\hat{a}_1^2 + \left(\frac{\sigma_2}{\sigma_1}\right)^2}$$

$$m = \frac{x_1\left(a\hat{a}_1 + \left(\frac{\sigma_2}{\sigma_1}\right)^2\right)}{\hat{a}_1^2 + \left(\frac{\sigma_2}{\sigma_1}\right)^2} \tag{B.12b}$$

$$\Phi(x) = \frac{1}{\sqrt{2\pi}} \int_{-\infty}^{x} e^{-x^2/2}\, dx$$

We now examine the two limiting cases, i.e., $\frac{x_1}{\sigma} \to 0$ and $\frac{x_1}{\sigma} \to \infty$. From (B.12a), it is readily seen that

(1) $$f(\hat{a}_1) = \frac{\sigma_2/\sigma_1}{\pi\left[\hat{a}_1^2 + (\sigma_2/\sigma_1)^2\right]}, \quad \text{as } \frac{x_1}{\sigma_1} \to 0, \ \frac{x_1}{\sigma_2} \to 0$$

(2) $$f(\hat{a}_1) = \frac{1}{\sqrt{2\pi}\,(\sigma_2^2/x_1)}\, e^{-\frac{1}{2}\left(\frac{x_1}{\sigma_2}\right)^2(\hat{a}_1 - a)^2}, \quad \text{as } \frac{x_1}{\sigma_1} \to \infty \tag{B.13a}$$

$$f(\hat{a}_1) = \begin{cases} 0 & \text{if } \hat{a}_1 \neq a \\ \infty & \text{if } \hat{a}_1 = a \end{cases} \tag{B.13b}$$

$$= \delta(\hat{a}_1 - a), \quad \text{as } \frac{x_1}{\sigma_1} \to \infty, \quad \frac{x_1}{\sigma_2} \to \infty$$

Thus, it is recognized that as signal x approaches zero, the estimate approaches the Cauchy distribution, resulting in a 100% bias. On the other hand, as the signal-to-noise ratio increases without bound, the distribution approaches a delta function occurring at $\hat{a}_1 = a$. The bias as well as the variance of the estimate is zero, indicating that the estimate is the true value of the parameter. Actually, this comes as no real surprise, because the problem at hand becomes purely a deterministic one.

Figures B-1 through B-3 show the plots of (B.12a) for different values of signal-to-noise ratio, i.e., $x/\sigma = 0$, 1, and 10, assuming that $\sigma_1 = \sigma_2 = \sigma$ and $a = 1$. Note that in these conditions, the percentage bias can be expressed as

$$\frac{1}{1 + (x/\sigma)^2} \times 100\% \tag{B.14}$$

We now proceed to examine the cases when more data are used. We may proceed as before for $n = 2, 3, \ldots,$ but the algebra becomes too complicated to warrant this approach, and we shall not pursue this line further. Rather, we shall examine, in detail, the asymptotical properties of the estimate $\hat{a}_n$, as $n \to \infty$.

With reference to equation (B.10c) it is readily seen that both the random sequences

$$y_1 z_1, \quad y_2 z_2, \cdots, y_n z_n$$
$$y_1^2, \; y_2^2, \; \cdots, \; y_n^2$$

are independent with respect to their own elements, that is, $y_i z_i$ and $y_j z_j$ are independent; further, y_i^2 and y_j^2 are also independent for all $1 \le i, j \le n$. By the central limit theorem, p_n and q_n defined in (B.10c) will both approach normal distributions as $n \to \infty$, i.e.,

$$p_n \triangleq \frac{1}{n}\sum_{i=1}^{n} y_i z_i \longrightarrow \text{normal variable}$$
$$q_n \triangleq \frac{1}{n}\sum_{i=1}^{n} y_i^2 \longrightarrow \text{normal variable}$$

as $n \to \infty$.

To provide a common ground for comparing the statistical properties of $\hat{a}_n$ as $n \to \infty$ and $\hat{a}_1$, and to simplify the algebra, it is convenient to consider that the signal-to-noise ratio is constant. (In practice this condition is relatively hard to realize, since $x(t)$ is changing. However, if $x(t)$ is a stationary random process such as the motion of the airplane resulting from random gust excitations, it is realistic to assume a constant signal-to-noise ratio.) With this assumption, we have

$$\begin{aligned} E\left[y_i z_i\right] &= a x_i^2 = a x^2 \\ E\left[y_i^2\right] &= x_i^2 + \sigma_1^2 = x^2 + \sigma_1^2 \end{aligned} \qquad \text{(B.15)}$$

Recall that p_n and q_n are sample mean for $\{y_i z_i\}$ and $\{y_i^2\}$ respectively; their mean and variance are respectively

$$\begin{aligned} E\left[p_n\right] &= a x^2 \\ E\left[(p_n - a x^2)^2\right] &= \sigma_{p_n}^2 \to 0 \quad \text{as} \quad n \to \infty \\ E\left[q_n\right] &= x^2 + \sigma_1^2 \\ E\left[(q_n - x^2 - \sigma_1^2)^2\right] &= \sigma_{q_n}^2 \to 0, \quad \text{as} \quad n \to \infty \end{aligned} \qquad \text{(B.16)}$$

Thus, the density functions of p_n and q_n as $n \to \infty$ are

$$\begin{aligned} \lim_{n \to \infty} f(p_n) &= \lim_{\sigma_{p_n} \to 0} N(\alpha C, \sigma_{p_n}^2) \\ \lim_{n \to \infty} f(q_n) &= \lim_{\sigma_{q_n} \to 0} N(C, \sigma_{q_n}^2) \end{aligned} \qquad \text{(B.17)}$$

where

$$\alpha \triangleq \frac{a(x/\sigma_1)^2}{1+(x/\sigma_1)^2}, \quad c \triangleq x^2 + \sigma_1^2$$

Since p_n and q_n both approach normal variables as $n \to \infty$, the results obtained for $\hat{a}_1$, which we recall is a ratio of two normal variables, can readily be used. By comparing (B. 17) with (B. 11), it is easy to see that

$$\lim_{n\to\infty} f(\hat{a}_n) = \lim_{\substack{\sigma_{q_n}\to 0 \\ \sigma_{p_n}\to 0}} \frac{\bar{K}}{\pi \sigma_{q_n} \sigma_{p_n}} \left\{ \bar{\sigma}_3^2 e^{-\frac{\bar{m}^2}{\bar{\sigma}_3^2}} + \sqrt{2\pi}\, \bar{\sigma}_3 \bar{m} \cdot \left[\Phi\left(\frac{\bar{m}}{\bar{\sigma}_3}\right) - \frac{1}{2} \right] \right\} \tag{B. 18a}$$

where

$$\bar{K} \triangleq \exp - \frac{c^2}{2\sigma_{q_n}^2} \left[\frac{\sigma_{q_n}^2}{\sigma_{p_n}^2} + \alpha^2 - \frac{(\sigma_{q_n}^2/\sigma_{p_n}^2 + \alpha \hat{a}_n)^2}{\hat{a}_n^2 + (\sigma_{q_n}/\sigma_{p_n})^2} \right].$$

$$\bar{\sigma}_3^2 \triangleq \frac{\sigma_{q_n}^2}{\hat{a}_n^2 + (\sigma_{q_n}/\sigma_{p_n})^2}$$

$$\bar{m} \triangleq \frac{c\left(\alpha \hat{a}_n + (\sigma_{q_n}/\sigma_{p_n})^2\right)}{\hat{a}_n^2 + (\sigma_{q_n}/\sigma_{p_n})^2}$$

$$\Phi(x) \triangleq \frac{1}{\sqrt{2\pi}} \int_{-\infty}^{x} e^{-\frac{x^2}{2}} dx$$

$$c = x^2 + \sigma_1^2$$

$$\alpha = \frac{a(x/\sigma_1)^2}{1+(x/\sigma_1)^2}$$

Carrying out the limiting process yields

$$\lim_{n\to\infty} f(\hat{a}_n) = \begin{cases} 0 & \text{if} \quad \hat{a}_n \neq \alpha \\ \infty & \text{if} \quad \hat{a}_n = \alpha \end{cases} \tag{B. 18b}$$

$$= \delta(\hat{a}_n - \alpha)$$

This new result serves to answer the two important questions previously raised. We conclude that

- The estimate $\hat{a}$ is <u>asymptotically biased.</u>
- The bias depends solely on the ratio of the signal to state variable measurement noise, x/σ_1 and is given by

$$\hat{a} - a = -a \left[\frac{1}{1 + (x/\sigma_1)^2} \right]$$

In the language of probability theory, equation (B. 18) says that the sequence of the estimates $\{\hat{a}_n\}$ converges to α with probability one, as $n \to \infty$.

The above asymptotical analysis for a single variable case can readily be extended to a multi-parameter case. Consider a two-parameter system

$$\begin{aligned} \dot{x} &= ax + by \\ q &= \dot{x} + u \\ \bar{x} &= x + v_1 , \; \bar{y} = y + v_2 \end{aligned} \qquad (B.19)$$

where

$$\begin{aligned} E[u] &= E[v_1] = E[v_2] = 0 \\ E[u^2] &= \sigma^2 \\ E[v_1^2] &= \sigma_x^2 , \; E[v_2^2] = \sigma_y^2 \end{aligned} \qquad (B.20)$$

and u, v_1 and v_2 are independent. By a similar analysis as for the single parameter case, it is not difficult to show that

$$\lim_{n \to \infty} \begin{bmatrix} \hat{a}_n \\ \hat{b}_n \end{bmatrix} = \begin{bmatrix} x^2 + \sigma_x^2 & xy \\ xy & y^2 + \sigma_y^2 \end{bmatrix}^{-1} \begin{bmatrix} x(ax + by) \\ y(ax + by) \end{bmatrix} \qquad (B.21)$$

with probability one. Namely, $\hat{a}_n$ and $\hat{b}_n$ converge, with probability one, to

$$\lim_{n \to \infty} \hat{a}_n = \frac{a\left(\frac{x}{\sigma_x}\right)^2 + b\left(\frac{\sigma_y}{\sigma_x}\right)\left(\frac{x}{\sigma_x}\right)\left(\frac{y}{\sigma_y}\right)}{1 + \left(\frac{x}{\sigma_x}\right)^2 + \left(\frac{y}{\sigma_y}\right)^2} \qquad (B.22A)$$

$$\lim_{n \to \infty} \hat{b}_n = \frac{b\left(\frac{y}{\sigma_y}\right)^2 + a\left(\frac{\sigma_x}{\sigma_y}\right)\left(\frac{x}{\sigma_x}\right)\left(\frac{y}{\sigma_y}\right)}{1 + \left(\frac{x}{\sigma_x}\right)^2 + \left(\frac{y}{\sigma_y}\right)^2} \qquad (B.22b)$$

For the general k-parameter case

$$\dot{x}_1 = p_1 x_1 + p_2 x_2 + p_3 x_3 + \cdots + p_k x_k \tag{B.23a}$$

with the measurements

$$z = \dot{x}_1 + u$$

$$\bar{x}_i = x_i + v_i \tag{B.23b}$$

where

$$E\left[v_i\right] = 0$$

$$E\left[v_i^2\right] = \sigma_i^2, \quad i = 1, 2, \ldots, k$$

and u, v_i are independent, the estimates of the parameters $(\hat{p}_1)_n$, $(\hat{p}_2)_n$, $\ldots$, $(\hat{p}_k)_n$ converge to

$$\lim_{n\to\infty} \begin{bmatrix} (\hat{p}_1)_n \\ (\hat{p}_2)_n \\ \cdot \\ \cdot \\ \cdot \\ (\hat{p}_k)_n \end{bmatrix} = \begin{bmatrix} x_1^2+\sigma_1^2 & x_1 x_2 & x_1 x_3 & \cdots & x_1 x_k \\ x_2 x_1 & x_2^2+\sigma_2^2 & \cdots & & x_2 x_k \\ \cdot & & \cdot & & \cdot \\ \cdot & & & \cdot & \cdot \\ \cdot & & & & \cdot \\ x_k x_1 & \cdots & & \cdots & x_k^2+\sigma_k^2 \end{bmatrix}^{-1} \begin{bmatrix} x_1 \\ x_2 \\ \cdot \\ \cdot \\ \cdot \\ x_k \end{bmatrix} (p_1 x_1 + \cdots p_k x_k) \tag{B.23c}$$

with probability one. Namely,

$$\lim_{n\to\infty} (\hat{p}_i)_n = \frac{p_i \left(\frac{x_i}{\sigma_i}\right)^2 + \left(\frac{x_i}{\sigma_i}\right) \sum\limits_{\substack{j=1 \\ j\neq i}}^{k} p_j \left(\frac{\sigma_j}{\sigma_i}\right)\left(\frac{x_j}{\sigma_j}\right)}{1 + \sum\limits_{i=1}^{k} \left(\frac{x_i}{\sigma_i}\right)^2} \qquad i = 1, 2, \ldots, k \tag{B.23d}$$

with probability one.

The other equation error methods discussed in Section 3.1 are also asymptotically biased estimators. The bias of these estimators, like that of using the equations-of-motion method discussed earlier in this section, stems from the fact that the regressor in the least square fit is stochastic (due to the errors in the state variable measurements) and the fact that the regressor and the errors in the least square fit are correlated.

Consider, for instance, the Denery's initial estimator (see Appendix C). The matrix

$$\int_0^{t_f} \left[H_0 \left(\frac{\partial \tilde{x}}{\partial p} \; \vdots \; \frac{\partial \tilde{x}}{\partial \tilde{x}_0} \right) \right]^T W \left[H_0 \left(\frac{\partial \tilde{x}}{\partial p} \; \vdots \; \frac{\partial \tilde{x}}{\partial \tilde{x}_0} \right) \right] dt$$

in (C.9) is stochastic, since $\frac{\partial \tilde{x}}{\partial p}(t)$ is a solution of the stochastic differential equation (C.8). Further, this matrix is clearly correlated with the vector in (C.9)

$$\int_0^{t_f} \left[H_0 \left(\frac{\partial \tilde{x}}{\partial p} \; \vdots \; \frac{\partial \tilde{x}}{\partial \tilde{x}_0} \right) \right]^T W (y - \tilde{y}_N) dt$$

Thus, the estimates $\left[p^T \; \vdots \; \Delta \tilde{x}_0^{\;T} \right]^T$ in (C.9) are asymptotically biased.

Consider next the polynomial estimator and the modified (floppy) spline function estimator. For the purposes of illustration, consider a single parameter case.

$$\begin{aligned} \dot{x} &= ax \\ y &= x + v \end{aligned} \tag{B.24}$$

First, we fit a time function $\hat{y}(t)$ using a set of deterministic base vectors (polynomials or modified spline functions) to the state measurement $y(t)$. For N sample points (see Equation 3.7).

$$\begin{aligned} \hat{y}_N &= A_N \hat{a} \\ &= A_N (A_N^T A_N)^{-1} A_N^T y_N \\ &= \mathcal{K} y_N = \mathcal{K}(x_N + v_N) \end{aligned} \tag{B.25}$$

where $\mathcal{K} = A_N (A_N^T A_N)^{-1} A_N^T$ is a deterministic matrix.

Then, since $\dot{x}_N = a x_N$, (B.25) yields

$$\overset{\circ}{\hat{y}}_N = a\hat{y}_N + \left[\mathcal{K}\dot{v}_N - a\mathcal{K}v_N \right] \tag{B.26}$$

and the least square fit $\hat{a}_N$ to a in (B.26) gives

$$\begin{aligned} \hat{a}_N &= (\hat{y}_N^T \hat{y}_N)^{-1} \hat{y}_N^T \overset{\circ}{\hat{y}}_N \\ &= a + (\hat{y}_N^T \hat{y}_N)^{-1} \hat{y}_N^T (\mathcal{K}\dot{v}_N - a\mathcal{K}v_N) \end{aligned} \tag{B.27}$$

Since $\hat{y}_N$ is a random vector and is correlated with $(\mathcal{K}\dot{v}_N - a\mathcal{K}v_K)$ in (B.27), the estimate $\hat{a}_N$ is again asymptotically biased.

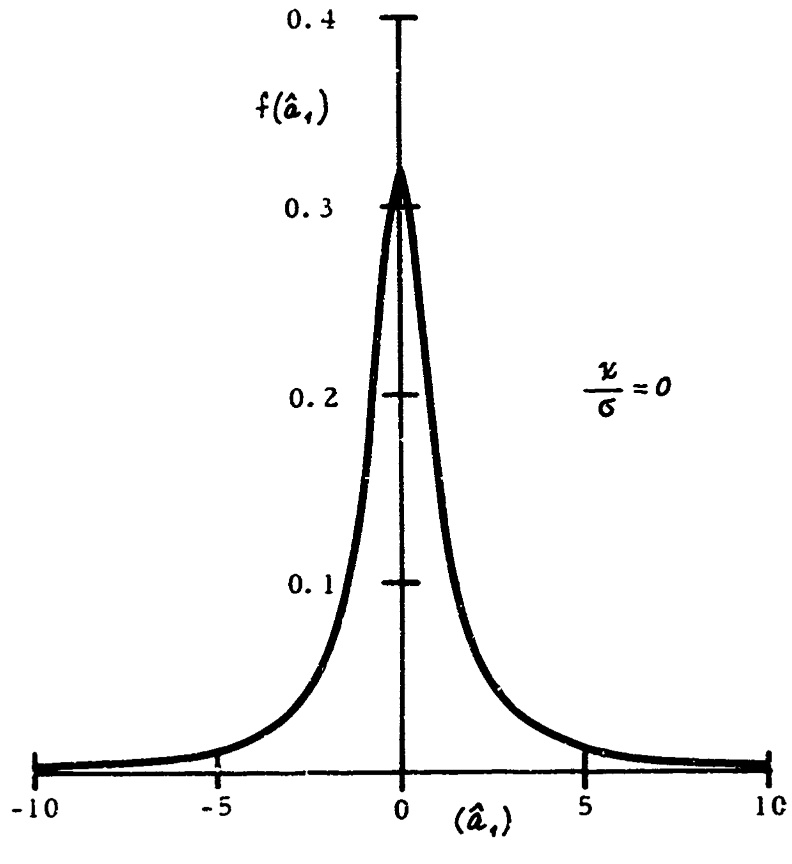

Figure B-1 $f(\hat{a}_1)$ for $\frac{x}{\sigma} = 0$

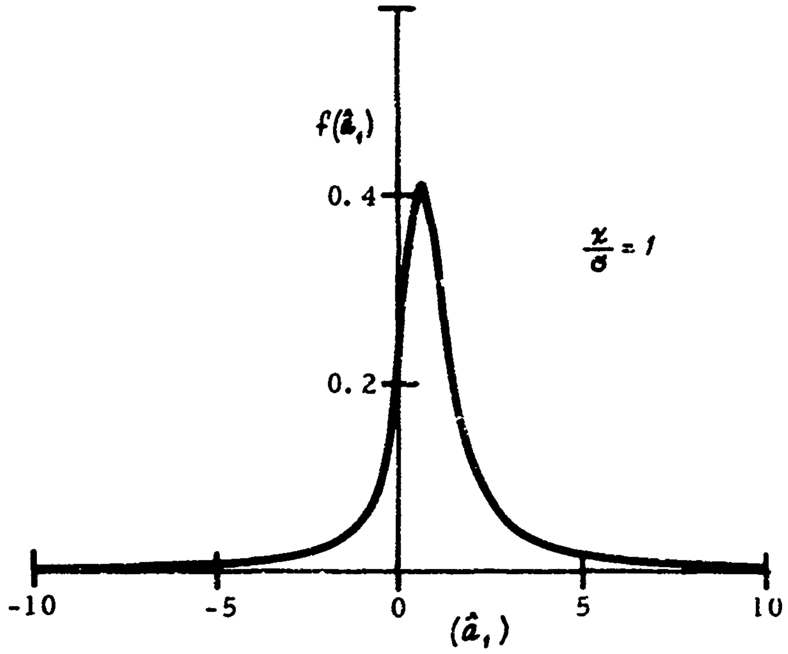

Figure B-2 $f(\hat{a}_1)$ for $\frac{\kappa}{\sigma} = 1.0$

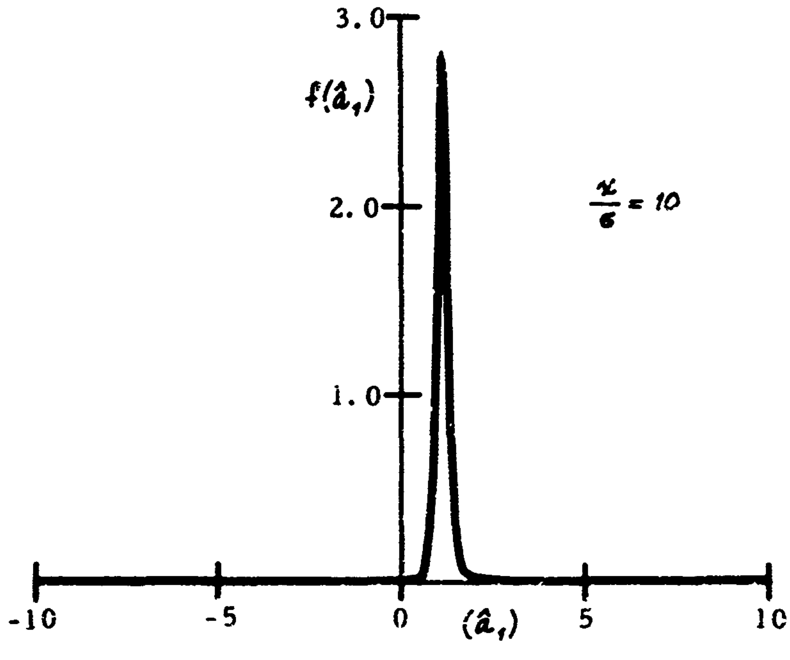

Figure B-3 $f(\hat{a}_1)$ for $\frac{\kappa}{\sigma} = 10$

APPENDIX C

DENERY'S INITIAL ESTIMATOR

In the following discussions of this technique, it appears to be easier, insofar as conveying the basic idea is concerned, to use a multi-output phase variable form (Reference 66) rather than using Denery's canonical form presented in his original work (Reference 12). Consider a linear system

$$\left.\begin{aligned} \dot{x} &= Fx + Gu \\ y &= Hx + v \end{aligned}\right\} \qquad \text{(C. 1)}$$

where x is the state vector, (n-vector); u is the control vector, (r-vector); y is the output vector, (m-vector); and v is the measurement error vector. If $m < n$, there are generally infinitely many sets of (F, G , H) that can fit (C. 1) as far as the input-output relationship is concerned. To be specific, therefore, we shall assume that we are to fit the system (C. 1) by the following system:

$$\begin{aligned} \dot{\tilde{x}} &= F_0 \tilde{x} + G_0 u \quad , \; \tilde{x}(0) = \tilde{x}_0 \\ \tilde{y} &= H_0 \tilde{x} \end{aligned} \qquad \text{(C. 2)}$$

where

$$F_0 = \left(\begin{array}{c:c} 0 & \\ \hdashline I_{n-m} & \alpha \end{array}\right) \quad , \quad H_0 = \left(0 \; \vdots \; I_m\right),$$

which is represented in the phase variable form (see Reference 66). Notice that, as far as the input-output relationship is concerned, the two systems are equivalent if noise v is not present in (C. 1). It is to be noted also that the unknown parameters in α affect the output $\tilde{y}$ in a nonlinear fashion, but the parameters in G_0 affect the output linearly. The n x m parameters in α are to be related to a set of n x m parameters that affect the output linearly.

Consider a "filter" with gain matrix K, which has a total of n x m parameters, that operates on the output y in conjunction with the system (C. 2):

$$\begin{aligned} \dot{\tilde{x}} &= F_0 \tilde{x} + G_0 u + K\left(y - H_0 \tilde{x}\right) , \; \tilde{x}(0) = \tilde{x}_0 \\ \tilde{y} &= H_0 \tilde{x} \end{aligned} \qquad \text{(C. 3)}$$

Notice that, in the absence of the measurement noise v in (C. 1), (C. 3) reduces to (C. 2) regardless of the filter gain matrix K. Let

$$\begin{aligned} F_N &= F_0 - K H_0 \\ G_N &= G_0 - SG \end{aligned} \qquad \text{(C. 4)}$$

Preceding page blank

Then, by choosing F_N and G_N, F_o and G_o are uniquely determined if K and δG are first determined. Using (C.4), (C.3) becomes

$$\dot{\tilde{x}} = F_N \tilde{x} + G_N u + (Ky + \delta G u), \quad \tilde{x}(0) = \tilde{x}_o$$

$$\tilde{y} = H_o \tilde{x} \tag{C.5}$$

It is seen from (C.5) that $\tilde{y}(t)$ is linearly related to K, δG, and $\Delta \tilde{x}_o$, where $\tilde{x}_o = \tilde{x}_{N_o} + \Delta \tilde{x}_o$. Indeed,

$$\begin{aligned}\tilde{y}(t) &= H_o\left\{ \tilde{x}_N(t) + e^{F_N t}\int_0^t e^{-F_N \tau}\left[\delta G u(\tau) + K y(\tau)\right] d\tau + e^{F_N t}\Delta\tilde{x}_o \right. \\ &= \tilde{y}_N(t) + H_o e^{F_N t}\left\{\Delta\tilde{x}_o + \int_0^t e^{-F_N\tau}\left[\delta G u(\tau) + K y(\tau) d\tau\right]\right\}\end{aligned} \tag{C.6}$$

where

$$\tilde{y}_N(t) = H_o \tilde{x}_N(t),$$

and

$$\tilde{x}_N(t) = e^{F_N t}\left[\tilde{x}_{N_o} + \int_0^t e^{-F_N \tau} G_N u(\tau) d\tau\right]$$

Let us now arrange the unknown parameters in δG and K as the components in the parameter vector p. Then

$$\tilde{y}(t) - \tilde{y}_N(t) = H_o \begin{bmatrix} \dfrac{\partial \tilde{x}}{\partial p} & \dfrac{\partial \tilde{x}}{\partial \tilde{x}_o} \end{bmatrix} \begin{bmatrix} p \\ \Delta\tilde{x}_o \end{bmatrix} \tag{C.7}$$

where the matrices $\dfrac{\partial\tilde{x}}{\partial p} = \left[\dfrac{\partial\tilde{x}}{\partial p_1} \cdots \dfrac{\partial\tilde{x}}{\partial p_{n(m+r)}}\right]$, $\dfrac{\partial\tilde{x}}{\partial\tilde{x}_o}$ are the solutions of the following linear differential equations:

$$\begin{aligned}&\frac{d}{dt}\frac{\partial\tilde{x}}{\partial p_i} = F_N \frac{\partial\tilde{x}}{\partial p_i} + \frac{\partial}{\partial p_i}(\delta G)u(t) + \frac{\partial K}{\partial p_i} y(t) \quad , \frac{\partial\tilde{x}}{\partial p_i}(0) = 0 \ , \ i = 1,2,\ldots,n(m+r) \\ &\frac{d}{dt}\frac{\partial\tilde{x}}{\partial\tilde{x}_o} = F_N \frac{\partial\tilde{x}}{\partial\tilde{x}_o} \quad , \quad \frac{\partial\tilde{x}}{\partial\tilde{x}_o}(0) = I_N\end{aligned} \tag{C.8}$$

Using the same performance index as in the measurement error methods,

$$J = \frac{1}{2}\int_0^{t_f} (y-\tilde{y})^T W (y-\tilde{y}) dt$$

the parameter vector p and $\Delta\tilde{x}_o$ can be computed by minimizing J without iteration.

$$\begin{aligned}\begin{bmatrix} p \\ \hdashline \Delta\tilde{x}_o \end{bmatrix} &= \left\{\int_0^{t_f}\left[H_o\left(\frac{\partial\tilde{x}}{\partial p} \,\vdots\, \frac{\partial\tilde{x}}{\partial\tilde{x}_o}\right)\right]^T W \left[H_o\left(\frac{\partial\tilde{x}}{\partial p} \,\vdots\, \frac{\partial\tilde{x}}{\partial\tilde{x}_o}\right)\right] dt\right\}^{-1} \\ &\quad \times \int_0^{t_f}\left[H_o\left(\frac{\partial\tilde{x}}{\partial p} \,\vdots\, \frac{\partial\tilde{x}}{\partial\tilde{x}_o}\right)\right]^T W (y - \tilde{y}_N) dt\end{aligned} \tag{C.9}$$

For the special case in which all the state variables are measured, $H_0 = I_n$ and (C.9) is further simplified. By comparing (C.8) and (C.9) with equations (4) and (5) of Reference 21, it is seen that they are identical in form with the exception of the term $\frac{\partial K}{\partial \varphi_i} y(t)$ in (C.8). Thus, this term can be replaced by $\frac{\partial F}{\partial \varphi_i} x(t)$ after the first iteration (which computes the initial estimates), and a unified estimation procedure is thereby achieved.

When measurement noise is present in (C.1), the term $\frac{\partial K}{\partial \varphi_i} y(t)$ in (C.8) is a random process and the solution (C.9) resulting from applying the linear regression is biased. This and other statistical properties of the equation-error methods presented here are discussed in greater detail in Appendix B.

APPENDIX D

COMPUTER-GENERATED DATA FOR IDENTIFICATION STUDY

Several possible techniques exist for parameter estimation of nonlinear dynamic systems, as discussed in Section III. In order to evaluate the relative merits of these various techniques, such as accuracy, convergence properties, computing time, storage requirements, etc., time histories of a system representative of the X-22A, with known parameters and noise statistics, are needed.

The subject set of data was generated by integrating a set of longitudinal, three-degree-of-freedom equations of motion. The values of the stability and control derivatives used as shown in Table D-1 were the best approximations to the "global aerodynamic" data (Reference 1). In all the cases, independent unfiltered random noise sequences with Gaussian distribution and zero mean were added to the outputs of the state variables and their derivatives, simulating measurement noise. In addition, for some of the cases the same type of noise sequences was added in the equations of motion to simulate gusts. The trim values were:

λ_0 = 30 degree	θ_0 = 2.362 degree
u_0 = 130 ft/sec	β_0 = 17.257 degree
w_0 = 5.362 ft/sec	δ_{ES_0} = -.637 in.

Both linear and nonlinear models were used. They are:

1. Nonlinear Model:

<u>Dynamic System Equations</u>

$$\begin{bmatrix} \dot{u} \\ \dot{w} \\ \dot{\theta} \\ \dot{q} \end{bmatrix} = \begin{bmatrix} X_w(u)w - qw - g\sin\theta \\ Z_w(u)w + qu + g\cos\theta \\ q \\ M_w(u)w + M_q(u)q \end{bmatrix} + \begin{bmatrix} X_0(u) & X_\lambda(u) & X_\beta(u) & X_{\delta_{es}}(u) \\ Z_0(u) & Z_\lambda(u) & Z_\beta(u) & Z_{\delta_{es}}(u) \\ 0 & 0 & 0 & 0 \\ M_0(u) & M_\lambda(u) & M_\beta(u) & M_{\delta_{es}}(u) \end{bmatrix} \begin{bmatrix} 1 \\ \Delta\lambda \\ \Delta\beta \\ \Delta\delta_{es} \end{bmatrix}$$

$$+ \begin{bmatrix} X_u(u) & X_w(u) & 0 \\ Z_u(u) & Z_w(u) & 0 \\ 0 & 0 & 0 \\ M_u(u) & M_w(u) & M_q(u) \end{bmatrix} \begin{bmatrix} u_g \\ w_g \\ q_g \end{bmatrix} \qquad \text{(D-1a)}$$

where the components u_g : w_g and q_g are the components of the disturbance or gust vector and g is the gravitational constant.

Measurement System

$$y = x + Bn$$
$$z = z' + Cm$$

where

$$x = \begin{bmatrix} u \\ w \\ \theta \\ q \end{bmatrix} \qquad z' = \begin{bmatrix} \dot{u} \\ \dot{w} \\ n_x = \frac{1}{g}(\dot{u} + q\,w) + \sin\theta \\ n_z = \frac{1}{g}(\dot{w} - q\,u) - \cos\theta \\ \dot{q} \end{bmatrix} \qquad \text{(D-1b)}$$

n and m are the noise vectors, whose elements are sequences of random numbers, and B and C are diagonal matrices made up of the standard deviations σ_i for the noise sequences. Two levels of noise were used. The one considered to be "low" has standard deviations chosen to approximate the requirements in Reference 67. The other, considered to be "moderate", is five times greater (see Table D. 2).

2. Linearized Model:

Dynamic Equations

$$\begin{bmatrix} \Delta\dot{u} \\ \Delta\dot{w} \\ \Delta\dot{\theta} \\ \Delta\dot{q} \end{bmatrix} = \begin{bmatrix} X_u & X_w & -g\cos\theta_0 & -w_0 \\ Z_u & Z_w & -g\sin\theta_0 & u_0 \\ 0 & 0 & 0 & 0 \\ M_u & M_w & 0 & M_q \end{bmatrix} \begin{bmatrix} \Delta u \\ \Delta w \\ \Delta\theta \\ \Delta q \end{bmatrix} \qquad \text{(D. 2a)}$$

$$+ \begin{bmatrix} X_\beta & X_{\delta_{es}} \\ Z_\beta & Z_{\delta_{es}} \\ 0 & 0 \\ M_\beta & M_{\delta_{es}} \end{bmatrix} \begin{bmatrix} \Delta\beta \\ \Delta\delta_{es} \end{bmatrix} + \begin{bmatrix} X_u & X_w & 0 \\ Z_u & Z_w & 0 \\ 0 & 0 & 0 \\ M_u & M_w & M_q \end{bmatrix} \begin{bmatrix} u_g \\ w_g \\ q_g \end{bmatrix}$$

Measurement System

$$\Delta y = \Delta x + \mathcal{B} n$$

$$\Delta z = \Delta z' + \mathcal{C} m$$

where (D. 2b)

$$\Delta z' = \begin{bmatrix} \Delta \dot{u} \\ \Delta \dot{w} \\ \Delta n_x = \frac{1}{g}(\dot{u} + q w) + \sin\theta - \sin\theta_0 \\ \Delta n_z = \frac{1}{g}(\dot{w} - q u) - \cos\theta + \cos\theta_0 \\ \Delta \dot{q} \end{bmatrix} \begin{matrix} \\ \\ * \\ * \\ \\ \end{matrix}$$

---

* These expressions were slightly in disagreement with (D. 2a). Thus, a term $\frac{1}{g}\Delta q \Delta w$ in Δn_x and a term $\frac{1}{g}\Delta q \Delta u$ in Δn_z will occur if acceleration measurements are used in this linearized model.

TABLE D-1 Actual Parameter Values Used in Generating Data

LINEAR EQS. OF MOTION										
NOTATION OF PARAMETERS	m_u	m_w	m_q	$m_{\delta_{es}}$	x_u	x_w	$x_{\delta_{es}}$	z_u	z_w	$z_{\delta_{es}}$
DIMENSION	1/FT-SEC	→	1/SEC	1/IN.-SEC^2	1/SEC	→	FT/IN.-SEC^2	1/SEC	→	FT/IN. SEC^2
VALUE	-.0044	-.0075	-.625	.480	-.150	.021	1.370	-.216	-.650	1.66

NONLINEAR EQS. OF MOTION

COMBINED PARAMETER		$m_o(u)$	$m_w(u)$	$m_q(u)$	$m_{\delta_{es}}(u)$	$x_o(u)$	$x_w(u)$	$x_{\delta_{es}}(u)$	$z_o(u)$	$z_w(u)$	$z_{\delta_{es}}(u)$
COMBINED DIMENSION		1/SEC^2	1/FT-SEC	1/SEC	1/IN.-SEC^2	FT/SEC^2	1/SEC	FT/IN.-SEC^2	FT/SEC^2	1/SEC	FT/IN.-SEC^2
COEFFICIENTS OF THE POLYNOMINAL IN u	u^0	.50518	-.001747	-.497	.3275	18.30	.2211	-.778	-32.17	-.2939	-.3507
	u^1	-.00306	-.0000553	-.00103	.001167	-.09167	-.001587	.0184	.91	-.00287	.01667
	u^2	-.0000062	-	-	-	-.0003	-	-	-.007	-	-
	u^3	-	-	-	-	-	-	-	-	-	-

TABLE D-2 Measurement and Process Noise Characteristics

MODEL	NOISE ADDED	LEVEL OF NOISE	DESIGNATION
CONSTANT COEFFICIENTS	MEASUREMENT NOISE ONLY	LOW	1-A
		MODERATE	1-C
	MEASUREMENT NOISE PLUS "GUST" NOISE	LOW	1-B
		MODERATE	1-D
COEFFICIENTS ARE 1st ORDER FUNCTION OF u EXCEPT $m_o(u)$, $x_o(u)$ AND $z_o(u)$ BEING 2nd ORDER	MEASUREMENT NOISE ONLY	LOW	2-A
		MODERATE	2-C
	MEASUREMENT NOISE PLUS "GUST" NOISE	LOW	2-B
		MODERATE	2-D

		STANDARD DEVIATION σ	
		LOW	MODERATE
GUSTS * (PROCESS NOISE)	u_g	1.0 FPS	5.0 FPS
	w_g	1.0 FPS	5.0 FPS
	$\dot{\theta}_g$	0.2 DEG/SEC	1.0 DEG/SEC
MEASUREMENT NOISE	u	0.5 FPS	2.5 FPS
	w	0.075 FPS	0.375 FPS
	θ	0.03 DEG	0.15 DEG
	$\dot{\theta}$	0.01 DEG/SEC	0.05 DEG/SEC
	n_x	0.001 g	0.005 g
	n_z	0.005 g	0.025 g
	$\dot{q}$	0.0025 DEG/SEC^2	0.0125 DEG/SEC^2

COMBINED PARAMETER		$m_u(u)$	$x_u(u)$	$z_u(u)$
COMBINED DIMENSION		1/FT-SEC	1/SEC	1/SEC
COEFFICIENTS OF THE POLYNOMINAL IN u	u^0	.1308	2.066	3.243
	u^1	-.0031	-.05491	-.07327
	u^2	.0000232	.000445	.00052
	u^3	$-.569 \times 10^{-7}$	$-.1187 \times 10^{-5}$	$-.1236 \times 10^{-5}$

* In integrating the equations of motion, these gusts were held constant during each integration step. Because of "zero-order hold", the variances of these gust become $\frac{\sigma^2}{\Delta t}$.

APPENDIX E

PERTURBED PARAMETERS

From equations (2.8) and (2.10), it is seen that the aerodynamic terms are expressed as third degree polynomial in forward speed u. Based on numerical experience, it was suggested by Dr. J.T. Fleck and Mr. D.B. Larson of the Computer Mathematics Department of CAL that a better numerical condition would result if the parameters were expressed in the perturbed values during the identification process. Consider a typical term in (2.10) (with reference notation R dropped).

$$m_0(u) = a_1^T \vec{u} \tag{E.1}$$

Let us express the parameter vector a_1 as a "perturbed" value, i.e.,

$$m_0(u) = a_1^T \vec{u} = \tilde{a}_1^T \vec{\tilde{u}} \tag{E.2}$$

where
$$\tilde{u} \triangleq u - u_0 \tag{E.3}$$

and
$$u_0 \triangleq u(t)\Big|_{t=t_0} = u(0)$$

Using (E.1), (E.2), and (E.3), it is readily shown that a_1 is related to $\tilde{a}_1$ by

$$a_1 = T\tilde{a}_1 \tag{E.4}$$

where

$$T = \begin{bmatrix} 1 & -u_0 & u_0^2 & -u_0^3 \\ 0 & 1 & -2u_0 & 3u_0^2 \\ 0 & 0 & 1 & -3u_0 \\ 0 & 0 & 0 & 1 \end{bmatrix} \tag{E.4a}$$

and

$$T^{-1} = \begin{bmatrix} 1 & -u_0 & u_0^2 & -u_0^3 \\ 0 & 1 & -2u_0 & 3u_0^2 \\ 0 & 0 & 1 & -3u_0 \\ 0 & 0 & 0 & 1 \end{bmatrix} \tag{E.4b}$$

These transformation pairs are the same for all the 16 parameter vectors in (2.10).

APPENDIX F

DESIGN OF INPUT

The design of input signals for parameter identification has long been recognized as an important ingredient to a successful identification of parameters. However, design procedures based on optimization techniques have not been discussed until recently (References 68-71).

In our early numerical experiments using sensitivity of the aircraft motion to parameter variation as a criterion, we found that a better input function did exist and did drastically improve the parameter estimation. Tables F-1 and F-2 show the results of applying an initial estimator and the linear Kalman program to a system responding to two different control inputs. The results clearly show the effects of the control input on the quality of the parameter identified.

In fact, if we use mean square estimation error as the criterion for the quality of the parameter estimation, the best performance for a given set of input functions (and hence the data)is given by the Cramer-Rao lower bound (Reference 29). Therefore, the design of inputs may be formulated by attempting to minimize the Cramer-Rao lower bound. Since the Cramer-Rao lower bound is related to the inverse of a norm of the sensitivity vector functions, the problem then amounts to a maximization of the sensitivity vector functions.

To make the minimization problem meaningful, constraints on the magnitudes of inputs and the state variables must be added so that the equations of motion for the vehicle will remain valid. Unfortunately, the design of an input, when formulated in this manner, becomes a typical optimal control problem requiring a solution of a two-point boundary value problem.

Instead of solving the two-point boundary value problem associated with a large number of differential equations, we present first an attempt to find a suboptimal solution using a technique similar to that used for parameter identification. We then present an attempt to solve the actual two-point boundary value problem with a smaller number of parameters.

Statement of the Problem

Consider the dynamic system and the measurement system (F. 1) and (F. 2) respectively, i. e.:

$$\dot{x} = f(x, p, m), \qquad x(0) = x_o$$
$$y = h(x, p, m) + v(t) \tag{F. 1}$$

where as usual $E\{v\} = 0$ and $E\{v(t)v^T(\tau)\} = R\,\delta(t-\tau)$ (F. 2)

It is desired to minimize some norm of the Cramer-Rao lower bound matrix for the covariance of the estimation error, where

$$CR = \left\{ \int_0^{t_f} \left[\frac{\partial h}{\partial x} \frac{\partial x}{\partial x_o} \,\Big|\, \frac{\partial h}{\partial p} + \frac{\partial h}{\partial x} \frac{\partial x}{\partial p} \right]^T R^{-1} \left[\frac{\partial h}{\partial x} \frac{\partial x}{\partial x_o} \,\Big|\, \frac{\partial h}{\partial p} + \frac{\partial h}{\partial x} \frac{\partial x}{\partial p} \right] dt \right\}^{-1} \tag{F. 3}$$

subject to the constraints on the sensitivity equations (F. 4) and (F. 5) i. e.,

$$\frac{d}{dt}\left(\frac{\partial x}{\partial x_o}\right) = \left(\frac{\partial f}{\partial x}\right)\left(\frac{\partial x}{\partial x_o}\right), \qquad \frac{\partial x}{\partial x_o}(0) = I_n \tag{F. 4}$$

$$\frac{d}{dt}\left(\frac{\partial x}{\partial p}\right) = \left(\frac{\partial f}{\partial x}\right)\left(\frac{\partial x}{\partial p}\right) + \frac{\partial f}{\partial p}, \qquad \frac{\partial x}{\partial p}(0) = 0 \tag{F. 5}$$

and to the constraints

$$|M| \leq M \quad \text{and} \quad |X| \leq X \tag{F. 6a}$$

or

$$\int_0^{t_f} Q(x, m)\, dt \leq K \tag{F. 6b}$$

The constraints (F. 6) are required for the mathematical model (F. 1) and (F. 2) to remain valid. In equation (F. 6), M and X are constant vectors; K is a scalar constant; and Q is some cost function.

A Suboptimal Input Design

The problem as stated in the preceding pages is a typical optimal control problem for a nonlinear system with a large number of equations. Indeed, even if one uses the linearized representation for VTOL aircraft dynamics, for instance, the input design for a ten-parameter problem becomes an optimal control problem with constraints on 44 differential equations (4 original equations of motion plus 40 sensitivity equations) instead of just the original fourth-order system. This is a formidable two-point boundary value problem!

To circumvent this difficulty, one may seek a much simpler suboptimal solution. Instead of choosing the control input function from all those admissible, one can restrict oneself to choose from those which are a linear combination of the solutions to a set of chosen linear time-invariant differential equations. This reduces the two-point boundary value problem to a much simpler problem of parameter minimization, much the same as the measurement error parameter identification problem. Thus, the design of the input can be carried out using the existing computer program for identification with some modifications.

Consider a linear time-invariant system

$$\dot{x} = Fx + Gm , \qquad x(0) = x_0 \tag{F.7a}$$

$$y = x + v \tag{F.7b}$$

Then a suboptimal control problem can be formulated as follows: Find $m(t), 0 \leq t \leq t_f$ to minimize

$$J = \frac{1}{2} \left\{ \sum_{i=1}^{q} \lambda_i \, C_{ii}^{2} + \lambda_{q+1} \int_0^{t_f} (x^T Q_1 x + m^T Q_2 m) dt \right\} \tag{F.8}$$ *

* C_{ii}^2 was used instead of $|C|_{ii}$ in the computer program. However, this should not adversely affect the results, as the diagonal terms of C are all positive anyway.

subject to the constraints

$$\dot{x} = F_N x + G_N m, \qquad x(0) = x_0 \tag{F.9a}$$

$$\dot{S}_N = F_N S_i + F_{\bar{p}_i} x + G_{\bar{p}_i} m, \qquad S_i(0) = 0, \quad i = 1, 2, \ldots, q \tag{F.9b}$$

where $C_R \triangleq \left\{ \int_0^{t_f} [S_1\ S_2 \cdots S_q]^T R^{-1} [S_1, S_2, \cdots S_q]\, dt \right\}^{-1} \triangleq (C_{R_{ij}})$

and the control functions $m(t)$ are restricted to those that can be generated from a linear system of known form,

$$\begin{aligned} \dot{z} &= A_N z \qquad z(0) = z_0 \\ m &= B z \end{aligned} \tag{F.10}$$

where the elements in B and the initial vector z_0 are unknown parameters to be determined by minimizing J.

NOTE: F_N, G_N are nominal system matrices, $F_{\bar{p}_i}$, $G_{\bar{p}_i}$ are partial derivatives of F and G with respect to stability and control derivatives to be identified.

The suboptimal input design problem as formulated above is a typical parameter optimization problem such as the measurement error method. Table F-3 shows a sample run using the conjugate gradient method. In this computer run, the following parameters were used.

$$z_0 = (1, 1, \cdots, 1)^T$$

$$q = 10; \qquad \lambda_i = 1, \quad i = 1, 2, \cdots, 10$$

$$\lambda_{11} = 0.01$$

$$R^{-1} = \begin{bmatrix} 1.384 & 0 & 0 & 0 \\ 0 & 7.716 & 0 & 0 \\ 0 & 0 & 67800 & 0 \\ 0 & 0 & 0 & 405700 \end{bmatrix}$$

$$x = (u, w, q, \theta)^T$$

$$Q_1 = I_4, \qquad Q_2 = 10 I_2, \qquad \Delta t = 0.1, \qquad t_f = 5.$$

and F_N and G_N are as shown in Appendix D.

Two cases were considered: one utilized 4 modes and the other one utilized 8 modes. The initial guess values and the final values for $\mathcal{B}$ as well as the time histories for the control inputs $m(t) \triangleq \delta_{ES}(t)$ were also shown in the table. Notice that, although the signal power is smaller for the 8-mode case than for the 4-mode case, the $\mathcal{CR}$ values are smaller for the 8-mode case, resulting in better parameter identification.

In the above numerical example, one may, of course, vary the weighting λ_{11} so that the final input power, $\int_0^{t_f} \left(B_f e^{A_w t}\right)^2 dt$, or signal power be made approximately equal to those of the initial input power, $\int_0^{t_f} (B_0 e^{A_w t}) dt$. However, due to limited time and money, this experimentation was not carried out.

We now discuss another method which is a direct solution to the actual two-point boundary value problem.

An Optimal Input Design Method

Instead of minimizing some norm of the Cramer Rao matrix, one may choose to maximize* some form of Fisher's information matrix (Reference 69).

$$\int_0^{t_f} \left[S_1 S_2 \cdots S_q\right]^T R^{-1} \left[S_1 \cdots S_q\right] dt$$

For instance, we may choose to maximize the trace of the above Fisher's information matrix, or equivalently, to minimize the negative of its trace. This would be equivalent to maximizing the sensitivities of the desired parameters. The easiest way to do this is to increase the signal-to-noise ratio of the measured responses by increasing the size of any given input. However, since the noise level is fixed, increasing the signal-to-noise ratio eventually leads to the point where the responses become too large to control or the model chosen for the airplane is no longer valid. In the example

* Goodwin (Reference 70) has pointed out that they are not exactly equivalent.

using the preceding suboptimal approach to the input design problem, increasing the signal level was essentially all that was accomplished. With that method, a final input had to be made up from a given set of base vector inputs, and the shape of the final input is not altered significantly. When the optimal approach is taken, however, the final input does not depend on any given base vector of inputs, and does change the shape of the initial input.

The optimal approach is basically a solution to a two-point boundary value problem using the conjugate gradient method to update the initial input (Reference 72). In this method we wish to minimize the performance index J :

$$J = -tr\left[\int_0^{t_f}\left[S_1, S_2 \cdots S_r\right]^T R^{-1}\left[S_1\, S_2\, \ldots\, S_r\right] dt\right] + c\int_0^{t_f} x^T R^{-1} x\, dt \qquad (F.11)$$

The first terms above are the negative of the trace of the Fisher information matrix, and the last term is a penalty function of the state vector X, which is added to keep the responses of the airplane within reasonable bounds. C is an inputted constant which determines the weight given to the penalty function. The system is:

$$\dot{x}_a = F_a x_a + G_a m \qquad x_a(0) = 0 \qquad (F.12)$$

where

$$x_a = \left(x^T\, S_1^T\, S_2^T \cdots S_q^T\right)^T \qquad (F.13a)$$

$$\dot{x} = Fx + Gm, \quad x(0) = 0 \qquad (F.13b)$$

$$\dot{S}_i = FS_i + \frac{\partial F}{\partial p_i} x + \frac{\partial G}{\partial p_i} m, \quad S_i(0) = 0 \quad i = 1, 2, \cdots, q \qquad (F.13c)$$

$$F_a = \begin{bmatrix} F & 0 & 0 & \cdots & 0 \\ \frac{\partial F}{\partial p_1} & F & 0 & & 0 \\ \frac{\partial F}{\partial p_2} & 0 & F & & \cdot \\ \vdots & & & \ddots & \vdots \\ \frac{\partial F}{\partial p_q} & 0 & \cdots & & F \end{bmatrix} \tag{F.13d}$$

$$G_a = \begin{bmatrix} G \\ \frac{\partial G}{\partial p_1} \\ \vdots \\ \frac{\partial G}{\partial p_q} \end{bmatrix} \tag{F.13e}$$

x - 4 x 1 state vector
m - 2 x 1 control vector
F - 4 x 4 stability derivative matrix
G - 4 x 2 control matrix
S_i - 4 x 1 sensitivity vector of parameter, $i = 1, 2, \cdots q$
p_i - parameter of interest, $i = 1, 2, \ldots q$

Define the Hamiltonian H,

$$H(t) = \lambda^T \left[F_a x_a + G_a m \right] - \sum_{i=1}^{r} S_i^T W S_i + x^T C R^{-1} x \tag{F.14}$$

where

$$\dot{\lambda}(t) = -\frac{\partial H}{\partial x_a}$$

or

$$\dot{\lambda}(t) = -F_a^T \lambda + 2 \begin{bmatrix} CR^{-1} & & & 0 \\ & R^{-1} & & \\ & & R^{-1} \ddots & \\ 0 & & & R^{-1} \end{bmatrix} x_a, \quad \lambda(t_f) = 0 \tag{F.15}$$

The gradient is

$$g(t) = \frac{\partial H}{\partial u} = G_i^T \lambda(t) \tag{F.16}$$

To update the control, $m(t)$, the standard conjugate gradient method is used: (i = iteration no.)

$$u_i(t) = u_{i-1}(t) - \alpha_i \, a_i(t) \tag{F.17}$$

where $a_1(t) = g_1(t)$

$$a_i(t) = g_i(t) + \beta_{i-1} \, a_{i-1}(t) \qquad i \neq 1 \tag{F.18}$$

$$\beta_{i-1} = \frac{\int_0^{t_f} [g_i(t)]^2 dt}{\int_0^{t_f} [g_{i-1}(t)]^2 dt} \tag{F.19, F.20}$$

In the iteration scheme the control, $m(t)$, is also bounded at chosen values, so the inputs will not become unrealistic.

The procedure is to first initialize the control input, then evaluate $x_a(t)$ by integrating (F.12) forward in time. Next, $\lambda(t)$ is evaluated by integrating (F.15) backward in time from t_f. Now $g(t)$ is evaluated from (F.16) and $m(t)$ is updated by (F.17)-(F.20). J is calculated and the iteration is stopped if it has reached a minimum; if not, the procedure is repeated by evaluating $x_a(t)$ with the new $m(t)$.

For a preliminary look at this method it was decided to use a linear model of the X-22 with just δ_{ES} control, and to maximize the sensitivities of M_u, M_w, M_q, and Z_w. This reduces the size of information matrix down to a 4 x 4 matrix.

Figure F-1 shows a computer run which utilized the following parameters.

$$\mathcal{C} = 10{,}000$$

$$R^{-1} = \begin{bmatrix} 1.4 & 0 & 0 & 0 \\ 0 & 9.0 & 0 & 0 \\ 0 & 0 & 70{,}000 & 0 \\ 0 & 0 & 0 & 400{,}000 \end{bmatrix}$$

$$\Delta t = 0.1, \qquad t_f = 5 \text{ sec}, \qquad m(t) = \Delta \delta_{es}(t)$$

and the F and G are the same as the preceding example. The initial control perturbation was $\Delta \delta_{ES} = 0.12$ inch. Notice that the initial and final signal to noise ratios

$$\int_0^{t_f} x^T R^{-1} x \, dt$$

were approximately the same, but that the sensitivities of the parameters were doubled. It is interesting to note that the control reversing occurred at approximately 1.5 seconds which is about one-half period of the oscillatory mode of the X-22A at this flight condition.

Concluding Remarks

As a result of our studies on input design discussed in this Appendix, the following remarks are in order:

(i) Sensitivity of the aircraft motion to parameter variation is a good criterion for the input design. An increase in sensitivity results in an increase in parameter identifiability.

(ii) Input design using the exact optimization technique is not practical for all the parameters simultaneously; however, suboptimal techniques appear to be feasible by grouping the parameters into several groups with a smaller number of parameters in each group for sequential parameter identification. Also, cut-and-try methods based on past experience and using sensitivity as the criteria have been demonstrated to be practical.

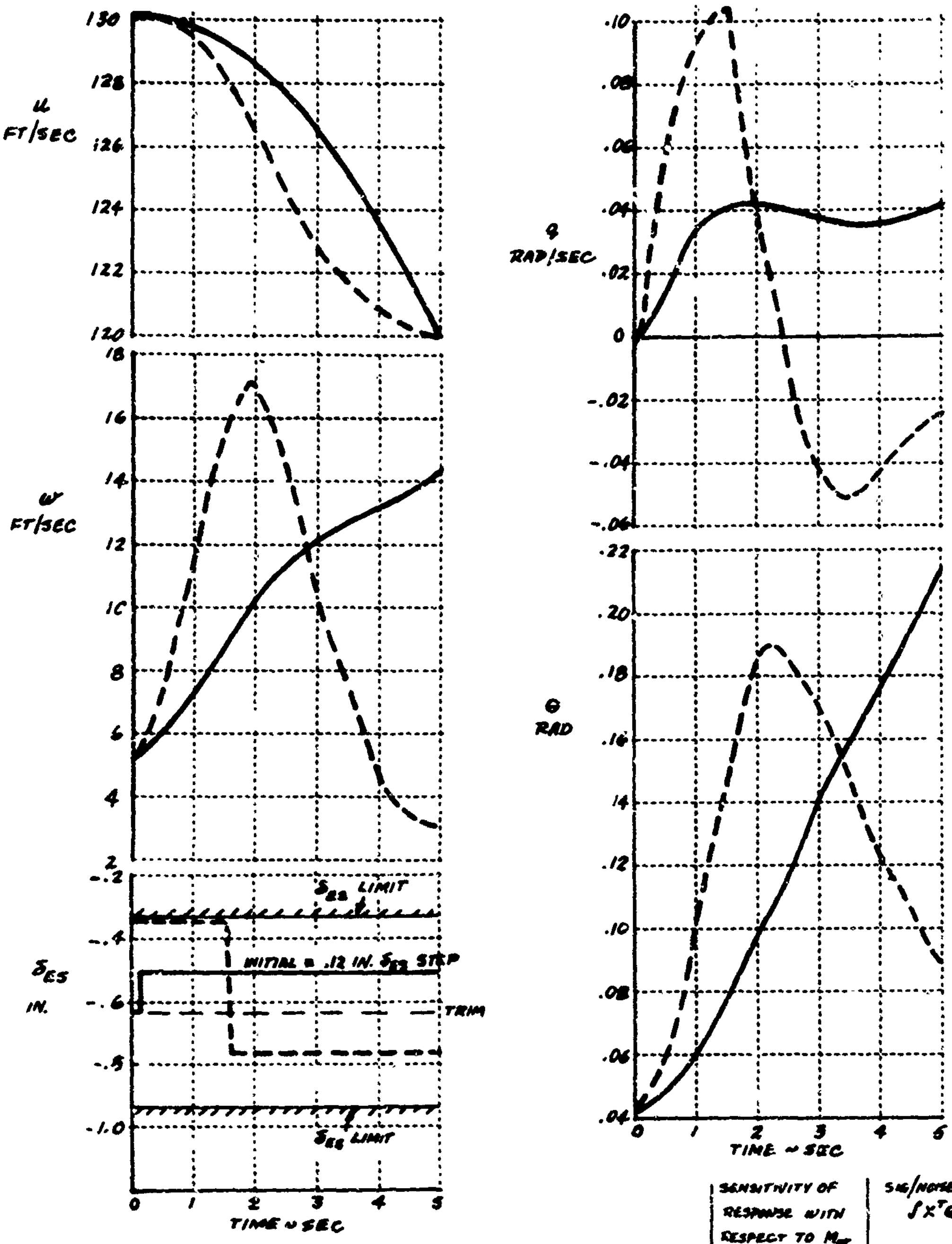

	SENSITIVITY OF RESPONSE WITH RESPECT TO M_w	SIG/NOISE RATIO $\int X^T Q X$
——— INITIAL INPUT	1.2×10^9	$.212 \times 10^6$
– – – FINAL INPUT	2.5×10^9	$.220 \times 10^6$

Input Design:

1 Signal to noise ratio of response stays approximately the same

2 Sensitivities doubled (i.e., the variance of the identified parameter would be one half)

Figure F-1 State Responses to Designed Input

TABLE F-1

EFFECT OF INPUT ON THE INITIAL ESTIMATOR
(EQUATIONS-OF-MOTION METHOD)

PARAMETER	TRUE VALUE	OLD INPUT		NEW INPUT	
		MODERATE MEAS. NOISE 1 - C	MODERATE MEAS. AND PROCESS NOISE 1 - D	MODERATE MEAS. NOISE 1 - C	MODERATE MEAS. AND PROCESS NOISE 1 - D
M_u	-.0044	-.001711	-.00319	-.004037	-.004131
M_w	-.0075	-.002301	-.00619	-.006573	-.006778
M_q	-.6250	-.548800	-.29660	-.656700	-.698900
$M_{\delta_{es}}$	.4800	.299000	.40470	.459800	.491400
X_u	-.1500	-.065310	-.09615	-.139200	-.148500
X_w	.0210	.188900	.13240	.004557	.021590
$X_{\delta_{es}}$	1.3700	-3.571600	-3.00800	.626000	1.262000
Z_u	-.2160	-.076190	-.18450	-.197700	-.198800
Z_w	-.6500	-.365700	-.60450	-.607700	-.625400
$Z_{\delta_{es}}$	1.6600	-7.506000	3.90700	.265300	1.249000
INPUT		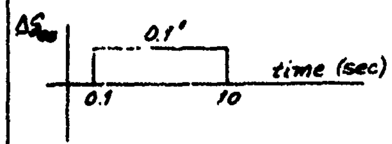		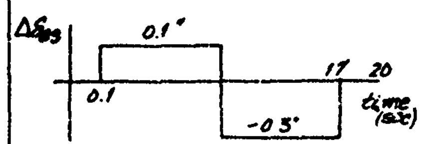	

TABLE F-2

EFFECTS OF INPUT ON KALMAN FILTERING *

PARAMETER	TRUE PARAMETER VALUES	1-D DATA: MODERATE MEASUREMENT AND PROCESS NOISE	
		OLD INPUT**	NEW INPUT*
M_u	-.0044	-.00424	-.00454
M_w	-.0075	-.00847	-.00749
M_q	-.6250	-.32170	-.74280
$M_{\delta_{es}}$	.4800	.49670	.52260
X_u	-.1500	-.19650	-.15420
X_w	.0210	-.02290	.01495
$X_{\delta_{es}}$	1.3710	.61270	1.68330
Z_u	-.2160	-.16160	-.19710
Z_w	-.6500	-.59160	-.61060
$Z_{\delta_{es}}$	1.6600	4.73220	1.07400

* Without Accel. Measurements

** Old Input

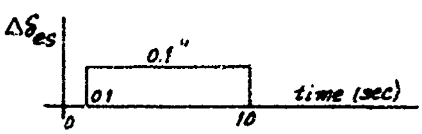

New Input

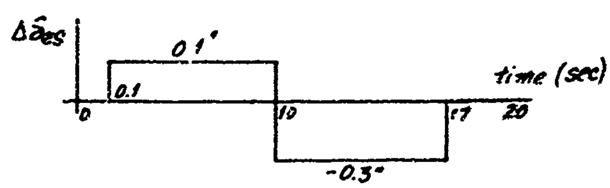

TABLE F-3 A Sample Run of Suboptimal Input Design

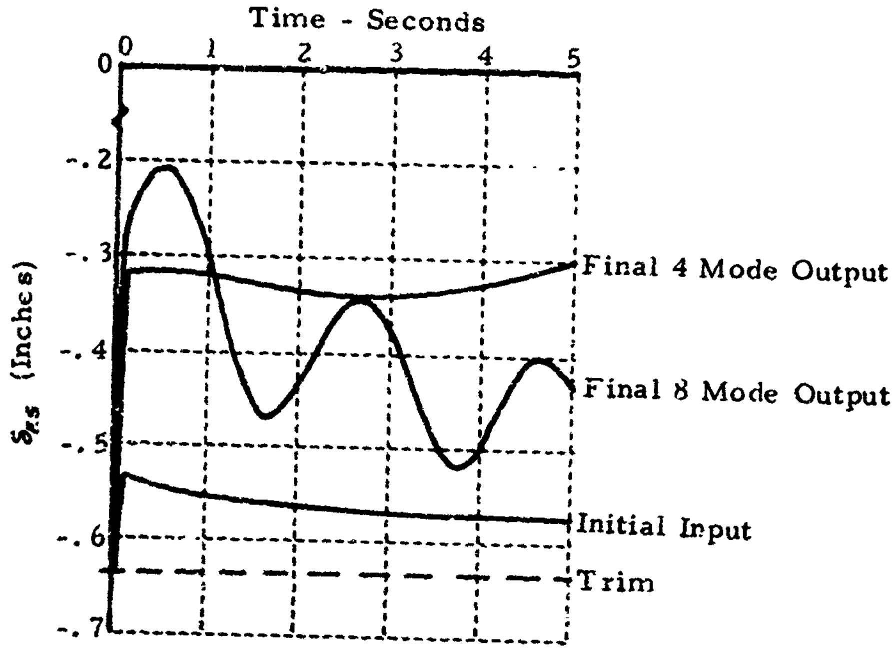

$$\delta_{ES} = \mathcal{B} e^{A_N t}$$

$$z_0 = (1, 1, \ldots, 1)^T$$

4 Mode Case

$$\mathcal{B}_o = (.1, 0, 0, 0)$$

$$\mathcal{B}_f = (.179, .128, .0065, .0043)$$

$$A_N = \begin{bmatrix} -1 & 0 & 0 & 0 \\ 0 & 1 & 0 & 0 \\ 0 & 0 & 0 & 1 \\ 0 & 0 & -1.44 & -.096 \end{bmatrix}$$

8 Mode Case

$$\mathcal{B}_c = (.1, 0, 0, 0, \ldots, 0)$$

$$\mathcal{B}_f = (.213, .033, .0068, .0018, .0919, .019, .014, -.0336)$$

$$A_N = \begin{bmatrix} -.1 & 0 & 0 & 0 & 0 & 0 & 0 & 0 \\ 0 & -1 & 0 & 0 & 0 & 0 & 0 & 0 \\ 0 & 0 & 0 & 1 & 0 & 0 & 0 & 0 \\ 0 & 0 & -1.44 & -.096 & 0 & 0 & 0 & 0 \\ 0 & 0 & 0 & 0 & -.2 & 0 & 0 & 0 \\ 0 & 0 & 0 & 0 & 0 & -.2 & 0 & 0 \\ 0 & 0 & 0 & 0 & 0 & 0 & 0 & 1. \\ 0 & 0 & 0 & 0 & 0 & 0 & -9. & -.24 \end{bmatrix}$$

TABLE F-3

A SAMPLE RUN OF SUBOPTIMAL INPUT DESIGN (CONTINUED)

PARAMETER	TRUE VALUE	INITIAL	4 MODES		8 MODES	
		$\sqrt{10\, c e_{ii}}$	$\sqrt{10\, c e_{ii}}$	EQ. OF MOTION ESTIMATES	$\sqrt{10\, c e_{ii}}$	EQ. OF MOTION ESTIMATES
M_u	-[illegible]	.00348	.0011	-.0015	.0008	-.0023
M_w	-.[illegible]	.00438	.0013	-.0046	.0010	-.0053
M_q	-.6250	.66780	.2045	-.8430	.1533	-.6620
$M_{\delta_{es}}$	.4800	.08780	.0210	.5100	.0206	.4700
X_u	-.1500	.57430	.1772	-.1020	.1410	-.1140
X_w	.0210	.51150	.1584	.0610	.1306	.0490
$X_{\delta_{es}}$	1.3700	11.20000	3.3960	.8130	3.0300	1.0430
Z_u	-.2160	.29670	.0916	-.1530	.0727	-.1730
Z_w	-.6500	.27590	.0854	-.5860	.0692	-.6140
$Z_{\delta_{es}}$	1.6600	6.77800	2.0530	.1560	1.7920	.8420
J		87.13000	17.20		13.75	

APPENDIX G

MATHEMATICAL PRELIMINARIES

In this appendix, several pertinent properties of Gaussian random variables are first discussed. The importance of the conditional expectation to parameter estimation is then stressed. Finally, some useful properties and formulae for Gaussian conditional expectation and covariance are given. These formulae are necessary for the development of locally iterated filter-smoother and fixed-point smoothing algorithms.

Some Properties of Joint Gaussian Random Variables

Let x be a random vector of n-variables x_i, $i = 1, 2, \ldots, n$. The random variables x_i are said to be jointly normal if their joint density function $f(x) \triangleq f(x_1 x_2 \ldots x_n)$ is

$$f(x) = \frac{1}{\sqrt{2\pi^n}\,|P_{xx}|^{\frac{1}{2}}} \exp\left\{-\frac{1}{2}(x-\bar{x})^T P_{xx}^{-1}(x-\bar{x})\right\} \tag{G.1}$$

where the mean $\bar{x}$ and the covariance matrix P_{xx} are defined by

$$\bar{x} = E(x) = E\begin{bmatrix} x_1 \\ x_2 \\ \vdots \\ x_n \end{bmatrix} = \begin{bmatrix} \bar{x}_1 \\ \bar{x}_2 \\ \vdots \\ \bar{x}_n \end{bmatrix} \tag{G.2a}$$

$$P_{xx} = E\left\{(x-\bar{x})(x-\bar{x})^T\right\}$$

$$= E\begin{bmatrix} (x_1-\bar{x}_1)^2, & (x_1-\bar{x}_1)(x_2-\bar{x}_2), & \cdots, & (x_1-\bar{x}_1)(x_n-\bar{x}_n) \\ (x_2-\bar{x}_2)(x_1-\bar{x}_1), & (x_2-\bar{x}_2)^2, & \cdots, & (x_2-\bar{x}_2)(x_n-\bar{x}_n) \\ \text{---} & \text{---} & \text{---} & \text{---} \\ (x_n-\bar{x}_n)(x_1-\bar{x}_1), & (x_n-\bar{x}_n)(x_2-\bar{x}_2), & \cdots, & (x_n-\bar{x}_n)^2 \end{bmatrix} \tag{G.2b}$$

E is the expectation operator and $|P_{xx}|$ is the determinant of P_{xx}. Note that the density function $f(x)$ in (G. 1) is characterized by only two parameters, the mean $\bar{x}$ and the covariance matrix P_{xx}. For this reason, it is of symbolic simplicity to express the sensity function (G. 1) as

$$f(x) = N(\bar{x}, P_{xx}) \tag{G. 3}$$

Consider next the random vector $u = (x^T, y^T)^T$ where x is a n-vector and y is m-vector. Assume that x and y are jointly normal. Then

$$f(u) = N(\bar{u}, P_{uu}) \tag{G. 4}$$

where by definition

$$\bar{u} = \begin{pmatrix} \bar{x} \\ \bar{y} \end{pmatrix} \tag{G. 5a}$$

$$P_{uu} = \begin{pmatrix} P_{xx} & P_{xy} \\ P_{yx} & P_{yy} \end{pmatrix} \tag{G. 5b}$$

It is easy to establish the the following important properties of the joint Gaussian random variables.

(i) A linear transformation of Gaussian random variables yields Gaussian random variables. For example, let $w = Tu$, where T is a linear transformation. Then

$$f(w) = N(T\bar{u}, TP_u T')$$

(ii) Let x, y be jointly normal. If x and y are uncorrelated, then x and y are independent. This fact is readily seen from (G. 1), (G. 4), and (G. 5).

(iii) If x, y are jointly normal with joint density function (G. 4), then x and y are both marginally normal with marginal density functions $f(x) = N(\bar{x}, P_{xx})$ and $f(y) = N(\bar{y}, P_{yy})$ respectively. To show that x is normal one simply chooses the transformation T to be

$$T = \begin{pmatrix} I_x & 0 \\ -P_{yx} P_{xx}^{-1} & I_y \end{pmatrix} \quad \text{(G.6)}$$

where I_x is an identity matrix with the same dimensions as x. Similarly, to show that y is normal, one chooses

$$T = \begin{pmatrix} I & -P_{xy} P_{yy}^{-1} \\ 0 & I \end{pmatrix} \quad \text{(G.7)}$$

(iv) Let x, y be jointly normal with joint density function (G.4). Then the conditional random vector x|y (x given y) is also normal. Indeed, using $f(x|y) = \frac{f(x,y)}{f(y)}$ it can be shown that

$$f(x|y) = N(m, Q) \quad \text{(G.8)}$$

where

$$m = E\left[x|y\right] = \bar{x} + P_{xy} P_{yy}^{-1} (y - \bar{y}) \quad \text{(G.9a)}$$

$$Q = P_{x|y} = P_{xx} - P_{xy} P_{yy}^{-1} P_{yx} \quad \text{(G.9b)}$$

In particular, if x and y are uncorrelated, then $f(x|y) = f(x) = N(\bar{x}, P_{xx})$. Thus, the condition on y is removed.

(v) Let x, y, z be jointly normal with joint density function

$$f(v) = N(\bar{v}, P_{vv}) \quad \text{(G.10)}$$

where

$$v^T = (x^T, \; y^T, \; z^T) \quad \text{(G.11a)}$$

$$\bar{v}^T = (\bar{x}^T, \; \bar{y}^T, \; \bar{z}^T) \quad \text{(G.11b)}$$

$$\mathcal{P}_{vv} = \begin{pmatrix} \mathcal{P}_{xx} & \mathcal{P}_{xy} & \mathcal{P}_{xz} \\ \mathcal{P}_{yx} & \mathcal{P}_{yy} & \mathcal{P}_{yz} \\ \mathcal{P}_{zx} & \mathcal{P}_{zy} & \mathcal{P}_{zz} \end{pmatrix} \qquad \text{(G. 11c)}$$

If x, y are individually uncorrelated with z, then x and y are jointly independent of z. This is easily seen from (G. 5b) and (G. 11c).

These important properties will be utilized to establish some useful properties of Gaussian conditional expectation and conditional covariance later. The importance of the conditional expectation is discussed in the next section.

Fundamental Theorems of Estimation

Problem Statement

The general estimation problem can be formulated as follows: Let x be the state vector (which may include the unknown parameters) to be estimated. A set of measurements $y_1, y_2, \ldots, y_N$ is made which are related to the state by

$$y_i = h(x_i, v_i) \; , \; i = 1, 2, \ldots, N \qquad \text{(G. 12)}$$

where

y_i is the measurement vector, an m-vector

x_i is the state vector, an n-vector

v_i is the noise vector, an m-vector

The problem is to estimate x_k, $1 \leq k \leq N$ based on the observation $Y(n) \triangleq (y_1^T, y_2^T, \ldots, y_n^T)^T$, $1 \leq n \leq N$. Depending on whether $k > n$, $k = n$, or $k < n$, the problem is said to be of prediction, of filtering, or of smoothing respectively.

Criteria of Estimation

Denote an estimate $\hat{x}_{t|n}$. Since there is available only a set of measurements $Y(n)$, $1 \leq n \leq N$, $\hat{x}_{t|n}$ must be of some function of the observation $Y(n)$, i.e.,

$$\hat{x}_{t|N} = F(Y(n)) \tag{G.13}$$

If F is a linear function of $Y(n)$, it is called a linear estimator of x_t.

Regardless of whether it is linear or nonlinear, an estimator depends on the criterion used for the estimation. The criteria of estimation may be divided into two major groups: Bayesian and non-Bayesian. Bayesian criteria stem from the Bayesian estimation philosophy which assumes that the entire information available to an estimator is contained in the a posteriori density function $f(x_t/Y(n))$. On the other hand, the non-Bayesian criteria are based on the likelihood function $\log_e f(Y(n)/x_t)$. Merits or debits of the Bayesian and non-Bayesian criteria are long standing problems in statistics. Discussions on these are beyond the scope of this report. The approach we shall take here is Bayesian. Consider the estimation error

$$\tilde{x}_t \triangleq x_t - \hat{x}_{t|n} \tag{G.14}$$

Since $\hat{x}_{t|n}$ is a random vector (some function of random vector $Y(n)$), $\tilde{x}_t$ is also a random vector. Thus, the ideal situation that $\tilde{x}_t = 0$ cannot be met. Rather, we use some criteria which are average values of some scalar functions of $\tilde{x}_t$. For instance, consider a commonly used mean square error criterion

$$L_1 \triangleq E\|\tilde{x}_t\|^2 \tag{G.15}$$

i.e., we want to estimate the random vector x_t by a suitable function $F(Y(n))$ of $Y(n)$ so that the mean square estimation error

$$E\left\{\left[x_t - F(y(n))\right]^2\right\} = \int_{-\infty}^{\infty}\int_{-\infty}^{\infty} \left[x_t - F(y(n))\right]^2 f(x_t, Y(n))\, dx_t\, dY(n) \tag{G.16}$$

is minimum. We shall see later that the mean square error criterion is only a special case of a broader criterion called an admissible function. $L_a \triangleq L_a(\tilde{x}_k)$ is said to be an admissible function, if:

(i) L_a is a scalar function of $\tilde{x}_k$

(ii) $L_a(0) = 0$

(iii) $L_a(\tilde{x}_k^{\alpha}) \geq L_a(\tilde{x}_k^{\beta})$ whenever $\rho(\tilde{x}_k^{\alpha}) \geq \rho(\tilde{x}_k^{\beta})$ where ρ is a scalar valued, non-negative, convex function of $\tilde{x}_k$

(iv) $L_a(\tilde{x}_k) = L_a(-\tilde{x}_k)$

Note that L_a as defined in (iii) need not be a convex function. Some examples of L_a are depicted in the following figure.

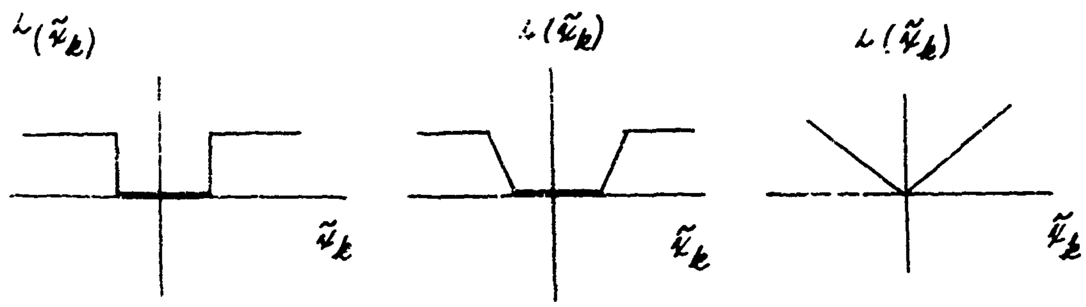

Clearly, L_f is a member of L_a.

Some Important Theorems of Estimation

Three important theorems are given in the following. These are the basis for our subsequent development.

Theorem 1: The conditional mean $E\left[x_k \mid Y(n)\right]$ is the optimal estimator for the criterion function L_f in (G.15) for any conditional density function $f(x_k \mid Y(n))$.

This theorem is very easy to establish; one simply substitutes

$$f\left(x_k, Y(n)\right) = f\left(x_k \mid Y(n)\right) f\left(Y(n)\right)$$

into (G. 16), yielding

$$E\left\{\left[x_t - F(Y(n))\right]^2\right\} = \int_{-\infty}^{\infty} dY(n) f(Y(n)) \int_{-\infty}^{\infty} \left[x_t - F(Y(n))\right]^2 f\left(x_t \mid Y(n)\right) dx_t$$

From this equation, it is readily seen that $\hat{x}_{t|n} = E\left(x_t \mid Y(n)\right)$ minimizes the second integral, and hence, since the integral above is non-negative, the criterion function L_1. In the above theorem, the criterion function L_1 can be relaxed considerably at the expense of imposing some constraints on the conditional density functions. Shereman (Reference 42) has established the following important theorem.

Theorem 2: If the conditional density $f\left(x_t \mid Y(n)\right)$ is symmetrical and unimodal. then the conditional mean is the optimal estimate for all the admissible criteria functions L_a.

The importance of theorems 1 and 2 is further enhanced by the fact that the conditional mean is an efficient estimator, i.e., the conditional mean is unbiased and minimum variance. Indeed, it is easy to establish (Reference 31):

Theorem 3: The conditional mean is an efficient estimator (i.e., unbiased and minimum variance).

We see from theorems 1 - 3 that the conditional mean is a very desirable estimator. In order to obtain the estimate, one has to first obtain the conditional density function. However, as we shall see later, the availability of the conditional density function is often one thing, but the evaluation of its mean is quite another, and this difficulty is often encountered in nonlinear problems.

It is also appropriate here to point out that if the conditional density function $f\left(x_t \mid Y(n)\right)$ is symmetric and unimodal, then its mean and mode coincide. The conditional mode is closely related to the weighted least square criteria as discussed in Section III.

The importance of the Gaussian case will now be discussed. Clearly, a normal density function is symmetrical and unimodal. Thus, if x_t and $Y(n)$ are jointly normal we see from (G.8) and (G.9) that $f\left(x_t \middle| Y(n)\right)$ is also normal. Thus, the conditional mean $\hat{x}_{t|n} = E\left(x_t \middle| Y(n)\right)$ is the optimal estimate for all the admissible criteria functions L_a. Furthermore, we also see from (G.9a) that this estimate $\hat{x}_{t|n}$ is a linear function of the available data $Y(n)$. Thus, for the Gaussian case, the conditional mean is a linear estimator. Further, it is optimum with respect to all the admissible criteria.

Before we proceed to use these theorems to develop our filter-smoother algorithms, we shall first present some useful formulae pertinent to the Gaussian conditional mean and covariance in the next section.

Some Useful Formulae for Gaussian Conditional Expectation and Conditional Covariance

From the fundamental theorems of estimation discussed in the preceding section, we see that the conditional expectation is of paramount importance in our subsequent development of the estimation algorithms. We will see later that the conditional covariance is also an important parameter for assessing the quality of the estimate. For use in subsequent developments we present here several useful properties and formulae for Gaussian conditional expectation and conditional covariance.

(i) The conditional expectation of x given y, $E(x|y)$ is a Gaussian random vector which is a linear function of y. This is readily seen from (G.9a).

(ii) The random vector $\tilde{x} = x - E(x|y)$ is independent of any linear transformation of y. Since the random vector $x - E(x|y)$ has a zero mean (this is easy to see, since $E\left[E(x|y)\right] = E(x)$), the above statement implies that the random vector x, which is the estimate error of x given y, is orthogonal to any linear transformation of y.

This is one of the most important properties of the minimum mean square estimation.

(iii) Let x, y, and z be jointly normal with joint density function as given by (G. 10). Then the covariance of x, y given z is

$$\begin{aligned} P_{x,y/z} &\triangleq E\left\{[x-E(x/z)][y-E(y/z)]^T / z\right\} \\ &= E\left\{[x-E(x/z)][y-E(y/z)]^T\right\} \end{aligned} \qquad (G.18)$$

indicating that the condition on z can be removed. Furthermore,

$$\begin{aligned} P_{x,y/z} &= E\left\{(x-\bar{x})[Y-E(y/z)]^T\right\} \\ &= P_{x\tilde{y}} = P_{\tilde{x}y}^T \end{aligned} \qquad (G.19)$$

where
$$\tilde{y} \triangleq y - E(y/z)$$
$$\tilde{x} \triangleq x - E(x/z)$$

Equation (G. 18) is an immediate consequence of the property (ii) and the property (v) discussed in Gaussian variables. (G. 19) is obtained using the property (ii), equation (G. 9a) and the fact that $E(\tilde{y}) = E(\tilde{x}) = 0$.

(iv) Let x, y, and $\tilde{z}$ be jointly normal with density function as given by (G. 10) (with z replaced by $\tilde{z}$). If y and $\tilde{z}$ are independent, then

$$E(x/y,\tilde{z}) = E(x/y) + P_{x\tilde{z}} P_{\tilde{z}\tilde{z}}^{-1} (\tilde{z} - \bar{\tilde{z}}) \qquad (G.20)$$

This relationship can be easily obtained from (G. 9a) and the fact that $P_{y\tilde{z}} = P_{\tilde{z}y} = 0$.

(v) Using (G. 14) it can be shown in a straightforward manner that

$$E(x|y,z) = E(x|y,\tilde{z})$$
$$= E(x|y) + P_{x\tilde{z}} P_{\tilde{z}\tilde{z}}^{-1} \tilde{z} \qquad \text{(G.21)}$$

where $\quad \tilde{z} = z - E(z-y)$

Note that y and z are not independent. By interchanging y and z it is readily seen from (G. 18) and (G. 19) that

$$P_{x\tilde{z}} = P_{x,z|y}$$

and

$$P_{\tilde{z}\tilde{z}} = P_{z|y}$$

Thus (G. 21) can also be expressed as

$$E(x|y,z) = E(x|y) + P_{x,z|y} P^{-1}_{z|y} (z - E(z|y)) \qquad \text{(G.21a)}$$

(vi) From (G. 9b), (G. 21) and (G. 21a), it is straightforward to establish the following important results of the conditional covariance of x given y and z.

$$P_{x|y,z} = P_{x|y} - P_{x\tilde{z}} P^{-1}_{\tilde{z}\tilde{z}} P_{x\tilde{z}}^{T} \qquad \text{(G.22)}$$

where

$$\tilde{z} = z - E(z|y)$$

or

$$P_{x|y,z} = P_{x|y} - P_{x,z|y} P^{-1}_{z|y} P^{T}_{x,z|y} \qquad \text{(G.22a)}$$

The formulae (G. 21), (G. 21a), (G. 22), and (G. 22a) are of fundamental importance in the recursive estimation of parameters. One may interpret x as the parameter to be estimated; and y and z are respectively old and new data. Thus (G. 21) indicates that the optimal estimates of the parameter x given all the data is a linear combination of the old estimate and new data, if x, y, z are jointly distributed normally.

The results of this Appendix are used to develop filter-smoother algorithms in Section 5.2.

APPENDIX H

ACTUAL BIAS AND COVARIANCE IN MULTI-CORRECTED EXTENDED KALMAN FILTER

Consider the dynamic system

$$x_k = g_k(x_{k-1}) + w_k \tag{H. 1a}$$

$$y_k = h_k(x_k) + v_k \tag{H. 1b}$$

where the random vector sequences w_k and v_k are white Gaussian with zero mean and covariance matrices.

$$E(w_k w_j^T) = Q_k \delta_{kj}$$

$$E(v_k w_j^T) = R_k \delta_{kj}$$

$$E(v_k w_j^T) = 0$$

Assume that the nonlinear functions g_k and h_k may be adequately represented by a two-term Taylor series expansion

$$g(x) \approx g(\bar{x}) + \frac{\partial g}{\partial x}(x-\bar{x}) + \frac{1}{2}\frac{\partial^2 g}{\partial x^2} : \left[(x-\bar{x})(x-\bar{x})^T\right] \tag{H. 2a}$$

$$h(x) \approx h(\bar{x}) + \frac{\partial h}{\partial x}(x-\bar{x}) + \frac{1}{2}\frac{\partial^2 h}{\partial x^2} : \left[(x-\bar{x})(x-\bar{x})^T\right] \tag{H. 2b}$$

where $\frac{\partial^2 g}{\partial x^2} : \left[(x-\bar{x})(x-\bar{x})^T\right]$ is a vector whose i^{th} element is

$$\left\{\frac{\partial^2 g}{\partial x^2} : \left[(x-\bar{x})(x-\bar{x})^T\right]\right\}_i = \sum_j^n \sum_k^n \frac{\partial^2 g_i}{\partial x_j \partial x_k} \left[(x-\bar{x})(x-\bar{x})^T\right]_{jk} \tag{H. 3}$$

and $\frac{\partial g}{\partial x} \triangleq \left.\frac{\partial g}{\partial x}\right|_{\bar{x}}$, etc.

It is known that the extended Kalman filter (5. 32) is a biased estimator. To show this, let us begin with an unbiased estimate $\hat{x}_{k-1|k-1}$ with covariance matrix P_{k-1}, i.e.,

$$E\left[\hat{x}_{k-1|k-1}\right] = x_{k-1}$$

$$\mathrm{cov}\left[\hat{x}_{k-1|k-1}\right] = P_{k-1}$$

and define

$$\hat{e}_{k|k-1} \triangleq x_k - \hat{x}_{k|k-1} \tag{H. 4a}$$

$$\hat{e}_{k|k} \triangleq x_k - \hat{x}_{k|k} \tag{H. 4b}$$

Then from Reference 32

$$E\left[\hat{e}_{t|t-1}\right] = \frac{1}{2}\, g_{xx} : P_{t-1} \tag{H.5a}$$

$$\mathrm{cov}\left[\hat{e}_{t|t-1}\right] = \Phi_{t|t-1} P_{t-1} \Phi^T_{t,t-1} + Q_t \triangleq P_{t|t-1} \tag{H.5b}$$

and

$$E\left[\hat{e}_{t|t}\right] = \left(I - \psi_t H_t\right) E\left[\hat{e}_{t|t-1}\right] - \frac{1}{2}\psi_t h_{xx} : \left\{E\left(\hat{e}_{t|t-1}\hat{e}^T_{t|t-1}\right)\right\} \tag{H.5c}$$

$$\mathrm{cov}\left[\hat{e}_{t|t}\right] = \left(I - \psi_t H_t\right) P_{t|t-1} \left(I - \psi_t H_t\right)^T + \psi_t R_t \psi_t^T \tag{H.5d}$$

showing that the extended Kalman filter gives biased estimates. However, the computed covariances are identical to the actual covariances approximated to the second order. We note in (H.5) $g_{xx} \triangleq g_{xx}\big|_{\hat{x}_{t-1|t-1}}$, $h_{xx} \triangleq h_{xx}\big|_{\hat{x}_{t|t-1}}$

We wish to examine the bias at the second correction. To this end, we first consider the one state smoothing (5.38). Define

$$\hat{e}_{t-1|t} = x_t - \hat{x}_{t-1|t}$$

then from (5.38) and the fact that $\left(I - \psi_t H_t\right)^T H_t R_t^{-1} = P^{-1}_{t|t-1}\psi_t$,

$$\hat{e}_{t-1|t} = x_{t-1} - \hat{x}_{t-1|t-1} - P_{t-1}\Phi^T_{t,t-1} P^{-1}_{t|t-1}\psi_t \left\{v_t + H_t \hat{e}_{t|t-1} + \frac{1}{2} h_{xx} : \left[\hat{e}_{t|t-1}\hat{e}^T_{t|t-1}\right]\right\} \tag{H.6}$$

and hence

$$E\left[\hat{e}_{t-1|t}\right] = -P_{t-1}\Phi^T_{t,t-1} P^{-1}_{t|t-1}\psi_t \left\{H_t E\left[\hat{e}_{t|t-1}\right] + \frac{1}{2} h_{xx} : \left[P_{t|t-1} + E\left(\hat{e}_{t|t-1}\right) E\left(\hat{e}^T_{t|t-1}\right)\right]\right\} \tag{H.7}$$

From (H.6) and (H.7) we have

$$\begin{aligned} \hat{e}_{t-1|t} - E\hat{e}_{t-1|t} = \hat{e}_{t-1|t-1} - P_{t-1}\Phi^T_{t|t-1} P^{-1}_{t|t-1}\psi_t \Big\{ & v_t + H_t\left[\hat{e}_{t|t-1} - E\left(\hat{e}_{t|t-1}\right)\right] \\ & + \frac{1}{2} h_{xx} : \left[\hat{e}_{t|t-1}\hat{e}^T_{t|t-1} - \left(P_{t|t-1} + E\left(\hat{e}_{t|t-1}\right) E\left(\hat{e}_{t|t-1}\right)^T\right)\right]\Big\} \end{aligned} \tag{H.8}$$

Thus,

$$
\begin{aligned}
cov\left[\hat{e}_{t-1|t}\right] &= E\left[(\hat{e}_{t-1|t}-E(\hat{e}_{t-1|t}))(\hat{e}_{t-1|t}-E(\hat{e}_{t-1|t}))^T\right] \\
&= E\Big\{\left[\hat{e}_{t-1|t-1}-P_{t-1}\Phi^T_{t,t-1}P^{-1}_{t|t-1}\psi_t\left(v_t+H_t\left(\hat{e}_{t|t-1}-E(\hat{e}_{t|t-1})\right)\right)\right] \\
&\quad \times\left[\hat{e}_{t-1|t-1}-P_{t-1}\Phi^T_{t,t-1}P^{-1}_{t|t-1}\psi_t\left(v_t+H_t\left(\hat{e}_{t|t-1}-E(\hat{e}_{t|t-1})\right)\right)\right]^T\Big\} \\
&\quad + \text{higher order terms} \\
&= P_{t-1}-E\left\{\hat{e}_{t-1|t-1}\hat{e}_{t|t-1}\right\}H^T_t\psi^T_t P^{-1}_{t|t-1}\Phi_t P_{t-1} \\
&\quad -P_{t-1}\Phi^T_{t,t-1}P^{-1}_{t|t-1}\psi_t H_t E\left\{\hat{e}_{t|t-1}\hat{e}^T_{t|t-1}\right\} \\
&\quad +P_{t-1}\Phi^T_{t|t-1}P^{-1}_{t|t-1}\psi_t\left(R_t+H_t P_{t|t-1}H^T_t\right)\psi^T_t P^{-1}_{t|t-1}\Phi_{t|t-1}P_{t-1} \\
&\quad + \text{higher order terms}
\end{aligned}
\tag{H.9}
$$

It is easy to see that to second-order approximation

$$
\begin{aligned}
E\left[\hat{e}_{t|t-1}\hat{e}^T_{t-1|t-1}\right] &= E\left[\Phi_t(\hat{e}_{t-1|t-1}\hat{e}^T_{t-1|t-1})+\frac{1}{2}\left\{f_{xx}:\left[\hat{e}_{t-1|t-1}\hat{e}^T_{t-1|t-1}\right]\right\}\hat{e}^T_{t-1|t-1}\right] \\
&\approx \Phi_t P_{t-1}
\end{aligned}
\tag{H.10}
$$

Similarly $E\left[\hat{e}_{t-1|t-1}\hat{e}^T_{t|t-1}\right] \approx P_{t-1}\Phi^T_{t,t-1}$

Hence to the second-order approximation the actual covariance matrix for the one-stage smoothed estimate is

$$cov\left[\hat{e}_{t-1|t}\right] = P_{t-1} - P_{t-1}\Phi^T_{t,t-1}H^T_t\psi^T_t P^{-T}_{t|t-1}\Phi_{t,t-1}P_{t-1}$$
$$- P_{t-1}\Phi^T_{t,t-1}P^{-T}_{t|t-1}\psi_t H_t\Phi_{t,t-1}P_{t-1} + P_{t-1}\Phi^T_{t,t-1}P^{-1}_{t|t-1}\psi_t \tag{H.11}$$
$$\times\left(H_t P_{t|t-1}H^T_t + R_t\right)\psi^T_t P^{-T}_{t|t-1}\Phi_t P_{t-1}$$
$$= P_{t-1} - P_{t-1}\Phi^T_{t,t-1}P^{-T}_{t|t-1}\psi_t H_t\Phi_{t,t-1}P_{t-1}$$

which is identical to the computed covariance for the one-stage smoothed estimate (5.37).

To see the error statistics of the second corrected estimate, we first consider those of the second extrapolated estimate. Define

$$\hat{e}^{(2)}_{t|t-1} \triangleq x_t - \hat{x}^{(2)}_{t|t-1}$$
$$\approx \Phi^{(2)}_{t,t-1}\hat{e}_{t-1|t-1} + \frac{1}{2}g_{xx} : \left[\hat{e}^{(1)}_{t-1|t}\,\hat{e}^{(1)T}_{t-1|t}\right] + w_t \tag{H.12}$$

to the second-order approximation. In (H.12), $\Phi^{(2)}_{t,t-1} \triangleq \Phi_{t,t-1}\left(\hat{x}^{(1)}_{t-1|t}\right)$, $\hat{x}^{(1)}_{t-1|t} \triangleq \hat{x}_{t-1|t}$, and $\hat{e}^{(1)}_{t-1|t} \triangleq \hat{e}_{t-1|t}$. Hence:

$$E\left[\hat{e}^{(2)}_{t|t-1}\right] = \frac{1}{2}g_{xx} : \left[P^{(1)}_{t-1|t} + E\left[\hat{e}^{(1)}_{t-1|t}\right]E\left[\hat{e}^{(1)}_{t-1|t}\right]^T\right]$$
$$\approx \frac{1}{2}g_{xx} : P^{(1)}_{t-1|t} \tag{H.13}$$

to the second-order approximation.

Thus, to the second-order approximation the actual covariance of the second prediction is

$$cov\left[\hat{e}^{(2)}_{t|t-1}\right] = \Phi^{(2)}_{t,t-1}P_{t-1}\Phi^{(2)T}_{t,t-1} + Q_t \tag{H.14}$$

which is the same as the computed value. Now consider the second corrected estimate

$$\hat{x}^{(2)}_{t|t} = \hat{x}^{(2)}_{t|t-1} + \psi^{(2)}_t\left[y_t - h_t\left(\hat{x}^{(1)}_{t|t}\right) - H_t\left(\hat{x}^{(1)}_{t|t}\right)\left(\hat{x}^{(2)}_{t|t-1} - \hat{x}^{(2)}_{t|t}\right)\right]$$

Define $\hat{e}^{(2)}_{t|t} \triangleq x_t - \hat{x}^{(2)}_{t|t}$

Then to the second-order approximation

$$\hat{e}^{(2)}_{t|t} = \left[I - \psi^{(2)}_t H^{(2)}_t\right] \hat{e}^{(2)}_{t|t-1} - \frac{1}{2} \psi^{(2)}_t h_{xx} : \left[\hat{e}^{(1)}_{t|t} \hat{e}^{(1)\,T}_{t|t}\right] - \psi^{(2)}_t v_t \qquad \text{(H. 15)}$$

Hence,

$$E\left[\hat{e}^{(2)}_{t|t}\right] = \left[I - \psi^{(2)}_t H^{(2)}_t\right] E\left[\hat{e}^{(2)}_{t|t-1}\right] - \frac{1}{2} \psi^{(2)}_t h_{xx} : E\left\{\hat{e}^{(1)}_{t|t} \hat{e}^{(1)T}_{t|t}\right\} \qquad \text{(H. 16)}$$

and, to the second-order approximation, the actual covariance for $\hat{e}^{(2)}_{t|t}$ is

$$\operatorname{cov}\left[\hat{e}^{(2)}_{t|t}\right] = \left(I - \psi^{(2)}_t H^{(2)}_t\right) P^{(2)}_{t|t-1} \left(I - \psi^{(2)}_t H^{(2)}_t\right)^T + \psi^{(2)}_t R_t \psi^{(2)T}_t \qquad \text{(H. 17)}$$

which is the same as computed covariance matrix for the second corrected estimate.

Now, we are in a position to compare the bias and variance of the first and second corrected estimates, based on equations (H. 5c), (H. 5d), (H. 16), and (H. 17). Assume that $\Phi^{(1)}_{t,t-1} \approx \Phi^{(2)}_{t,t-1}$ and $H^{(1)}_t \approx H^{(2)}_t$, which implies that $P^{(1)}_{t|t-1} \approx P^{(2)}_{t|t-1}$ and $\psi^{(1)}_t \approx \psi^{(2)}_t$. Then from (H. 17) and (H. 5d) it is seen that the variance of the first corrected estimate (from the extended Kalman filter) is approximately the same as that of the second corrected estimate. However, the bias of the second corrected estimate is substantially different from that of the first corrected estimate as evident from (H. 5a), (H. 5c), (H. 13), and (H. 16). Indeed,

$$E\left[\hat{e}^{(1)}_{t|t-1}\right] = \frac{1}{2} g_{xx} : P_{t-1} \quad \text{and} \quad E\left[\hat{e}^{(2)}_{t|t-1}\right] = \frac{1}{2} g_{xx} : P^{(1)}_{t-1|t}$$

Since $P^{(1)}_{t|t-1}$ is the covariance of the one-stage smoothed estimate which is "smaller" than $P_{t-1} \triangleq P_{t-1|t-1}$ we see that the effect of nonlinearity of the system is reduced by the multi-correction.

Similarly, noting that the last terms in (H. 5c) and (H. 16) are

$$E\left[\hat{e}_{t|t-1} \hat{e}^T_{t|t-1}\right] \approx P_{t|t-1}$$

$$E\left[\hat{e}^{(1)}_{t|t} \hat{e}^{(1)T}_{t|t}\right] \approx P^{(1)}_{t|t}$$

to the second-order approximation, we see that the effect of the nonlinearity in the measurement system is also reduced.

APPENDIX I

CORRELATED PROCESS AND MEASUREMENT NOISE

In the derivation of the locally iterated filter-smoother algorithm, it was explicitly assumed that the process and measurement noise vector sequences were uncorrelated. With the incorporation of acceleration measurements into the measurement system, a direct correlation exists between the resulting measurement noise and process noise. This fact can readily be seen by considering the nonlinear dynamic system

$$\dot{x} = f(x,t) + w(t) \tag{I.1}$$

and discrete time noise measurements of both states, x, and state derivatives, $\dot{x}$, (accelerations) represented by

$$y_i = \begin{bmatrix} x_i \\ \hdashline \dot{x}_i \end{bmatrix} + \begin{bmatrix} v_{1i} \\ \hdashline v_{2i} \end{bmatrix} \triangleq \ell(x_i, \dot{x}_i) + v_i' \tag{I.2}$$

from which estimates are to be based where $x(t_i) \triangleq x_i$, $w(t_i) = w_i$ for $t_i \le t < t_{i+1}$, and v_i' and w_i are zero mean white Gaussian sequences with

$$E\left\{\begin{bmatrix} w_i \\ v_i' \end{bmatrix}\begin{bmatrix} w_j^T & v_j'^T \end{bmatrix}\right\} = \begin{bmatrix} Q_i & 0 \\ 0 & R_i \end{bmatrix} \delta_{i,j} \tag{I.3}$$

As in Section 5.2, we express the nonlinear system (I.1) in discrete form as

$$x_i = g_i(x_{i-1}) + \Gamma_i w_i \tag{I.4}$$

where $g_i(x_{i-1})$ in (I.4) is defined to be the solution, at time t_i , to (I.1) with initial condition x_{i-1} and $w(t) = 0, t_{i-1} \le t < t_i$ and Γ_i is an appropriate noise effectiveness matrix for this discrete representation. From (I.1) and (I.2), the measurement system can be expressed as a function of x_i only or

$$\begin{aligned} y_i &= \begin{bmatrix} x_i \\ \hdashline f(x_i, t_i) \end{bmatrix} + \begin{bmatrix} v_{1i} \\ \hdashline v_{2i} + w_i \end{bmatrix} \\ &\triangleq h_i(x_i) + v_i \end{aligned} \tag{I.5}$$

Clearly, w_i and v_i in (I.4) and (I.5) are correlated, with

$$E\{w_i v_j^T\} = [0 \vdots Q_i]\,\delta_{i,j-1} \triangleq C_i \delta_{i,j-1}\,, \tag{I.6}$$

thus verifying the previous assertion.

However, by a proper transformation, the process and measurement noise can be made uncorrelated. From (I.5), since

$$y_{i-1} - h_{i-1}(x_{i-1}) - v_{i-1} = 0$$

(I.3) can be equivalently written as

$$x_i = g_i(x_{i-1}) + \Gamma_i w_i + D_{i-1}\left(y_{i-1} - h_{i-1}(x_{i-1}) - v_{i-1}\right) \tag{I.7}$$

or

$$x_i = g_i(x_{i-1}) + D_{i-1}\left(y_{i-1} - h_{i-1}(x_{i-1})\right) + \omega_i \tag{I.8}$$

where

$$\omega_i = \Gamma_i w_i - D_{i-1} v_{i-1} \tag{I.9}$$

It is desired to adjust D such that

$$E\{\omega_i v_{i-1}^T\} = 0$$

or

$$E\left\{\left(\Gamma_i w_i - D_{i-1} v_{i-1}\right) v_{j-1}^T\right\} = \Gamma_i C_i - D_{i-1} R_{i-1} = 0 \tag{I.10}$$

From (I.10) it is clearly seen that ω_i and v_i will be uncorrelated if

$$D_{i-1} = \Gamma_i C_i R_{i-1}^{-1} \tag{I.11}$$

We note, from (I.9) and (I.11), that $cov(\omega_i) = \Gamma_i (Q_i - C_i R_{i-1}^{-1} C_i^T)\Gamma_i^T \delta_{ij}$.

Therefore, with D_i given by (I-11) and noting that the measurements y_i can be considered as deterministic (known) inputs to the system described by (I.9), the locally iterated filter-smoother and fixed-point smoother algorithms are directly applicable to the models (I.5) and (I.8). The results are summarized below.

Locally Iterated Filter-Smoother:

$$\hat{x}_{i|i}^{(j+1)} = \hat{x}_{i|i-1}^{(j)} + \psi_i^{(j)} \left[y_i - h_i\left(\hat{x}_{i|i}^{(j)}\right) - H_i^{(j)}\left\{ \hat{x}_{i|i-1}^{(j)} - \hat{x}_{i|i}^{(j)} \right\} \right]$$

where

$$\hat{x}_{i-1|i}^{(j+1)} = \hat{x}_{i-1|i-1} + P_{i-1}\,\Phi_{i,i-1}^{(j)T} H_i^{(j)T} \left[H_i^{(j)} P_{i|i-1}^{(j)} H_i^{(j)T} + R_i \right]^{-1} \cdot RES_i^{(j)}$$

$$P_{i|i-1}^{(j)} = \Phi_{i,i-1}^{(j)} + P_{i-1}\,\Phi_{i,i-1}^{(j)T} + \Gamma_i\left(Q_i - C_i R_i^{-1} C_i^T\right)\Gamma_i^T$$

$$\psi_i^{(j)} = P_{i|i-1}^{(j)} H_i^{(j)T} \left[H_i^{(j)} P_{i|i-1}^{(j)} H_i^{(j)T} + R_i \right]^{-1}$$

$$\hat{x}_{i|i-1}^{(j)} = g_i\left(\hat{x}_{i-1|i}^{(j)}\right) - D_{i-1} h_{i-1}\left(\hat{x}_{i-1|i}^{(j)}\right) + D_{i-1} y_{i-1} + \Phi_{i,i-1}^{(j)} \left[\hat{x}_{i-1|i-1} - x_{i-1|i}^{(j)} \right]$$

$$P_i^{(j)} = \left[I - \psi_i^{(j)} H_i^{(j)} \right] P_{i|i-1}^{(j)}$$

$$RES_i^{(j)} \triangleq y_i - h_i\left(\hat{x}_{i|i}^{(j)}\right) - H_i^{(j)}\left\{ \hat{x}_{i|i-1}^{(j)} - \hat{x}_{i|i}^{(j)} \right\}$$

$$\Phi_{i,i-1}^{(j)} \triangleq \Phi_{i,i-1}\left(\hat{x}_{i-1|i}^{(j)}\right) - D_{i-1} H_{i-1}\left(\hat{x}_{i-1|i}^{(j)}\right)^{*}$$

$$H_{i-1}^{(j)} \triangleq \left.\frac{\partial h_{i-1}}{\partial x}\right|_{\hat{x}_{i-1|i}^{(j)}}$$

$$D_{i-1} \triangleq \Gamma_i C_i R_{i-1}^{-1}$$

with the initial or starting conditions

$$\hat{x}_{i-1|i}^{(1)} = \hat{x}_{i-1|i-1} \quad , \quad \hat{x}_{i|i}^{(1)} = \hat{x}_{i|i-1}$$

$^{*}\Phi_{i,i-1}\left(x_{i-1|i}^{(j)}\right)$ is defined in Section 5.2

The iteration scheme starts with $j = 1$ and terminates when

$$\hat{x}^{(j)}_{i|i} \approx \hat{x}^{(j-1)}_{i|i}$$

or after a prespecified number of iterations. The converged values of $\hat{x}^{(j)}_{i|i}$, $\hat{x}^{(j-1)}_{i-1|i}$ and $P_i^{(j-1)}$ are taken as the estimates $\hat{x}_{i|i}$, $\hat{x}_{i-1|i}$ and the covariance P_i , respectively, for the next data point.

Fixed-Point Smoother:

$$\hat{x}_{0|i-1} = \hat{x}_{0|i} + B_{i+1} H^{(f)^T}_{i+1} R^{-1}_{i+1} RES^{(f)}_{i+1}$$

where

$$B_{i+1} = B_i \Phi^{(f)^T}_{i+1|i} \left[I - \psi^{(f)}_{i+1} H^{(f)}_{i+1} \right]^T , \quad B_0 = P_0$$

All symbology is as previously defined and the superscript (f) implies the final trajectory in the locally iterated filter-smoother.

A few general comments can be made about the estimation algorithms when correlation between the process noise and measurement noise sequences exists and this correlation is incorporated into the algorithms.

1. The algorithms for the locally iterated filter-smoother become slightly more complicated by the introduction of additional terms in each of the matrix equations.

2. An added nonlinearity, $h_i(x_i)$, is introduced into the system dynamics.

3. The estimation of the unknown forcing function, w_i , employing the redefined system equation (I.8), will consist of both the original process noise sequence (w_i) and the measurement noise sequence (v_i) as defined in (I.9).

4. If C_i is about the same order of magnitude as Q_i and R_i, increased accuracy could be expected.

However, C_i was set equal to zero in the locally iterated filter-smoother for computational simplicity.

APPENDIX J

EFFECTS OF CALIBRATION ERRORS AND SENSOR/FILTER DYNAMICS

In the development of the identification techniques, consistent errors in flight test data have not been considered. Three major types of consistent errors exist: sensor offsets, errors in calibration constants, and sensor/filter lags introduced by the recording system. Di Franco (Reference 10) has shown that for the equations-of-motion estimator, consistent calibration slope errors bias the extracted parameters but consistent instrument offsets can be removed by the addition of constant bias terms in the model equations. Similar degradation in parameter identification results for the iterative techniques used in the second and third stage refining process. Since at the time of this analysis, the extended Kalman filter was emerging as the best technique for use in the second stage and is an obvious requirement for the third stage, it was considered appropriate to conduct an error or sensitivity analysis around this technique. The primary goal of this analysis was to evaluate the effects of sensor and filter dynamics on the quality of the parameters identified employing the extended Kalman filter.

Two approaches were initially taken: (1) numerical experiments were conducted in which data were generated from a realistic model formulated using noise levels from the X-22A MPE II flight test data and the sensor/filter characteristics of the X-22A. Data sets were generated with and without sensor/filter dynamics. Both sets of data were then applied to the extended Kalman identification technique without modification and the resulting parameters estimated were compared; (2) a sensitivity analysis was initiated to determine the effects of erroneous models on the covariance of the estimation error from the Kalman filter. If modeling errors (e.g., unmodeled sensor lags and biases errors) and imperfect knowledge of the plant and measurement noise covariances exist, the calculated error covariance matrix in the filtering algorithm no longer represents the actual error covariance matrix. Since the actual covariance matrix of the estimation error gives an indication of the error which can occur when an incorrect model is used, this covariance matrix will indicate filter performance degradation due to inaccuracy in modeling.

A brief summary of the results and conclusions from the numerical experiments are discussed below. A derivation of the recursive matrix equations for an error or sensitivity analysis of the Kalman filtering algorithm is given in Appendix K.

Numerical Results

To determine the effects of neglected sensor/filter lags in the X-22A instrumentation on the Kalman filter identification technique, three sets of data were generated on the computer employing the linear equations of motion of the X-22A at fixed-duct incidence. Data generation is shown pictorially in Table J-1 for each case, and noise characteristics, sensor/filter dynamics used, trim conditions and control input are given in Table J-2.

An investigation of the X-22A instrumentation revealed that the models included three of four sources of possible error. These are:

1. Sensor/filter dynamics
2. Individual channel filter dynamics
3. Colored measurement noise
4. Consistent bias and calibration slope errors*

Values of each error source are given in Table J-2. These values were estimated using MPE II flight test data and the instrumentation characteristics on the X-22A. Calibration and bias errors are considered "maximum worst case" and are commensurate with the existing instrumentation accuracy.

Frequency response characteristics of the sensor/filter combinations in all measurement channels, except u and w, were considered to be flat to frequencies high enough to have negligible effect and thus were not included. Since $\dot{q}$ is obtained by differentiating q in the X-22A, a differentiator was simulated by the transfer function

* This source of error was not considered

$$\frac{s(50)^2}{(s+50)^2} \; . \tag{J.1}$$

To include the effects of colored measurement noise, the measurement noise statistics were assumed to be an isotropic zero mean random process with experimental autocorrelation function

$$E\left\{ m(t)\, m(t+\tau) \right\} = \sigma_m^2 \, e^{-B|\tau|} \tag{J.2}$$

where σ_m^2 is the variance and B is the bandwidth. Since at the present time the statistical properties of these errors (e.g., power spectral density) are not well defined, it is reasonable to adopt the model specified by (J.2). B for each measurement source was chosen to be consistent with the bandwidth of its particular sensor and filter.

Data 3A also included the individual channel filters. Note that process noise was assumed absent.

Results employing the linear version of the extended Kalman filter without acceleration measurements and the systematic recycling technique discussed in Section V are given in Tables J-3 through J-6. Tables J-4 and J-5 depict sensitivity of the parameter estimates for different selections of P_0. In all cases, the P_0 matrix was formed from the equations-of-motion variances multiplied equally by a constant factor. From these results, the following general conclusions can be made.

- The parameter estimates from the equations-of-motion initial estimator are "very poor" when sensor dynamics are present. This degradation is contributed to by the way $\dot{q}$ is measured in the X-22A, i.e., differentiating q, and simulated here. However, the systematic recycling of data through the extended Kalman filter improves the estimates considerably.

- Sensor dynamics and correlated measurement noise (as defined here) have "very little" or no effect on the quality of the parameters estimated using the systematic approach. Small degradation is due to a poor initial estimate because of the $\dot{q}$ measurement.

- Additional filtering of the responses, assuming all filters are the same, improves identification by reducing noise levels. The added dynamics of the filters, if the filter cutoff frequency is 6 Hz or better, does not affect the Kalman technique.

TABLE J-1

Data Generation

CASE 2A (NO ERROR MODEL)

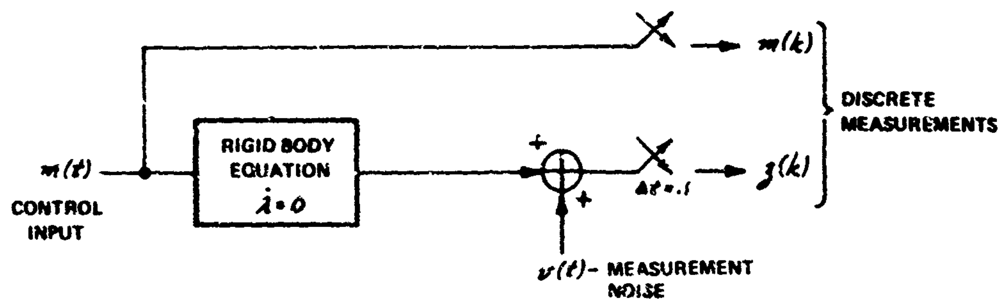

CASE 1A (ERROR MODEL, SENSOR OUTPUTS)

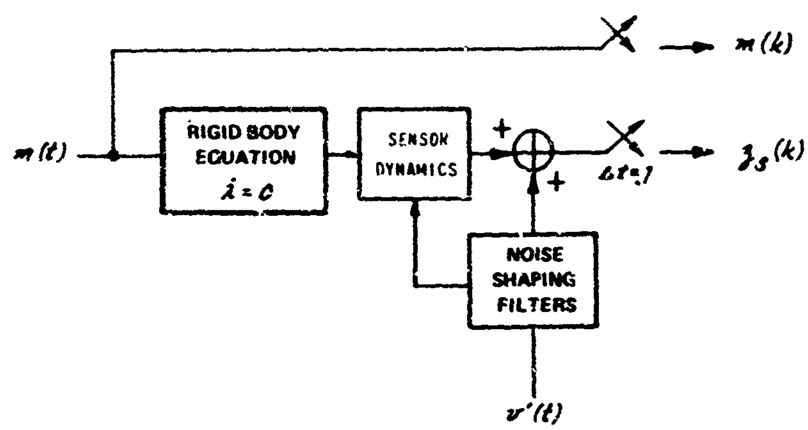

CASE 3A (ERROR MODEL, FILTER OUTPUTS)

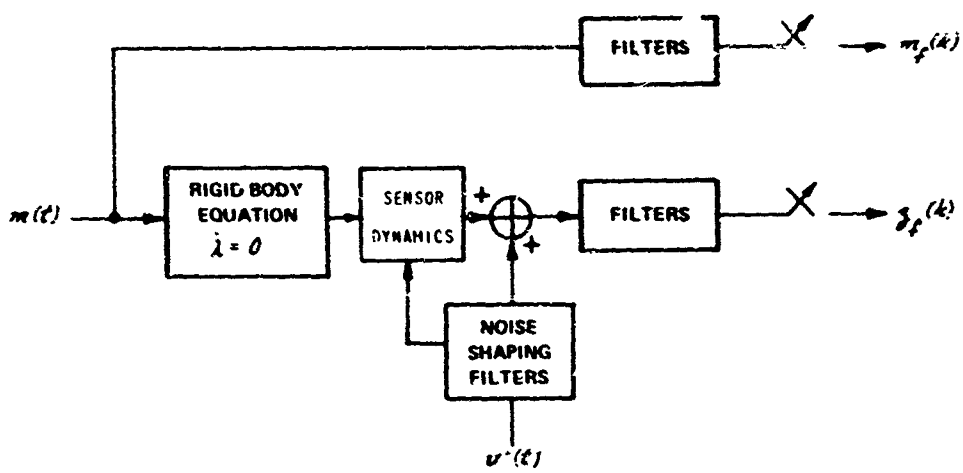

TABLE J-2

Measurement Noise Characteristics and Sensor and Filter Dynamics

SENSOR	MEASUREMENT NOISE		SENSOR & FILTER DYNAMICS		(3) CALIBRATION ERRORS	
	STANDARD DEVIATION	(1) BANDWIDTH SHAPING FILTER	SENSOR	FILTER	FUNCTIONAL SLOPE (3σ)	BIAS (3σ)
u	2.6 fps	3Hz	ω_n = 3.2 Hz δ = .707	ω_n = 6 Hz δ = .707	.02	1.3 fps
(2) w	.36 fps	3 Hz	1st ORDER 3 Hz	"	.02	.75 fps
θ	.09	10 Hz	NONE	"	.01	.12
q	.22 /sec	10 Hz	NONE	"	.015	.25 /sec
n_x	.012 g	10 Hz	NONE	"	.005	.005 g
n_z	.05 g	10 Hz	NONE	"	.005	.01 g
(2) $\dot{q}$	2.3 /sec	N.A.	(4)	"	.015	.47/sec^2
δ_{es}	NONE	N.A.	NONE	"	0	0

(1) ESTIMATED
(2) NO SENSOR ON X-22A
(3) MAX WORST CASE. SET TO ZERO IN DATA GENERATION
(4) DIFFERENTIATE q AS INSTRUMENTED IN X-22A

-TRIM CONDITIONS-

$\lambda_o = 30°$	$\theta_o = 2.35$
$g_o = 0$	$B_o = 17.257$
$w_o = 5.36$ fps	$\delta_{eso} = -.637''$
$u_o = 130$ fps	

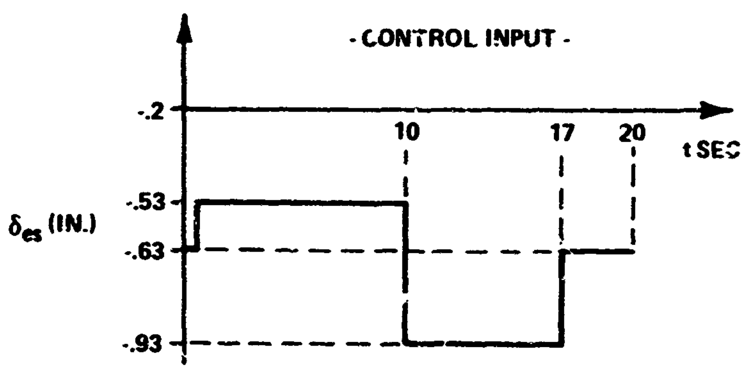

TABLE J-3

Summary of Initial Estimator - Equations of Motion

PARAMETER	TRUE VALUE	NO ERROR MODEL 2A	ERROR MODEL - SENSOR 1A	ERROR MODEL - FILTERED 3A
		NO PROCESS NOISE	NO PROCESS NOISE	NO PROCESS NOISE
M_u	-.0044	-.00346	-.00206	-.00209
M_w	-.0075	-.00559	-.00286	-.00599
M_q	-.625	-.5003	-.0821	.20146
$M_{\delta_{es}}$	.48	.3654	.2131	.1502
X_u	-.15	-.137	-.1347	-.1372
X_w	.021	.0503	.0555	.0459
$X_{\delta_{es}}$	1.37	.4635	.2675	.3536
Z_u	-.216	-.198	-.1930	-.2052
Z_w	-.65	-.6131	-.5308	-.5587
$Z_{\delta_{es}}$	1.66	.4808	-.47902	.4660

TABLE J-4

Case 1A - Sensitivity With Respect to $P(0)$

PARAMETER	TRUE VALUE	INITIAL ESTIMATE -EQ. OF MOTION		$P(0) = \left[\begin{array}{c:c} R & 0 \\ \hdashline 0 & 10P_{22} \end{array}\right]$		$P(0) = \left[\begin{array}{c:c} R & 0 \\ \hdashline 0 & 1000P_{22} \end{array}\right]$	
		ESTIMATE	σ^2	ESTIMATE - 5 PASS	FINAL σ	ESTIMATE - 5 PASS	FINAL σ
M_u	-.0044	-.00206	2.166×10^{-7}	-.0048	1.00×10^{-5}	-.00507	1.919×10^{-5}
M_w	-.0075	-.00286	1.365×10^{-6}	-.00770	2.398×10^{-5}	-.00795	4.882×10^{-5}
M_q	-.625	-.08212	7.469×10^{-2}	-.8517	3.984×10^{-3}	-.997	9.488×10^{-3}
$M_{\delta_{es}}$	.48	.2131	4.177×10^{-3}	.5460	9.904×10^{-4}	.5746	2.189×10^{-3}
X_u	-.15	-.1347	8.993×10^{-6}	-.1357	7.602×10^{-4}	-.0755	3.14×10^{-3}
X_w	.021	.05546	4.033×10^{-5}	.0594	1.888×10^{-3}	.1874	6.707×10^{-3}
$X_{\delta_{es}}$	1.37	.2675	6.793×10^{-4}	.6391	.09087	-4.809	.2854
Z_u	-.216	-.19301	5.627×10^{-5}	-.1922	5.382×10^{-4}	-.1894	1.095×10^{-3}
Z_w	-.65	-.5308	2.523×10^{-4}	-.5973	1.265×10^{-3}	-.5944	2.373×10^{-3}
$Z_{\delta_{es}}$	1.66	-.4790	.4251	-.2999	.0644	-1.371	.1138

TABLE J-5

Case 2A - Sensitivity With Respect to $P(0)$

PARAMETER	TRUE VALUE	INITIAL ESTIMATE -EQ. OF MOTION		$P(0) = \left[\begin{array}{c:c} R & 0 \\ \hdashline 0 & 10P_{22} \end{array}\right]$		$P(0) = \left[\begin{array}{c:c} R & 0 \\ \hdashline 0 & 1000P_{22} \end{array}\right]$	
		ESTIMATE	σ^2	ESTIMATE - 5 PASS	FINAL σ	ESTIMATE - 5 PASS	FINAL σ
M_u	-.0044	-.00346	1.188×10^{-7}	-.00450	9.54×10^{-6}	-.00456	1.015×10^{-5}
M_w	-.0075	-.00559	9.60×10^{-7}	-.00747	2.314×10^{-5}	-.00753	2.53×10^{-5}
M_q	-.625	-.5003	4.108×10^{-2}	-.71825	3.805×10^{-3}	-.7748	4.059×10^{-3}
$M_{\delta_{es}}$	.48	.3654	2.099×10^{-3}	.50241	9.228×10^{-4}	.5044	9.781×10^{-4}
X_u	-.15	-.137	9.571×10^{-6}	-.1361	7.974×10^{-4}	-.0877	1.033×10^{-3}
X_w	.021	.0503	4.873×10^{-5}	.0533	1.975×10^{-3}	.1546	2.45×10^{-3}
$X_{\delta_{es}}$	1.37	.4635	7.188×10^{-2}	.4541	.09528	-3.887	.1139
Z_u	-.216	-.198	3.489×10^{-5}	-.2055	5.581×10^{-4}	-.2049	5.882×10^{-4}
Z_w	-.65	-.6131	1.777×10^{-4}	-.62799	1.31×10^{-3}	-.6310	1.372×10^{-3}
$Z_{\delta_{es}}$	1.66	.4808	.2621	.6845	.06623	.0593	.06771

TABLE J-6

Summary of Extended Kalman - 5 Passes

PARAMETER	TRUE VALUE	$P(0) = \left[\begin{array}{c:c} R & 0 \\ \hdashline 0 & 1000\,P_{22} \end{array}\right]$		
		2A	1A	3A
M_u	-.0044	-.00456	-.00507	-.00492
M_w	-.0075	-.00753	-.00795	-.00757
M_q	-.625	-.7748	-.997	-.8936
$M_{\delta_{es}}$	.48	.5044	.5746	.5620
X_u	-.15	-.0877	-.0755	-.1499
X_w	.021	.1546	.1874	.0294
$X_{\delta_{es}}$	1.37	-3.887	-4.809	1.787
Z_u	-.216	-.2049	-.1894	-.1921
Z_w	-.65	-.6310	-.5944	-.5756
$Z_{\delta_{es}}$	1.66	.0593	-1.371	-.3138

APPENDIX K

SENSITIVITY FUNCTIONS FOR THE KALMAN FILTER

The recurrence relations in the Kalman filter algorithm yield the correct error covariance or performance of the filter if the a priori statistics ($P(0)$, R and Q) and choice of the mathematical model truly represent the actual process. If this is not the case, the calculated error covariance no longer represents the actual error covariance of the filter. Since this latter covariance matrix gives an indication of filter performance (on the average) due to unknown a priori statistics and modeling errors, it is of prime importance in determining filter degradation or performance sensitivity with respect to variations in the assumed model.

Matrix difference equations are briefly derived in this appendix for the actual error covariance of the linear discrete filter. Since these equations appear elsewhere in the literature (References 31, 73, and 74), a detailed derivative is not given. However, for the interested reader, a complete development is given by Griffin in Reference 74. If the estimation errors are small, the equations are directly applicable for a sensitivity analysis of the extended Kalman filter.

Derivation of Actual Covariance Matrices

Assume the actual or exact process and measurement vector is described by the vector difference equation

$$\begin{aligned} y^a(k+1) &= \Phi^a(k)\,y^a(k) + \Gamma^a(k)\,w^a(k) && \text{(dynamics)} \\ z^a(k) &= H^a(k)\,y^a(k) + v^a(k) && \text{(measurements)} \end{aligned} \tag{K.1}$$

with the moments

$$\begin{aligned} E\{w^a(k)\} &= 0 \qquad & E\{w^a(k)w^{a^T}(j)\} &= Q^a(k)\delta_{kj} \\ E\{v^a(k)\} &= 0 \qquad & E\{v^a(k)v^{a^T}(j)\} &= R^a(k)\delta_{kj} \\ & & E\{v^a(k)w^{a^T}(j)\} &= 0 \end{aligned} \tag{K.2}$$

where the superscript " a " refers to the actual process. The assumed model, used to derive the filter equation, is postulated to have the same form as linearized equations (5.13) and (5.14), and is given by

$$y(k+1) = \Phi(k)y(k) + \Gamma(k)w(k) \tag{K.3}$$

$$z(k) = H(k)y(k) + v(k)$$

with the moments

$$E\{w(k)\} = 0 \qquad E\{w(k)w^T(j)\} = Q(k)\delta_{kj}$$

$$E\{v(k)\} = 0 \qquad E\{v(k)v^T(j)\} = R(k)\delta_{kj} \tag{K.4}$$

$$E\{v(k)w^T(j)\} = 0$$

In the sequel, all unsuperscripted variables will refer to the assumed model or calculated covariances.

Using the assumed model and statistics as defined in equation (K.3) and (K.4), the estimator gain $K(k)$ and calculated error covariance are given by equation (K.5).

$$K(k) = M(k)H^T(k)\left[H(k)M(k)H^T(k) + R(k)\right]^{-1}$$

$$M(k) = \Phi(k-1)P(k-1)\Phi^T(k-1) + \Gamma(k-1)Q(k-1)\Gamma^T(k-1)$$

$$P(k) = \left[I - K(k)H(k)\right]M(k)\left[I - K(k)H(k)\right]^T + K(k)R(k)K^T(k)^T \tag{K.5}$$

$P(0)$ = initial error covariance

The estimation equation then becomes

$$\hat{y}(k) = \bar{y}(k) + K(k)\left[z^a(k) - H(k)\bar{y}(k)\right] \tag{K.6}$$

where $\bar{y}(k) = \Phi(k-1)\hat{y}(k-1)$

$\hat{y}(0) = E\{y(0)\}$

Subtracting the estimation vector from the state vector of the actual process gives the actual estimation errors. Therefore,

$$\tilde{y}^a(t) \triangleq y^a(t) - \hat{y}(t)$$
$$\tilde{\tilde{y}}^a(t) \triangleq y^a(t) - \bar{y}(t) \qquad (K.7)^*$$

where $\tilde{y}^a$ and $\tilde{\tilde{y}}^a$ are the actual estimation errors given data up to t and $t-1$, respectively. The actual covariance of the estimation errors are defined as usual in equation (K.8)

$$P^a(t) \triangleq E\left\{\tilde{y}^a(t)\tilde{y}^{a^T}(t)\right\}$$
$$M^a(t) \triangleq E\left\{\tilde{\tilde{y}}^a(t)\tilde{\tilde{y}}^{a^T}(t)\right\} \qquad (K.8)^{**}$$

Using equations (K.1), (K.6) and (K.7), matrix difference equations for $M^a(t)$ and $P^a(t)$ can easily be shown to be given by

$$\begin{aligned} M^a(t) = {} & \Phi(t-1)P^a(t-1)\Phi^T(t-1) + \Delta\Phi(t-1)P_c(t-1)\Phi^T(t-1) \\ & + \Phi(t-1)P_c^T(t-1)\Delta\Phi^T(t-1) + \Delta\Phi(t-1)P_y^a(t-1)\Delta\Phi^T(t-1) \\ & + \Gamma^a(t-1)Q^a(t-1)\Gamma^{a^T}(t-1) \end{aligned} \qquad (K.8a)$$

$$\begin{aligned} P^a(t) = {} & \left[I - K(t)H(t)\right] M^a(t)\left[I - K(t)H(t)\right]^T - K(t)\Delta H(t)M_c(t)\left[I - K(t)H(t)\right]^T \\ & - \left[I - K(t)H(t)\right] M_c^T(t)\Delta H^T(t)K^T(t) + K(t)R^a(t)K^T(t) \\ & + K(t)\Delta H(t)P_y^a(t)\Delta H^T(t)K^T(t) \end{aligned}$$

---

* This equation is also valid when the actual process and assumed model have different order. For the usual case where the order of the actual process is greater than the order of the assumed model, equations (K.3) and (K.6) should be interpreted as though fictitious zero states were augmented to the assumed model equations. This implies $K(t)$ will have the partitioned form

$$K(t) = \begin{bmatrix} K_1(t) \\ \hline 0 \end{bmatrix}$$

** It is not strictly correct to refer to $P^a(t)$ as a covariance matrix because error in the assumed model dynamics could make $E\{\tilde{y}^a(t)\} \neq 0$. However, $P^a(t)$ does provide a direct measure of the actual estimation error.

where

$$\begin{aligned}
\Delta\Phi(t) &\triangleq \Phi^a(t)-\Phi(t)\\
\Delta H(t) &\triangleq H^a(t)-H(t)\\
P_c(t) &\triangleq E\left\{y^a(t)\tilde{y}^a(t)\right\}\\
M_c(t) &\triangleq E\left\{y^a(t)\tilde{\tilde{y}}^a(t)\right\}\\
P_y^a(t) &\triangleq E\left\{y^a(t)y^{a^T}(t)\right\}
\end{aligned} \tag{K.8b}$$

with the initial condition

$$P^a(0) \triangleq E\left\{\left[y^a(0)-E\{y^a(0)\}\right]\left[y^a(0)-E\{y^a(0)\}\right]^T\right\} \tag{K.8c}$$

and $K(t)$ is generated from (K.5).

Similarly, difference equations for the cross-covariance and auto-correlation matrices defined in (K.8b) can be shown to be given by the following:

$$\begin{aligned}
M_c(t) &= \Phi^a(t-1)P_c(t-1)\Phi^T(t-1)+\Phi^a(t-1)P_y^a(t-1)\Delta\Phi^T(t-1)\\
&\quad+\Gamma^a(t-1)Q^a(t-1)\Gamma^{a^T}(t-1)\\
P_c(t) &= M_c(t)\left[I-K(t)H(t)\right]^T - P_y^a(t)\Delta H^T(t)K^T(t)\\
P_y^a(t) &= \Phi^a(t-1)P_y^a(t-1)\Phi^{a^T}(t-1)+\Gamma^a(t-1)Q^a(t-1)\Gamma^{a^T}(t-1)
\end{aligned} \tag{K.9}$$

The particular differences between the actual process and assumed model usually indicate the initial conditions used in (K.9). In general, if $E\left\{y^a(0)\right\} = 0$ the initial conditions are easily shown to be given by

$$P_y^{(a)}(0) = P_c(0) = P^a(0) \tag{K.10}$$

For the case where the assumed model and actual process are of the same order, (K.10) holds for the less severe condition that $\hat{y}(0) = E\left\{y^a(0)\right\}$.

The optimal filter performance, $P^o(t)$, achievable when the assumed model correctly characterizes the actual process, is obviously given by (K.5), when the actual process parameters are used.

Mean of Estimation Error

It was indicated in the footnote to equation (K.8) that if modeling errors exist ($\Delta\Phi(k)\neq 0$ and $\Delta H(k)\neq 0$), the mean of the actual estimation error may not be zero. If $E\{\tilde{y}^a(k)\}\neq 0$, the covariance of the estimation error is not $P^a(k)$ but is more correctly given by

$$cov\{\tilde{y}^a(k),\tilde{y}^a(k)\} = P^a(k) - E\{\tilde{y}^a(k)\}E\{\tilde{y}^a(k)\}^T \tag{K.11}$$

Taking the expectation of $\tilde{y}^a(k)$, the means of the extrapolated and a posteriori estimation errors are given by

$$E\{\tilde{\tilde{y}}^a(k)\} = \Phi(k-1)E\{\tilde{y}^a(k-1)\} + \Delta\Phi(k-1)E\{y^a(k-1)\} \tag{K.12a}$$

$$E\{\tilde{y}^a(k)\} = \ell(k)E\{\tilde{\tilde{y}}^a\} - K(k)\Delta H(k)E\{y^a(k)\} \tag{K.12b}$$

Substituting (K.12a) into (K.12b) and using $E\{y^a(k)\} = \Phi^a(k-1)E\{y^a(k-1)\}$, the mean of the a posteriori estimation error results. That is,

$$E\{\tilde{y}^a(k)\} = \ell(k)\Phi(k-1)E\{\tilde{y}^a(k-1)\} + \left[\ell(k)\Delta\Phi(k-1) - K(k)\Delta H(k)\Phi^a(k-1)\right] E\{y^a(k-1)\} \tag{K.13}$$

where
$$\ell(k) = I - K(k)H(k)$$

The first term in (K.13) represents the mean of the estimation error due to non-zero mean initial estimation error, i.e., $E\{\tilde{y}^L(0)\}\neq 0$.

If,
$$\prod_{k=1}^{n}\left[I-K(k)H(k)\right]\Phi(k-1)\rightarrow 0 \text{ as } n\rightarrow\infty \tag{K.14}$$

then the estimator is asymptotically unbiased if no modeling errors exist. If modeling error exists, the second term in (K.13) <u>may</u> force the estimation error to be non-zero mean or the estimator to be biased; in which case (K.11) gives the correct covariance of the estimation error and (K.13) the mean. From the second term in (K.13), it is seen that the bias is a function of modeling errors and $E\{y^a(0)\}$. Similar results hold for the extrapolated estimation error and its covariance.

Error Bounds

Conditions have been reported by Nishimura (References 75 and 76) such that a set of error bounds can be computed for the variances of the estimation error for the Kalman filtering algorithms and are correct for the linear continuous or discrete case. The main results are given in the following theorem and corollary.

Theorem 1

If $P(0) \geq P^a(0)$, $Q(t) \geq Q^a(t)$, and $R(t) \geq R^a(t)$ for all $t \geq 0$, then

$$P(t) \geq P^a(t)$$

for all $t \geq 0$. Equivalently,

$$\left[P(t)\right]_{ii} \geq \left[P^a(t)\right]_{ii} \quad \forall t \geq 0$$

where the elements $\left[P(t)\right]_{ii}$ and $\left[P^a(t)\right]_{ii}$ are the respective diagonal components of $P(t)$ and $P^a(t)$. The greater than or equal to sign used with matrices, e.g., $P(0) \geq P^a(0)$, indicates that the difference matrix $P(0) - P^a(0)$ is positive semi-definite. Hence, upper bounds on the variances of the error in the estimate are available even when the variances of the actual process are not known provided the conservative conditions in Theorem 1 are satisfied.

Corollary 1

If $P^a(0) \geq P(0)$, $Q^a(t) \geq Q(t)$, and $R^a(t) \geq R(t)$ for all $t \geq 0$,

then

$$P^a(t) \geq P(t)$$

or

$$\left[P^a(t)\right]_{ii} \geq \left[P(t)\right]_{ii} \quad \forall t \geq 0.$$

Obviously, the optimal estimation error, $P^o(t)$, when correct a priori information is employed is always less than or equal to $P^a(t)$ by definition, i.e.,

$$P^o(t) \leq P^a(t) \quad \forall t \geq 0$$

Therefore, if the conditions in Theorem 1 hold

$$P(t) \geq P^a(t) \geq P^o(t) \qquad \forall t \geq 0 \tag{K.15}$$

and $P(t)$ can be considered an upper bound on the estimation error.

However, if instead the conditions in Corollary 1 are valid, this implies

$$\begin{aligned} P^a(t) &\geq P(t) \\ P^a(t) &\geq P^o(t) \end{aligned} \qquad \forall t \geq 0 \tag{K.16}$$

and no relationship can be given between $P^o(t)$ and $P(t)$.

The above theorems establish upper bounds on the estimation error to be expected when incorrect a priori information is used in the filtering algorithm. The lower error bound is given by $P^o(t)$ for the linear Kalman filter and the Cramer-Rao lower bound for arbitrary estimator. For the extended Kalman filter, the validity of these relationships is conditioned upon the accuracy of the approximation made in the linearization.

APPENDIX L

DERIVATION OF THE EQUATIONS OF MOTION FOR PDMT QUAD DUCT TEST MODEL

The geometric configuration and the coordinate systems have been depicted as shown in the schematic diagram of Figure 7-1. With reference to the coordinate system X_s, Y_s, Z_s, the vector $\vec{l}$ can be written as

$$\vec{l} = \begin{pmatrix} X'_{cg} \\ 0 \\ Z'_{cg} \end{pmatrix} = \begin{pmatrix} (X_{cg} - r)\cos\theta + Z_{cg}\sin\theta \\ 0 \\ -(X_{cg} - r)\sin\theta + Z_{cg}\cos\theta \end{pmatrix} \qquad \text{(L. 1)}$$

With respect to this same coordinate system the linear acceleration at the model c.g. is

$$\vec{a}_{cg} = \vec{a}_p + \vec{\omega} \times (\vec{\omega} \times \vec{l}) + \dot{\vec{\omega}} \times \vec{l}$$

or

$$\begin{pmatrix} \dot{u}'_s \\ 0 \\ \dot{w}'_s \end{pmatrix} = \begin{pmatrix} \dot{u}_s \\ 0 \\ \dot{w}_s \end{pmatrix} + \left\{ \begin{pmatrix} 0 & 0 & q \\ 0 & 0 & 0 \\ -q & 0 & 0 \end{pmatrix}^2 + \begin{pmatrix} 0 & 0 & \dot{q} \\ 0 & 0 & 0 \\ -\dot{q} & 0 & 0 \end{pmatrix} \right\} \begin{pmatrix} X'_{cg} \\ 0 \\ Z'_{cg} \end{pmatrix}$$

$$= \begin{bmatrix} \dot{u}_s + \dot{q}\left[-(X_{cg} - r)\sin\theta + Z_{cg}\cos\theta\right] - q^2\left[(X_{cg} - r)\cos\theta + Z_{cg}\sin\theta\right] \\ 0 \\ \dot{w}_s - \dot{q}\left[(X_{cg} - r)\cos\theta + Z_{cg}\sin\theta\right] - q^2\left[-(X_{cg} - r)\sin\theta + Z_{cg}\cos\theta\right] \end{bmatrix} \qquad \text{(L. 2)}$$

The total inertia force F_I acting at the model c.g. is then

$$F_I = -\left\{ M \begin{pmatrix} \dot{u}'_s \\ 0 \\ \dot{w}'_s \end{pmatrix} + \begin{pmatrix} (M_v + M_h)\dot{u}_s \\ 0 \\ M_v \dot{w}_s \end{pmatrix} \right\} \qquad \text{(L. 3)}$$

Expressing $\dot{u}_s$ and $\dot{w}_s$ in the above equation in terms of $\dot{u}'_s$, $\dot{w}'_s$, the space-fixed variables at the c.g. (Figure 7-1), equation (L. 3) becomes:

$$F_I \equiv \begin{pmatrix} X_{inertia} \\ 0 \\ Z_{inertia} \end{pmatrix}$$

$$= \begin{bmatrix} -(M+M_v+M_h)\dot{u}_s' + \dot{q}(M_v+M_h)Z_{cg}' - q^2(M_v+M_h)X_{cg}' \\ 0 \\ -(M+M_v)\dot{w}_s' - M_v(\dot{q}X_{cg}' + q^2 Z_{cg}') \end{bmatrix} \tag{L.4}$$

With respect to the body axis system X_B , Y_B , Z_B the above inertia force and the gravitational force can be written as

$$\begin{bmatrix} (X_{inertia})_B \\ 0 \\ (Z_{inertia})_B \end{bmatrix} = T \begin{bmatrix} X_{inertia} \\ 0 \\ Z_{inertia} \end{bmatrix}_S \tag{L.5}$$

$$\begin{bmatrix} (X_g)_B \\ 0 \\ (Z_g)_B \end{bmatrix} = T \begin{bmatrix} 0 \\ 0 \\ g(M_v+M) \end{bmatrix}_S \tag{L.6}$$

where $T \equiv \begin{pmatrix} \cos\theta & 0 & -\sin\theta \\ 0 & 0 & 0 \\ \sin\theta & 0 & \cos\theta \end{pmatrix}$

Equating

$$\begin{aligned} (X_{inertia})_B + (X_g)_B + (X_{aero})_B &= 0 \\ (Z_{inertia})_B + (Z_g)_B + (Z_{aero})_B &= 0 \end{aligned} \tag{L.7}$$

and expressing the inertia acceleration $\dot{u}_s'$, $\dot{w}_s'$ in (L.4) in terms of body system variables, i.e.,

$$\begin{pmatrix} \dot{u}'_s \\ 0 \\ \dot{w}'_s \end{pmatrix} = \begin{bmatrix} (\dot{u}_B + q w_B)\cos\theta + (\dot{w}_B - q u_B)\sin\theta \\ 0 \\ -(\dot{u}_B + q w_B)\sin\theta + (\dot{w}_B - q u_B)\cos\theta \end{bmatrix} \tag{L.8}$$

the following equations of motion, expressed in body axis system are obtained:

$$\dot{u}_B = \frac{1}{(M+M_v)(M+M_v+M_h)} \Big\{ (M+M_v+M_h\sin^2\theta)\left[I_3\cos\theta - I_4\sin\theta - (M+M_v)g\sin\theta + X_{aero_B}\right]$$

$$- M_h\sin\theta\cos\theta\left[I_3\sin\theta + I_4\cos\theta + g(M+M_v)\cos\theta + Z_{aero_B}\right]\Big\}$$

$$\dot{w}_B = \frac{1}{(M+M_v)(M+M_v+M_h)} \Big\{ -M_h\sin\theta\cos\theta\left[I_3\cos\theta - I_4\sin\theta - g(M+M_v)\sin\theta + X_{aero_B}\right]$$

$$+ (M+M_v+M_h\cos^2\theta)\left[I_3\sin\theta + I_4\cos\theta + g(M+M_v)\cos\theta + Z_{aero_B}\right]$$

where

$$I_3 = -(M+M_v+M_h)\left[q w_B\cos\theta - q u_B\sin\theta\right] + \dot{q}(M_h+M_v)\left[-(X_{cg}-r)\sin\theta + Z_{cg}\cos\theta\right]$$
$$- q^2(M_v+M_h)\left[(X_{cg}-r)\cos\theta + Z_{cg}\sin\theta\right]$$

$$I_4 = -(M+M_v)\left[-q w_B\sin\theta - q u_B\cos\theta\right] - \dot{q}M_v\left[(X_{cg}-r)\cos\theta + Z_{cg}\sin\theta\right]$$
$$- q^2 M_v\left[-(X_{cg}-r)\sin\theta + Z_{cg}\cos\theta\right]$$

Using the following shorthand notations:

$$\sigma \equiv \frac{M+M_v}{M+M_v+M_h} \qquad X_{aero_B} = \frac{1}{M+M_v} X_{aero_B}$$

$$\mu \equiv \frac{M_v}{M+M_v+M_h} \qquad Z_{aero_B} = \frac{1}{M+M_v} Z_{aero_B}$$

$$\xi \equiv \frac{M_h}{M+M_v+M_h} = 1-\sigma$$

the above equations of motion can finally be written as

$$-\dot{u}_B - \dot{w}_B q - g\sin\theta + \mu\left\{ Z_{cg}\left[\left(1+\frac{\xi}{\mu}\right)\cos^2\theta + \frac{1}{\sigma}\sin^2\theta\right] + (X_{cg}-r)\left(\frac{1}{\sigma}-1-\frac{\xi}{\mu}\right)\sin\theta\cos\theta \right\}\dot{q}$$

$$+\mu\left\{ Z_{cg}\left(\frac{1}{\sigma}-1-\frac{\xi}{\mu}\right)\sin\theta\cos\theta - (X_{cg}-r)\left[\left(1+\frac{\xi}{\mu}\right)\cos^2\theta + \frac{1}{\sigma}\sin^2\theta\right] \right\}q^2$$

$$+\left[\sin^2\theta + \sigma\cos^2\theta\right] X_{aero_B} - \left[(1-\sigma)\sin\theta\cos\theta\right] Z_{aero_B} = 0 \qquad \text{(L.9a)}$$

$$-\dot{w}_B + u_B q + g\cos\theta - \frac{\mu}{\sigma}\left\{ (X_{cg}-r)\left[\cos^2\theta + \sigma\left(1+\frac{\xi}{\mu}\right)\sin^2\theta\right] + Z_{cg}\left[1-\sigma\left(1+\frac{\xi}{\mu}\right)\right]\sin\theta\cos\theta \right\}\dot{q}$$

$$+\frac{\mu}{\sigma}\left\{ (X_{cg}-r)\left[1-\sigma\left(1+\frac{\xi}{\mu}\right)\right]\sin\theta\cos\theta - Z_{cg}\left[\cos^2\theta + \sigma\left(1+\frac{\xi}{\mu}\right)\sin^2\theta\right] \right\}q^2$$

$$+\left[\cos^2\theta + \sigma\sin^2\theta\right] Z_{aero_B} - \left[(1-\sigma)\sin\theta\cos\theta\right] X_{aero_B} = 0 \qquad \text{(L.9b)}$$

We now turn to the derivation of the pitching moment equation. The pitching moment equation about the model c.g. is

$$M_{inertia} + M_g + M_{aero} = 0 \qquad \text{(L.10)}$$

The inertia moment is

$$M_{inertia} = -\left[I_{cg}\dot{q} - (M_V+M_h)\dot{u}_s Z'_{cg} + M_V X'_{cg}\dot{w}_s\right]$$

Using equations (L.1), (L.2), and (L.3), the above equation can be rewritten as

$$\begin{aligned} M_{inertia} = -\Big\{ & I_{cg}\dot{q} - (M_V+M_h)\left[-(X_{cg}-r)\sin\theta + Z_{cg}\cos\theta\right]\Big[(\dot{u}_B + q w_B)\cos\theta + (\dot{w}_B - q u_B)\sin\theta \\ & - \dot{q}\left(-(X_{cg}-r) + Z_{cg}\cos\theta\right) + q^2\left((X_{cg}-r)\cos\theta + Z_{cg}\sin\theta\right)\Big] \\ & + M_V\left[(X_{cg}-r)\cos\theta + Z_{cg}\sin\theta\right]\Big[-(\dot{u}_B + q w_B)\sin\theta + (\dot{w}_B - q u_B)\cos\theta \\ & + \dot{q}\left((X_{cg}-r)\cos\theta + Z_{cg}\sin\theta\right) + q^2\left(-(X_{cg}-r)\sin\theta + Z_{cg}\cos\theta\right)\Big]\Big\} \end{aligned} \qquad \text{(L.11)}$$

The gravitational moment M_g is simply

$$M_g = M_V g X'_{cg} = M_V g\left[(X_{cg}-r)\cos\theta + Z_{cg}\sin\theta\right] \tag{L.12}$$

Combining equations (L.10), (L.11), and (L.12), the pitching moment equation about the model c.g. is obtained:

$$\begin{aligned}
&-\dot{q}\left\{I_{cg} + (X_{cg}-r)^2\left[M_h\sin^2\theta + M_V\right] + Z_{cg}^2\left[M_h\cos^2\theta + M_V\right] - 2M_h(X_{cg}-r)Z_{cg}\sin\theta\cos\theta\right\} \\
&-M_h\left\{-(X_{cg}-r)\sin\theta + Z_{cg}\cos\theta\right\}\left\{(\dot{u}_B + q w_B)\cos\theta\right. \\
&\left.+(\dot{w}_B - q u_B)\sin\theta + q^2\left[(X_{cg}-r)\cos\theta + Z_{cg}\sin\theta\right]\right\} \\
&+M_V\left\{(X_{cg}-r)(g\cos\theta + \dot{w}_B - q u_B) - Z_{cg}(\dot{u}_B + q w_B - g\sin\theta)\right\} + M_{aero_B} = 0
\end{aligned} \tag{L.13}$$

Linearization of the Equations

For fixed-duct tests at the PDMT, assume that small perturbations about a constant trim may be valid. Then the linearized version of the above equations about u_0, w_0, θ_0 can be written as

$$\begin{bmatrix} 1 & -X'_{\dot{w}} & 0 & -\mu f_4 \\ 0 & (1-Z'_{\dot{w}}) & 0 & \frac{\mu}{\sigma} f_5 \\ 0 & 0 & 1 & 0 \\ \frac{-1}{K_1(\theta_0)} & -\left(\frac{1}{K_2(\theta_0)} + M'_{\dot{w}}\right) & 0 & 1 \end{bmatrix} \begin{bmatrix} \dot{u} \\ \dot{w} \\ \dot{\theta} \\ \dot{q} \end{bmatrix} =$$

$$\begin{bmatrix} X'_u & X'_w & (-g\cos\theta_0 + X_{\theta_0}) & (-w_0 + X'_q) \\ Z'_u & Z'_w & (-g\sin\theta_0 + Z_{\theta_0}) & (u_0 + Z'_q) \\ 0 & 0 & 0 & 1 \\ M'_u & M'_w & -\frac{g}{K_3} & \left(M'_q + \frac{w_0}{K_1} - \frac{u_0}{K_2}\right) \end{bmatrix} \begin{bmatrix} u \\ w \\ \theta \\ q \end{bmatrix} + \begin{bmatrix} X'_B & X'_{\delta_{ES}} & X'_\lambda \\ Z'_B & Z'_{\delta_{ES}} & Z'_\lambda \\ 0 & 0 & 0 \\ M'_B & M'_{\delta_{ES}} & M'_\lambda \end{bmatrix} \begin{bmatrix} \Delta B \\ \Delta\delta_{ES} \\ \Delta\lambda \end{bmatrix} \tag{L.14}$$

where the variables are perturbation values, and:

$$Z_{(\,)}, X_{(\,)} \equiv \frac{1}{M+M_v}\frac{\partial Z}{\partial(\,)}\ ,\ \frac{1}{M+M_v}\frac{\partial X}{\partial(\,)}$$

$$M_{(\,)} \equiv \frac{1}{I_{cg}}\frac{\partial M}{\partial(\,)}$$

$$X'_{(\,)} = f_1(\theta_o)X_{(\,)} - f_2(\theta_o)Z_{(\,)}$$

$$Z'_{(\,)} = f_6(\theta_o)Z_{(\,)} - f_2(\theta_o)X_{(\,)}$$

$$X_{t_o} = 2f_2(\theta_o)X_o - f_3(\theta_o)Z_o$$

$$Z_{t_o} = -2f_2(\theta_o)Z_o - f_3(\theta_o)X_o$$

$$f_1(\theta_o) = \sin^2\theta_o + \sigma\cos^2\theta_o$$

$$f_2(\theta_o) = (1-\sigma)\sin\theta_o\cos\theta_o$$

$$f_3(\theta_o) = (1-\sigma)(\cos^2\theta_o - \sin^2\theta_o)$$

$$f_4(\theta_o) = Z_{cg}\left[\left(1-\frac{\xi}{\mu}\right)\cos^2\theta_o + \frac{1}{\sigma}\sin^2\theta_o\right] - (X_{cg}-r)\left(\frac{1}{\sigma}-1-\frac{\xi}{\mu}\right)\sin\theta_o\cos\theta_o$$

$$f_5(\theta_o) = (X_{cg}-r)\left[\cos^2\theta_o + \left(1+\frac{\xi}{\mu}\right)\sigma\sin^2\theta_o\right] + Z_{cg}\left(1-\sigma-\sigma\frac{\xi}{\mu}\right)\sin\theta_o\cos\theta_o$$

$$f_6(\theta_o) = \cos^2\theta_o + \sigma\sin^2\theta_o$$

$$I'_{cg} = I_{cg} + (X_{cg}-r)^2(M_h\sin^2\theta_o + M_v) + Z_{cg}^2(M_h\cos^2\theta_o + M_v) - 2M_h(X_{cg}-r)Z_{cg}\sin\theta_o\cos\theta_o$$

$$M'_{(\,)} = \frac{1}{I'_{cg}}\frac{\partial M}{\partial(\,)}$$

$$\frac{1}{K_h^2(\theta_o)} = \frac{M_h}{I'_{cg}}\ ,\ \frac{1}{K_v^2(\theta_o)} = \frac{M_v}{I'_{cg}}$$

$$\frac{1}{K_1(\theta_o)} = \frac{(X_{cg}-r)}{K_h^2}\sin\theta_o\cos\theta_o - \frac{Z_{cg}}{K_h^2}\cos^2\theta_o - \frac{Z_{cg}}{K_v^2}$$

$$\frac{1}{K_2(\theta_o)} = \frac{(X_{cg}-r)}{K_h^2}\sin^2\theta_o - \frac{Z_{cg}}{K_h^2}\sin\theta_o\cos\theta_o + \frac{(X_{cg}-r)}{K_v^2}$$

$$\frac{1}{K_3(\theta_o)} = \frac{(X_{cg}-r)}{K_v^2}\sin\theta_o - \frac{Z_{cg}}{K_v^2}\cos\theta_o$$

A primary advantage in the linearization of the general nonlinear equations, (L.9) and (L.13), is the fact that the inertial coupling through the square of pitch rate is eliminated, and the equations may thus be written in terms of conventional state and control variables. A straightforward matrix inversion enables us to write the equations in the general form $\dot{\bar{x}} = A\bar{x} + B\bar{u}$, that is:

$$\begin{bmatrix} \dot{u} \\ \dot{w} \\ \dot{\theta} \\ \dot{q} \end{bmatrix} = \frac{1}{\Delta}\begin{bmatrix} A_{11} & A_{12} & A_{13} & A_{14} \\ A_{21} & A_{22} & A_{23} & A_{24} \\ A_{31} & A_{32} & A_{33} & A_{34} \\ A_{41} & A_{42} & A_{43} & A_{44} \end{bmatrix}\begin{bmatrix} u \\ w \\ \theta \\ q \end{bmatrix} + \frac{1}{\Delta}\begin{bmatrix} B_{11} & B_{12} & B_{13} \\ B_{21} & B_{22} & B_{23} \\ B_{31} & B_{32} & B_{33} \\ B_{41} & B_{42} & B_{43} \end{bmatrix}\begin{bmatrix} \Delta B \\ \Delta\delta_{ES} \\ \Delta\lambda \end{bmatrix} \quad \text{(L. 15)}$$

where

$$\Delta = (1-Z'_{\dot{w}}) + \frac{X'_{\dot{w}}}{K_1}\frac{\mu}{\sigma}f_5 + \frac{\mu f_4}{K_1}(1-Z'_{\dot{w}}) + \frac{\mu}{\sigma}f_5\left(\frac{1}{K_2}+M'_{\dot{w}}\right)$$

$$A_{11} = \left[1 + Z'_{\dot{w}} + \frac{\mu}{\sigma}f_5\left(\frac{1}{K_2}+M'_{\dot{w}}\right)\right]X'_u + \left[X'_{\dot{w}} - \mu f_4\left(\frac{1}{K_2}+M'_{\dot{w}}\right)\right]Z_u$$

$$- \left[\mu f_4(1-Z'_{\dot{w}}) + \frac{\mu}{\sigma}f_5 X'_{\dot{w}}\right]M'_u$$

$$A_{21} = \left[\frac{1}{K_1}\frac{\mu}{\sigma}f_5\right]X'_u + \left[1 + \frac{1}{K_1}\mu f_4\right]Z'_u - \frac{\mu}{\sigma}f_5 M'_u$$

$$A_{31} = 0$$

$$A_{41} = \left[\frac{1}{K_1}(1-Z'_{\dot{w}})\right]X'_u + \left[\frac{X'_{\dot{w}}}{K_1} + \left(\frac{1}{K_2}+M'_{\dot{w}}\right)\right]Z'_u + (1-Z'_{\dot{w}})M'_u$$

$$A_{12} = \left[1 - Z'_{\dot{w}} + \frac{\mu}{\sigma} f_5 \left(\frac{1}{K_2} + M'_{\dot{w}}\right)\right] X'_w + \left[X'_{\dot{w}} - \mu f_4 \left(\frac{1}{K_2} + M'_{\dot{w}}\right)\right] Z'_w$$

$$- \left[\mu f_4 (1 - Z'_{\dot{w}}) + \frac{\mu}{\sigma} f_5 X'_{\dot{w}}\right] M'_w$$

$$A_{22} = \left[\frac{1}{K_1} \frac{\mu}{\sigma} f_5\right] X'_w + \left[1 + \frac{1}{K_1} \mu f_4\right] Z'_w - \frac{\mu}{\sigma} f_5 M'_w$$

$$A_{32} = 0$$

$$A_{42} = \left[\frac{1}{K_1} (1 - Z'_{\dot{w}})\right] X'_w + \left[\frac{X'_{\dot{w}}}{K_1} + \left(\frac{1}{K_2} + M'_{\dot{w}}\right)\right] Z'_w + (1 - Z'_{\dot{w}}) M'_w$$

$$A_{13} = \left[1 - Z'_{\dot{w}} + \frac{\mu}{\sigma} f_5 \left(\frac{1}{K_2} + M'_{\dot{w}}\right)\right]\left[-g \cos \theta_0 + X_{t_0}\right] + \left[X'_{\dot{w}} - \mu f_4 \left(\frac{1}{K_2} + M'_{\dot{w}}\right)\right]\left[-g \sin \theta\right.$$

$$\left. + Z_{t_0}\right] + \left[\mu f_4 (1 - Z'_{\dot{w}}) + \frac{\mu}{\sigma} f_5 X'_{\dot{w}}\right] \frac{g}{K_3}$$

$$A_{23} = \left[\frac{1}{K_1} \frac{\mu}{\sigma} f_5\right]\left[-g \cos \theta_0 + X_{t_0}\right] + \left[1 + \frac{1}{K_1} \mu f_4\right]\left(-g \sin \theta_0 + Z_{t_0}\right) + \frac{\mu}{\sigma} f_5 \frac{g}{K_3}$$

$$A_{33} = 0$$

$$A_{43} = \left[\frac{1}{K_1} (1 - Z'_{\dot{w}})\right]\left[-g \cos \theta_0 + X_{t_0}\right] + \left[\frac{X'_{\dot{w}}}{K_1} + \left(\frac{1}{K_2} + M'_{\dot{w}}\right)\right]\left[-g \sin \theta_0 + Z_{t_0}\right]$$

$$- (1 - Z'_{\dot{w}}) \frac{g}{K_3}$$

$$A_{14} = -\left[1 - Z'_{\dot{w}} + \frac{\mu}{\sigma} f_5 \left(\frac{1}{K_2} + M'_{\dot{w}}\right)\right](w_0 - X'_q) + \left[X'_{\dot{w}} - \mu f_4 \left(\frac{1}{K_2} + M'_{\dot{w}}\right)\right](u_0 + Z'_q)$$

$$- \left[\mu f_4 (1 - Z'_{\dot{w}}) + \frac{\mu}{\sigma} f_5 X'_{\dot{w}}\right]\left[M'_q + \frac{w_0}{K_1} - \frac{u_0}{K_2}\right]$$

$$A_{24} = -\left[\frac{1}{K_1}\frac{\mu}{\sigma}f_5\right](w_0 - X'_q) + \left[1 + \frac{1}{K_1}\mu f_4\right](u_0 + Z'_q)$$

$$- \frac{\mu}{\sigma}f_5\left[M'_q + \frac{w_0}{K_1} - \frac{u_0}{K_2}\right]$$

$$A_{34} = \Delta$$

$$A_{44} = -\left[\frac{1}{K_1}(1 - Z_{\dot{w}})\right](w_0 - X'_q) + \left[\frac{X'_{\dot{w}}}{K_1} + \left(\frac{1}{K_2} + M'_{\dot{w}}\right)\right](u_0 + Z'_q)$$

$$+ (1 + Z'_{\dot{w}})\left(M'_q + \frac{w_0}{K_1} - \frac{u_0}{K_2}\right)$$

$$B_{11} = \left[1 - Z'_{\dot{w}} + \frac{\mu}{\sigma}f_5\left(\frac{1}{K_2} + M'_{\dot{w}}\right)\right]X'_\beta + \left[X'_{\dot{w}} - \mu f_4\left(\frac{1}{K_2} + M'_{\dot{w}}\right)\right]Z'_\beta$$

$$- \left[\mu f_4(1 - Z'_{\dot{w}}) + \frac{\mu}{\sigma}f_5 X'_{\dot{w}}\right]M'_\beta$$

$$B_{21} = \left[\frac{1}{K_1}\frac{\mu}{\sigma}f_5\right]X'_\beta + \left[1 + \frac{1}{K_1}\mu f_4\right]Z'_\beta - \frac{\mu}{\sigma}f_5 M'_\beta$$

$$B_{31} = 0$$

$$B_{41} = \left[\frac{1}{K_1}(1 - Z'_{\dot{w}})\right]X'_\beta + \left[\frac{X'_{\dot{w}}}{K_1} + \left(\frac{1}{K_2} + M'_{\dot{w}}\right)\right]Z'_\beta + (1 - Z'_{\dot{w}})M'_\beta$$

$$B_{12} = \left[1 - Z'_{\dot{w}} + \frac{\mu}{\sigma}f_5\left(\frac{1}{K_2} + M'_{\dot{w}}\right)\right]X'_{\delta_{ES}} + \left[X'_{\dot{w}} - \mu f_4\left(\frac{1}{K_2} + M'_{\dot{w}}\right)\right]Z_{\delta_{ES}}$$

$$- \left[\mu f_4(1 - Z'_{\dot{w}}) + \frac{\mu}{\sigma}f_5 X'_{\dot{w}}\right]M'_{\delta_{ES}}$$

$$B_{22} = \left[\frac{1}{K_1}\frac{\mu}{\sigma}f_5\right]X'_{\delta_{ES}} + \left[1 + \frac{1}{K_1}\mu f_4\right]Z'_{\delta_{ES}} - \frac{\mu}{\sigma}f_5 M'_{\delta_{ES}}$$

$$B_{32} = 0$$

$$B_{42} = \left[\frac{1}{K_1}(1 - Z'_{\dot{w}})\right]X'_{\delta_{ES}} + \left[\frac{X'_{\dot{w}}}{K_1} + \left(\frac{1}{K_2} + M'_{\dot{w}}\right)\right]Z'_{\delta_{ES}} + (1 - Z'_{\dot{w}})M'_{\delta_{ES}}$$

$$B_{13} = \left[1 - Z'_{\dot{w}} + \frac{\mu}{\sigma} f_5 \left(\frac{1}{K_2} + M'_{\dot{w}}\right)\right] X'_\lambda + \left[X'_{\dot{w}} - \mu f_4 \left(\frac{1}{K_2} + M'_{\dot{w}}\right)\right] Z'_\lambda$$

$$- \left[\mu f_4 \, (1 - Z'_{\dot{w}}) + \frac{\mu}{\sigma} f_5 X'_{\dot{w}}\right] M'_\lambda$$

$$B_{23} = \left[\frac{1}{K_1} \frac{\mu}{\sigma} f_5\right] X'_\lambda + \left[1 + \frac{1}{K_1} \mu f_4\right] Z'_\lambda - \frac{\mu}{\sigma} f_5 M'_\lambda$$

$$B_{33} = 0$$

$$B_{43} = \left[\frac{1}{K_1} (1 - Z'_{\dot{w}})\right] X'_\lambda + \left[\frac{X'_{\dot{w}}}{K_1} + \left(\frac{1}{K_2} + M'_{\dot{w}}\right)\right] Z'_\lambda + (1 - Z'_{\dot{w}}) M'_\lambda$$

REFERENCES

1. D. Key and L. Reed: VTOL Transition Dynamics and Equations of Motion With Application to the X-22A. CAL Report No. TB-2312-F-1, June 1968.

2. W. Davies, et al: Final Report, Phase I MPE of the X-22A VTOL Research Aircraft. NATC TR FT-80R-68, December 1968.

3. W. B. Rhodes: Initial Military Flight Tests of the X-22A VTOL Research Aircraft. AIAA Paper No. 69-319, March 1969.

4. A. E. Bryson and M. Frazier: Smoothing for Linear and Nonlinear Dynamic Systems. AF-TDR-63-119, pp 353-364, Wright-Patterson AFB, Ohio, February 1963.

5. H. Cox: "On the Estimation of State Variables and Parameters for Noisy Dynamic Systems" IEEE Trans. on Automatic Control. pp 5-12, 1964.

6. H. Cox: "Estimation of State Variables via Dynamic Programming" Proc. JACC 1964, pp 376-381, June 1964.

7. J. S. Meditch: A Successive Approximation Procedure for Nonlinear Data Smoothing. Boeing Sci. Res. Lab. Document D-1-82-0803.

8. M. Shinbrot: On the Analysis of Linear and Nonlinear Dynamical Systems. NACA TND 3288, December 1954.

9. F. Eckhart and R. P. Harper, Jr.: Analysis of Longitudinal Responses of Unstable Aircraft. CAL Report No. BA-1610-F-1, September 1964.

10. D. A. DiFranco: In-Flight Parameter Identification by Equations of Motion Technique - Application to the Variable Stability T-33 Airplane. CAL Report No. TC-1921-F-3, December 1965.

11. D. Larson, et al: Modified Spline Interpolation Function. Contributed paper given at S. I. A. M. Meeting at Philadelphia, Pa., October 1968.

12. D. G. Denery: An Identification Algorithm Which Is Insensitive to Initial Parameter Estimates. Paper presented at 8th Aerospace Sci. Conf., January 19-21, 1970.

13. R. A. Westerwick: System Identification Using Transient Response Data. Paper presented at SAE Aerospace Vehicle Flight Controls Committee, Atlanta, Georgia, March 1970.

14. K. Y. Wong and E. Polak: "Identification of Linear Discrete Time Systems Using the Instrumental Variable Method" IEEE Trans. AC-12, pp 707-718, December 1967.

15. A. S. Goldberger: Econometric Theory. J. Wiley & Sons, 1964.

16. R. Bellman, et al: Quasilinearization, System Identification, and Prediction. Rand Memo RM-3812-PR, Rand Corporation, Santa Monica, Calif., August 1963.

17. K. Kumar and R. R. Sridhar: "On the Identification of Control Systems by the Quasilinearization Method" Transactions of the Institute of Electrical and Electronics Engineers on Automatic Control, Vol. 9, pp 151-154, April 1964.

18 D. B. Larson: Identification of Parameters by the Method of Quasilinearization. CAL Report No. 164, 1968.

19. G. C. Goodwin: "Application of Curvature Methods to Parameter and State Estimation" Proceedings of the Institution of Electrical Engineers, Vol. 116, No. 6, pp 1197-1200, June 1969.

20. L. W. Taylor and K. W. Iliff: A Modified Newton Raphson Method for Determining Stability Derivatives from Flight Data. Paper presented at the Second International Conference on Computational Methods in Optimal Problems, San Remo, Italy, September 9-13, 1968.

21. R. T. N. Chen: "A Recurrence Relationship for Parameter Estimation via Method of Quasilinearization and Its Connection with Kalman Filtering" J AIAA. pp 1696-1698, September 1970.

22. R. F. Brown and G. C. Goodwin: "Hybrid Method of State and Parameter Estimation for Use in Gradient Techniques" Electronics Letters, December 1967.

23. J. Greenstadt: "On the Relative Efficiencies of Gradient Methods" Math. of Comp. Vol. 21, pp 360-367, 1967.

24. G. C. Goodwin: Estimation of Process Parameters and State. IFAC Symposium, Sydney, August 1968.

25. R. Fletcher and C. Reeves: "Function Minimization by Conjugate Gradients" Computer J., Vol. 7, No. 2, pp 149-154, 1964.

26. L. S. L. Lason, et al: "The Conjugate Gradient Method for Optimal Control Problems" IEEE Trans. AC-12, pp 132-138, April 1967.

27. D. M. Detchmendy and R. Sridhar: Sequential Estimation of States and Parameters in Noisy Nonlinear Dynamical Systems. JACC preprint, pp 56-63, 1965.

28. R. Bellman, et al: Invariant Imbedding and Nonlinear Filtering Theory. Rand Memo RM-4374-PR, December 1964.

29. N. E. Nahi: Estimation Theory and Application. John Wiley & Sons, New York, 1969.

30. A. Bryson and Y. C. Ho: Applied Optimal Control. Ginn Blaisdell, 1969.

31. A. H. Jazwinski: Stochastic Processes and Nonlinear Filtering Theory. Academic Press, 1970.

32. B. L. Ho: Sensitivity of Kalman Filter With Respect to Parameter Variations. Memorandum 33, SRI, Menlo Park, Calif., March 1968.

33. B. Dolbin, Jr.: A Differential Correction Method for the Identification of Airplane Parameters From Flight Test Data. MS Thesis, State University of New York at Buffalo, December 1968.

34. G. W. Hall: A Quasilinearization Technique for Obtaining Lateral-Directional Modal Parameters From Digitally Recorded Flight Test Records. MS Thesis, State University of New York at Buffalo, 1970.

35. J. D. McLean, et al: Optimal Filtering and Linear Prediction Applied to a Midcourse Navigation System for the Circumlunar Mission. NASA TND-1208, March 1962.

36. G. L. Smith, et al: Application of Statistical Filter Theory to the Optimal Estimation of Position and Velocity On Board a Circumlunar Vehicle. NASA TR-T-135, 1962.

37. R. Roy and K. Jenkins: Identification and Control of a Flexible Launch Vehicle. NASA CR-551, August 1966.

38. L. Schwartz and E. B. Stear: "A Computational Comparison of Several Nonlinear Filters" IEEE Trans. on Automatic Control AC-13, pp 83-86, 1968.

39. H. E. Rauch: "Solution to the Linear Smoothing Problem" IEEE Trans. on Automatic Control, pp 371-372, 1963.

40. H. E. Rauch, et al: "Maximum Likelihood Estimation of Linear Dynamic Systems" J AIAA, Vol. 3, pp 1445-1450, August 1965.

41. D. C. Fraser: A New Technique for the Optimal Smoothing of Data. ScD. Thesis, MIT, January 1967.

42. J. S. Meditch: Stochastic Optimal Linear Estimation and Control. McGraw-Hill, 1969.

43. J. S. Meditch: Optimal Fixed-Point Continuous Linear Smoothing. JACC Preprint, pp 249-257, 1967.

44. J. S. Meditch: "On Optimal Fixed-Point Linear Smoothing" Int. J. Control, Vol. 6, No. 2, pp 189-199, 1967.

45. H. H. Kagiwada, et al: "Invariant Imbedding and Sequential Interpolating Filters for Nonlinear Processes" J. Basic Engr., pp 195-200, June 1969.

46. R. C. K. Lee: Optimal Estimation, Identification, and Control. MIT Press, 1964.

47. E. E. Fisher: The Identification of Linear Systems. JACC Preprint, pp 473-475, 1965.

48. C. G. Pfeiffer: "On the Identification of Observable Orbit Parameters With Application to Lunar Orbiter Tracking" J. Ast. Sci., pp 22-31, January-February 1969.

49. A. Lavi and J. Strauss: "Parameter Identification in Continuous Dynamic Systems" IEEE Int. Conv. Record, pp 49-61, 1965.

50. B. Friedman: Principles and Techniques of Applied Mathematics. J. Wiley & Sons, 1956.

51. L. Zadeh and C. Desoer: Linear Systems Theory. McGraw-Hill, 1963.

52. R. T. N. Chen: "On the Construction of State Observers in Multi-Variable Control Systems" Proc. NEC, pp 62-67, December 1969.

53. M. Athans, et al: "Suboptimal State Estimation for Continuous Time Nonlinear System With Discrete Noisy Measurements" IEEE Trans. AC-13, pp 504-518, 1968.

54. H. E. Rauch: "Optimum Estimation of Satellite Trajectories Including Random Fluctuations in Drag" J AIAA, pp 717-722, April 1965.

55. J. S. Tyler, et al: The Use of Smoothing and Other Techniques for VTOL Aircraft Parameter Identification. SCI Report, June 30, 1970.

56. R. G. Mortensen: Mathematical Problems of Modeling Stochastic Nonlinear Dynamic Systems. NASA CR-1168, September 1968.

57. R. P. Wishner, et al: "A Comparison of Three Nonlinear Filters" Automatica, Vol. 5, pp 487-496, 1969

58. Maj. W. J. Scheuren, et al: Phase II Military Preliminary Evaluation of the X-22A Variable Stability Research Aircraft. Final Report, Report No. FT-47R-69, 28 May 1969.

59. H. C. Curtiss, Jr.; W. F. Putman; and J. J. Traybar: General Description of the Princeton Dynamic Model Track. USAAVLABS Technical Report 66-73, U.S. Army Aviation Material Laboratories, Fort Eustis, Virginia, November 1966.

60. H. C. Curtiss, Jr.: An Investigation of the Dynamic Stability Characteristics of a Quad Configuration, Ducted-Propeller V/STOL Model. Volume IV, The Longitudinal Stability Characteristics of a Quad Configuration, Ducted-Propeller V/STOL Model at High Duct Incidence. USAAVLABS Technical Report 68-49D, U.S. Army Aviation Material Laboratories, Fort Eustis, Virginia, May 1969.

61. Letter from W. F. Putman to J. V. Lebacqz of CAL, April 13, 1970.

62. M. Parrag: Static Calibration of the Elevon Control System With Feedforward System Operating. CAL X-22A TM-56, November 20, 1968.

63. M. Parrag: Static Calibration of the Propeller Pitch Control System With Feedforward System Operation. CAL X-22A TM-58, June 15, 1968.

64. R. D. Till: Additional Static Calibration of the Basic X-22A Propeller Pitch Control System. CAL X-22A TM-61, April 30, 1969.

65. A. Papoulis: Probability, Random Variables, and Stochastic Processes. McGraw-Hill, 1965.

66. R. T. N. Chen: "On the Construction of State Observer in Multivariable Control Systems" Proc. NEC, pp 62-67, December 1969.

67. R. W. Hill; I. L. Clinkenbeard; and N. F. Bolling: V/STOL Flight Test Instrumentation Requirements for Extraction of Aerodynamic Coefficients. AFFDL TR-68-154, Vol. 1, December 1968.

68. N. E. Nahi and D. E. Wallis, Jr.: Optimal Control for Information Maximization in Least-Square Parameter Estimation. SAMSO-TR-68-177, January 1968.

69. N. E. Nahi and D. E. Wallis, Jr.: Optimal Inputs for Parameter Estimation in Dynamic Systems With White Observation Noise. Preprint of 1969 JACC, pp 506-516, 1969.

70. G. C. Goodwin: "Input Synthesis for Minimum Covariance State and Parameter Estimation" Electronic Letters, Vol 5, No. 21, 16 October 1969.

71. D. R. VanderStoep: "Trajectory Shaping for the Minimization of State-Variable Estimation Error" IEEE Transactions on Automatic Control, pp 284-286, June 1968.

72. B. Pagurek and C. M. Woodside: "The Conjugate Gradient Method for Optimal Control Problems With Bounded Control Variables" Automatics, Vol. 4, pp 337-349, 1968.

73. R. Griffin and A. P. Sage: "Large and Small Scale Sensitivity Analysis of Optimum Estimation Algorithms" IEEE Trans. Automatic Control, Vol. AC-13, pp 320-328. April 1966.

74. R. E. Griffin and A. P. Sage: Sensitivity Analysis of Discrete Filtering and Smoothing Algorithms. AIAA Guidance, Control and Flight Dynamics Conf., Pasadena, California, August 1968.

75. T. Nishimura: "On the A Priori Information in Sequential Estimation Problems" IEEE Trans. Automatic Control, Vol. AC-11, pp 197-204, April 1966.

76. T. Nishimura: "Error Bounds of Continuous Kalman Filters and the Application to Orbit Determination Problems" IEEE Trans. Automatic Control, Vol. AC-12, pp 268-275, June 1967.